INFORMATION TO USERS

This manuscript has been reproduced from the microfilm master. UMI films the text directly from the original or copy submitted. Thus, some thesis and dissertation copies are in typewriter face, while others may be from any type of computer printer.

The quality of this reproduction is dependent upon the quality of the copy submitted. Broken or indistinct print, colored or poor quality illustrations and photographs, print bleedthrough, substandard margins, and improper alignment can adversely affect reproduction.

In the unlikely event that the author did not send UMI a complete manuscript and there are missing pages, these will be noted. Also, if unauthorized copyright material had to be removed, a note will indicate the deletion.

Oversize materials (e.g., maps, drawings, charts) are reproduced by sectioning the original, beginning at the upper left-hand corner and continuing from left to right in equal sections with small overlaps. Each original is also photographed in one exposure and is included in reduced form at the back of the book.

Photographs included in the original manuscript have been reproduced xerographically in this copy. Higher quality 6" x 9" black and white photographic prints are available for any photographs or illustrations appearing in this copy for an additional charge. Contact UMI directly to order.

UMI

A Bell & Howell Information Company
300 North Zeeb Road, Ann Arbor MI 48106-1346 USA
313/761-4700 800/521-0600

Synthesis, Characterization and Metal Complexation of Novel Pentacoordinate N_4S-Donor Macrobicyclic Ligands

by

Kevin Robert Coulter

B. Sc., University of Victoria, 1989

A DISSERTATION SUBMITTED IN PARTIAL FULFILLMENT
OF THE REQUIREMENTS FOR THE DEGREE OF
DOCTOR OF PHILOSOPHY

in the Department of Chemistry

We accept this dissertation as conforming
to the required standard

Dr. A. McAuley

Dr. T. M. Fyles

Dr. K. R. Dixon

Dr. D. V. Ellis

Dr. R. C. Thompson

Supervisor: Professor Alexander McAuley

ABSTRACT

The syntheses of three structurally isomeric pentacoordinate N_4S-donor macrobicyclic ligands are reported. The isomers differ only in the identity of the two nitrogen atoms of the cyclam ring across which the $-CH_2-CH_2-S-CH_2-CH_2-$ fragment ("sulphur bridge") has been linked. The first isomer, 15-Thia-1,5,8,12-tetraazabicyclo[10.5.2]nonadecane (**L1**), consists of a 9-membered N_2S-donor ring fused to the 14-membered 1,5,8,11-tetraazacyclotetradecane (cyclam) ring. The ligand was synthesized by a copper(II) templated ring closure followed by borohydride reduction. A novel side product (**4**), a monoamide derivative of (**L1**), was also isolated and characterized. The second isomer, 17-Thia-1,5,8,12-tetraazabicyclo[6.6.5]nonadecane (**L2**), consists of linking the sulphur bridge across the diagonally opposed [1,8]-nitrogens. The ligand was synthesized by cyclizing cyclam (1,4,8,11-tetraazacyclotetradecane) with thiodiglycolic acid chloride under high dilution conditions. The third isomer, 14-Thia-1,4,8,11-tetraazabicyclo[9.5.3]nonadecane (**L3**), consists of linking the sulphur bridge across the adjacent [1,5]-nitrogens of the cyclam ring. The ligand was synthesized by cyclization of 1-thia-4,8-diazacyclododecane (**20**) with N,N'-*bis*(α-chloro amido)diaminopropane (**27**) which afforded the diamide derivative, 14-Thia-1,4,8,11-tetraazabicyclo[9.5.3]nonadecane-3,9-dione (**30**), in high yield. Reduction of **30** with diborane gave the third structural isomer, (**L3**).

A novel, convenient synthesis of 1-thia-4,8-diazacyclododecane-3,9-dione (**23**) from diaminopropane and thiodiglycolic acid chloride was developed. It was shown that high dilution conditions were necessary to obtain high product yields. The nature of the product obtained from reduction of **23** was shown to depend on the conditions used. In the presence of excess borane and methanol, the major product was a boron complex of the reduced ligand. Several changes to the conditions used avoided production of the boron complex and yielded the intended product (**20**) in sufficient quantity.

The parent 1-Thia-4,7-diazacyclononane ([9]aneN_2S) and 1,4,8,11-tetraazacyclotetradecane ([14]aneN_4) ligands exhibit first order coupling behaviour as a

result of time averaging of molecular motions. However, the ambient temperature ^{1}H-NMR spectrum of the [9]aneN_4S bicyclic free ligand (**L1**) exhibited second-order couplings and line broadening indicative of an exchange process. This result indicates that the rigidity of the macrobicyclic structure has hindered certain molecular motions. The variable-temperature ^{1}H-NMR spectra of (**L1**) were recorded in deuterated chloroform. It was found that the geminal coupling (> 15 Hz) of the C-C$\underline{H}_2$-C (propylene fragment) methylene group approached 0 Hz as the temperature was raised beyond 40°C. It is believed that nitrogen inversion processes are responsible for the collapse of these signals.

In order to determine if the rigidity of the N_4S macrobicyclic free ligand structure would have a significant effect on the chemistry of the metal complexes, the copper(II) and nickel(II) complexes of each of the N_4S isomers (**L1-L3**) were prepared and characterized. Any differences observed between these isomers can be attriubuted to ring strain effects.

Electronic spectroscopy of the copper(II) complexes determined the absorption maxima of the [Cu(**L1**)]$(ClO_4)_2$, [Cu(**L3**)]$(ClO_4)_2$ and [Cu(**L2**)]$(ClO_4)_2$ isomers to be 532, 532.5 and 603 nm respectively. ESR spectroscopy showed each complex to have similar g_{iso} values (2.092, 2.090 and 2.089), and the frozen solution (77 K) spectra were indicative of tetragonally elongated axial symmetry ($g_z \neq g_x = g_y$) with the unpaired electron predominantly in the d_{x2-y2} orbital.

The synthesis and characterization of the corresponding nickel(II) complexes of each ligand are reported. The electronic spectra of each of the [Ni(**L1**)]$(ClO_4)_2$, [Ni(**L3**)](acetate)$_2$ and [Ni(**L2**)]$(ClO_4)_2$ isomers were consistent with that expected for O_h coordination of nickel(II). Electrochemical studies of the nickel(II)/(III) oxidations showed that there was a 170 mV difference between the $E_{1/2}$ values of the [Ni(**L1**)]$(ClO_4)_2$ ($E_{1/2}$ = 0.709 V) and [Ni(**L2**)]$(ClO_4)_2$ ($E_{1/2}$ = 0.878 V) complexes.

These results implied that the (**L1**) and (**L3**) bicycle isomers are similar in coordination properties such that significant differences were not observed. The coordination properties of the third N_4S bicycle (**L2**) differ markedly from those of the

other two isomers. That the unique diagonally bridged structure resulted in significantly different absorption maxima and redox potentials, indicates that the coordination of the N_4S donor set has been perturbed (relative to the (L1) and (L3) bicyclic ligands) by the strain energies unique to that isomer.

The molecular structures of the $[Co(L1)(OH_2)](ClO_4)_3$ and $[Pd(L1)](PF_6)_2$ complexes were determined by X-ray crystallographic techniques. The cobalt(III) complex was shown to contain "true" octahedral coordination. The palladium(II) complex was shown to consist of square planar N_4 coordination with the axial sulphur donor positioned 2.87Å from the palladium atom with the M-S vector deviating 16° from the perpendicular to the N_4 plane.

Dr. A. McAuley

Dr. T. M. Fyles

Dr. K. R. Dixon

Dr. D. V. Ellis

Dr. R. C. Thompson

TABLE OF CONTENTS

LIST OF TABLES

LIST OF FIGURES

LIST OF SCHEMES

LIST OF COMPOUNDS

L1 15-Thia-1,5,8,12-tetraazabicyclo[10.5.2]nonadecane (p. 270)

L2 17-Thia-1,5,8,12-tetraazabicyclo[6.6.5]nonadecane (p. 270)

L3 14-Thia-1,4,8,11-tetraazabicyclo[9.5.3]nonadecane (p. 271)

4 15-Thia-1,5,8,12-tetraazabicyclo[10.5.2]nonadecane-6-one (p. 272)

5a N,N'-*Bis*((4-methylphenyl)sulphonyl)-*bis*(2-aminoethyl)sulphide (p. 273)

5b $TsNH(CH_2)_2S(CH_2)_2NHTs$ disodium salt (p. 273)

6 ethylene glycol ditosylate (tosylate = (4-methylphenyl)sulphonate) (p. 273)

7 4,7-*Bis*((4-methylphenyl)sulphonyl)-1-thia-4,7-diazacyclononane (p. 273)

8 1-Thia-4,7-diazacyclononane (p. 274)

9 monoethanolamine ditosylate (p. 274)

10 tosylaziridine (p. 275)

11 4,7-*Bis*(2-cyanoethyl)-1-thia-4,7-diazacyclononane (p. 275)

12 4,7-*Bis*(3-aminopropyl)-1-thia-4,7-diazacyclononane (p. 275)

13 $[Cu(\mathbf{12})](ClO_4)_2$ (p. 276)

14 1,4,8,11-tetraazacyclotetradecane (cyclam) (p. 276)

15 Thiodiglycolic acid chloride (p. 276)

16 **CRUDE** 17-Thia-1,5,8,12-tetraazabicyclo[6.6.5]nonadecane-15,19-dione (p. 277)

17 1-(3-Thia-pentanol)-tetraazacyclotetradecane (p. 277)

18 propylene glycol ditosylate (tosylate = (4-methylphenyl)sulphonate)(p. 278)

19 4,8-*Bis*((4-methylphenyl)sulphonyl)-1-thia-4,8-diazacyclodecane (p. 278)

LIST OF ABBREVIATIONS

[9]aneN_4S bicycle	15-Thia-1,5,8,12-tetraazabicyclo[10.5.2]nonadecane (p. 270)
hemi-cryptateN_4S bicycle	17-Thia-1,5,8,12-tetraazabicyclo[6.6.5]nonadecane (p. 271)
[10]aneN_4S bicycle	14-Thia-1,4,8,11-tetraazabicyclo[9.5.3]nonadecane (p. 272)
monoamido [9]aneN_4S bicycle	15-Thia-1,5,8,12-tetraazabicyclo[10.5.2]nonadecane-5-one (p. 272)
[10]aneN_4S diamide bicycle	14-Thia-1,4,8,11-tetraazabicyclo[9.5.3]nonadecane-5,7-dione (p. 284)
[20]aneN_4S_2	1,11-Dithia-4,8,14,18-tetraazacycloeicosane (p. 281)
[10]aneN_4O bicycle	14-Oxa-1,4,8,11-tetraazabicyclo[9.5.3]nonadecane (p. 283)
[10]aneN_2S	1-Thia-4,8-diazacyclododecane (p. 278)
[9]aneN_2S	1-Thia-4,7-diazacyclononane (p. 274)
[10]aneN_2S diamide	1-Thia-4,8-diazacyclododecane-3,9-dione (p. 279)
[15]aneN_4S linear	*bis*(3,7-diaaminoheptane)sulphide (p. 280)
[10]aneN_4O diamide	14-Oxa-1,4,8,11-tetraazabicyclo[9.5.3]nonadecane-5,7-dione (p. 282)
[14]aneN_4 or cyclam	1,4,8,11-tetraazacyclotetradecane (p. 276)
2-3-2-tet	1,4,8,11-tetraazaunadecane

ACKNOWLEDGEMENTS

I would like to thank my supervisor, Dr. A. McAuley, for the academic freedom given to me and his patience and encouragement throughout the course of this project. I would also like to thank the members of the group, S. Subramanian, S. Chandrasakar, B. Cameron, B. Chak, C. Xu, A. Ingham, M. Rodopoulos and T. Rodopoulos, for their much appreciated assistance.

I would especially like to thank my parents, Florence and Robert Douglas Coulter, and my sister, Marilyn Coulter, for their support, without which this would not have been possible.

Chapter 1
Introduction

1.1 Coordination Chemistry and the Chelate Effect:

The term "coordination chemistry" refers to those compounds which are observed to form when simple metal anion salts are reacted with certain neutral molecules called coordinating ligands. For transition metals, such compounds are often brightly coloured. Perhaps the earliest known of all coordination compounds[1] is the bright red dye, alizarin, a calcium aluminate compound of hydroxyanthraquinone. It was first used in India and known to the ancient Persians and Egyptians then later used by the Greeks and the Romans. Joseph's "coat of many colours" may possibly have been treated with it.

The first scientifically recorded observation[2] of a completely inorganic coordination complex is the formation of the familiar tetraamine copper(II) ion, $[Cu(NH_3)_4]^{2+}$. The 16th century German physician and alchemist Andreas Libavius noticed that *aqua calcis* (limewater) containing *sal ammoniac* (ammonium chloride) became blue in contact with brass (an alloy of copper and zinc)[2]. Another of the early recorded coordination compounds is Prussian Blue, potassium iron(III) hexacyanoferrate(II), a complex of empirical formula $KCN{\bullet}Fe(CN)_2{\bullet}Fe(CN)_3$. It was first obtained[3] accidentally in 1704 by Diesbach, a manufacturer of artist's colours from Berlin.

In 1913, Alfred Werner[4] won the nobel prize for recognizing the true nature of these complex compounds. Werner showed that that the neutral molecules were bound directly to the metal so that the complex salts such as $CoCl_3{\bullet}6NH_3$ were correctly formulated as $[Co(NH_3)_6](Cl)_3$.

$[Co(NH_3)_6](Cl)_3$ =

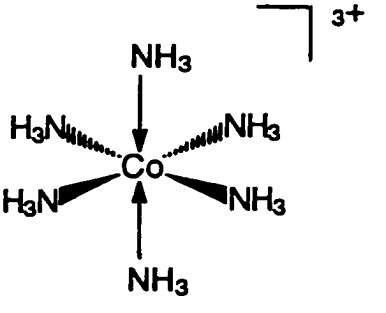

Werner also showed that the molecules or ions around the metal center occupied positions at the corners of an octahedron or a square, giving rise to stereochemical consequences.

The field of coordination chemistry was next advanced by the development of crystal field theory by Bethe[5]. Since then, there have been considerable theoretical and experimental advances in coordination chemistry[6]. Indeed, a diverse range of coordinating ligands has been synthesized and their coordination chemistry investigated. In particular, the coordination chemistry of polydentate ligands has recieved considerable attention[7]. This is because the presence of more than one donor in the coordinating ligand results in a bidentate, or chelate, complex in which the stability of the metal-ligand interaction is greatly enhanced. This effect is referred to as the "chelate effect"[7]. The chelate effect is illustrated by comparing the stability of the tris-ethylenediamine nickel(II) complex shown below to that of the similar, but non-chelated, hexa-amino nickel(II) analogue.

$$Ni^{2+}(aq) + 6NH_3(aq) \Rightarrow [Ni(NH_3)_6]^{2+}(aq) \qquad \log \beta = 8.61$$

$$Ni^{2+}(aq) + 3en(aq) \Rightarrow [Ni(en)_3]^{2+}(aq) \qquad \log \beta = 18.28$$

The system $[Ni(en)_3]^{2+}$, in which three chelate rings are formed, is ten orders of magnitude more stable than that in which no such ring is formed. Although the effect is not always so pronounced, such a chelate effect is a very general one. If one invokes the thermodynamic relationships $\Delta G^\circ = -RT\ln\beta$ and $\Delta G^\circ = \Delta H^\circ - T\Delta S^\circ$, it can be seen that the thermodynamic driving force of the chelate effect is attributable primarily to the presence of a favourable entropy term. The experimentally[7] determined parameters for the cadmium complexes shown below are illustrative of this effect.

Although the ΔH° values are equal within experimental error, the ΔS° values indicate a much more favourable entropy contribution for the chelating ethylenediamine ligand. Extending the level of chelation from bidentate to tridentate and tetradentate donor ligands also provides a compelling demonstration of the chelate effect. This effect is illustrated by the competition reaction between ethylenediamine (en) and

$Cd^{2+}(aq) + 4CH_3NH_2(aq) \Rightarrow [Cd(CH_3NH_2)_4]^{2+}(aq) \quad \log\beta = 6.52$

$Cd^{2+}(aq) + 2H_2NCH_2CH_2NH_2(aq) \Rightarrow [Cd(en)_2]^{2+}(aq) \quad \log\beta = 10.6$

Ligands	ΔH° (kJ/mol)	ΔS° (kJ/mol)	$-T\Delta S^\circ$ (kJ/mol)	ΔG° (kJ/mol)
$4CH_3NH_2$	-57.3	-67.3	20.1	-37.2
2 en	-56.5	+14.1	-4.2	-60.7

Note: Data obtained from reference 126, p. 72.

tris-(2-aminoethyl)amine (tren) in the presence of nickel(II).

$[Ni(en)_2(H_2O)_2]^{2+}(aq) + tren(aq) \Rightarrow [Ni(tren)(H_2O)_2]^{2+}(aq) + 2en(aq) \quad \log\beta = 1.88$

For this reaction, $\Delta H^\circ = +13.0$ kJ/mol while $-T\Delta S^\circ = -23.7$ kJ/mol. The unfavourable positive enthalpy[7] can be attributed to greater steric strain imposed by the presence of three fused chelated rings in tren and to the weaker M-N bond formed by tertiary amines, as opposed to the primary amines in en. Nevertheless, the unfavourable enthalpy is offset by a favourable entropy term due to the presence of three chelate rings in tren (as opposed to two rings).

1.2. Macrocyclic Effect:

A macrocyclic ligand is defined[8] as a cyclic compound with nine or more members (including all heteroatoms) and with three or more donor (ligating) atoms. Prior to 1960, reports of synthetic macrocyclic ligands were few in number. The synthetic macrocycles that were reported were not usually prepared for the purpose of studying their coordination chemistry. For example, the now ubiquitous[9] tetraaza macrocycle, 1,4,8,11-

tetraazacyclotetradecane (cyclam), was first reported[10] in 1936, however the cobalt and nickel complexes were not reported[11] until the mid-1960's. The only well-established category of synthetic macrocycles was that of the highly conjugated (and therefore brightly coloured) phthalocyanines which bear a structural and electronic resemblance to the natural porphyrin systems:

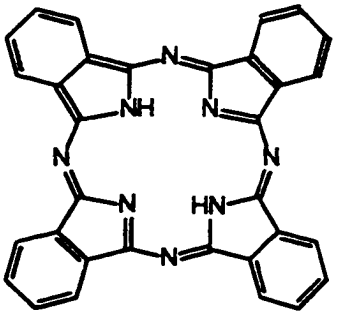

The primary interest in these systems was in their commercial importance as dyes and catalysts.

In the early 1960's, Curtis[12] reported that the reaction between *tris*-ethylenediaminenickel(II) perchlorate and acetone produced the unexpected tetraaza macrocycle shown below:

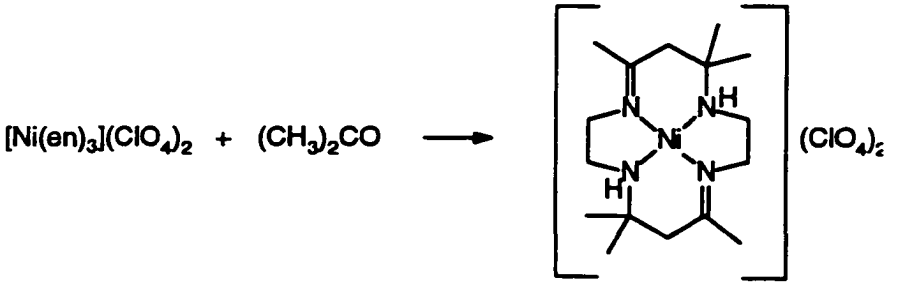

Figure 1.1. Template synthesis of Curtis[12] tetraazadienato macrocycle.

Considerable interest in the coordination properties of macrocyclic complexes developed in the early 1970's when it was reported by Cabbiness and Margerum[13,14] that the stability constant for the Cu(II) complex of the reduced Curtis macrocycle is approximately 10^4 times higher than for the related open-chain tetraza analogue, 1,4,8,11-tetraazaunadecane (2-3-2-tet). Although the presence of an additional chelate ring in the macrocyclic complex is expected to increase the stability of the complex (via the chelate effect), the stability was still an order of magnitude greater than anticipated. The authors ascribed this additional stability to the presence of a "macrocyclic effect".

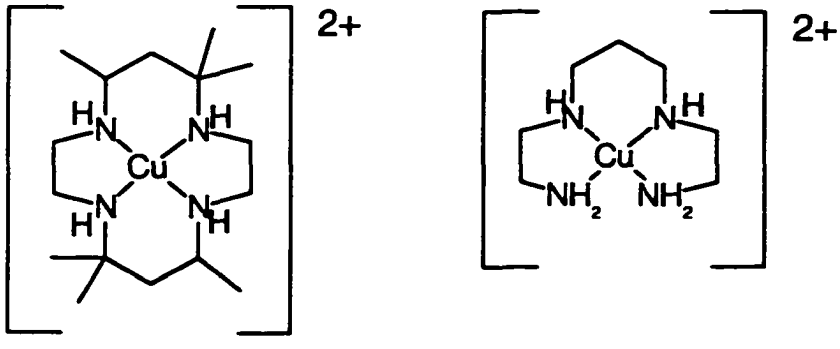

Figure 1.2. Curtis macrocycle and open-chain tetraaza analogue (2-3-2-tet).[12]

The thermodynamic origin (enthalpic or entropic) of this macrocyclic effect, particularly for complexes of tetraaza ligands, has been the subject of much debate[15,16]. More recent studies[17], using more reliable calorimetric data, have largely resolved the uncertainty. Table 1.1 shows the thermodynamic data determined for a series of tetraaza ligands.

The data shown in table 1.1, together with a range of similar studies of tetraaza macrocycles, illustrate the present understanding of the macrocyclic effect. It is now clear

that the entropic term tends to be favourable while the enthalpic term tends to vary and, in some instances, has been found to be unfavourable relative to the analogous open-chain

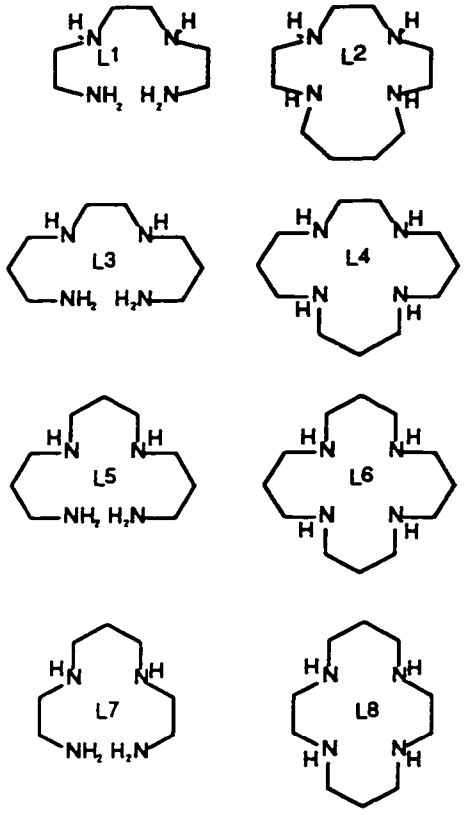

$[Ni(L_{OC})]^{2+} + L_{MAC}{}^{2+} \rightleftharpoons [Ni(L_{MAC})]^{2+} + L_{OC}$ (OC = open chain; MAC = macrocyclic)

L_{OC}/L_{MAC}	$-\Delta G$ /kJ mol^{-1}	ΔH /kJ mol^{-1}	$T\Delta S$ /kJ mol^{-1}
L^1/L^2	2.43	5.1	7.4
L^3/L^4	21.05	5.3	26.4
L^5/L^6	15.69	3.5	19.2
L^7/L^8	33.67	-20.5	13.2

Table 1.1. Thermodynamic data for a series of tetraaza ligands in the presence of high-spin Ni(II). Data obtained from ref. 9.

ligand. In the case of the 14-membered tetraaza macrocycle (cyclam), shown in table 1.1, both the enthalpic and entropic terms are favourable which is one of the reasons that the coordination chemistry of cyclam has generated considerable interest.

Although the thermodynamic contributions to the macrocyclic effect are not consistently substantial, the observed kinetic stabilities of macrocyclic complexes are consistently greater than that of their open-chain analogues. For example, the observed[14] decomposition rate data shown in table 1.2 illustrate that the decomposition rate of the Cu(II) complex of the reduced Curtis macrocycle is much slower than that of its linear analogue, 2-3-2-tet.

Ligand	Solvent	k_f (M^{-1} s^{-1})	k_d (s^{-1})
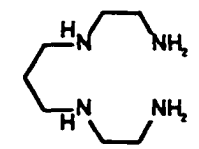	H_2O	8.9×10^4	4.1
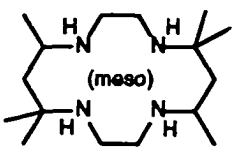	H_2O	5.8×10^{-2}	3.6×10^{-7}
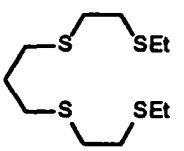	80% MeOH	4.1×10^5	3.0×10^4
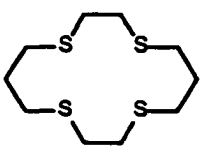	80% MeOH	2.8×10^4	9

Table 1.2. Decomposition rates[14] of copper(II)-tetraaza macrocyclic complexes and their open-chain analogues.

In the case of macrocyclic amines, the kinetic stability is readily observed at low pH because the dissociation of the amines is facilitated by protonation of the amine donor such that it can no longer bind the metal. Indeed, mono- and polydentate amine ligands dissociate rapidly in the presence of acid, while macrocyclic ligands do not. For example, the half-life of the nickel(II) complex of 1,4,8,11-tetraazaunadecane (2-3-2-tet) is less than 5 sec in acidic media, while the half-life of the square-planar Nickel(II) complex of cyclam is approximately 30 years[18].

These results conform to the hypothesis that the open-chain ligand can undergo successive S_N1 replacement steps of the nitrogen donors by solvent molecules, beginning at one end of the ligand. The stripping of successive donors in this fashion is sometimes referred to as the "zippering" mechanism. In acidic media, the dissociated groups are quickly protonated (and solvated) such that they can no longer bind to the metal center. The initial protonation of one of the ends of the open-chain ligand leads to a dissociated, but tethered, intermediate. The cyclic ligand, however, cannot be displaced by such a simple proton scavenging mechanism because the ring has no end. Although the zippering mechanism could still occur in principle, the rigidity of the ring structure prevents the amine donors from leaving the inner coordination sphere.

Busch and co-workers[19] coined the term "multiple juxtapositional fixedness" to describe this kinetic effect. It should, however, be pointed out that a considerable contribution to the observed kinetic stability is also made by the closeness of fit of the macrocyclic ligand cavity to the optimum coordination size required by the metal. For the nickel(II) cyclam complex mentioned above, the 14-membered ring is well-matched to the requirements of the nickel(II) center. However, the addition of one nitrogen donor into the ring to form a 15-membered pentaaaza macrocycle results in complexes which are considerably more labile in acidic solution due to the increasing flexibility in larger ring systems[20].

1.3. Chemistry of Macrocyclic Complexes:

1.3(a). Modeling Aspects of Metalloenzymes:

As the chemistry of macrocyclic complexes was developing, it was realized that such complexes could serve as appropriate models for the active sites of natural metalloenzymes. Bio-inorganic chemistry is concerned with the function of metallic elements in biology and encompasses a broad range of enzymes and reactivities. Approximately 30% of all known enzymes contain metals[21]. A thorough treatment of bio-inorganic chemistry is beyond the scope of this introduction and the reader is referred to more comprehensive sources[21-23].

The use of the term "model" has drawn considerable criticism regarding its proper use. "Purists" argue in favour of concern only with the facts without biases introduced by the prejudices of individual backgrounds. Although this view is fundamental to the scientific method, even the isolation and study of native biological systems requires alteration of the systems such that the rigorous criteria of the purist are not met either.

In practice, two general approaches have been taken by investigators in bio-inorganic chemistry, the biochemical approach and the inorganic approach. The biochemical approach[21] to elucidation of structure/function relationships of metalloenzymes involves alteration (e.g. modification of the protein ligand by site-directed mutagenesis, substitution of one metal for another) of the native material and investigation of the resulting changes in spectroscopic properties and reactivity. The synthetic inorganic chemist instead tends to focus on the central metal ions in the active sites of metalloenzymes and therefore approaches the development of model systems by constructing synthetic ligands and metal complexes which approximate the environment about a given metal in a given active site. This approach generally takes the form of introducing the proper number of donor atoms, geometry, type of donor atoms, steric requirements, etc. into the ligand. For the purposes of the present study, a model system is

considered valid if it modifies or isolates certain salient features pertinent to the real system.

Unlike the metalloenzymes, which have complicated spectra and reactivities due to the large number of functional groups present, these model systems are relatively simple to study and therefore it is easier to draw conclusions about structure/reactivity relationships. Detailed structures of metalloenzymes are known only in relatively few cases such that direct investigation does not definitively determine which aspects of the metalloenzyme (e.g. nature of the donors, coordination geometry, bond lengths, etc.) are responsible for the observed reactivity.

A relevant example of a macrocyclic model is that of the "lacunar ligands" developed by Busch and co-workers[24] for the purpose of modeling the reversible dioxygen binding of hemoglobin and myoglobin. The first barrier to model studies that had to be overcome was to prevent the irreversible formation of μ-oxo bridged di-iron species (the pocket of the native enzyme prevents such interactions). Many modified prophyrins have been successful in preventing μ-oxo bridging and have been used to delineate the structure/function relationships of the native heme site (see the "picket fence"[21] derivatives for example).

This task, however, was also accomplished [24] by the lacunar ligand framework in which a tetraaza macrocycle has been protected on one side by the hydrophobic "void" (figure 1.3) provided by strapping a non-polar bridge across the ring. The iron(II) and

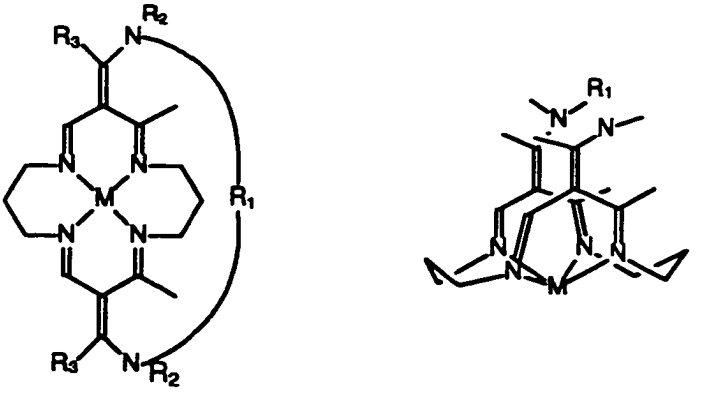

Figure 1.3. Lacunar macrobicyclic ligand framework synthesized by Busch et al.[24]

cobalt(II) complexes of this ligand system have been shown[24] to display oxygen binding behaviours that compare favourably with those of the natural hemoglobins and coboglobins. That such reversible dioxygen binding should occur in a greatly simplified non-aromatic macrocycle, shows that the more subtle features of the aromaticity and rigidity of the heme group are not a necessary requirement for reversible dioxygen binding.

Another successful example of modeling metalloenzymes with macrocyclic complexes is provided by Kimura and co-workers[25]. The metalloenzymes responsible for the hydrolysis of esters, amides (or peptides) and phosphates almost exclusively contain zinc(II) in the active site. The active sites of carbonic anhydrase (CA) and carboxypeptidase are as shown:

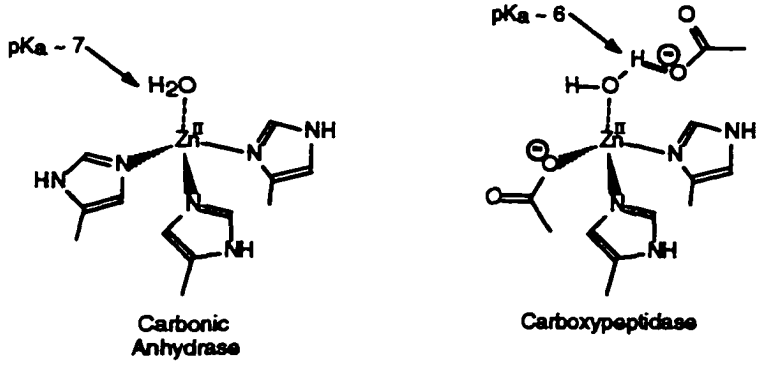

It can be seen that the zinc(II) center is bound by three histidine donors (one carboxylate donor replaces a histidine in carboxyypeptidase) and one water molecule. Although various hypotheses have been presented to explain the role of the zinc(II) center in these enzymes, it is difficult to study the native enzyme unambiguously. It is generally believed that the action of the enzyme involves attack of the substrate by Zn-OH. The pKa of the Zn-OH_2 group in carbonic anhydrase (CA) is 7. By synthesizing macrocyclic model complexes of zinc(II) (see figure 1.4), Kimura[26] has shown that the tetraaza macrocyclic complexes have relatively high pKa values such that they do not model the active site reactivity.

It can be seen, however, that the triamines, particularly [12]aneN$_3$, have pKa values that are very close to that of CA. It has also been found[26] that the mono-aquo Zn(II) complex of [12]aneN$_3$ shows hydrolysis activity that closely resembles the natural metalloenzymes. Elucidation of the model hydrolysis mechanism therefore plays a key role in understanding the mechanism of the metalloenzymes.

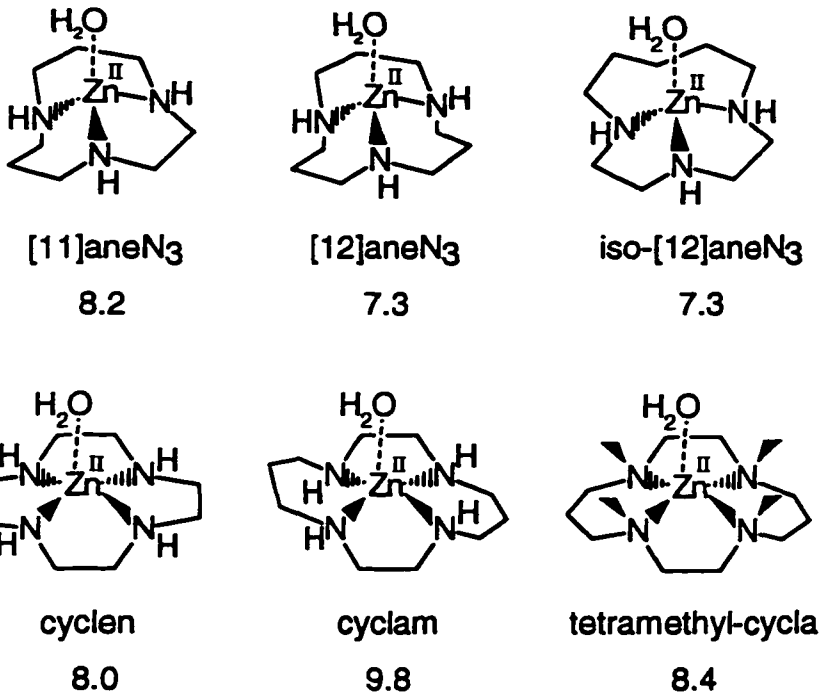

Figure 1.4. Acid dissociation constants of coordinated water in various triaza and tetraaza macrocyclic zinc(II) complexes.[26]

Although the use of macrocyclic complexes as models for metalloenzymes is often limited in scope, the unusual and varied chemistry of these macrocyclic complexes has proven to be of considerable interest in its own right. The salient features of interest in inorganic macrocyclic chemistry are now presented.

1.3(b). The Macrocyclic Cavity:

The mean radius of a macrocyclic ligand is referred to as its "hole size". The hole size influences the properties of the resultant metal complexes relative to those of the corresponding non-cyclic ligands. It is affected most by the number of atoms in the ring. As the number of atoms in the ring increases, the hole size of the free ligand increases by *ca.* 0.10-0.15 Å[27] per atom. However, for complexes of the relatively flexible saturated tetraaza macrocycles, the ligands are able to fold via expansion of the smaller chelate rings and contraction of the larger ones (to accomodate the bond length demands of the metal) such that the observed hole sizes of the metal complexes increase by only *ca.* 0.04-0.05 Å as the number of atoms increases.

The folding of the ligand to accomodate the demands of the metal results in a concomitant increase in ligand strain energy which may induce distortion of the coordination geometry about the metal. Thus, the observed hole sizes reflect a balance between the dictates of the metal ion versus that of the macrocyclic ligand. When the ligand contains a more rigid backbone, the capacity for radial expansion or contraction to accomodate the metal is compromised. This effect may result in metal-donor bond lengths which are compressed or stretched relative to their normal values[28].

1.3(c). Polyaza Macrocycles:

The tridentate, [9-12]aneN_3, macrocycles are too small to encircle a metal ion and thus coordinate facially to the metal ion (below), as opposed to the corresponding open-chain ligands which can adopt either a facial or meridional geometry.

The [12-16]aneN_4 series of tetradentate macrocycles can enircle the plane of the metal ion thereby adopting a *trans*-planar geometry. However, the [12]aneN_4 macrocycle tends to bind in a *cis*-octahedral geometry[29] (with two co-ligands), while the [13]aneN_4

macrocycle tends to yield square pyramidal geometries[30] (especially for larger metals) due to their smaller ring sizes.

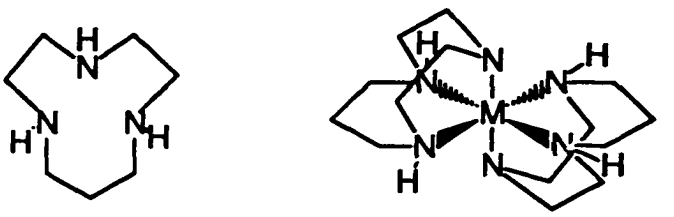

The 14-membered macrocycle, 1,4,8,11-tetraazacyclotetradecane (cyclam), has been studied extensively because it is large enough to encircle a range of metal ions and has sufficient flexibility to expand or contract to accomodate different sized metals[8,9].

Coordinated polyamine ligands exhibit stereochemistry at the nitrogen centers since the metal-nitrogen bond locks them into a certain chirality. The different possibilities for cyclam are illustrated in figure 1.5. The different combinations will have different overall strain energies because such energies depend significantly on the conformations of the individual chelated rings in the macrocycle.

Different ring configurations result in different conformations. For planar coordination, the lowest energy structure for 5-membered chelate rings is the gauche conformation (carbon atoms equally displaced on opposite sides of the MN_2 plane), while the lowest energy structure for 6-membered chelate rings is the chair conformation (as occurs in cyclohexane). The trans-III configuration for cyclam (figure 1.5) is the only one which permits both 5-membered chelate rings to be gauche and both 6-membered rings to be chair. Molecular mechanics calculations[31] on the different configurations of $[Ni(II)cyclam]^{2+}$ confirm that the trans-III configuration has the lowest energy but suggest that the trans-I configuration is only slightly less stable (*ca.* 2.3 kcal/mole).

The involvement of configurational isomers has been postulated in mechanistic schemes of formation, substitution and isomerization[32]. Except for the case of Co(III), the

observation of configurational isomers is difficult. For the more labile metal ions, N-substitution of the ligand slows the process of isomerization thereby permitting the isolation of the thermodynamically less stable configurational isomers. Using this approach, Barefield and co-workers[33] isolated complexes of Ni(II) with the N,N',N'',N'''-tetramethylated cyclam ligand in both the trans-III and trans-I configurations. Moore and coworkers[32] showed that these two isomers equilibrate readily in donor solvents, presumably via an intermediate trans-II isomer. The trans-II isomer was detected by NMR.

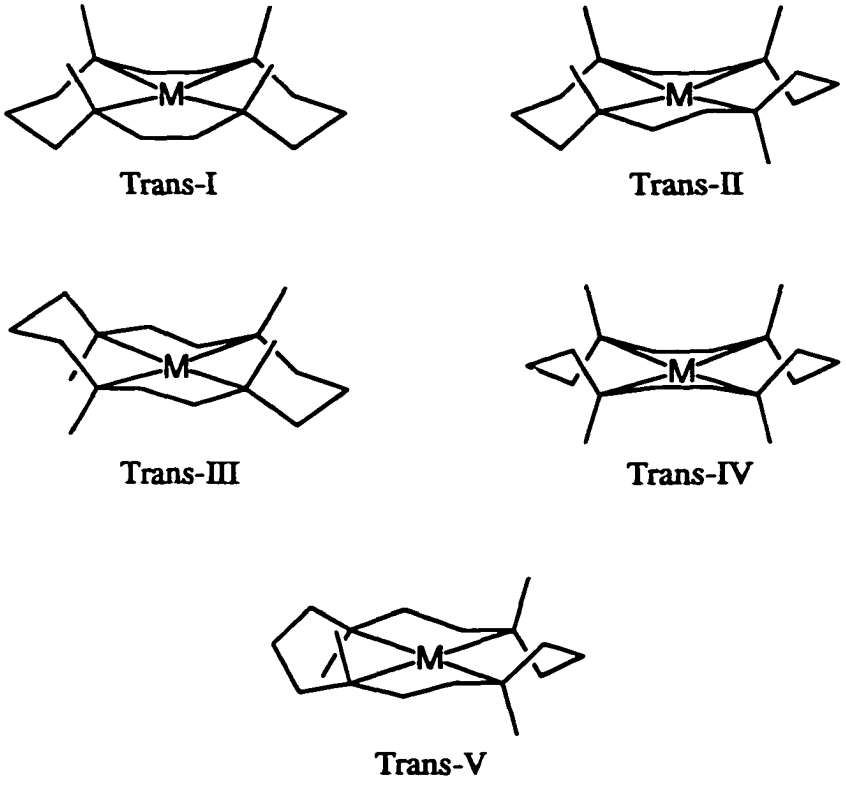

Figure 1.5. Trans-I to trans-V configurational isomers of coordinated [14]aneN$_4$ (cyclam).

New synthetic procedures have been developed which allow the synthesis of larger pentaaza and hexaaza macrocyclic rings. The series[34] of [15-16]aneN$_5$ macrocycles is potentially quinquedentate while those of the [18-20]aneN$_6$ series[35] are potentially sexidentate. These ligands generally have not been found to further stabilize octahedral complexes relative to the *bis*[9]aneN$_3$ complexes according to the macrocyclic effect. In fact, complexes with these ligands tend to be acid labile, unlike the tetraaza macrocyclic complexes. Presumably, the reason for this lack of stability is because the rings are too large too accomodate the metal effectively and protonation of the secondary amines is possible. These results underscore the need for the macrocyclic ligand to have a structure that is relatively "pre-oriented" appropriately for the intended coordination geometry.

1.3(d). Other Donors:

An important feature of macrocyclic ligands is the ability to systematically incorporate other donor atoms in place of the nitrogen donors. For example, the substitution of sulphurs in place of the nitrogens of the tetraaza macrocycles to produce the [13-15]aneS$_4$ series results in stabilization of the copper(I) ion such that it can be readily studied[36].

Macrocyclic ligands containing phosphorous and arsenic donors have been prepared as well, however, such chemistry has been much less explored[8,9].

1.3(e). Stabilization of Less Common Oxidation States:

The ability of cyclic ligands to stabilize less common oxidation states of a coordinated metal has been well-documumented.[37] For example, both the high-spin and low-spin nickel(II) complexes of cyclam are more readily oxidized to nickel(III) species

than are the corresponding open-chain complexes. Unlike the open-chain complexes, macrocyclic complexes of the nickel(III) ion have been shown to persist long enough to permit spectroscopic and kinetic investigations[38]. Oxidations have been achieved by chemical, electrochemical, pulse radiolysis and flash photolysis techniques. Although unusual oxidation states of many metals have been stabilized by macrocyclic ligands, the majority of studies have focussed on nickel and copper.

An investigation[39] of the factors influencing the electrochemical behaviour of twenty-seven nickel(II) complexes of tetraaza macrocycles has demonstrated that the redox properties of a given system are affected by the ring size, charge on the ligand, the nature of the ligand substituents and the degree of ligand unsaturation. An empirical partitioning of the electronic and structural factors was found to be possible. Overall, for square planar complexes of nickel(II), a potential range spanning almost two volts has been observed.

It has been found[37] that there is not necessarily a direct correlation between the redox potentials and ring size and that, for the [13-15]aneN_4 macrocycles, it is the 14-membered cyclam ring which most favours the nickel(III) oxidation state. The degree of ring strain was found to influence the redox behaviour. It was also proposed that the stronger the in-plane ligand field, the more readily oxidation to nickel(III) occurs. This behaviour appears to reflect the raising of the d_{x2-y2} orbital by strong equatorial interactions such that the electron is more easily removed from the nickel(II) precursor. These results imply that cyclam has the strongest equatorial interaction of the series.

1.3(f). Kinetic Aspects:

Inorganic reactions can be classified into two general catagories, substitution reactions and electron transfer (redox) reactions.

Substitution Reactions:

In substitution reactions, one or more of the coordinating ligands is substituted by an initially unbound ligand. The intermediate metal complex can have a dissociated (D) transition state of lower coordination number, or an associative (A) transition state of higher coordination number. In most cases, the reaction has no chemically significant intermediate and is referred to as an interchange (I_D or I_A) mechanism. The "D" and "A" subscripts then refer to the relative degree of bond-breaking versus bond-forming in the transition state. The details of substitution mechanisms are beyond the scope of this introduction and the reader is referred to recent reviews[40-43] presented in the literature.

The mechanism of a substitution reaction is largely determined by the electronic configuration of the metal center. A given d-electron configuration will have a preferred coordination number and geometry in both the ground and transition states, depending on the Crystal Field Stabilization Energy[43] (CFSE) for that state. This effect tends to be the controlling influence on the nature of the transition state, however, changes in effective charge and size of the metal center, the structure of the reacting and unreacting ligands, and the reaction conditions can also have significant effects on the reaction mechanism.

Investigations of the substitution kinetics of macrocyclic complexes have made considerable contributions[44] to the mechanistic understanding of such reactions. Equatorial coordination of a metal by a cyclic tetradentate ligand results in complexes with properties that are significantly different than that observed in complexes of the corresponding monodentate or linear polydentate ligands. An important difference is that the equatorial cyclic ligand is inert to substitution (macrocyclic effect) such that substitution is

constrained to the axial coordination sites of the metal center. This effect serves to simplify the kinetic expressions involved.

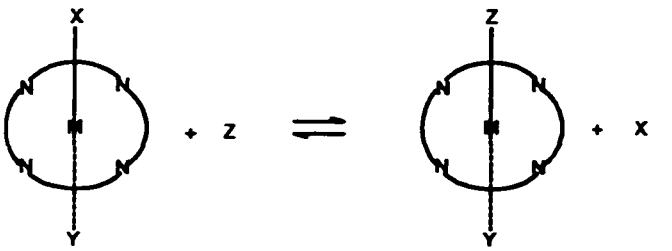

Figure 1.6. Axial substitution in *trans* $[Co(N_4)XY]^{n+}$ complexes.

For most macrocyclic complexes, the substitution proceeds without an accompanying stereochemical change as shown in figure 1.6.

The majority of substitution reactions studied to date have been of cobalt(III) complexes. This is because, of the first row transition metals, only the chromium(III)/d^3 and cobalt(III)/d^6 ions are of sufficient kinetic inertness to allow direct investigations. The data obtained from the reactions of the type shown in figure 1.6 can be used to determine the relative *trans*-directing influence of the the axial ligand, Y, and the labilizing influence of the equatorial (N_4) ligands ("*cis*-effect"). With synthetic macrocyclic ligands, the hope is to isolate the ligand features that most affect lability.

It should also be noted that the ability of the tetradentate macrocyclic ligands to stabilize unusual oxidation states of certain metals can be exploited to allow investigation of its substitution reactions. For example, nickel(III) has a d^7 electron configuration. It is of interest[45] to see how this configuration affects the substitution mechanism. The high effective charge on the nickel(III) center should favour an I_A mechanism, however, weakening of the axial bond via the Jahn Teller effect is expected to favour an I_D mechanism.

Electron Transfer Reactions:

Electron transfer reactions[43,46] are classified into two general categories, inner-sphere and outer-sphere. Inner-sphere electron transfers are those in which formation of the transition state involves a substitution reaction on one of the metal centers such that the two reactants are bridged by one (inner-sphere) ligand. Electron transfer occurs after this step. When the inner coordination spheres of the two participating reactants remain intact, the electron transfer process is referred to as outer-sphere. For macrocyclic complexes, the ligand is inert with respect to dissociation such that electron transfers are frequently outer-sphere. Outer-sphere reactions are also more simple overall, and therefore easier to study theoretically.

The simplest reactions in solution chemistry are electron self-exchange reactions in which the reactants and products are identical:

$$*A_{ox} + A_{red} \Rightarrow *A_{red} + A_{ox}$$

The usual way to establish chemically that a reaction has taken place is to introduce an isotopic label. There is no change in free energy ($\Delta G^\circ = 0$) for this type of reaction. The self-exchange rate provides an assessment of the activation barrier to electron transfer for a given complex. The experimental measurement of self-exchange rates is complex and frequently only results in order-of-magnitude estimates of the rate constant. Direct measurements of the self-exchange rates are obtained by NMR line-broadening or temperature-jump techniques.

Much more common are cross-reactions wherein the two reactants are different species:

$$A_{ox} + B_{red} \Rightarrow A_{red} + B_{ox}$$

For these reactions, ΔG° is not equal to zero. The experimental measurement of cross-reaction rates is generally more straightforward than that of self-exchange reactions.

The changes in oxidation states of the donor and acceptor centers result in a change in their equilibrium nuclear configurations. This process involves geometric changes, the magnitudes of which vary according to the nature of the ligand. In addition, changes in the interactions of the donor and acceptor with the surrounding solvent will occur.

The Franck-Condon principle[46] states that, during an electronic transition, the electronic motion is so rapid that the nuclei (including the ligands and solvent molecules) do not have time to move. Hence, electron transfer occurs at a fixed nuclear configuration. In a self-exchange reaction, the energies of the donor and acceptor orbitals, and hence the bond lengths and angles of both donor and acceptor, must be the same before efficient electron transfer can take place. Incorporation of this restriction leads to partitioning[47] of an electron transfer reaction into reactant (precursor complex) and product (successor complex) configurations.

Marcus[48] pioneered the use of potential energy diagrams as an aid to describing electron transfer processes. In classical transition state theory, the expression for the rate constant of a bi-molecular reaction in solution is

$$k = \kappa \nu_n \exp(-\Delta G^*/RT),$$

where ν_n, the nuclear frequency factor, is approximately 10^{11} M^{-1} s^{-1} for small molecules and ΔG^* is the Gibbs free-energy difference between the activated complex and the

precursor complex. The transmission coefficient, κ, is usually assumed to be unity. Thus, the problem of calculating the rate constant requires the calculation of ΔG^*, which Marcus partitioned into several parameters:

$$\Delta G^* = w^r + (\lambda/4)(1 + \Delta G^{o\prime}/\lambda)^2,$$

$$\Delta G^{o\prime} = \Delta G^o + w^p - w^r.$$

Here, w^r is the electrostatic work involved in bringing the two reactants to the mean reactant separation distance in the activated complex, and w^p is the analogous work term for dissociation of the products. ΔG^o is the Gibbs free-energy change when the two reactants are an infinite distance apart, and $\Delta G^{o\prime}$ is the Gibbs free-energy of the reaction when the reactants are a distance r apart in the medium. The quantity $-\Delta G^o$ is called the "driving force" of the reaction.

The reorganization energy, λ, is a parameter that contains both inner-sphere (λ_i) and outer-sphere (λ_o) components; $\lambda = \lambda_i + \lambda_o$. The inner-sphere reorganization energy is the free energy change associated with changes in the bond lengths and angles of the reactants.

The biological electron transfer proteins (e.g. cytochromes, blue copper proteins) have rate constants[49] which are several orders of magnitude greater than the corresponding inorganic metal complexes (see table 1.3). It has been proposed[50] that the metal-donor bond lengths are held rigidly at bond lengths which are intermediate between the preferences of the oxidized and reduced forms of the metal involved. Williams[50] has used the term "entatic state" to describe this phenomenon.

Table 1.3. Self-exchange rates of blue copper proteins. Data obtained from ref. 49.

Reduction potentials and self-exchange rate constants for inorganic reagents.

Reagent	E° (V *vs.* NHE)	k_{22} /M^{-1} s^{-1}
$Fe(EDTA)^{-/2-}$	0.12	6.9×10^4
$Co(phen)_3^{3+/2+}$	0.37	9.8×10^1

Reactions of blue copper proteins with inorganic reagents.

Protein	Reagent	k_{12} (obs)[a]	ΔE_{12}° /V	k_{11} (obs)[a]	k_{11} (calc)[a]
Stellacyanin	$Fe(EDTA)^{2-}$	4.3×10^5	0.064	1.2×10^5	2.3×10^5
	$Co(phen)_3^{3+}$	1.8×10^5	0.186	1.2×10^5	1.6×10^5
	$Ru(NH_3)_5py^{3+}$	1.94×10^5	0.069	1.2×10^5	3.3×10^5
Plastocyanin	$Fe(EDTA)^{2-}$	1.72×10^5	0.235	$\sim 10^3$-10^4	7.3×10^1
	$Co(phen)_3^{3+}$	1.2×10^3	0.009	$\sim 10^3$-10^4	1.1×10^4
	$Ru(NH_3)_5py^{3+}$	3.88×10^3	-0.100	$\sim 10^3$-10^4	4.9×10^4
Azurin	$Fe(EDTA)^{2-}$	1.39×10^3	0.184	2.4×10^6	2.8×10^{-2}
	$Co(phen)_3^{3+}$	2.82×10^3	0.064	2.4×10^6	7.0×10^3
	$Ru(NH_3)_5py^{3+}$	1.36×10^3	-0.058	2.4×10^6	1.1×10^3

[a]The rate constants, in M^{-1} s^{-1}, refer to the following electron-transfers:

k_{12} = rate of cross reaction: $A_1(ox) + A_2(red) \rightarrow A_1(red) + A_2(ox)$

k_{11} = self-exchange for A_1: $A_1(ox) + A_1(red) \rightarrow A_1(red) + A_1(ox)$

k_{22} = self-exchange for A_2: $A_2(ox) + A_2(red) \rightarrow A_2(red) + A_2(ox)$

1.3(g). Applications of Macrocyclic Complexes:

In recent years, a broad range of applications of macrocyclic complexes has been studied[51,52]. For example, of continuing interest is the result that metal complexes with cyclam have been shown to act as catalysts[53] for H_2O and CO_2 reduction. In nature, it has been shown that methanogenic bacteria require a nickel tetrapyrrole as one of six coenzymes in methanogenesis[54] (anaerobic reduction of CO_2 to CH_4). Several synthetic nickel and cobalt tetraaza macrocyclic complexes[55], including porphyrins and phthalocyanines, have been investigated and shown to function as electrocatalysts for the reduction of CO_2 in aqueous or mixed solvents at potentials between *ca.* -1.1 and -1.5 V *vs.* n.h.e. In such systems, CO is the major product; however, the selectivity for reduction of CO_2 versus that of H_2O is usually not very high resulting in low CO/H_2 ratios.

In contrast, Beley *et al*[56] achieved excellent results for the electrochemical reduction of CO_2 to CO in aqueous solution, using $[Ni(cyclam)]^{2+}$ as a homogeneous catalyst. In this system, CO is produced with considerable selectivity ($CO/H_2 = 10^2 - 10^3$) with almost 100% current efficiency and turnover numbers (mols product per mol catalyst) of 100. The authors suggested that the large selectivity is related to the macrocyclic ring size and the presence of NH groups.

Creutz and co-workers[57] have shown that the cobalt(I) complex of the Curtis tetraaza-diene macrocycle has similar electroreduction properties, and have characterized the interaction of CO_2 with the complex in water and acetonitrile solutions.

The synthesis of polycyclic frameworks via intramolecular cyclizations is an important methodology in organic chemistry[58]. Reductive cyclizations of *ortho*-substituted aromatic rings (below) generally require the use of stoichiometric amounts of tin hydrides, Sm(II) species or other reducing agents.

The electrochemical version of similar intramolecular processes has been studied in only a few cases[59] in the presence of nickel or cobalt complexes as catalysts. The non-

catalyzed electrochemical reaction of similar substrates mainly affords protodehalogenation and isomerization of the double bond, with no cyclization.

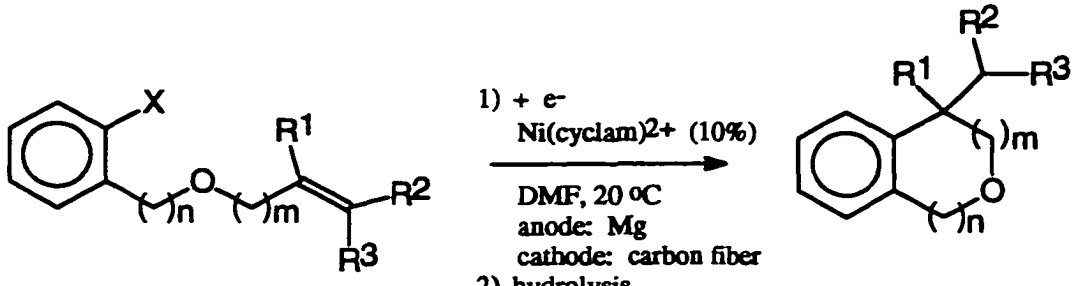

X = Cl, Br, I
n = 0, 1
m = 1, 2

R^1, R^2 = H, Me
R^3 = H, Me, alkyl, homoallyl

It has recently been shown[60] that reaction of the allyl *ortho*-halophenyl ether shown above depends very strongly on the nature of the ligand when using nickel complexes as the catalyst. When $[Ni\{bipy)_3]^{2+}$ is used as the catalyst, cleavage of the oxygen-allyl carbon bond, along with protodehalogenation occurred. However, when $[Ni(cyclam)]^{2+}$ is used as the catalyst, the same substrate undergoes cyclization.

1.4. Goals of the Present Study:

As mentioned in section 1.3(c), extension of the tetraaza macrocyclic rings to include additional donors does not necessarily lead to the intended octahedral coordination. Furthermore, complexes of the larger rings do not possess a significant macrocyclic effect because the ligand is not preoriented for octahedral coordination.

Macrobicyclic ligands, however, are suitably preoriented for axial coordination in addition to the equatorial coordination. The macrobicyclic polyethers synthesized by Lehn and co-workers[61] form "cryptate" complexes and have been shown to possess considerably enhanced thermodynamic stability relative to their monocyclic analogues. For example, the potassium complex of the cryptand 2.2.2 (structure 3 in table 1.4) shows an approximate

10^5-fold increase in stability relative to the corresponding pendant-armed monocyclic analogue (structure 2 in table 1.4). This enhanced stability was named the "cryptate effect", as an extension of the macrocyclic effect into three dimensions. As with the macrocyclic effect, the thermodynamic origin of the cryptate effect is difficult to determine. Thermodynamic data[62] suggest that the enthalpic terms are responsible.

	logK with metal ion				
Ligand	Na^+	K^+	Ca^{2+}	Sr^{2+}	Ba^{2+}
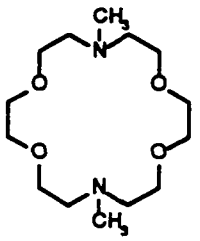	3.26	4.38	4.4	6.1	6.7
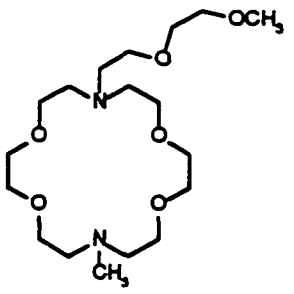	3.35	4.80			
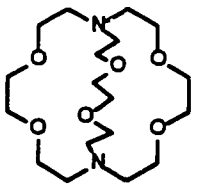	7.21	9.75	7.60	11.5	12

Table 1.4. Formation constants of Lehn's[61] macrobicyclic polyether cryptand (1) with alkali metals as compared to that of analogous monocyclic and pendant arm macrocycles.

In this laboratory, a template synthesis of the novel cyclam-based macrobicyclic ligand 15-thia-1,5,8,11-tetraazabicyclo[10.5.2]nonadecane (below) has been achieved[90]. Whereas the polyether macrobicycles are suitable for complexation of alkali metals, this thia-polyaza system is suitable for the coordination of transition metal ions.

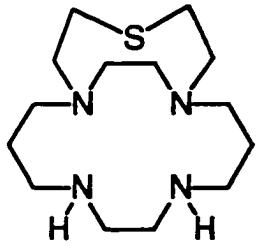

[9]aneN$_4$S macrobicycle (L1)

In addition to the possibility of a cryptate effect, the coordination of transition metals with this macrobicyclic ligand allows the study of the classical "trans-effect"[43] in axial substitution reactions within the context of a macrocyclic ligand system. Syntheses[63] of the corresponding 15-aza and 15-oxo analogues then allows comparison of the effects of different axial donors.

There are both biological and chemical motivations for studying thioether donors[64]. The observation of methionine thioether coordination in the blue copper proteins[65] and in nickel-containing methanogenic bacterial enzymes[66] has generated speculation that the unusual optical, redox and EPR properties of these proteins originate from the Cu-thioether interaction.

Irrespective of the possible biological relevance, the use of macrocyclic ligands to facilitate coordination of thioethers is of considerable interest because simple acyclic thioethers bind metal ions only very weakly[67]. Their relatively low σ-donor and π-acceptor abilities, combined with the steric encumbrance of the alkyl groups, makes homoleptic complexes of thioethers (e.g. Me_2S) virtually impossible to prepare. The framework of a

macrocyclic ligand, however, can induce the sulphur to remain coordinated to the metal center. For example, the homoleptic *bis*-[9]aneS_3 and [18]aneS_6 complexes of nickel(II) have unusually short Ni-S bond distances[68]. The average bond distances are 2.38Å which is 0.06Å shorter than than the sum of the atomic radii. It should be noted that a 0.06Å compression is equivalent to an external pressure of thousands of atmospheres[64].

There is also considerable interest in the electronic consequences of thioether coordination, such as the potential for moderate π-acidity (in analogy with phosphine ligands). This effect is expected to be responsible for the observed stabilization of lower oxidation states, as in copper(I), which has been observed in polythiaether macrocyclic complexes.[69]

There are two general ligand features which influence the chemistry of the resulting metal complexes, namely the electronic nature of the donors involved and the structural features of the ligand. Varying the nature of the donor gives insight into the electronic consequences of coordination of each donor. However, it is also of interest to vary the ligand structure systematically (while keeping the nature of the donors constant) in order to gain insight into the effects of such properties as ligand field strength and ligand rigidity. Most macrocylic complexes reported to date are not directly comparable with each other because the ligands differ both in the nature of the donors and in the structure of the ligand. Hence, it is difficult or impossible to determine the effects of these two influences separately. In this respect, it can be said that these studies lack "proper" scientific controls wherein only one feature is varied at a time.

A systematic variation of ligand structure for the tetraaza macrocyles, wherein the nature of the donors remains as similar as possible, has been reported by Busch.[70] This study involved comparison of the effects of the [12-16]aneN_4 series of macrocycles. The ligand field strengths of the series of nickel(II) complexes were determined by analysis of the electronic spectra using the ligand field model. The quantity Dq^{xy}, which is a measure of the equatorial ligand field strength provided by the tetraaza ring, was found to vary strongly with ring size (with the axial ligands remaining identical). This result provided

compelling evidence that a constant ligand set (e.g. N_4Cl_2 in this case) does not yield a constant ligand field strength. The Dq^{xy} value (see table 1.5) of [14]aneN_4 (cyclam) shows that the ligand field induced by this ligand is unusually high (1480 cm^{-1}) relative to that expected (1200 cm^{-1}) for similar donors in analogous acyclic ligands. This result was interpreted as an indication that the natural macrocyclic hole-size of cyclam is smaller than the optimum value for nickel(II) coordination. Conversely, the Dq^{xy} value for [15]aneN_4 is 1242 cm^{-1}, which is very close to the expected value of 1200 cm^{-1}. This result was interpreted as an indication that the natural hole-size of the 15-membered tetraaza macrocycle is closely matched to the requirements (i.e. optimum bond lengths) of the nickel(II) center.

Table 1.5. Ligand field values for the [Ni([14-16]aneN_4)$(X)_2$] series of complexes (data obtained from reference 70). Dq^{xy} and Dq^{z} values are defined in figure 5.4.

Complex	Dq^{xy} /cm^{-1}	Dq^{z} /cm^{-1}
Ni([15]aneN_4)Br_2	1283	452
Ni([14]aneN_4)Cl_2	1480	379
Ni([15]aneN_4)Cl_2	1242	589
Ni([16]aneN_4)Cl_2	1116	510
Ni([15]aneN_4)$(N_3)_2$	1227	764
Ni([15]aneN_4)$(NCS)_2$	1202	908

The same study was applied to the cobalt(III) complexes and the resulting data are presented in table 1.6. In the case of cobalt(III), the "normal" value of Dq^{xy} expected in the absence of structural effects is 2530 cm^{-1}. It can be seen that the Dq^{xy} value of the [14]aneN_4 complex matches the closest. This result was interpreted to indicate that the natural hole-size of [14]aneN_4 matches the shorter bond length requirements of cobalt(III) best. It is necessary to point out that these results do not imply that the actual bond lengths of these complexes vary significantly with ring size. It does, however, mean that,

even if the bond lengths are similar for each complex, the relative amount of strain energy in the macrocyclic ligand varies with ring size. The "ideal" ring size values shown in table 1.6 refer to the natural hole-size of the free ligand as calculated by molecular mechanics methods (with the four nitrogen donors constrained to remain square planar). The strain energy values reported in table 1.6 refer to the amount of strain calculated to develop in the macrocycle as it compresses or expands to accomodate the bond length requirements of the metal.

Table 1.6. Ligand field values for $[Co([13\text{-}16]aneN_4)(Cl)_2]^+$ series of complexes (data obtained from reference 70).

Ligand	Dq^{xy} /cm^{-1}	Ideal M-N Å	Strain Energy,[a] ΔH_f /kcal • mol^{-1}
[13]aneN$_4$	2750	2.01	19.7
[14]aneN$_4$	2562	2.13	11.5
[15]aneN$_4$	2303	2.28	21.3
[16]aneN$_4$	2249	2.42	35.6

[a]Calculated using MM2 parameters,[70] including the Co-N stretching force constant.

Busch then expanded the investigation and noted a linear correlation between the calculated ligand strain energies for the series of cobalt(III) complexes with the observed rates of aquation of the $[Co([13\text{-}16]aneN_4)(Cl)_2]^+$ complexes:

In the same way that Lehn's "cryptate effect" (discussed above) is an extension of the macrocyclic effect to the three dimensional coordination of alkali metals provided by the macrobicyclic cryptand complexes, it was of interest to extend Busch's correlations of ligand strain effects to macrobicyclic complexes of transition metals. This would require a

systematic variation of the macrobicyclic ligand structure while keeping the nature of the donor atoms as similar as possible. An ideal set of macrobicyclic ligands for this purpose would therefore be the following three structural isomers of the N_4S cyclam-based macrobicycle:

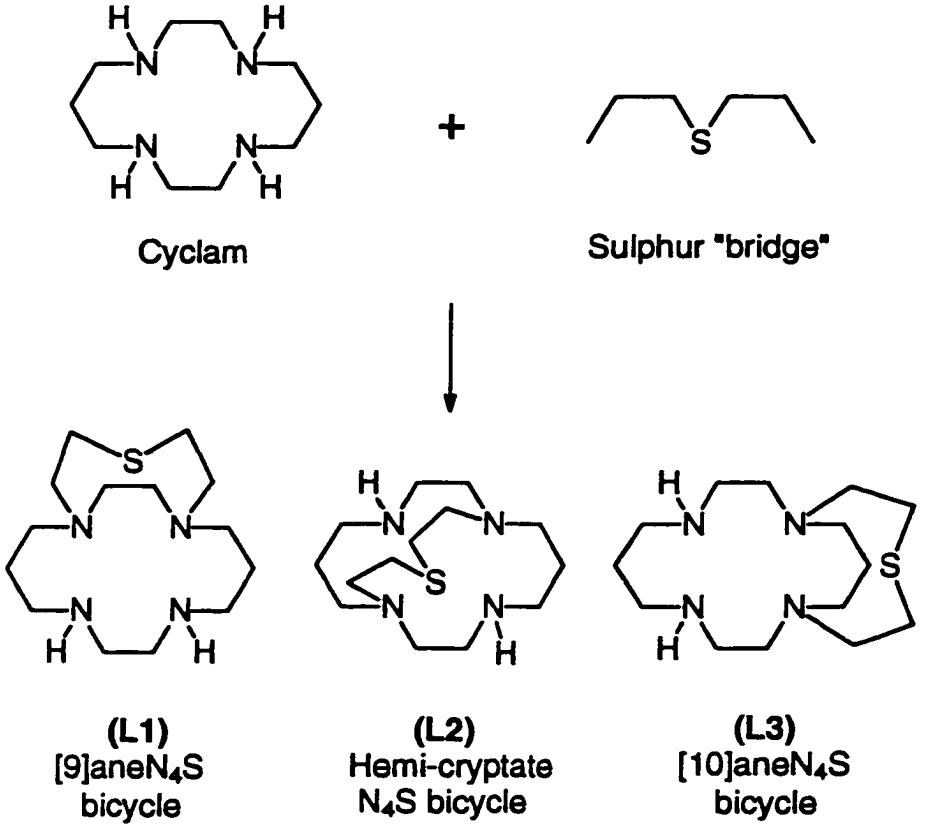

Figure 1.7. The three structural isomers of the N_4S macrobicyclic ligand series.

(L1) = 15-Thia-1,5,8,12-tetraazabicyclo[10.5.2]nonadecane

(L2) = 17-Thia-1,5,8,12-tetraazabicyclo[6.6.5]nonadecane

(L3) = 14-Thia-1,4,8,11-tetraazabicyclo[9.5.3]nonadecane

Each of these ligands contains a tetraaza cyclam ring (with two tertiary and two secondary N-donors) suitable for equatorial coordination and a CH_2-CH_2-S-CH_2-CH_2 "bridge" strapped across two of the nitrogens which is suitable for axial thioether coordination. The corresponding metal complexes are therefore each expected to consist of N_4S coordination environments which are identical with respect to the electronic nature of the donors, yet dissimilar with respect to ligand strain and, most likely, coordination geometry also. Any differences in the observed chemistries of the metal complexes could therefore be attributed to structural effects rather than donor effects.

A further advantage to the study of this series of macrobicycles relates to the arguments regarding structural effects made by Hancock[71]. Using available thermodynamic data on several series of chelate and macrocyclic complexes, Hancock has provided compelling evidence that the most significant source of the various structural effects of these ligands is derived from the number and size of the chelate rings presented by the ligand rather than the macrocyclic hole size (which reflects ring strain), as was favoured by Busch. It was pointed out that the [12-16]aneN_4 series of ligands studied by Busch involve successive increases in chelate ring sizes. For example, [14]aneN_4 contains two ethylenediamine 5-membered chelate rings and two propylenediamine 6-membered chelate rings, whereas [15]aneN_4 contains only one ethylenediamine chelate and three propylenediamine chelates. The structural features, and hence optimum bond lengths and angles, of 5-membered chelate rings differ significantly from that of the 6-membered chelate rings.

Unlike the series of [12-16]aneN_4 macrocycles, the three N_4S macrobicyclic ligands of the present study are structural isomers of each other such that the number and size of the chelate rings presented to the metal remain constant for each ligand. Thus, any observed differences in the resulting metal complexes can not be caused by variation of chelate ring size.

CHAPTER 2

Synthesis, Isolation and Characterization of N_4S Donor Macrobicyclic Ligands.

2.1. Introduction:

The primary objective of this project was the preparation of macrobicyclic, pentacoordinate ligand systems for the purpose of binding d-block metal ions. Specifically, the target structures consist of the 14-membered, tetraazamacrocycle, cyclam, (1,4,8,11-tetraazacyclotetradecane)[72] with a diethyl sulphide fragment bridged across two of the cyclam nitrogens. There are three ways of connecting such a bridge across two cyclam nitrogens, leading two three structurally isomeric macrobicycles:

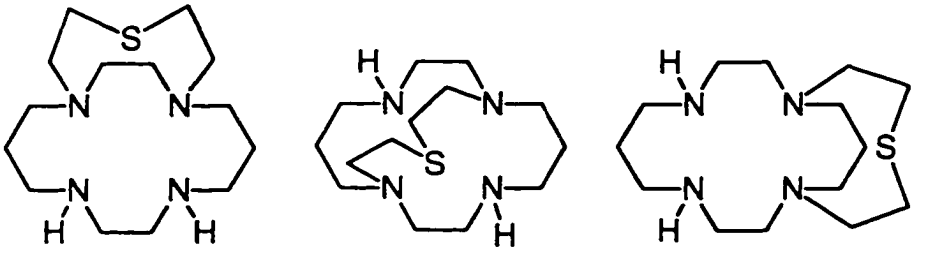

Figure 2.1. The three structural isomers of the N_4S macrobicyclic ligand system. [9]aneN_4S bicycle = 15-Thia-1,5,8,12-tetraazabicyclo[10.5.2]nonadecane. Hemi-cryptateN_4S bicycle = 15-Thia-1,5,8,12-tetraazabicyclo[6.6.5]nonadecane. [10]aneN_4S bicycle = 14-Thia-1,4,8,11-tetraazabicyclo[9.5.3]nonadecane.

These ligand systems are ideally suited for complexation of transition metal ions because of their ability to coordinate the four nitrogens of the cyclam ring equatorially and the sulphur donor axially. The resulting metal complexes are considerably stable[90] such that they can be considered inert towards demetallation in acidic media. The various

reasons for studying their metal chemistry will be discussed in subsequent chapters where appropriate. This chapter presents the synthesis of the 9ane-N_4S (**L1**) and Hemi-cryptateN_4S (**L2**) structural isomers. The synthesis of the following side product (**4**), a mono-amido derivative of the 9ane-N_4S macrobicycle, and its metal complexes is also presented:

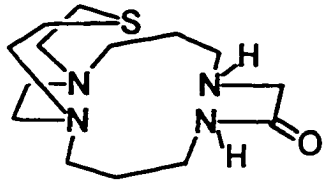

Figure 2.2. 15-Thia-1,5,8,12-tetraazabicyclo[10.5.2]nonadecane-5-one (**4**).

The various approaches to cyclization reactions can be divided into two general categories. The first of these, referred to as "direct methods", are those in which the cyclization proceeds as a conventional organic reaction. The second strategy is that of the "template" method in which the organic reactants are coordinated to a metal ion during the cyclization. Cyclization reactions generally require special circumstances or synthetic conditions in order to maximize the yield of cyclized product and, at the same time, inhibit the yield of competing linear polmerization reactions.

For direct methods, the general strategy for maximizing the yield of cyclized products is to perform the reaction under high dilution conditions. A typical high dilution reaction involves the reaction of two species which incorporate the required fragments for the target macrocycle, one of which contains nucleophiles on both ends of the fragment and another which contains complemetary electrophiles. The initial reaction of one of the nucleophiles with an electrophile of the other reactant leads to the "half condensed" intermediate depicted in Figure 2.3. This intermediate can either react

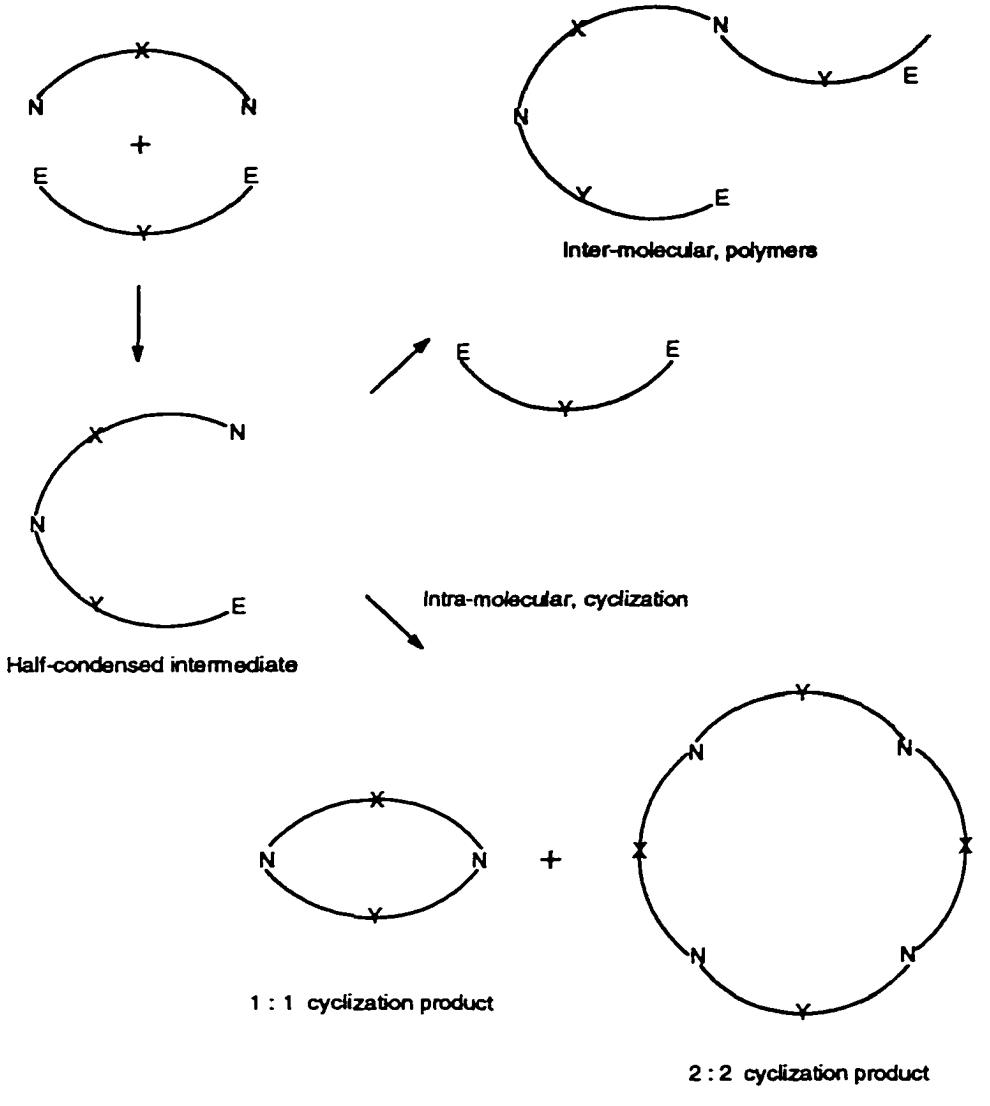

Figure 2.3. Generalized cyclization reaction and competing linear polymerization.

N = nucleophile, e.g. NH, O^-, S^-.

E = electrophile, e.g. Br, OTs, COCl.

X, Y = $-(CH_2)_n-Z-(CH_2)_m-$, Z = O, S, N-protected.

intramolecularly in a "head-to-tail" fashion to produce cyclized product(s), or it can react intermolecularly with other reactants to form polymer. By maintaining reaction conditions wherein both reagents are in high dilution, the intramolecular condensation is more favoured. This is because dilute conditions provide more time between intermolecular collisions, thereby providing a greater chance of cyclization of the half-condensed intermediate. High dilution conditions are achieved by special apparatus[73] designed to slowly dispense small, measured quantities of both reagents over long periods of time (hours to days) into the reaction vessel (see section 8.1(c) for details).

High dilution conditions are most useful for cyclizations in which the reactants are fast-reacting because intermolecular collisions are more likely to result in reaction. A good example of fast-reacting species is that of neutral primary and secondary amine nucleophiles reacting with neutral acid chloride electrophiles. Such reactivity was pioneered by Lehn and co-workers in the 1970's[74]. Another important early example of the success of high dilution techniques was the condensation of sodium thiolate nucleophiles with alkyl dibromide electrophiles. For example, Travis and Busch[75] reported that the yield of a [14]aneS$_4$ macrocycle was improved from 7.5% to 55% when high dilution conditions were used.

Conversely, for slowly reacting nucleophiles and electrophiles, the chance of a collision leading to reaction is lower such that the "extra time" provided by high dilution conditions is not as helpful. In fact, such slow-reactivity reactions make use of the alternative strategy to high dilution where, as in the case of amines and esters, both reagents are added together and reacted at normal concentrations for several days. Because the chance of a collision leading to reaction is low, the half-condensed intermediate will persist for long periods of time during which there will be as many or more chances to cyclize. Typically, reactions of this kind involving amines and esters in ethanol produce 20-40% cyclization yields, the rest forming polymer.[75]

Another significant development which allowed cyclizations to proceed in reasonable yields (up to 40-50% and sometimes better) at moderate to low dilution was

reported in 1974 by Richman and Atkins.[77] The Richman and Atkins reactivity consists of first tosylating the primary nitrogens of the nucleophile. The resulting tosyl amides are then deprotonated, usually with sodium hydride "in situ", and cyclization is achieved by the reaction of the appropriate tosylated alcohol. The improved cyclization yields are provided by the bulky tosyl groups. These groups reduce the number of conformational degrees of freedom, such as bond rotation, in the reactants and/or intermediates. Although not proven, it is believed that this effect is responsible for favouring cyclization relative to polmerization. The Richman-Atkins method has proven to be very effective and has found widespread use, particularly for syntheses of smaller nine to twelve membered rings, which are difficult to synthesize by other means.

An important concept pertinent to the success of macrocyclization reactions that has not yet been discussed is that of "pre-organization". In general, reactants and /or intermediates which have structural rigidity are referred to as pre-organized. Structural rigidity can be achieved by the presence of ring systems, π-bonding, or hydrogen bonding. The molecule need only be rigid on the time scale of the chemical reaction to be considered pre-organized.[78] An early example of such reactivity was provided by Ogawa, Yamaguchi and Gotoh[79], 1974. The authors found that the cyclization reaction involving the sterically rigid aromatic precursors shown in Figure 2.4 resulted in a greater than 90% yield despite the absence of high dilution conditions.

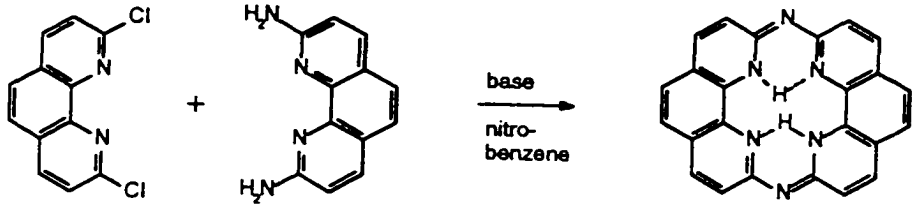

Figure 2.4. Cyclization to form a rigid aromatic macrocyle.[79]

A more recent example is provided by the work of Hunter et al.[80]. These workers observed a much higher cyclization yield when the 2,6-pyridyl derivative (Figure 2.5a) was used instead of the iso-phthaloyl derivative (Figure 2.5b). The authors attribute the increased yield to the presence of intramolecular hydrogen bonding between the pyridyl nitrogen lone pair and the amide protons of the 2,6-pyridyl reactant.

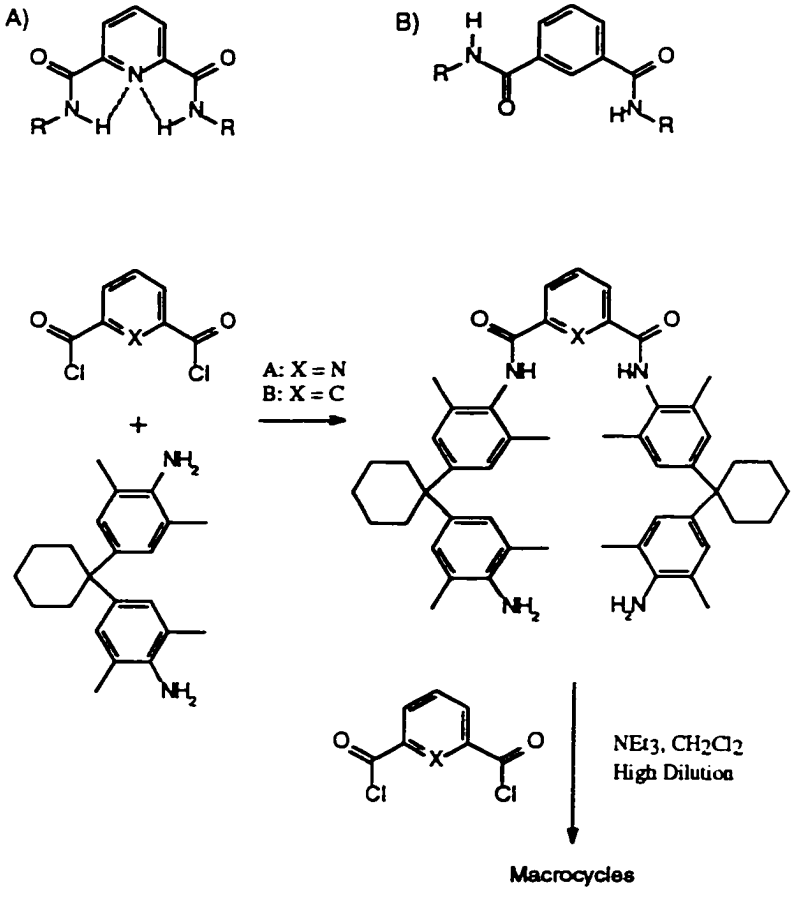

Figure 2.5. (a) Cyclization intermediate of a 2,6-pyridyl derivative with a benzyl diacid chloride. (b) Cyclization of an iso-phthaloyl derivative with a benzyl diacid chloride.[80]

Such hydrogen bonding "locks" the amides into the NH *cis* conformation in the half condensed intermediate such that it is favourably oriented for cyclization (Figure 2.6b). The iso-phthaloyl reactant has no such hydrogen bonding present and therefore adopts the lower energy *trans* conformation in the half-condensed intermediate (Figure 2.6a). Cyclization of this intermediate is much less likely to occur because the unreacted amine is oriented further away from the acid chloride.

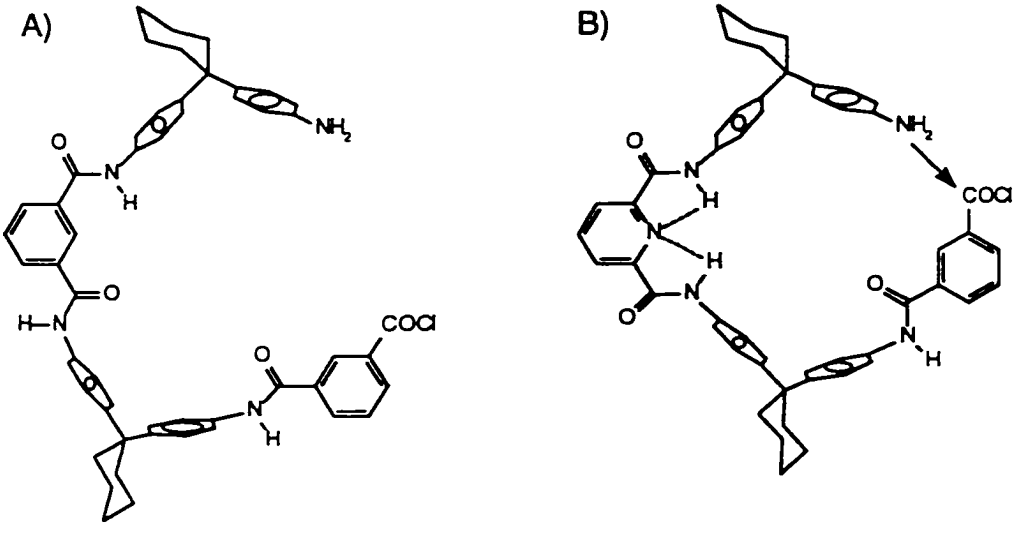

Figure 2.6. (a) Proposed[90] half-condensed intermediate in cyclization of the iso-phthaloyl derivative.

(b) Proposed[90] half-condensed intermediate in cyclization of the 2,6-pyridyl derivative.

Another important example of pre-orientation effects, pertinent to the syntheses described in chapter 3, has been reported by Bradshaw et al[81]. In this work, the desired polyaza macrocycles were prepared using *bis*(alpha-chloro) amides as the electrophiles, an example of which is shown in Figure 2.7. Although not nearly as rigid as the 2,6-pyridyl reactant just described, the presence of the rigid amides is sufficient to give reasonable (20-50%) cyclization yields. The authors refer to the preferred *cis* conformation of the *bis*(alpha chloro) amide reactant as "crab-like". The yields were also much greater when high dilution conditions were used. Another important feature of these reactions is that the presence of electron-withdrawing carbonyl carbons adjacent to the chloride substituted carbons, "activates" the chloride such that it is a much better leaving group than in a saturated alkyl chloride. This effect increases the reactivity which favours cyclization as well.

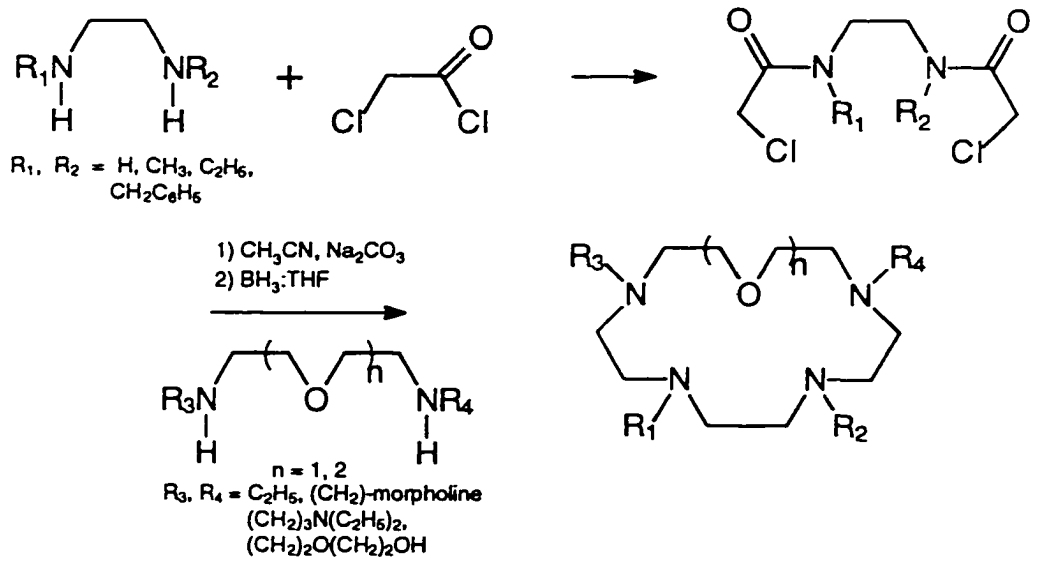

Figure 2.7. Formation of polyaza macrocyles using *bis*(alpha chloro) amides as the electrophilic reactants.[81]

The second class of macrocyclization reactions is referred to as "Template reactions". In these reactions, the cyclization is promoted by the presence of a metal ion. The template effect has been recognized for a long time. In fact, the first synthetic macrocycle[9] was obtained in 1928 as a side product from the reaction of phthalic anhydride with ammonia in an iron vessel. The dark blue side product was later shown to be an Fe(II) complex of the highly conjugated macrocycle phthalocyanine, which is very similar in structure to the naturally occurring porphyrin systems. There are many different classes of template reactions in the literature. For example, several reactions of dithiol nucleophile reactants with bis-alkyl bromides have been reported to give good yields of the cyclized products in the absence of high dilution conditions when the dithiol reactant is first coordinated to nickel(II). The presence of the metal ion "pre-organizes" the reactant(s) thereby facilitating cyclization and averting the need for high dilution conditions. Unlike the non-template reactions discussed above, the pre-organization, or conformational rigidity, is derived by the coordination of the metal center to the donor atoms of the reactants.

The most widely used class of template reactions are those involving coordination of linear tetradentate reactants to a metal ion, usually nickel(II). The reactant contains primary amine donor atoms at each end which are coordinated in a cis arrangement about the metal. The cyclization is then achieved by adding the appropriate electrophile, usually a dialdehyde which then reacts with the two primary amines. The template synthesis of the ubiquitous tetraazacyclotetradecane[82] (cyclam) is illustrative of such reactions. Syntheses of cyclam via direct methods gave low yields whereas the nickel(II) template method shown in figure 2.8 gave a yield in excess of 67%. If the metal is not present in this reaction, none of the cyclic product is obtained. The influence of the metal is considered to derive from both kinetic and thermodynamic factors[72] and has been discussed in great detail in the literature. The major disadvantage of templated cyclizations relative to the analogous direct methods is that the products obtained are determined by the chemistry of the metal and therefore the product may often differ

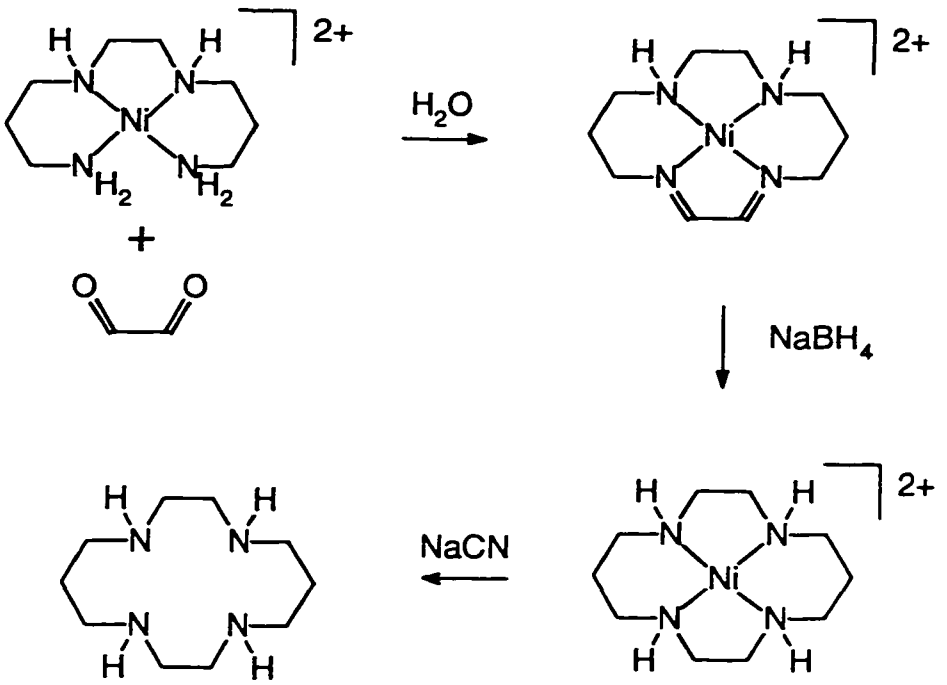

Figure 2.8. Synthesis of cyclam via nickel(II) templated reaction.[82]

significantly from the intended target macrocycle.

The preceding discussion presented only a few of the large number of macrocyclization reactions reported to date, and serves only to illustrate the various strategies involved. Each of the general strategies discussed has been used in the syntheses reported in this work. Much more comprehensive reviews of macrocyclization reactions are presented in references 83 and 84.

2.2. Synthesis of [9]aneN$_2$S (8):

The synthesis of [9]aneN$_2$S was first reported by Hancock[85] using the Richman and Atkins methodology shown in scheme 2.1. With respect to cost, route (a) was more attractive owing to the great expense of the bis-(2-aminoethyl) sulphide (**5a**) reagent required by route (b). However, the ditosylated thiodiglycol starting material required by route (a) proved to be very unstable to hydrolysis such that route (b) had to be followed.

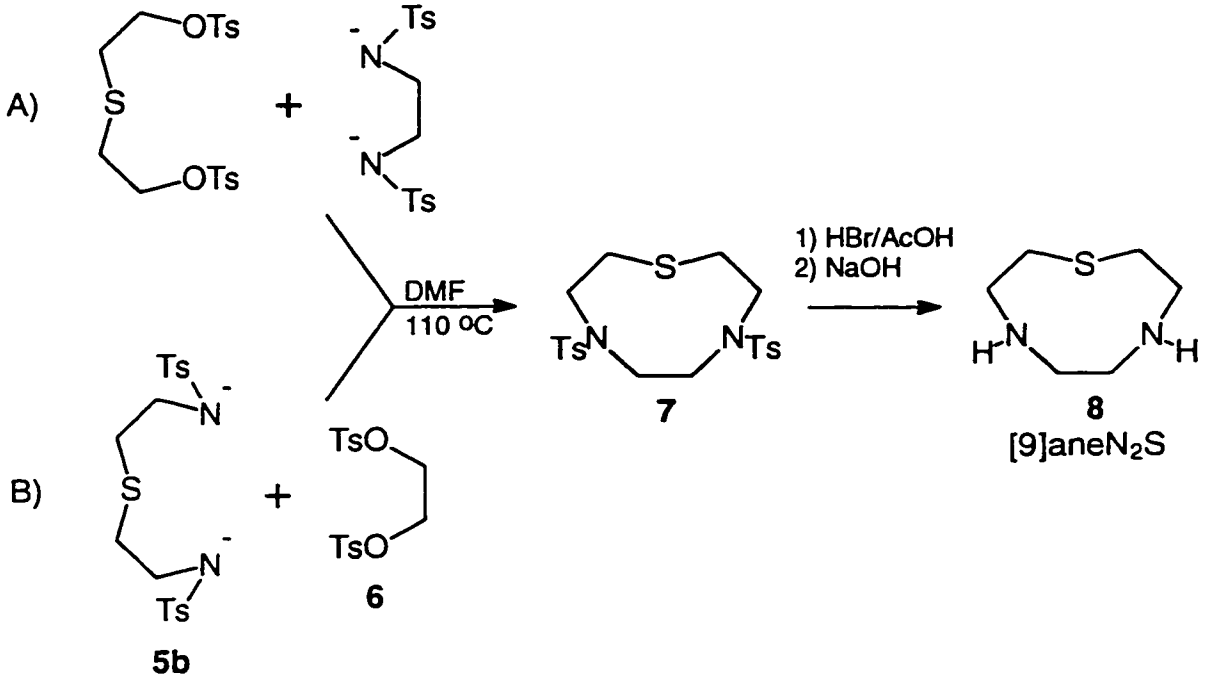

Scheme 2.1. Synthesis of [9]aneN$_2$S using the Richman and Atkins methodology.[85]

In order to avoid the high cost of commercially available **5a**, a novel synthetic route was developed, leading to the target ligand **8**. This synthetic route involves the reaction of two equivalents of tosylaziridine with sodium sulphide:

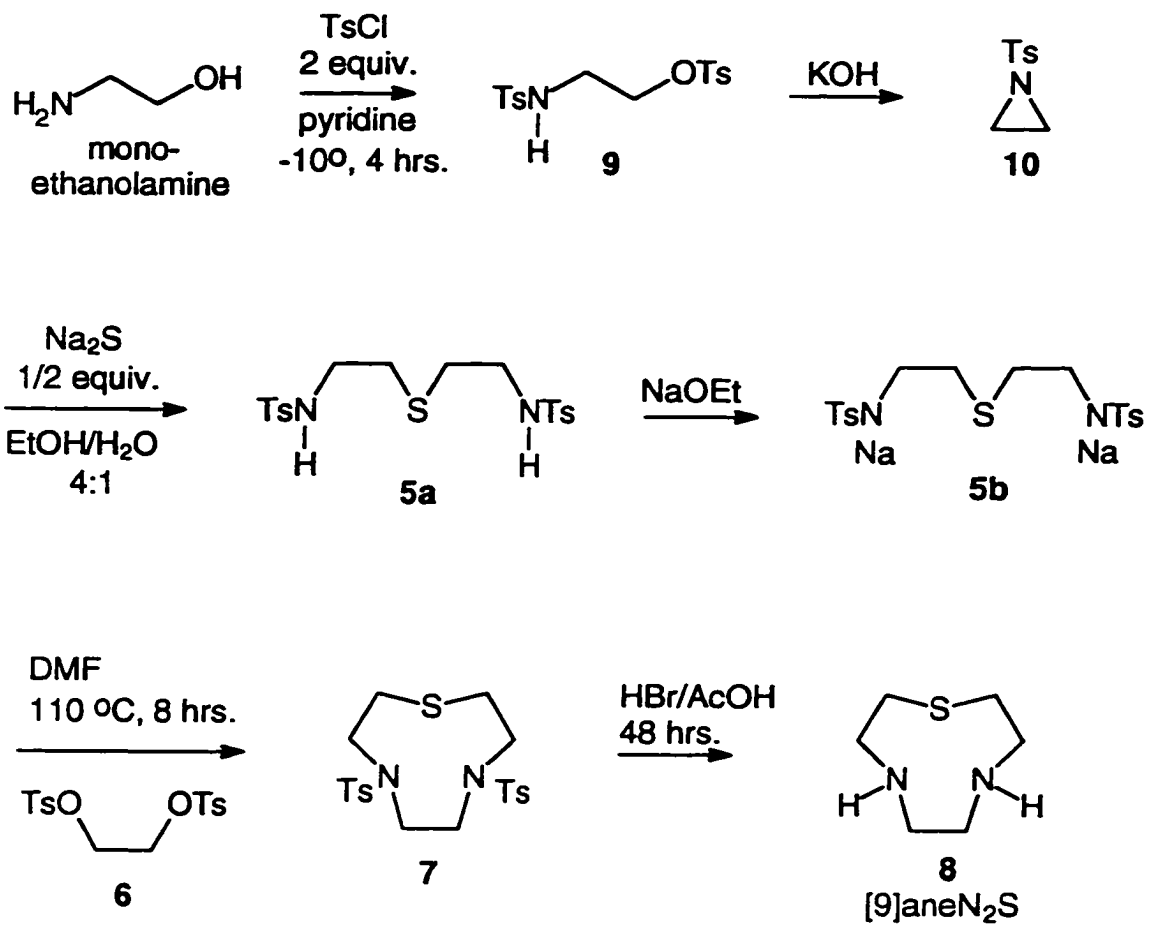

Scheme 2.2. Synthetic strategy for the preparation of [9]aneN$_2$S (**8**).

The synthetic procedure used to make tosylaziridine was an adaptation of the method reported by Wagnon and Jackels.[86]

2.3. Synthesis of [9]aneN$_4$S bicycle (L1):

15-Thia-1,5,8,12-tetraazabicyclo[10.5.2]nonadecane (L1). Ligand **L1** was first synthesized on a small scale by Fortier and McAuley[90] via the synthetic route shown in scheme 2.3. The uncyclized N_4S ligand **(12)** was produced by a Michael addition of 2-cyanoethyl arms onto each of the two secondary nitrogens of the precursor [9]aneN$_2$S, followed by reduction of the cyano groups with diborane. The final cyclization of the resulting primary amines was then achieved by a copper(II) templated Schiff base condensation with glyoxal. Usually without any work-up, sodium borohydride was added in situ to reduce the imino groups formed in the cyclization. Pure [Cu([9]aneN$_4$S)](ClO$_4$)$_2$ was then obtained by cation-exchange chromatography (Sephadex CM C-25 exchange packing from Aldrich) with 0.1M $NaClO_4$ as eulent. The copper was removed by refluxing for several hours with sodium sulphide in water. The CuS precipitate was removed by filtration or centrifugation. That sulphide was required to remove the copper is a testament to the stability of these complexes. The $NaClO_4$ and Na_2S contaminants were removed by addition of NaOH (pH > 14) and extraction of the free ligand **L1** into dichloromethane. This procedure was followed in this with work without any significant modifications. In the present study, the synthetic yield of **12** was 50% from **7** and the yield of **L1** was 50% - 60 % from **12.** The IR and ^{13}C-NMR spectra are shown in figure 2.9.

It is worthy to note that this successful glyoxal condensation promoted by copper(II), gave only uncharacterizable, brown polymeric material when first attempted[90] with nickel(II) as the templating metal. This is unusual because there are no other reports of successful copper(II) templated glyoxal condensations in the literature. For example, Barefield et al[91] were unable to prepare copper(II) cyclam by glyoxal condensation because of copper metal precipitation in the borohydride reduction step.

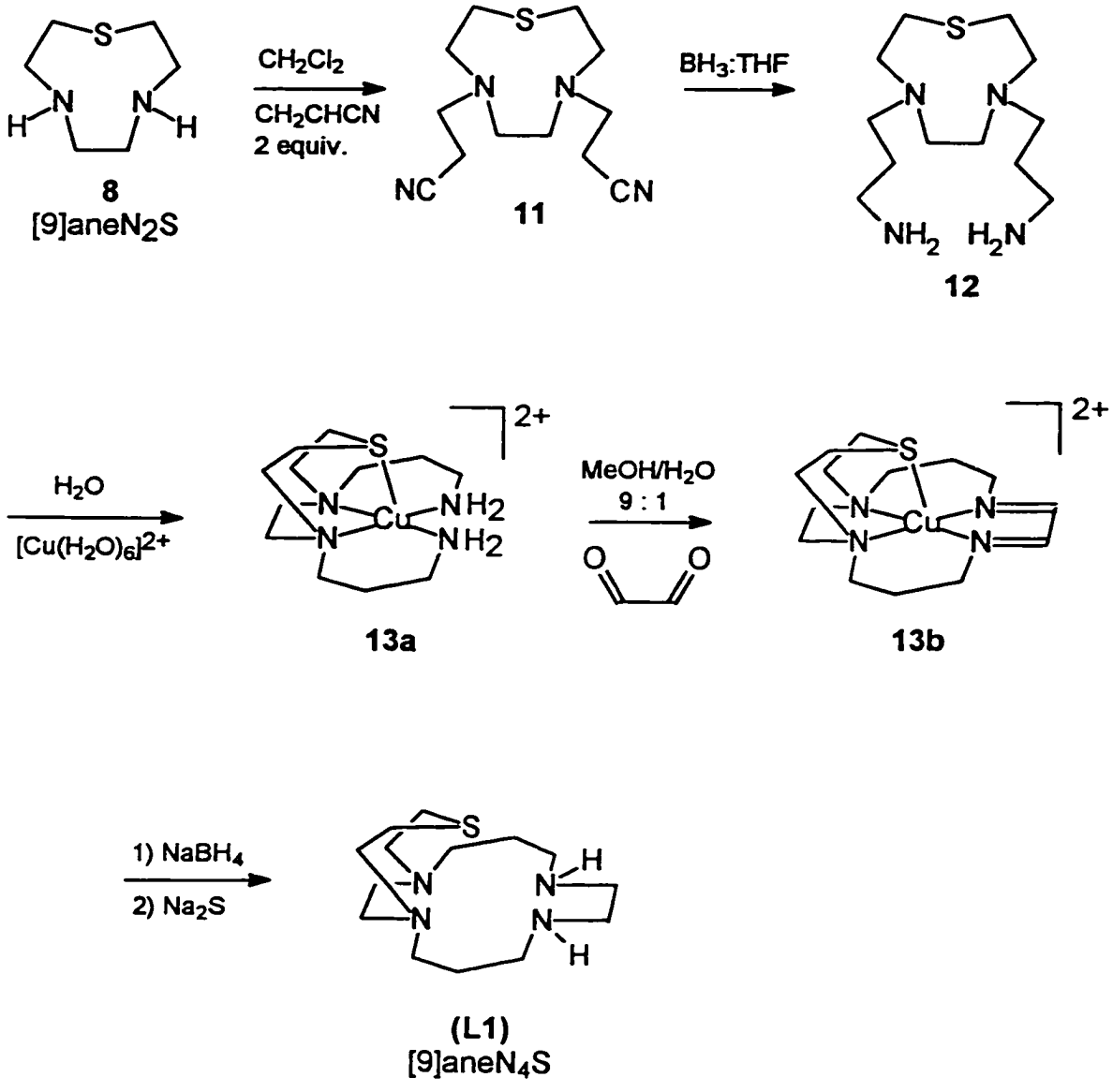

Scheme 2.3. Synthetic route to [9]aneN$_4$S bicycle (**L1**) via copper(II) template condensation. [90]

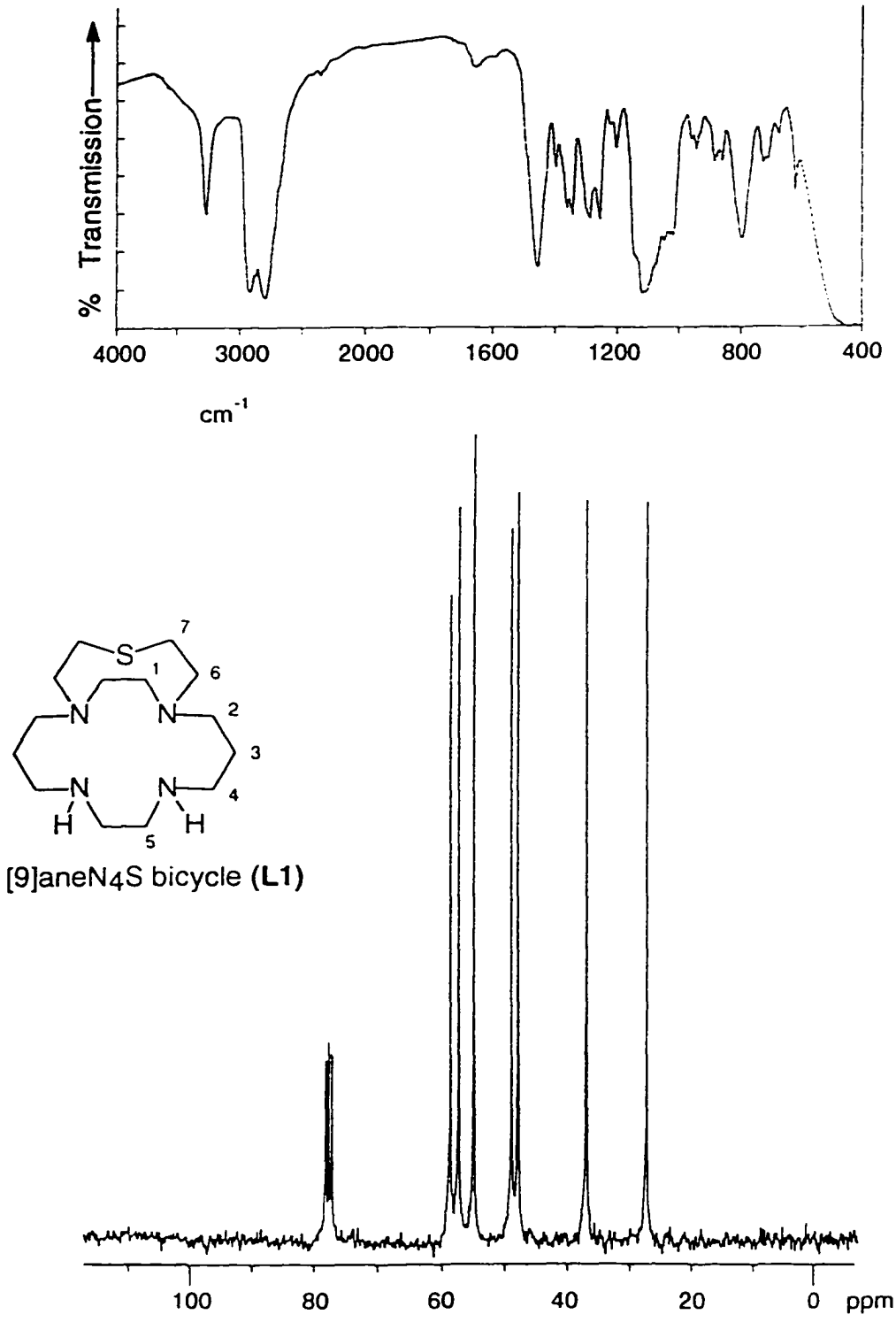

Figure 2.9. Infrared spectrum (top) and ^{13}C-NMR spectrum (bottom)of [9]aneN$_4$S bicycle (**L1**) free ligand.

2.4 Synthesis of monoamido-[9]aneN$_4$S bicycle (4):

The copper(II) templated synthesis of **L1** mentioned above generally proceeds with high purity; however it was noticed that if the pH during the glyoxal condensation step was greater than 9 (i.e. pH 10 - 12), a second, cyclized product was obtained in equal or greater yield than **L1**. In fact, when the pH was 12 or greater this side product was obtained exclusively. The blue color which persisted upon addition of acid (1 M HCl) to a small sample of the complex, indicated that cyclization to form an acid stable bicycle had occurred. The most notable feature of this side product was the presence of a strong infrared band at 1570 cm^{-1} in the copper(II) complex and, upon removal of the copper with sulphide, the free ligand exhibited a strong IR absorption at 1640 cm^{-1} (see figure 2.10). consistent with a carbonyl group in the ligand. The frequency of the absorption was shifted to a lower frequency (well below 1700 cm^{-1}) which is indicative of an amide carbonyl. The ^{13}C-NMR spectrum (figure 2.10) of the free ligand consisted of a fourteen line spectrum with one of the peaks occurring in the carbonyl region at 172.3 ppm. The only possible side product which would contain fourteen independent carbon resonances was one in which the N$_4$S bicycle had formed during the cyclization but one of the carbons adjacent to an amine had been oxidized to form an amide. Such a structure would no longer have a plane of symmetry bisecting the bicycle and therefore would give rise to a fourteen line spectrum rather than the expected seven. Mass spectroscopy was also consistent with such a structure. Furthermore, reduction of the amide group with BH_3·THF (1 M solution in THF) yielded the [9]aneN$_4$S bicycle **L1**.

The formation of unexpected side products such as **4** during the copper(II) templated cyclization and reduction has been previously investigated in this laboratory. Fortier and McAuley[92] and Beveridge, McAuley and Xu[93] investigated the [9]aneN$_5$ bicyclic and [9]aneN$_4$O ligand systems respectively. The majority of nickel(II) templated Schiff base condensations with glyoxal have been shown to yield the expected diimine intermediate which may then be reduced to the corresponding saturated macrocycle.[91]

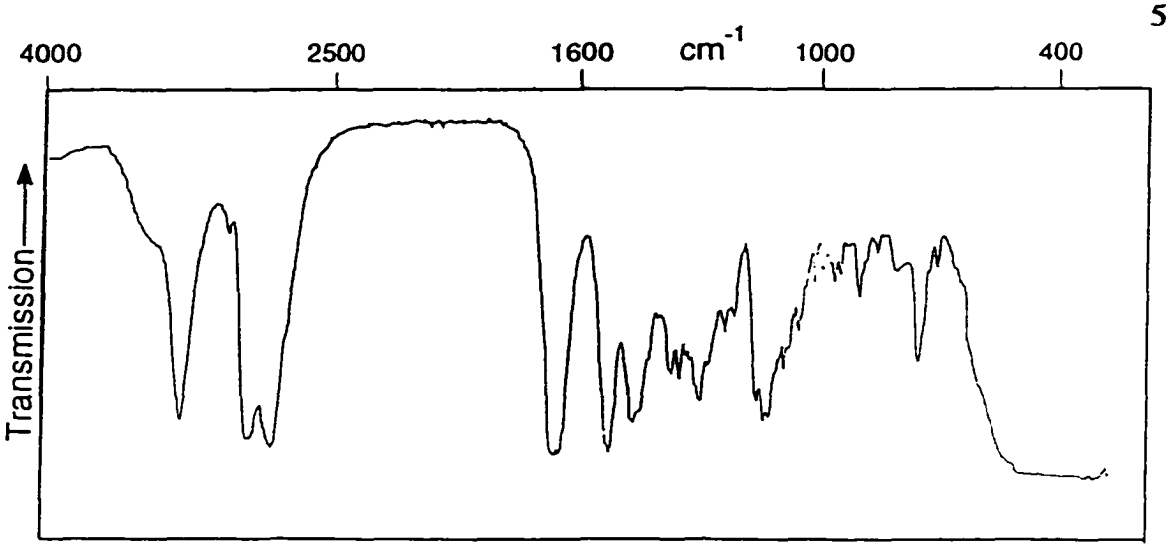

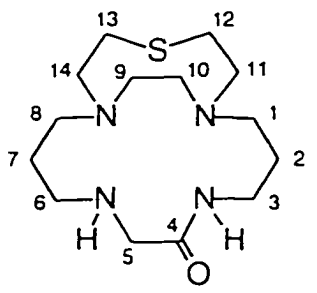

monoamido-
[9]aneN4S bicycle (4)

Figure 2.10. Infrared spectrum (top) and ^{13}C-NMR spectrum (bottom) of [9]aneN$_4$S-monoamido bicycle (**4**) free ligand.

Depending on the degree of dehydration that occurs during the Schiff-base condensation, there are three different possible products. These are the dicarbinolamine, imine-carbinolamine and diimine. Ideally, one would expect the fully dehydrated diimine species to form, however special circumstances are involved in the N_4X (X = NH, O, S) bicycle synthesis which destabilize the diimine. This is because the steric forces of the coordinated ligand are too strong to allow the formation of a planar, five-membered diimine ring around the metal center. The hydrated and semi-hydrated five-membered rings retain some flexibility and have much less strain in the ring by averting the need for planarity.

This effect has been reported in the literature[94]; however, when investigating the synthesis of the analogous N_5 bicyle via the route outlined in scheme 2.3, Fortier[92] successfully isolated and characterized a more unusual imidate intermediate (complex **2.4.5** in scheme 2.4). Fortier also observed that partial reduction of the imidate complex with a stoichiometric deficiency of borohydride led to an enamine intermediate. The N_4O analogue of the enamine intermediate was also observed and characterized by Xu.[93] Further reduction with borohydride led to the fully saturated macrobicyclic ligand. Scheme 2.4(a) presents the mechanism for the glyoxal condensation as proposed by Fortier and McAuley[92] based on the nature of the intermediates isolated and on deuterium-exchange experiments. It was proposed that the isolated imidate intermediate forms from the nucleophilic addition of methanol to the imine of an imine-carbinolamine intermediate (complex **2.4.2** in scheme 2.4). What is relevant to the formation of the monoamidoN_4S bicycle reported in this work, is that Fortier also observed that the addition of base to an equilibrium mixture of complexes **2.4.1** and **2.4.2** (scheme 2.4, X = NH) led to the mono-amidoN_5 macrobicylic ligand. This was the first example of the formation of an amide from a condensation reaction between a diamine and glyoxal. The proposed mechanism of formation of the amide in the presence of base is shown in scheme 2.4(b). That the imine-carbinolamine (complex **2.4.2**) should undergo such a base catalyzed proton shift is supported by the fact that ionization of methylene protons

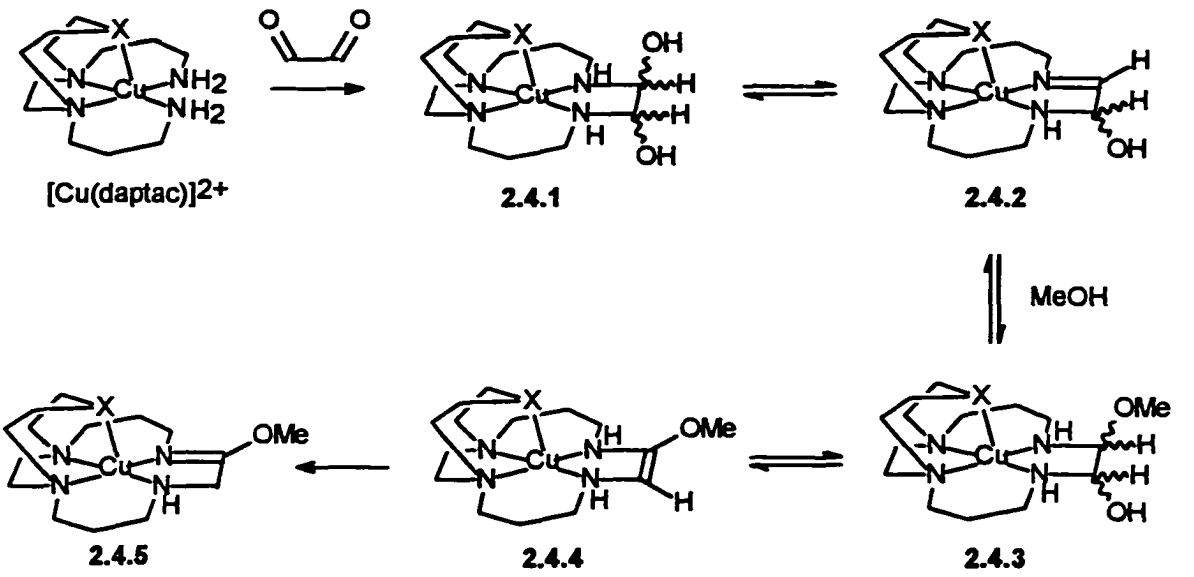

Scheme 2.4(a): Proposed Mechanism for the formation of imidate **5** from Cu(II)-templated glyoxal condensation: X = NH (ref 92); X = S (the present study).

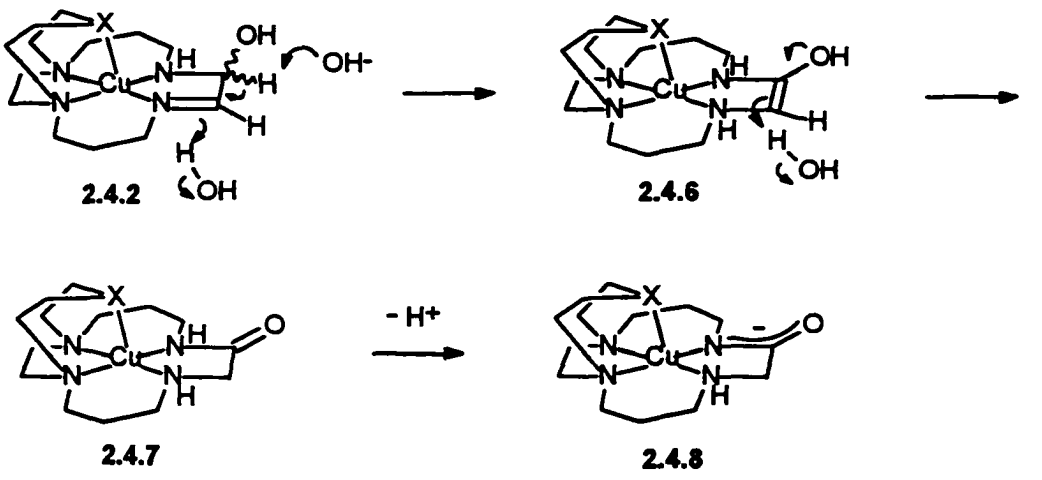

Scheme 2.4(b): Proposed Mechanism for Base Hydrolysis of **2** Leading to Amide **8**. X = NH (ref 92); X = S (the present study).

adjacent to an imine in a five-membered ring is well-documented.[95] The resulting enol then undergoes a tautomeric proton shift to form the amide **2.4.8**. Although Fortier and McAuley did not observe the imidate nor the amide side products during the synthesis of the N_4S bicycle, the fact that the amide species formed in quantity under basic conditions suggests that mechanism of the glyoxal condensation is the same as that established for the N_5 system.

It is important to note that no crystal structure determination has been carried out on the amido complex so the position of the amide carbonyl in the ligand was deduced indirectly from the observed chemistry and the NMR spectroscopy. The ^{13}C-NMR spectrum contained two upfield resonances (25.4 and 27.0 ppm) whose chemical shifts correspond to the middle methylene carbons of the propylene bridges. These methylene functions are unique from the rest because they are the only ones with two adjacent methylene groups, one on either side. The proton resonances of these middle methylene groups therefore are those which are split into quintets by having four adjacent protons. The chemical shift of these protons is also upfield from the other resonances. Two such resonances were observed in the ^{1}H-NMR spectrum. If the carbonyl carbon was present in the propylene chain, such chemical shifts and coupling patterns would not have been observed.

2.5 Synthesis of Hemi-cryptateN_4S bicycle (L2):

2.5(a) Introduction:

As discussed at the beginning of this chapter, the goal of this project was to synthesize all three isomers of the N_4S macrobicyclic ligand system. The synthesis of the [9]aneN_4S isomer via the copper(II)-templated glyoxal condensation had been well established, however synthesis of the other two isomers had not been previously attempted. It was not possible to devise a reasonable method of synthesizing the hemi-cryptate isomer via a template condensation because the ring closure must occur between *trans*, diagonally opposed, secondary amines. There are no literature precedents for metal-templated condensations across diagonally opposed amines; reported condensations invariably involve amine groups which are *cis* to each other. Also, there are no precedents for metal-templated ring closures involving secondary amines.

The most obvious and basic strategy for the synthesis of the hemi-cryptate isomer would be to react cyclam (1,4,8,11-tetraazacyclotetradecane) with the necessary -CH_2-CH_2-S-CH_2-CH_2- fragment via direct methods. The major disadvantage of such a strategy would be that all three isomers may be produced by such a reaction since the "sulphur bridge" could cyclize across any two of the cyclam nitrogens. The isomers would be produced in varying proportions depending on many factors such as the cyclam conformation, the relative nucleophilicity of the nitrogens, the size matching of the reactants, and steric factors.

A more reasonable synthetic strategy would therefore be to first protect the diagonally opposed nitrogens of the cyclam such that only the hemi-cryptate isomer could form. The disadvantage to such a strategy is that the synthesis of a diagonally protected cyclam would be an equally difficult task for the same reasons. Synthetic strategies in which the formation of more than one product is inherently allowed, are generally considered to be a bad practise. In this case, each of the possible products is a

target ligand. Furthermore, the main disadvantage of forming more than one product (and side products) is that purification becomes too difficult. However, cation-exchange chromatography of the corresponding copper(II) complexes has proved to be a very effective technique such that satisfactory purification may be possible. It was therefore decided to attempt reacting unprotected cyclam with the sulphur bridge.

2.5(b) Synthetic Routes to L2:

The first such synthesis attempted was an aminolysis reaction of cyclam with the diethyl ester derivatized sulphur bridge. The yield of product was so low that no further characterization was undertaken.

The relatively low reactivity of the diethyl ester sulphur bridge suggested that reaction of cyclam with the di-acid chloride derivative of the sulphur bridge (thiodiglycolic acid chloride) might give a better result. Most of the syntheses of sulphur containing macrocycles in the literature[83] involve either the use of thiolate nucleophiles which form thioethers after reaction, or amine nucleophiles with acid chloride electrophiles that contain thioether(s) which do not participate in the reactivity. In this work, the target ligand(s) contain only one thioether so a cyclization involving thiolate nucleophiles was not feasible. The main concern for cyclizations with a thioether reactant is that thioethers can be very reactive nucleophiles themselves. For example, thioethers readily displace alkyl halides to form sulphonium salts. If the electrophiles are acid chlorides, the reactivity of the thioether is attenuated because, upon displacement of the

chloride, the sulphonium cationic moiety would be adjacent to the electropositive carbonyl:

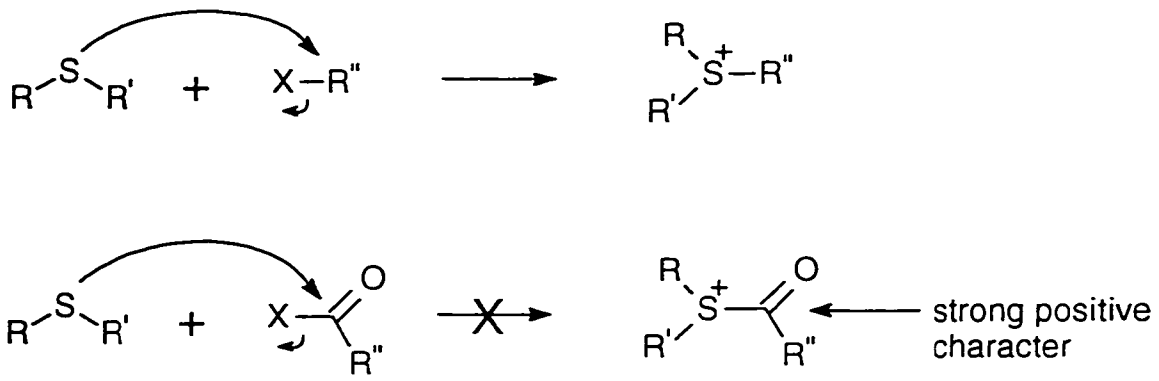

Figure 2.11. Formation of sulphonium salt.

Reactions between amines and acid chlorides are favoured both thermodynamically, where formation of the stable amide bond provides the driving force[96(a)], and kinetically, due to the relative lack of steric hindrance about the carbonyl carbon and the ease with which the tetrahedral intermediate can expel good leaving groups[96(b)]. These properties are ideal for cyclization reactions.

The cyclization of thiodiglycolic acid chloride **(15)** with cyclam was first carried out under high dilution conditions in dimethylformamide solvent with sodium carbonate serving as the base. The base neutralizes the hydrochloric acid liberated by the reaction, forming water and carbon dioxide gas such that the reaction is driven by the Le Chatelier principle. Dimethylformamide was chosen as the solvent firstly because it is the most polar organic solvent which would help to stabilize the polar transition state, and secondly because the only organic solvents in which the cyclam ligand is soluble are DMF, DMA, benzene and chloroform. The reaction was unsuccessful in DMF and DMA, mainly because the thiodiglycolic acid chloride was observed to decompose rapidly in

both solvents. Within minutes of dissolving thiodiglycolic acid chloride in DMF or DMA, the colorless solution turned dark and NMR spectroscopy showed that the reagent had decomposed into many uncharacterizable species.

In dry, distilled benzene, a very similar reaction involving the cyclization of thiodipropionic acid chloride across the diagonally opposed nitrogens of 1,7-dimethyl-1,4,7,10-tetraazacyclododecane (cyclen) had been reported[97] to have a 70% yield. Cyclam has a low solubility in benzene so the reagents were both dissolved in dichloromethane and then added dropwise into three litres of benzene. Triethylamine was used as the base. The reaction in benzene (dried over CaH_2) produced mostly polymer and a small amount of uncharacterizable products.

Perhaps the reaction should have been tried again using benzene which had been distilled over sodium metal. However, since both reagents were soluble and stable in chloroform, it was instead decided to try the reaction solely in chloroform. The chloroform was rigorously dried over phosphorous pentoxide to remove the ca. 0.75% ethanol. The ethanol must be removed to prevent hydrolysis of the thiodiglycolic acid chloride. Instead of adding an organic base to neutralize the liberated hydrochloric acid, it was decided to rely on the fact that two of the four cyclam nitrogens should be left unreacted and therefore could serve as the base. This effect would also serve to precipitate the bicyclic ligand product as its hydrochloride salt and drive the reaction according to the Le Chetalier principle. Inevitably, some unreacted cyclam would be precipitated out as well but the availability of cyclam rendered it suitable to serve as its own base to some extent.

Compound (15) was prepared using an adaptation of the procedure reported[97] for the synthesis of 3,3'-thiodipropionic acid chloride.The synthetic route is outlined in scheme 2.5. The synthesis produced an N_4S bicyclic product (**crude 16**) in low yield but sufficient quantity for reduction with borane followed by isolation and characterization of the compounds present in the reduction mixture.

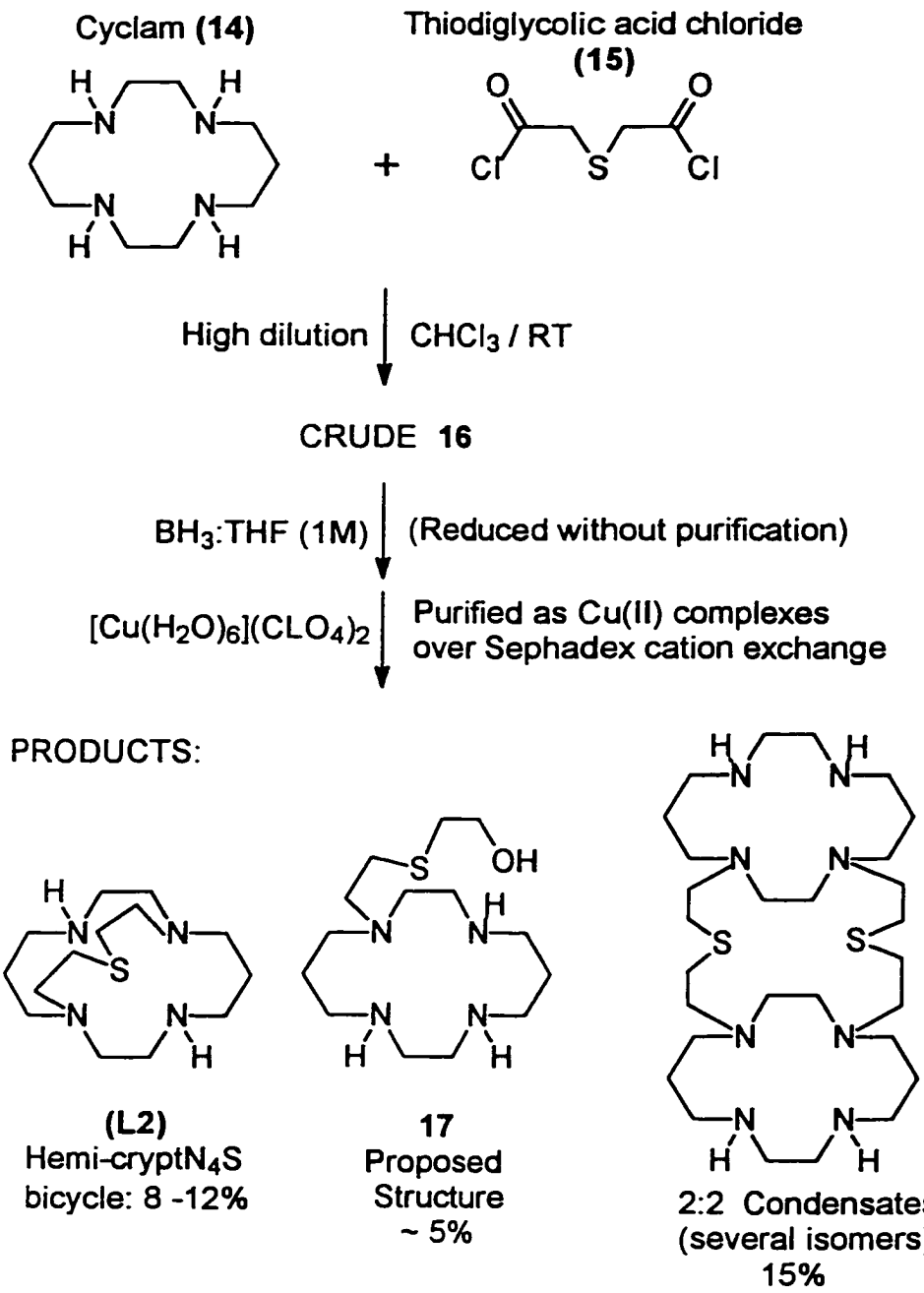

Scheme 2.5. Cyclization reaction between cyclam and thiodiglycolic acid chloride. Note: neither the [9]aneN$_4$S bicycle nor the [10]aneN$_4$S bicycle were produced.

2.5(c) Discussion of crude Hemi-cryptate bicyclic diamide (16) synthesis:

^{13}C-NMR spectroscopy of the sample of crude **16** showed it to be a mixture of many products plus some unreacted cyclam. Mass spectroscopy of the mixture identified peaks corresponding to the expected M+1 (315 m/e) and M+29 (343 m/e) of the bicyclic diamide product(s).

In order to determine if the product yield could be improved by not relying on the reactant cyclam and product species to neutralize the HCl generated by the reaction, the cyclization reaction was attempted under the same conditions in the presence of two equivalents of pyridine and also with one equivalent of 1,4-diazabicyclo[2.2.2]octane (DABCO). These reactions yielded mostly polymer and uncharacterizable oligimers. No bicyclic products were observed. The presence of base must have prevented the initial bicyclic product from precipitating out of the reaction solution as its hydrochloride salt and allowed further reaction of the unprotected secondary amines in the product.

Attempts at purifying the crude diamide reaction mixture were unsuccessful. Compounds containing primary and secondary amines are generally not amenable to normal phase chromatography over silica gel because the acidity of the silica causes the amine product to precipitate and "stick" to the silica. The presence of amide groups limited the solubility of the mixture such that it could be dissolved only in polar solvents such as water, alcohol and chloroform (sparingly). The diamide product could not bind metals such as copper(II) due to the presence of the tertiary amides. Only primary and secondary amides can coordinate transition metals because the amide must have an N-H bond which can then be deprotonated in order to provide sufficient donor strength. For this reason, purification of the mixture as its corresponding copper(II) complex could only be carried out after the diborane reduction.

^{13}C-NMR spectroscopy of the crude solid precipitate (diamide reaction mixture) after neutralizing with base and extracting into methanol, revealed the presence of *ca.* 40% unreacted starting materials in approximately a 1:1 ratio. The starting materials were

much more abundant than the products. The chemical shifts of the unreacted cyclam differed significantly from the known chemical shifts observed in the NMR spectra of the pure starting material. The ^{13}C-NMR chemical shifts of pure, free ligand cyclam in D_2O are 48.54, 48.47 and 29.26 ppm whereas, for the crude reaction mixture in D_2O, the chemical shifts were 41.3, 37.9 and 18.7 ppm. The chemical shifts of pure thiodiglycolic acid in D_2O are 173.9 and 33.9 ppm which agreed with the chemical shifts of 175.6 and 34.0 ppm found in the crude reaction mixture. The small difference in the chemical shift of the carbonyl carbon was significant. Infrared spectroscopy of the crude reaction mixture showed no carbonyl stretches in the 1700 cm^{-1} to 1750 cm^{-1} range, expected for carboxylate carbonyl groups. There were, of course, broad carbonyl stretches in the 1640 cm^{-1} to 1660 cm^{-1} range expected for amide carbonyl stretches. This result suggested that the putative unreacted thiodiglycolic acid was actually a reaction product. Removal of the thiodiglycolic acid reagent before reduction would avoid complications, however, a convenient method was not found. That the two reactant species remained in a 1:1 ratio after the work-up was unanticipated because it was expected that the differing reactivities and solubilities would result in an uneven ratio.

2.5(d) Discussion of borane reduction products:

After reduction of the crude diamide mixture (**16**) with diborane, the reactants were still present in a 1:1 ratio in the ^{13}C-NMR spectrum. The chemical shifts of the cyclam peaks still differed significantly from those of the known pure ligand. The chemical shifts of the thiodiglycolic acid also differed significantly from the known chemical shifts of thiodiglycolic acid and 2,2'-thiodiethanol, which was the expected product of the reduction. No satisfactory explanation for these observations was found. The unlikely possibility that the species present was actually a tricyclic 1:2 condensation product was ruled out by chromatographing a small portion of the reduction mixture over

DOWEX 50 X 8 cation exchange packing and eluting with pH 2 acidic water. If the two reactants were not chemically linked, only the the thiodiglycolic acid derivative would be able to pass through the packing without binding. Although some cyclam did pass through, the peaks assumed to be due to the thiodiglycolic acid derivative were present in a much greater amount which demonstrated that, despite the anomolous chemical shifts, the species present were not reaction products.

As mentioned in the experimental procedure, the presence of borate species was monitored by ^{11}B-NMR spectroscopy. The only ^{11}B species present were the expected polyborates. As disscussed in chapter 3, reduction of [10]aneN_2S diamide (**23**) to [10]aneN_2S (**20**) resulted in a boron coordinated side product. On the basis of the ^{11}B-NMR spectra, it was concluded that no such boron coordinated amines were present in this synthesis.

The high dilution reaction of cyclam with thiodiglycolic acid chloride produced several products: unreacted starting materials, a side product (**17**), a 1:1 condensation product (hemi-cryptateN_4S bicycle (**L2**)) and several 2:2 condensation products (table 2.1).

Table 2.1. Products obtained from purification of cyclam + thiodiglycolic acid chloride reaction mixture:

BAND #	[$NaClO_4$]	Ligand
1	0.10 M	Uncharacterizable
2	0.10 M	**17**, proposed half-condensed intermediate
3	0.15 M	1:1 Condensate, hemi-cryptateN_4S bicycle (**L2**)
4	0.20 M	Unreacted cyclam starting material
5	0.20 M	Unreacted cyclam starting material
6-10	0.40 M	several 2:2 Condensation products

Band #1:

During the separation of the copper(II) complexed reaction mixture, there were two distinct blue coloured bands eluted (0.1 M $NaClO_4$)$_2$ prior to the [Cu(**L2**)]$(ClO_4)_2$ band. The copper(II) was removed from a sample of the first band by refluxing with sodium sulphide. Characterization of the resulting free ligand by NMR and mass spectroscopy proved inconclusive. The ^{13}C-NMR spectrum contained thirty peaks of *ca.* equal intensity in the 20 ppm to 60 ppm range. There was no M+1, M+29, M+41 pattern in the mass spectrum such that the molecular weight of the ligand could not be determined. The mass spectrometer used in this work can only detect molecular weights of up to 600 m/e with assurance, so it is possible that the ligand had a higher mass. The presence of so many peaks in the ^{13}C-NMR also suggested that the ligand was a relatively large and asymmetric reaction product.

Band #2:

The complex [Cu(**17**)]$^{2+}$ was consistently produced as a side product from the reaction of cyclam and thiodiglycolic acid mentioned above. The pure blue complex eluted (0.1 M $NaClO_4$) as the second band from the column of sephadex CM-C25 ahead of the [Cu(**L2**)]$(ClO_4)_2$ product band. The complex did not decompose in the presence of strong acid which implied that the cyclam ring was present and intact.

The free ligand was obtained from this side product by removing the copper(II) with sodium sulphide. The ^{13}C-NMR spectrum consisted of fourteen peaks (figure 2.12) which suggested that an asymmetric 1:1 product had formed. The only significant parent ion observed in the mass spectrum of this side product corresponded to a mass $M^+ = 304$. On the basis of this evidence, the identity of the side product is proposed to be that of the half-condensed intermediate (1:1 cyclam:thiodiglycolic acid chloride).

The presence of a substantial amount of the half condensed intermediate would suggest that precipitation of the intermediate and products was occurring relatively rapidly. This result was expected because of the deficiency of base. The amount of **17** isolated was *ca.* 1/5 as much (by weight) as the bicyclic product (**L2**) which suggests that early precipitation of reactants and intermediates did not interfere significantly. Molecular modeling of the half-condensed, monoamide intermediate did not show any

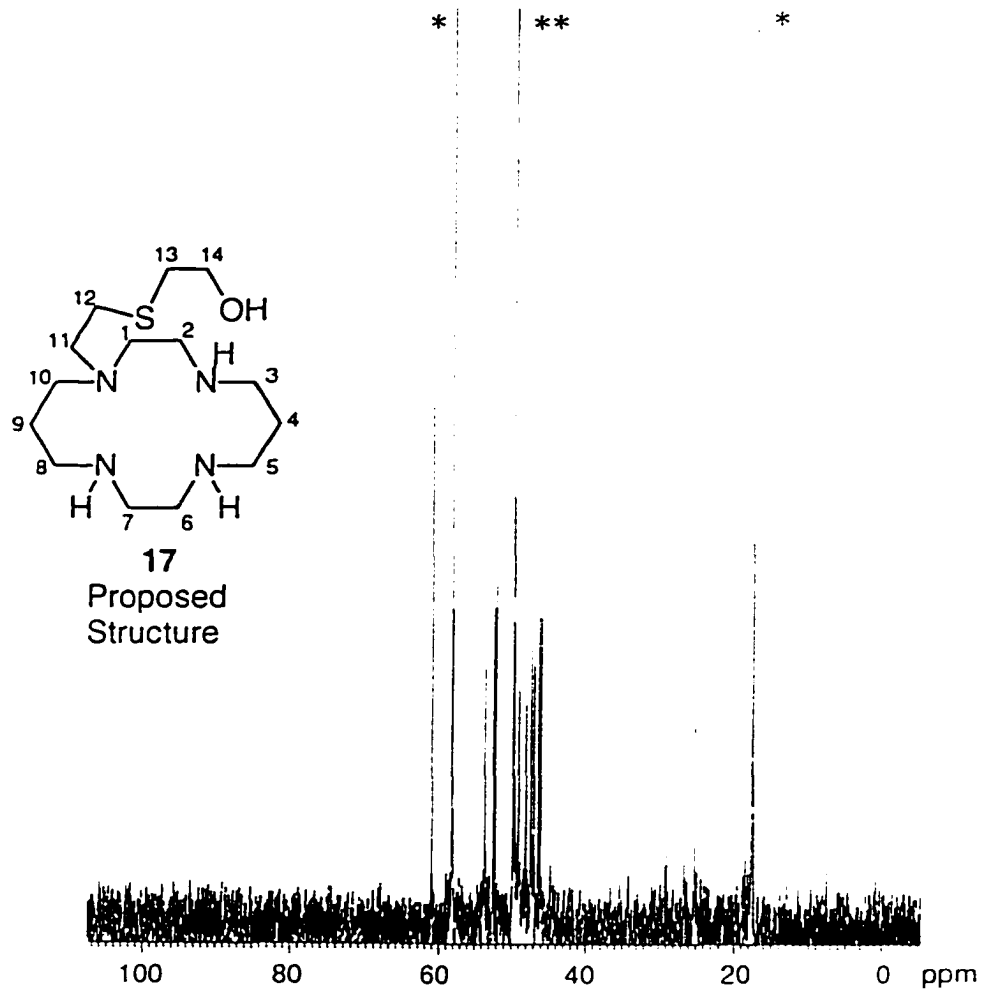

Figure 2.12. ^{13}C-NMR of side product (**17**, free ligand) from **L2** synthesis.
* = ethanol, ** = methanol.

unusual barriers preventing the thiodiglycolic acid chloride bridge from reaching another of the amine groups.

Band #3:

The most interesting aspect of the reaction was that only one of the three possible 1:1 condensation products was observed. No evidence was obtained for the formation of the [9]aneN_4S (**L1**) or [10]aneN_4S (**L3**) isomers. Mass spectroscopy of the free ligand of the isomer obtained established that it was an N_4S bicyclic ligand but could not distinguish which isomer. The identity of the isomer was concluded from the ^{13}C-NMR spectrum. The [9]aneN_4S (**L1**) free ligand possesses one mirror plane such that there are seven pairs of magnetically equivalent carbon nuclei present. The ^{13}C-NMR spectrum of **L1** therefore has seven peaks as was reported in section 2.3. The hemi-cryptate (**L2**) free ligand has no plane of symmetry, however, it does possess a C_2 rotation axis through the sulphur and perpendicular to the N_4 plane of the cyclam ring. The C_2 symmetry divides the ligand into seven pairs of magnetically equivalent carbon nuclei such that the ^{13}C-NMR spectrum is expected to have seven peaks as well. Although both **L1** and **L2** are expected to have seven ^{13}C-NMR peaks, the spectrum and chemical shift pattern of **L1** had already been unambiguously obtained via the template synthesis from [9]aneN_2S (**8**). The ^{13}C-NMR spectrum of the isomer formed in the cyclam reaction had seven peaks, but none of the chemical shifts corresponded to those observed for the [9]aneN_4S (**L1**) isomer. It was therefore concluded that the product was not **L1**.

The [10]aneN_4S (**L3**) isomer possesses one mirror plane which bisects the ligand and contains the sulphur and both of the middle methylene carbons (-CH_2-$\underline{C}H_2$-CH_2-) of the propyl bridges. Because the two middle methylene carbons are both in the mirror plane, they are not magnetically equivalent such that the isomer **L3** consists of six pairs

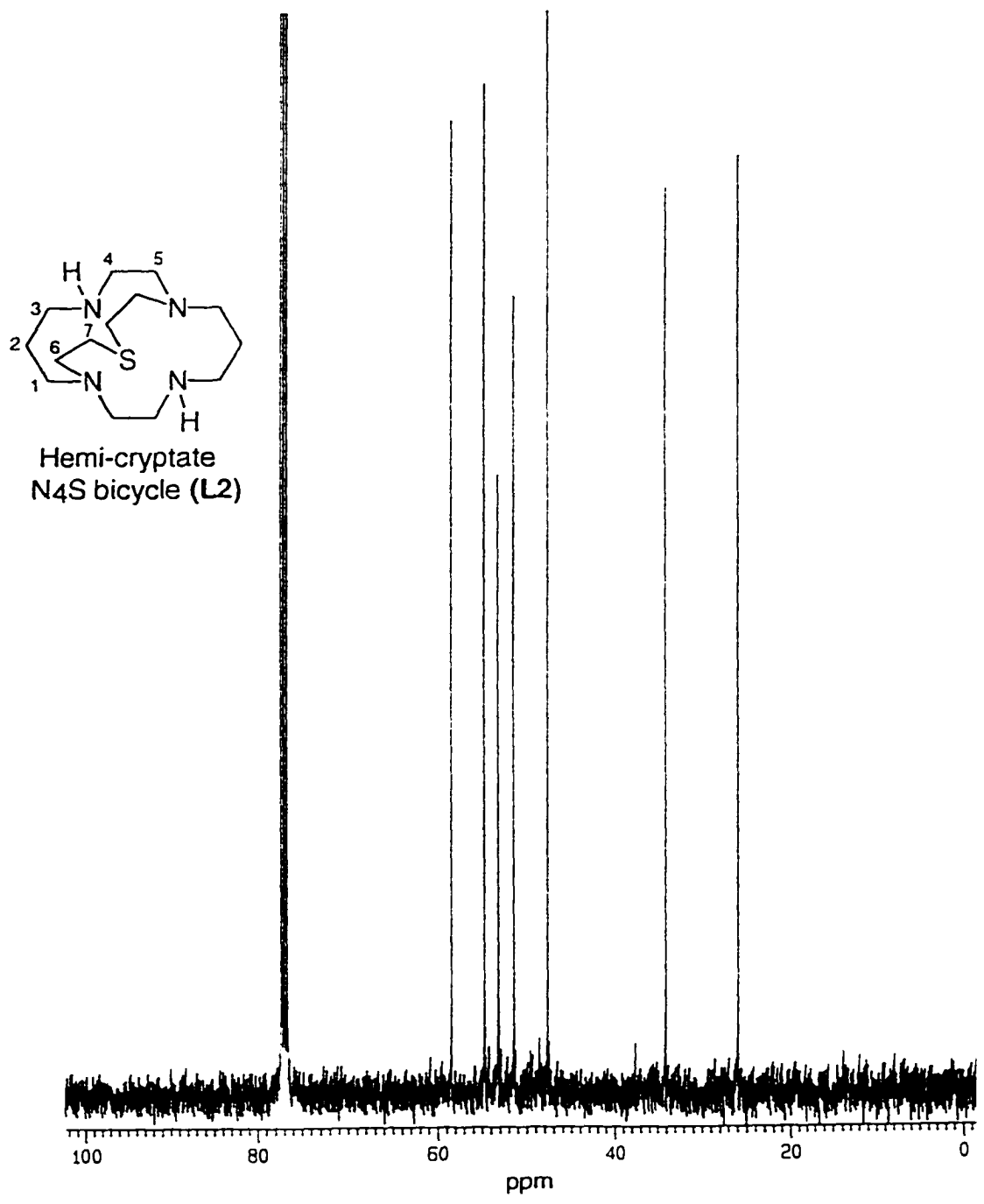

Figure 2.13(a). ^{13}C-NMR spectrum of Hemi-cryptateN_4S bicycle (L2) free ligand.

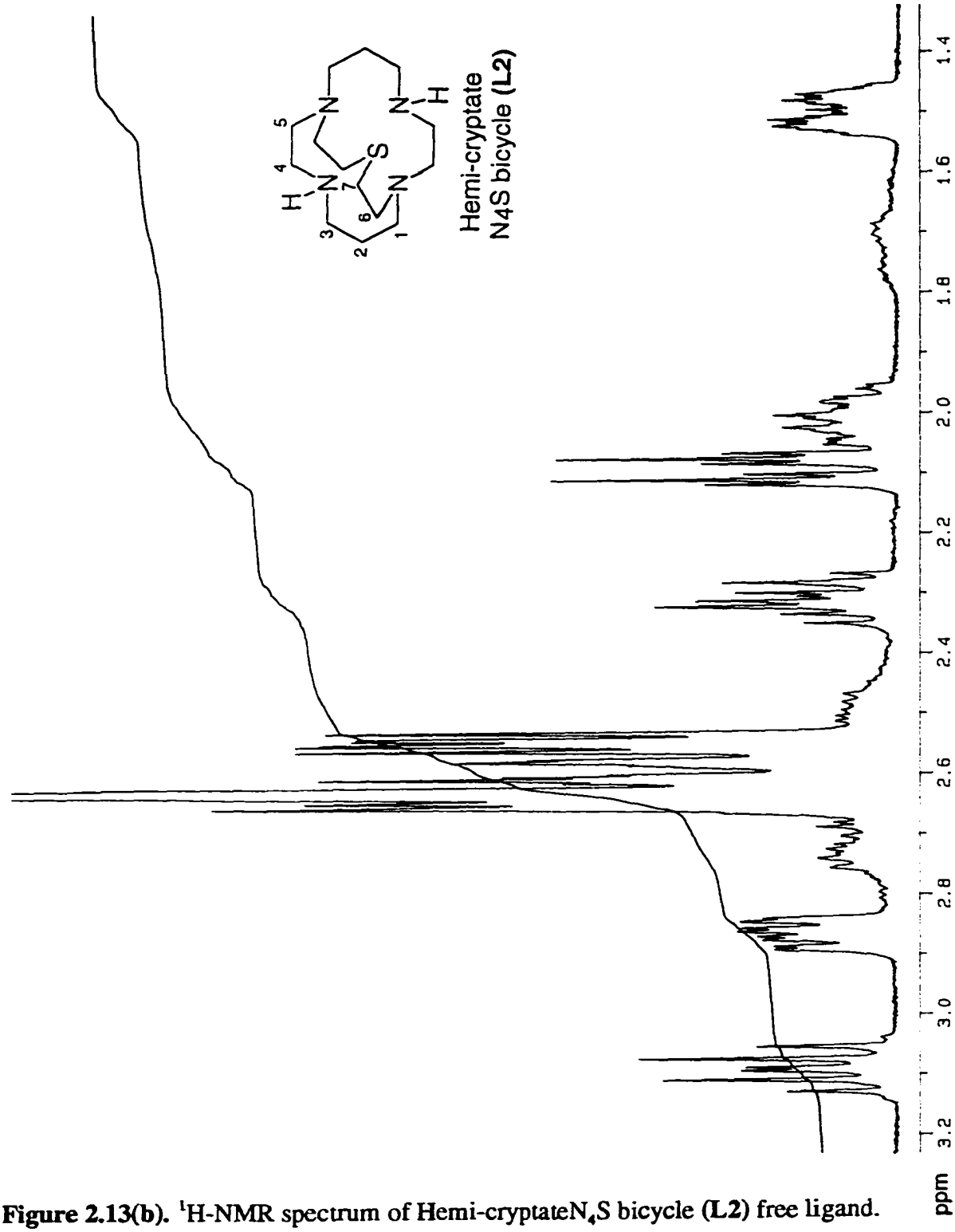

Figure 2.13(b). ^{1}H-NMR spectrum of Hemi-cryptateN_4S bicycle (**L2**) free ligand.

of identical carbon nuclei and two unique methylenes. The ^{13}C-NMR spectrum is therefore expected to have eight peaks, two of which would be only one half as intense as the other six. The ^{13}C-NMR spectrum of bicyclic ligand isolated consisted of seven peaks with roughly equal intensity, therefore it was concluded that the product was not **L3**.

That the only N_4S bicyclic isomer formed in the reaction was **L2** was unanticipated because there is no obvious reason why the bridge could not cyclize across adjacent nitrogen groups. In fact, such a cyclization was shown to occur in this laboratory when the [9]aneN_4O bicyclic ligand was reacted with diglycolic acid chloride[100]:

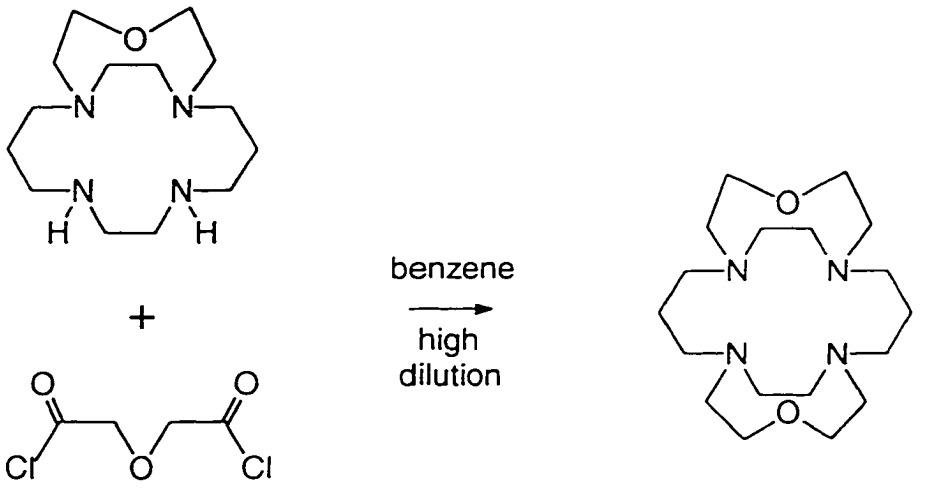

Figure 2.14. Cyclization across adjacent [1,12]-nitrogens of [9]aneN_4O bicycle with thiodiglycolic acid.[100]

In the above reaction, the oxo bridge serves to protect the adjacent 1,12-nitrogens from reaction by virtue of being tertiary substituted. The bridge was forced to cyclize across the two adjacent 5,8-nitrogens.

Cyclization across adjacent nitrogens was reported for the reaction of the unprotected 12-membered 1,4,7,10-tetraazacyclododecane (cyclen) with both the dibromoethane bridge[101(a)] and the triethyleneglycol ditosylate bridge[102]. The cyclization with dibromoethane yielded the 1,4-annelated (adjacent nitrogens) isomer exclusively, presumably because the ethylene bridge was too short to bridge diagonally. Cyclization with triethyleneglycol ditosylate gave both the 1,4-annelated (adjacent nitrogens) and 1,7-annelated (diagonally opposed nitrogens) isomers. The 1,4-annelated isomer predominated over the 1,7-annelated isomer by a factor of 5:1 which shows that, for that particular system, it is also more favourable for the bridge to cyclize across

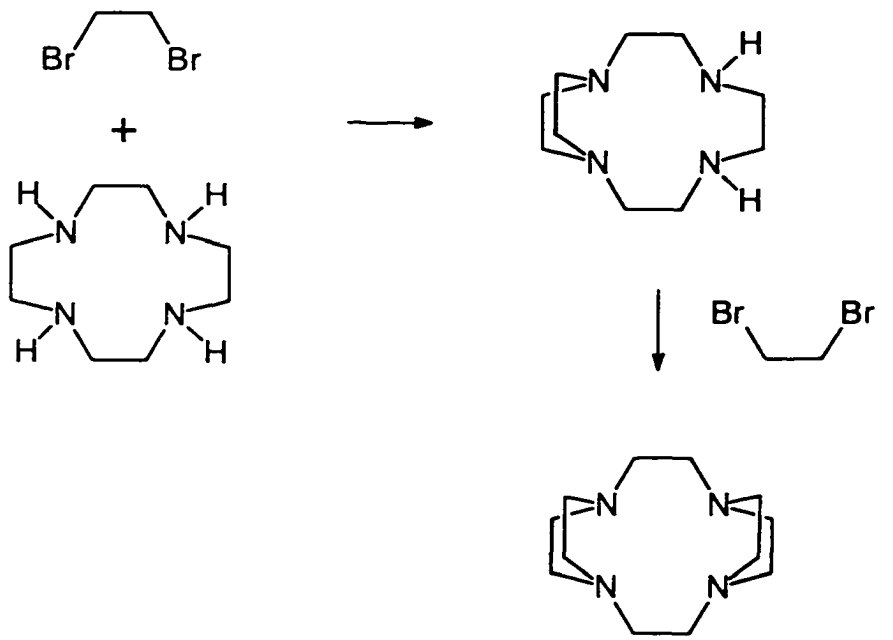

Figure 2.15. Cyclization of [12]aneN$_4$ (cyclen) with dibromoethane.[101]

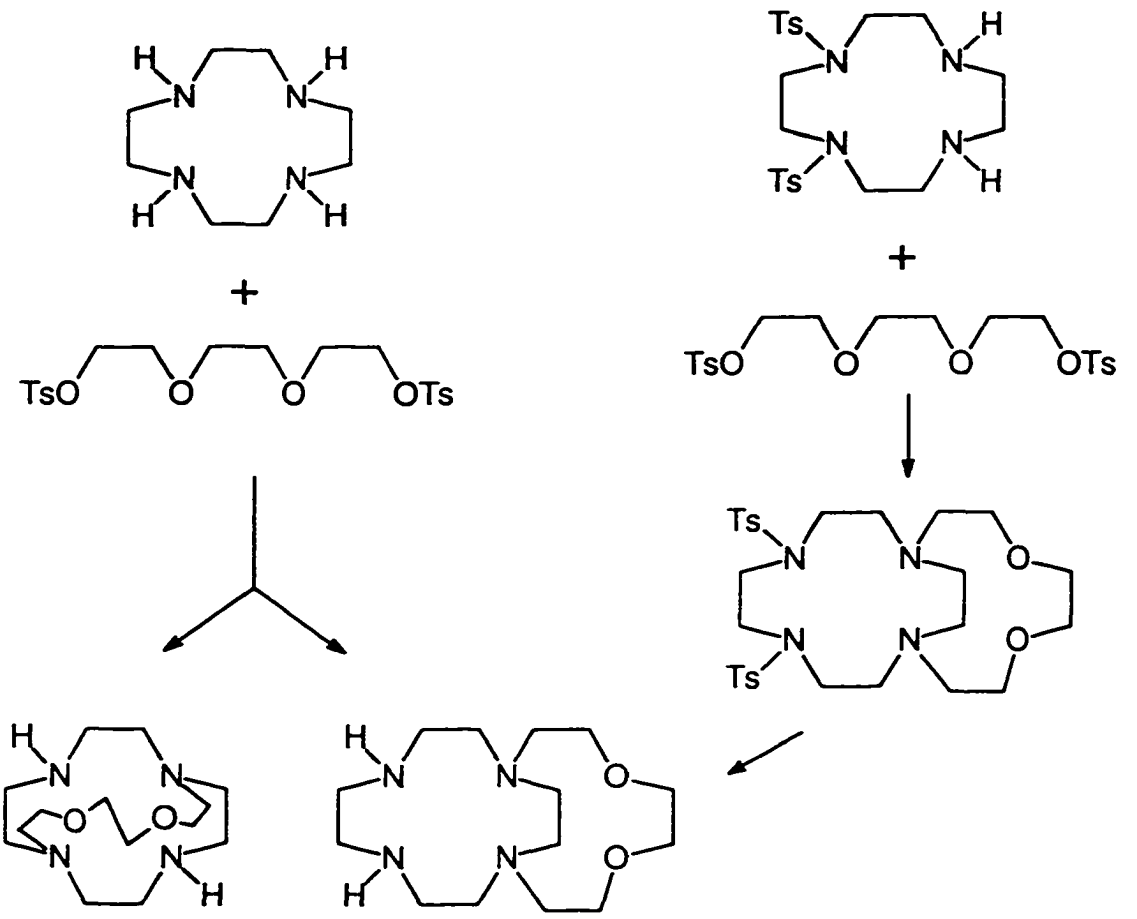

Figure 2.16. Cyclization of [12]aneN$_4$ (cyclen) with triethyleneglycol ditosylate.[102]

adjacent nitrogens. In fact, the authors had previously synthesized the 1,4-ditosyl protected cyclen to ensure cyclization occurred across the adjacent 7,10-secondary nitrogens, however, the high regioselectivity of the reaction with unprotected cyclen made that route more attractive because it avoided the difficult detosylation step.[102]

Why cyclization across adjacent nitrogen groups did not occur with the

unprotected cyclam has not been satisfactorily explained. However, several reports were subsequently found in the literature which help to corroborate such a result. Only two reports of a cyclization with unprotected cyclam have been found. The first [101(b)] involved reaction of cyclam with dibromoethane which yielded only the 1,4-annelated (adjacent) nitrogens, presumably because dibromoethane is too short to cyclize diagonally (see figure 2.19). The second report [103] involved the synthesis of the *bis*-aminal derivatized cyclam (figure 2.17 below) followed by exhaustive methylation with methyl iodide:

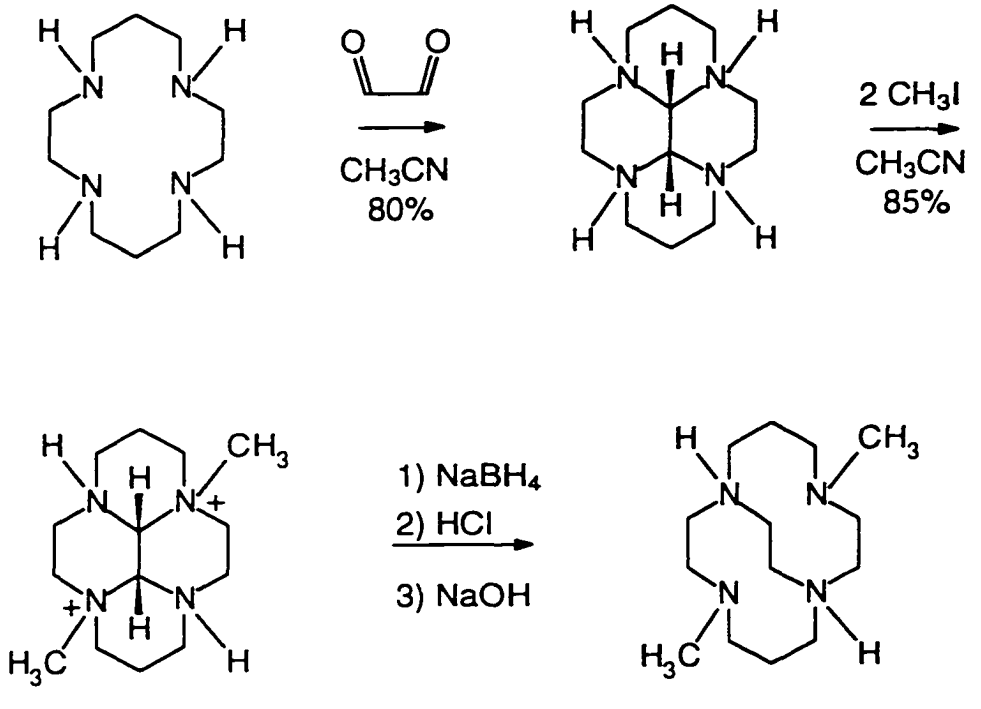

Figure 2.17. Synthesis of cross-bridged cyclam via formation of a *bis*-aminal intermediate. [103]

The methylation of the *bis*-aminal produced only the 1,8-dimethyl *bis*-quaternized derivative (see above). In principle, any of the three [1,4], [1,8] or [1,11] isomers could have formed, yet only the [1,8] isomer was observed. The authors attributed the high regioselectivity to the conformational preference of the *bis*-aminal intermediate. 1D-NMR and 2D-NMR results confirmed that the *bis*-aminal intermediate was locked in a conformation with a convex face and a concave face. The authors argued that only the two nitrogen lone pairs of the convex face were sterically available for alkylation:

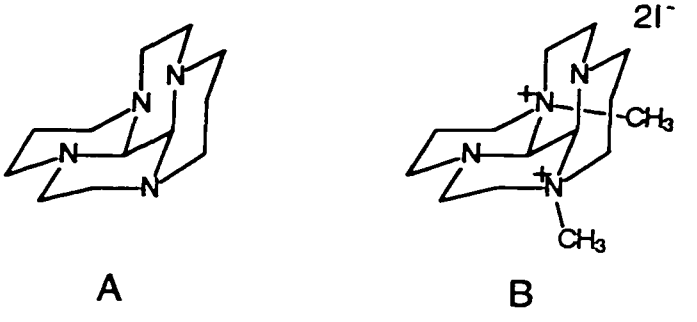

Figure 2.18. Proposed[103] structure of *bis*-aminal intermediate.

Diprotection of cyclam with 1.5 equivalents of tosyl chloride was reported[104] to give the [1,8] (diagonally opposed) and [1,11] (adjacent) isomers in reasonable yield and in the ratio 8:1. It is unlikely that the high regioselectivity in this case was caused by the conformational preference of the cyclam ring since all the nitrogen lone pairs would be available for reaction regardless of conformation. The authors gave no explanation for the regioselectivity, but perhaps the steric interactions of the bulky tosyl protecting groups were responsible in that case. The [1,8] isomer would be expected to offer the

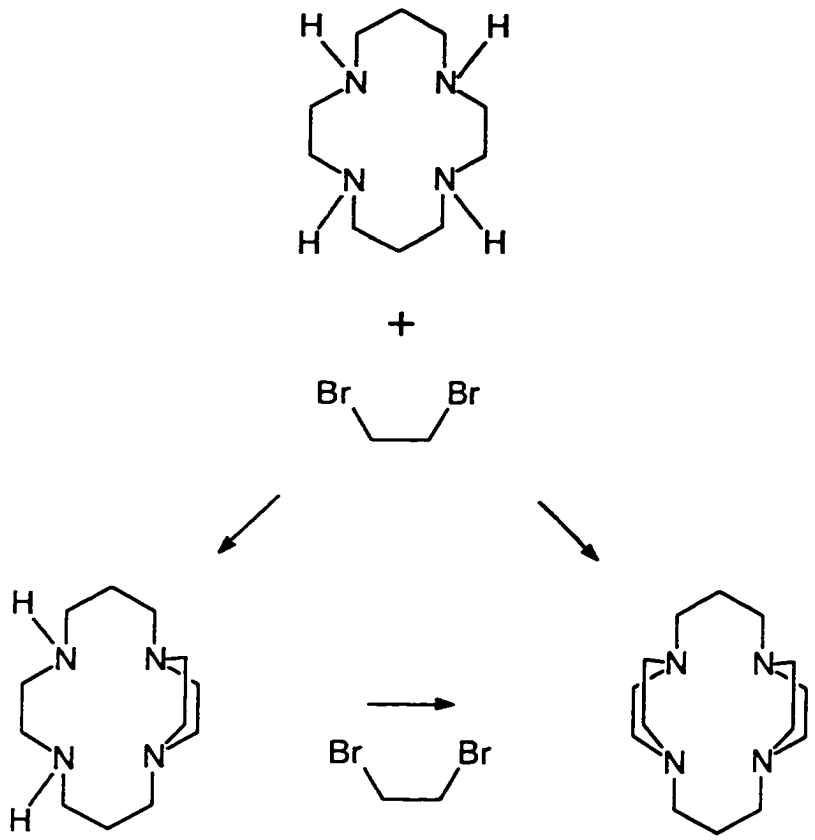

Figure 2.19. Cyclization of [14]aneN$_4$ (cyclam) with dibromoethane.[101(b)]

most relief of steric interactions between the tosyl groups. It would therefore be interesting to determine which isomer(s) form if cyclam is reacted with non-bulky protecting groups.

Although no other reports of diprotection of cyclam are available, the diprotection of cyclen with several chloroformates was recently reported.[105] Once again, the only disubstituted isomer observed was the 1,7-disubstituted (diagonally opposed) derivative. Several chloroformates of varying steric bulkiness were used and the same 1,7-di-substituted isomer was obtained in each case. The reactions were carried out in aqueous solution at pH *ca.* 2-3. It is known[106] that at pH < 2, two diagonally opposed nitrogens of

the cyclen are protonated. The authors suggest that this effect is likely to be responsible for the high regioselectivity. Di-protection of cyclen with two equivalents of tosyl chloride was recently reported[107] to give the 1,7-disubstituted isomer exclusively. In that case, cyclen was reacted with two equivalents of tosyl chloride in pyridine such that the cyclen would not have been protonated and therefore pH was not responsible for directing the tosyl groups onto the diagonally opposed nitrogens. These results are consistent with the ditosylation of cyclam discussed above.

There are insufficient reports available to determine the general regioselectivity of the unprotected cyclam reaction. Di-protection of both cyclen and cyclam results in disubstitution of the diagonally opposed nitrogens only. It is unlikely that both of these unprotected tetraaza rings are locked in a conformation in which only the diagonally opposed nitrogens can react since both ligands, when appropriately protected, have been shown to undergo cyclizations across adjacent nitrogens. The results of the diprotection reactions could be explained by steric interactions of the protecting groups except that the isomer formed appears to depend on the nature of the protecting group. Furthermore, for the reaction of unprotected cyclam with thiodiglycolic acid chloride reported in this work, there is no more relief of steric interactions in the 1,8-bridged isomer relative to the other two.

The formation of the cross-bridged isomer **L2** was expected because the length of the thiodiglycolic acid chloride bridge is best accommodated by the 1,8-nitrogens which are separated by a greater distance. Molecular modelling of the half-condensed intermediate did not reveal any significant conformational barriers to cyclization across adjacent nitrogens (relative to cyclization across the diagonally opposed nitrogens).

Bands 6-10:

The 2:2 condensation products produced by the reaction would be attractive target ligands for producing binucleating metal complexes. However, because the cyclam was reacted without protection of the other two amines, there are a total of nine structural isomers possible. During the purification of the copper(II) complexed mixture, there were at least five distinct violet-coloured bands which eluted only at relatively high (0.4 M) $NaClO_4$ concentrations. These bands were believed to be the various 2:2 condensation products because they would form binuclear copper(II) complexes with an overall 4+ charge, thereby requiring the higher ionic strength for elution from the sephadex CM C-25 packing.

The third band of the putative 2:2 condensation products eluted was characterized by microanalysis of the copper(II) complex. The mole ratios found were $CuN_4C_{14.20}H_{29.95}$ which corresponds well to the ratios of $CuN_4C_{14}H_{30}$ expected for a dicopper(II) complex of a 2:2 condensation product. Crystallographic characterization would be required to determine which ligand isomer was present, however attempts at obtaining X-ray quality crystals have been so far unsuccessful.

Because of the high eluent concentrations required for elution of the copper(II) complexes of the putative 2:2 condensation products and the similarity of the various isomers, it was not possible to completely separate each band. Also, the amount of each of these products was relatively low (between 50 - 150 mg of free ligand each). For these reasons, further purification and characterization of these products was not carried out.

CHAPTER 3

Synthesis, Isolation and Characterization of [10]aneN_2S Monocyclic and [10]aneN_4S Bicyclic Ligands.

3.1 Synthesis of [10]aneN$_2$S (20) via tosylate method:

The synthesis of [10]aneN$_2$S (20) was reported by Herman et al[109a] using a form of the Richman and Atkins[77] method (scheme 3.1). The synthesis was later used in this laboratory by Chandrasekhar and McAuley.[109b] The synthetic route was identical to that used to prepare [9]aneN$_2$S (section 2.2) except that tosylated 1,3-propanediol was used instead of glycol.

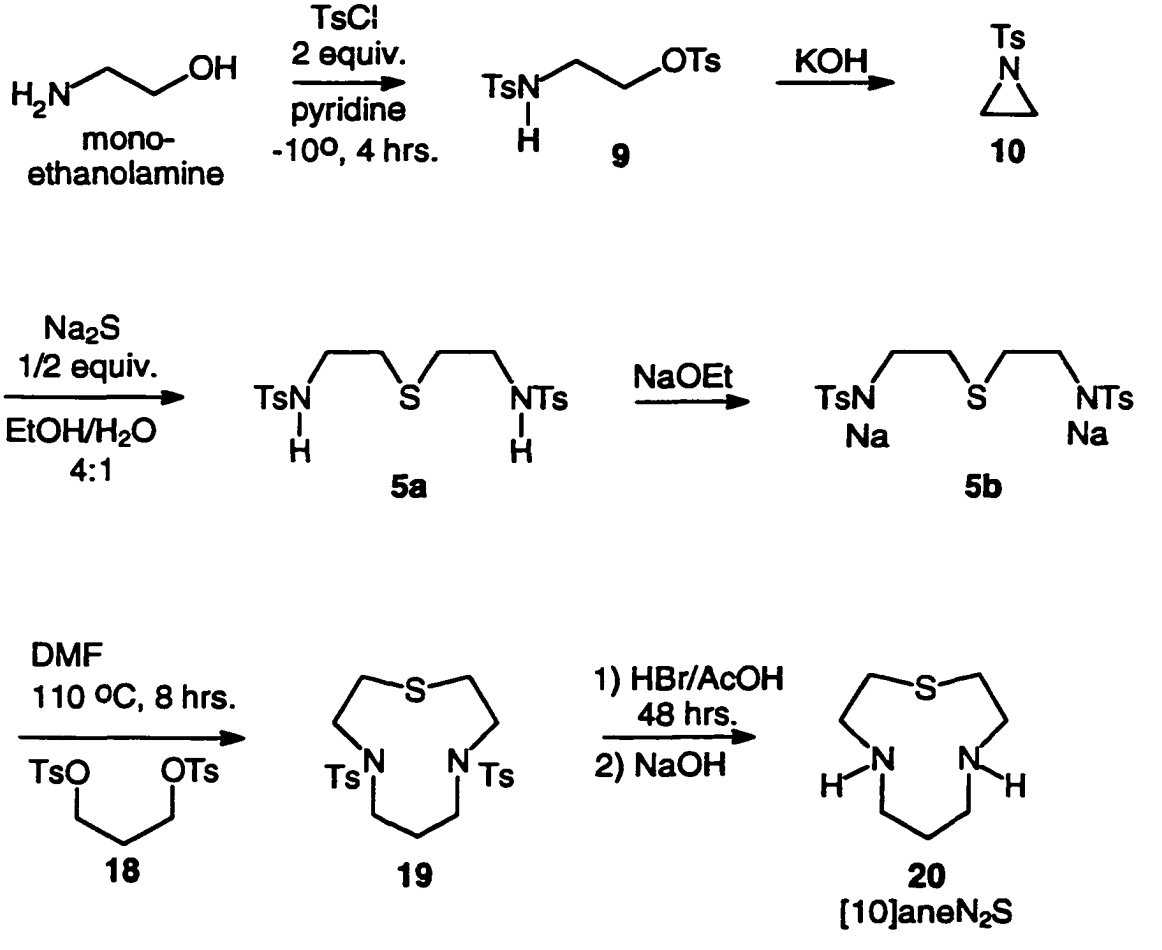

Scheme 3.1. Synthesis of [10]aneN$_2$S using Richman and Atkins methodology.

Several attempts at synthesizing [10]aneN_2S using that procedure met with varying success. Although the synthesis was found to give a 70% cyclization yield when working optimally, it was found that the synthesis failed on the order of two out of every three attempts. Steps were taken to identify the factors involved.

The most important variable affecting the success of the synthesis was determined to be the variation in the quality of the dimethylformamide (DMF) solvent used for the cyclization. The reason the synthesis was considered to have failed frequently was because of the presence of a specific side product in varying proportions. The only purification carried out in the work-up of a Richman and Atkins cyclization procedure consists of washing the water insoluble tosylated product(s) with water followed recrystallization from ethanol. If the cyclization produced mostly the intended product, the work-up was sufficient for the isolation of the intended product. The first batch of white solid isolated would be the N,N'-ditosylated [10]aneN_2S. The second and third batches isolated would contain increasingly larger amounts of the reaction byproduct, tosic acid. Batches containing too much tosic acid were not included.

Although the DMF solvent was purified by distillation before reaction, it was found that if the initial DMF solvent was impure, the resulting distillate was still impure. When the cyclization reaction was carried out with the impure DMF, a specific side product formed. After the work-up and recrystallization, ^{1}H-NMR and ^{13}C-NMR spectroscopy of the resulting white solid showed the presence of the intended ditosylated [10]aneN_2S product and the side product as well. The more impure the DMF was, the more the side product had formed. Mass spectroscopy of the mixture was unsuccessful at determining the molecular weight of the side product.

Several attempts at separating the mixture by column chromatography over silica gel (15% ethyl acetate in toluene) resulted in the isolation of 10% of the side product seen in the original mixture. Previously, a similar side product had been observed in the synthesis of N,N'-ditosylated [9]aneN_2S via the same method; however, in that case, the two products did not separate when chromatographed over silica gel. Once purified, the

identity of the side product was established by NMR and mass spectroscopy to be the 8-membered N,N'-ditosylated cyclization product, **21**. The ^{1}H-NMR spectrum consisted of: four aromatic peaks at 7.60, 7.56, 7.32 and 7.28 ppm, and one methyl peak at 2.41 ppm which are diagnostic of the presence of a tosyl group; two triplets at 3.55 ppm and 2.94 ppm which correspond to that expected for the -CH_2-CH_2- chain between the sulphur and nitrogen heteroatoms; and one singlet at 4.57 ppm which was presumably another methylene group. The integrations were consistent with the assignment made. The ^{13}C-NMR spectrum consisted of: four atomatic methine carbon peaks at 144.0, 136.3, 130.0 and 127.4 ppm, and one methyl peak at 21.5 ppm which are diagnostic of the presence of one tosyl group; two -CH_2- peaks at 32.7 and 48.8 ppm which correspond well to that expected for the -N-CH_2-CH_2-S- group; and one additional -CH_2- peak at 63.8 ppm which did not correspond to any of the chemical shifts reported for the intended product **(19)**.

The only reasonable mechanism for the formation of such a side product would be if the linear reactant, N,N'-ditosylated bis(aminoethyl)sulphide **(5b)** was cyclizing with formate rather than the intended propylene glycol ditosylate **(18)**. The impure DMF contained relatively high percentages of dimethylammonium formate, formed by cleavage of the DMF molecule (especially when exposed to light in the presence of oxygen for long periods of time). Titrations of the DMF used in this work (before and after distillation) revealed the presence of significant amounts of dimethylammonium formate[110]. In some cases, up to 10% dimethylammonium formate was present. Also, it was observed that diethylammonium formate distilled over with DMA. Since the Richman and Atkins methodology requires the ditosylated propanediol **(18)** to be added dropwise slowly, the relative amount of **18** present in solution at any given time was much less than the formate. This effect accounts for why the diamine **5b** reacted with the formate despite the fact that **18** is a more reactive electrophile.

Further evidence of this effect was provided by carrying out the same reaction in dimethylacetamide (DMA) solvent. It had been found by T. James and co-workers[110] that

DMA contains much less of the dimethylammonium acetate decomposition product than DMF.

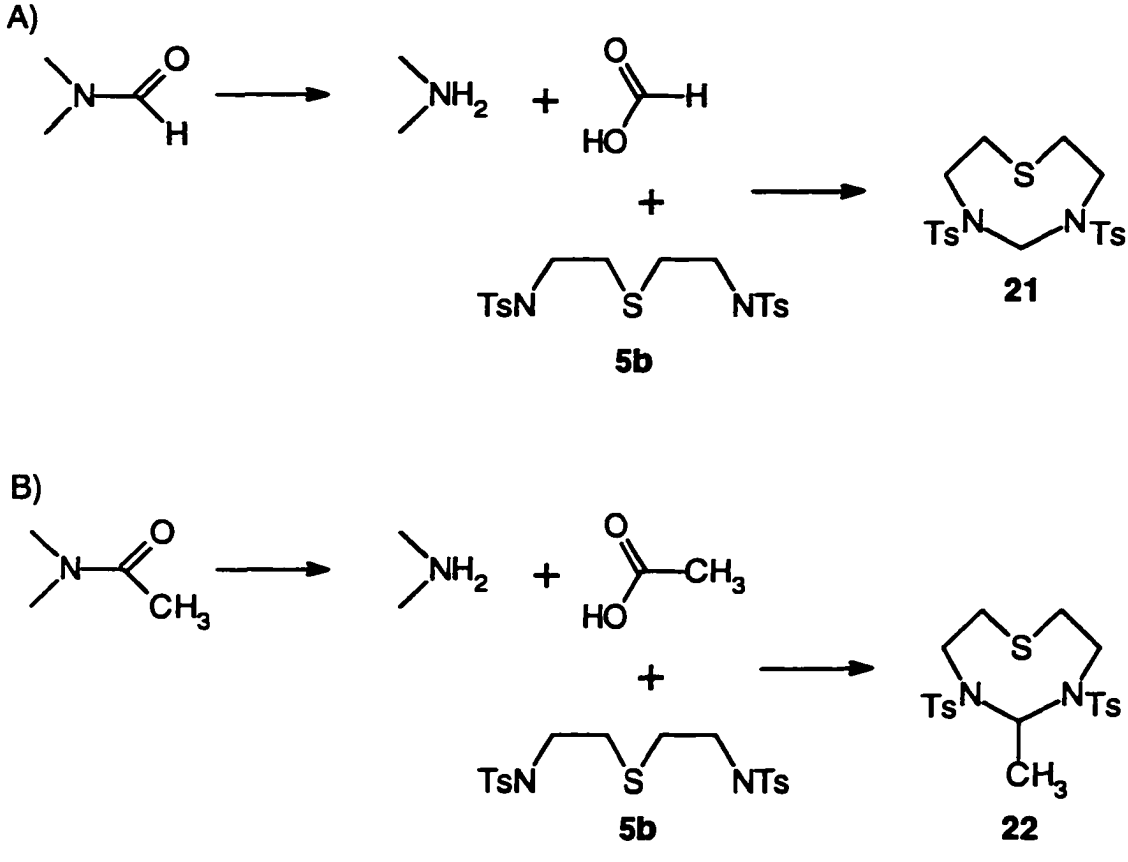

Figure 3.1. Cyclization of bis(aminoethyl)sulphide with formate (a) and methyl formate (b) to give [8]aneN_2S (**21**) and **22** side products.

A macrocyclic synthesis carried out in their laboratory had also started to fail due to the poor quality of the DMF purchased from the Aldrich Chemical Company, Inc. The use of DMA instead of DMF solved the problem. When the synthesis of N,N'-ditosylated

[10]aneN_2S **(19)** was carried out in DMA as the solvent, it was found that the acetate cyclization product **(22)** was obtained as a side product in a 1.5 : 1 ratio to the product. The result strongly implied that the solvent must have been cyclizing with **5b**. Although column chromatography over silica gel facilitated the isolation of small quantities of the product and side product(s), it was not effective enough to separate the bulk mixture. Not enough of the desired product **19** was ever isolated to carry on with the detosylation step. In retrospect, it has been pointed out[111] that the decomposition of the DMF and DMA solvents was probably enhanced by the method of distilling over calcium hydride. It is necessary to use a strongly reactive drying agent because traces of water in the reaction solvent prevent the reaction from working. However, DMF and DMA are too easily broken down by hydride. A milder drying method such as molecular sieves should be tried in the future.

No mention of such a cyclization with formate had been seen in the literature at the time, however, a report by G. Bradshaw[112] was later published which described the occurrence of similar single methylene cyclizations when preparing diaza polyether cryptands.

Even when the cyclization step worked optimally, the subsequent detosylation step tended to give variable yields as well. The optimum yield was found[109] to be 46%. Much lower yields were often encountered but the factors involved could not be easily determined. The greatest source of difficulty was the fact that thioethers are much more acid sensitive than the more commonly used ether and aza groups.[113] For example, triazacyclononane ([9]aneN_3) tritosylate can be detosylated in relatively good yield by several methods. One such method consists of refluxing the tritosylate in conc. sulphuric acid with phosphorous pentoxide added as a drying agent.[112] In this work, attempts at detosylating [9]ane and [10]ane N_2S ditosylates under identical conditions gave only decomposed material after 20 min. of refluxing, and only unreacted tosylated material was recovered if the reflux was conducted for less than 20 min.

Despite these problems, it was still feasible to synthesize the target [10]aneN_2S via these methods. However, these problems caused the preparation of large quantities of [10]aneN_2S to take much longer than desired. Previously, 9- to 12-membered rings synthesized by the Richman and Atkins methodology were used only for preparing various metal complexes. Large (> 10g) quantities were therefore not a necessity. The intention of using [10]aneN_2S as a starting material for the multistep synthesis of the N_4S-bicyclic target ligand required a more reproducible and less time consuming preparation. There was also an interest in avoiding the use of large quantities of carcinogenic tosylates.

3.2. Synthesis of [10]aneN_2S (20) Via Acid Chloride Methods:

3.2(a). Introduction:

The syntheses of small (9- to 12-membered) macrocycles reported in the literature usually employ the Richman and Atkins methodology. This is because the various other cyclization methods have not been as successful. Smaller, linear tridentate reactants do not coordinate transition metals in a well-defined planar geometry suitable for a template condensation. There are few ether donors present such that they tend not to bind alkali metals strongly enough for template assisted ring closure either. The smaller, linear reactants tend not to be rigid, or "pre-organized", and direct methods require the elaborate high dilution techniques.

A review of the literature[83] suggests that the synthetic yields of small macrocycles via direct methods are lower than that of their larger analogues. Indeed it has been shown[114] that relative rates of ring closure of cyclic monoamines reach a maximum for 6-membered rings, then drop by three or four orders of magnitude for 8- to 10- membered rings. The same general trend is observed for several types of ring closures. The various ring closure reactions all show some consistent features. The $\Delta H^{\ddagger}$ for three- and four-

membered rings is normally much higher than five- and six-membered rings while $\Delta S^{\ddagger}$ is smaller. The higher $\Delta H^{\ddagger}$ values reflect the fact that small three- and four-membered rings have large ring strain energies as a result of the unusually low bond angles involved. As the ring size increases from three to seven, the $\Delta S^{\ddagger}$ term remains relatively similar then decreases beyond seven members, reflecting the relative improbability of achieving the desired molecular orientation for ring closure.

There has been much discussion in the literature[116] that attributes the success of the Richman and Atkins reactivity to pre-orientation effects induced by the tosylate groups which result in lower cyclization entropies. However, relatively recent reports have focused on finding improved synthetic methods. An elegant example involves cyclization across two nitrogens of various guanidines followed by elimination of the single 'template' carbon atom[117]. The synthesis is however, limited to the preparation of triaza rings and cannot be modified to include thioethers. Another successful alternate method of preparing small macrocycles reported in the literature[118] is the double amidation reaction. This method gives reasonable yields (20% - 35%) and does not require high dilution conditions. The starting materials used by this method for aza and oxo macrocycles are inexpensive, however the bis(aminoethyl)sulphide starting material required for the synthesis of [10]aneN_2S via a double amidation is too expensive for large scale use. The material can be prepared relatively easily but it was desired to develop a synthesis that would avoid any unnecessary steps.

Although there are numerous reports[74,84] of syntheses of slightly larger (>10 members) aza, ether and thia macrocycles using acid chloride reactants, no results concerning the synthesis of smaller rings using acid chlorides have been found. Given that such reactions employ the most benign conditions for sulphur containing ligands and the starting materials required were inexpensive and readily available, it was decided that the synthesis was worthy of attempting. The general reaction scheme is shown in scheme 3.2. Thiodiglycolic acid chloride (**15**) was prepared as described in section 8.2. The reaction

was conducted with three different bases: K_2CO_3, NEt_3 or an additional equivalent of diaminopropane. Each of these three conditions will be reported separately.

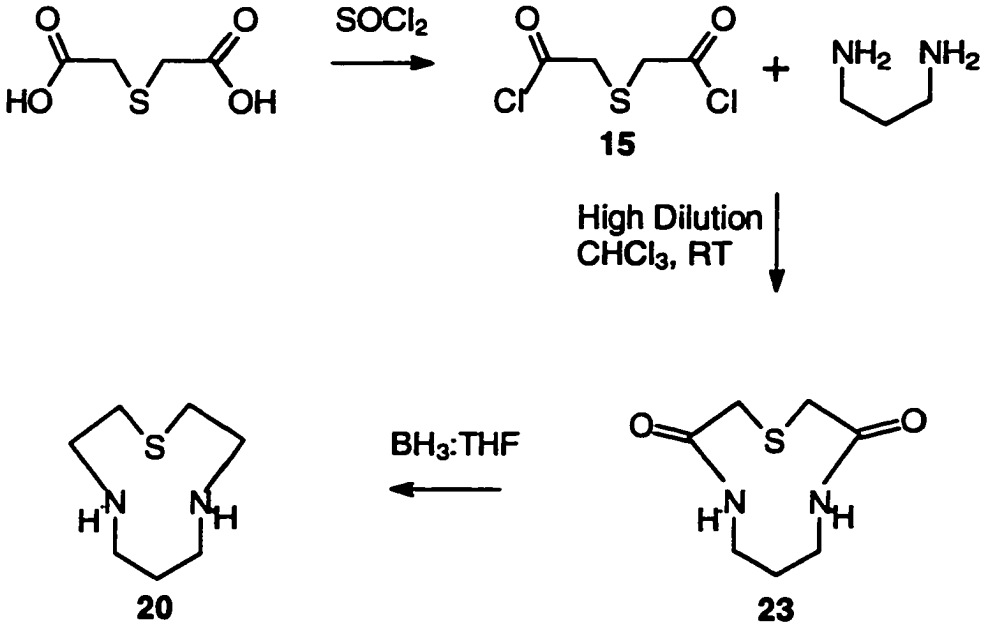

Scheme 3.2. Generalized synthetic route to [10]aneN_2S (**20**) using acid chloride reactivity.

3.2(b). Attempted synthesis of [10]aneN$_2$S via K_2CO_3 and amine: acid chloride (2:1) methods (moderate stirring conditions):

i) Cyclization of diaminopropane with thiodiglycolic acid chloride:

The synthesis of 1-thia-4,8-diazacyclodecane-3,9-dione (10aneN$_2$S diamide) was first attempted by reacting diaminopropane and thiodiglycolic acid chloride in equimolar amounts (using the high dilution procedure reported in section 8.1c) in the presence of excess potassium carbonate. The first solvent chosen was DMA. As mentioned in section 2.5, DMF and DMA are, in principle, ideal solvents for promoting cyclization of polar amine ligands. However, the thiodiglycolic acid chloride was observed to decompose into many uncharacterizable species within minutes of being dissolved in such solvents. Surprisingly, after evaporating the DMA reaction solution in vacuo and recrystallizing the crude solid from ethanol, the reaction yielded a small amount of precipitate which was shown by NMR and mass spectroscopy to be the intended [10]aneN$_2$S diamide (**23**) in high acceptable (see figure 3.2). The product yield was 0.7% which was much too small. Toluene was also tried as the solvent but the yield was too low also.

Since both reagents were soluble and stable in chloroform, the reaction was tried on a similar scale with chloroform as the solvent and potassium carbonate as the base. The reaction was initially conducted four times with only moderate stirring conditions, as reported in section 8.5. The procedure reported in section 8.5 does not contain the final optimized conditions but is merely presented for the benefit of the ensuing discussion about why these conditions were not as effective.

There were several products present (including the [10]aneN$_2$S diamide) and no evidence of polymer. The ^{13}C-NMR spectra of the crude cyclization mixtures using the potassium carbonate and 2:1 (amine : acid chloride) methods are shown in figures 3.3(a) and 3.3(b) respectively. The 2:1 (amine : acid chloride) method was identical except that

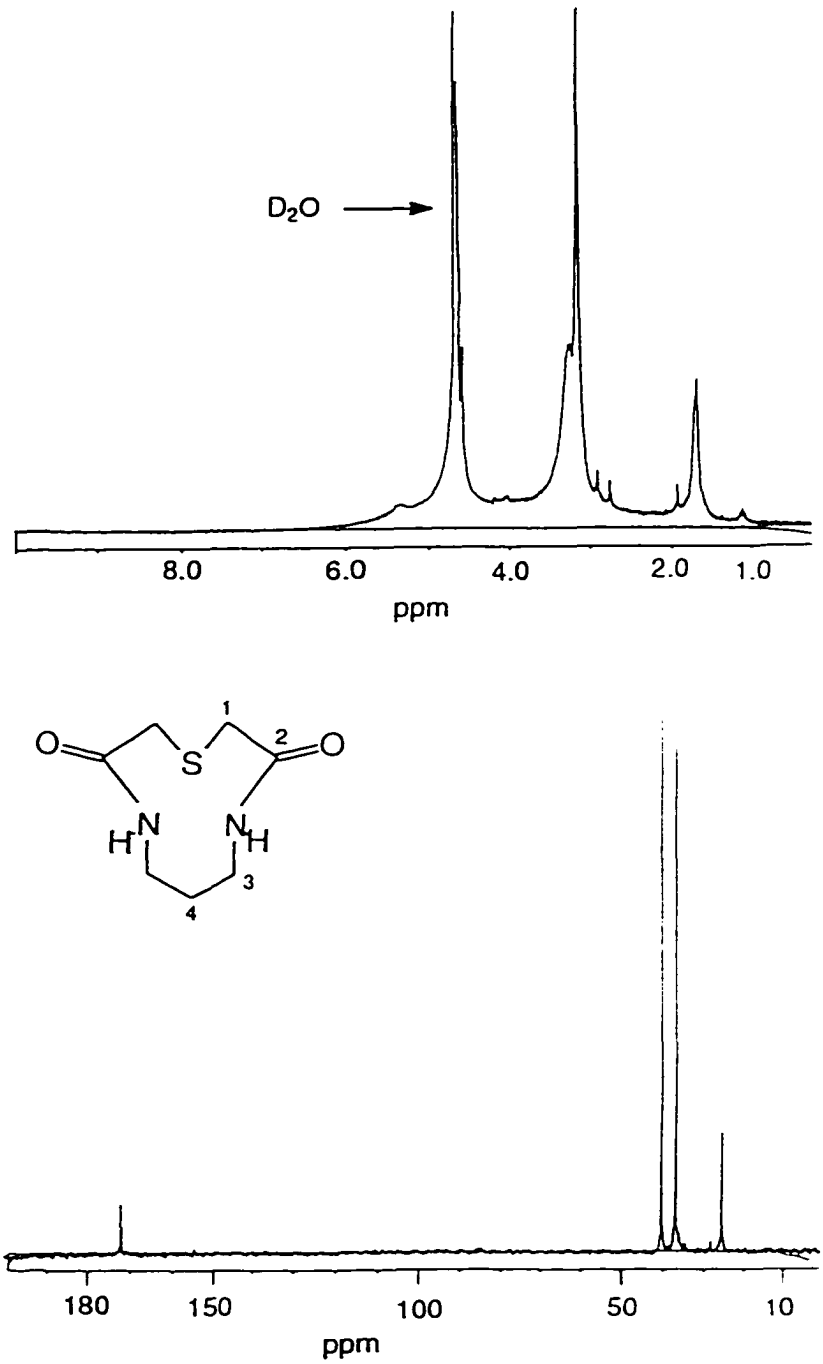

Figure 3.2. ^{1}H-NMR (top) and ^{13}C-NMR (bottom) of purified [10]aneN_2S diamide **(23)** using DMF as the cyclization solvent.

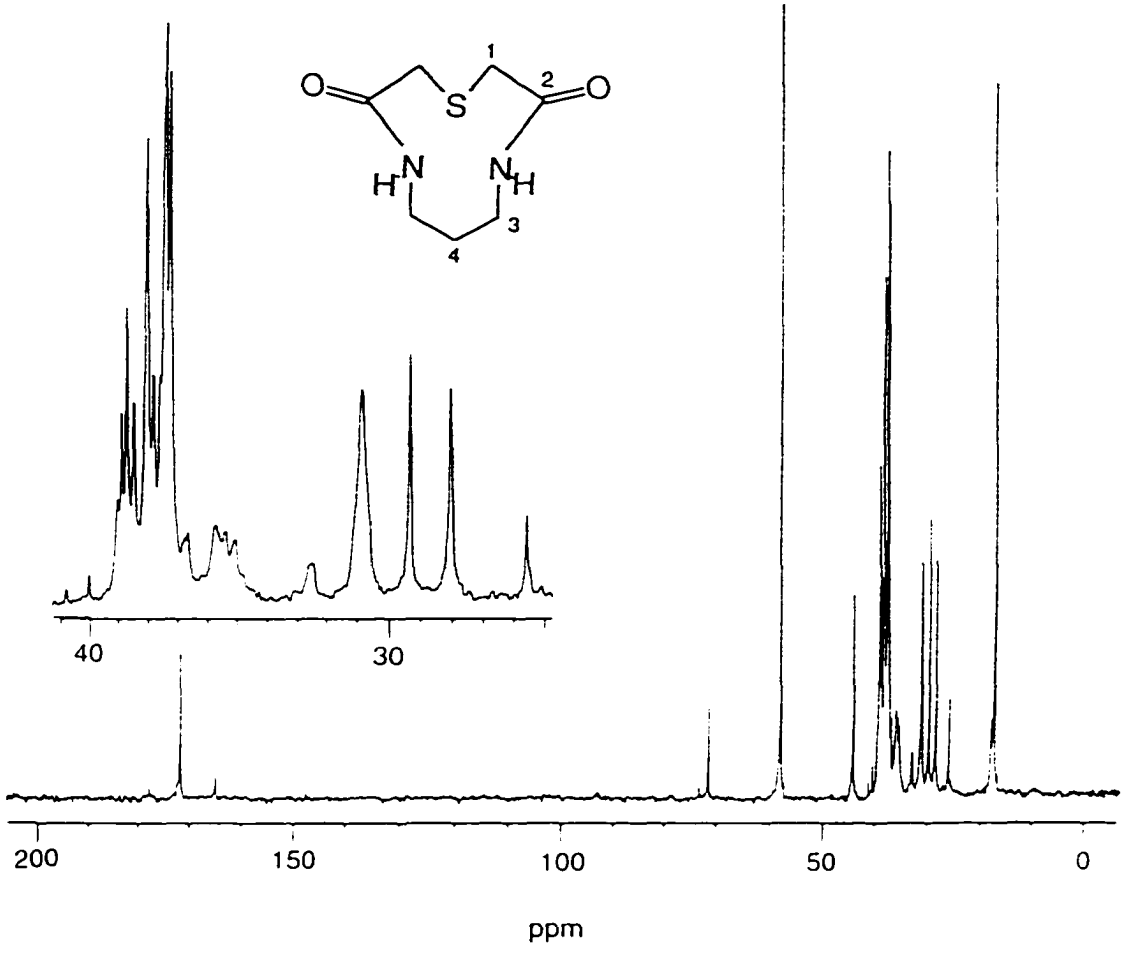

Figure 3.3(a). ^{13}C-NMR of crude [10]aneN_2S diamide **(23)** mixture using K_2CO_3 as the base.

two equivalents (8.88 g, 0.06 mol) of diaminopropane were used instead of adding potassium carbonate. Attempts at purifying the crude amide mixture by chromatography over silica gel failed. Mass spectroscopy of the mixture exhibited peaks corresponding to the M+1 (189 m/e) and M+29 (217 m/e) of the product. The crude mixture was therefore reduced without purification.

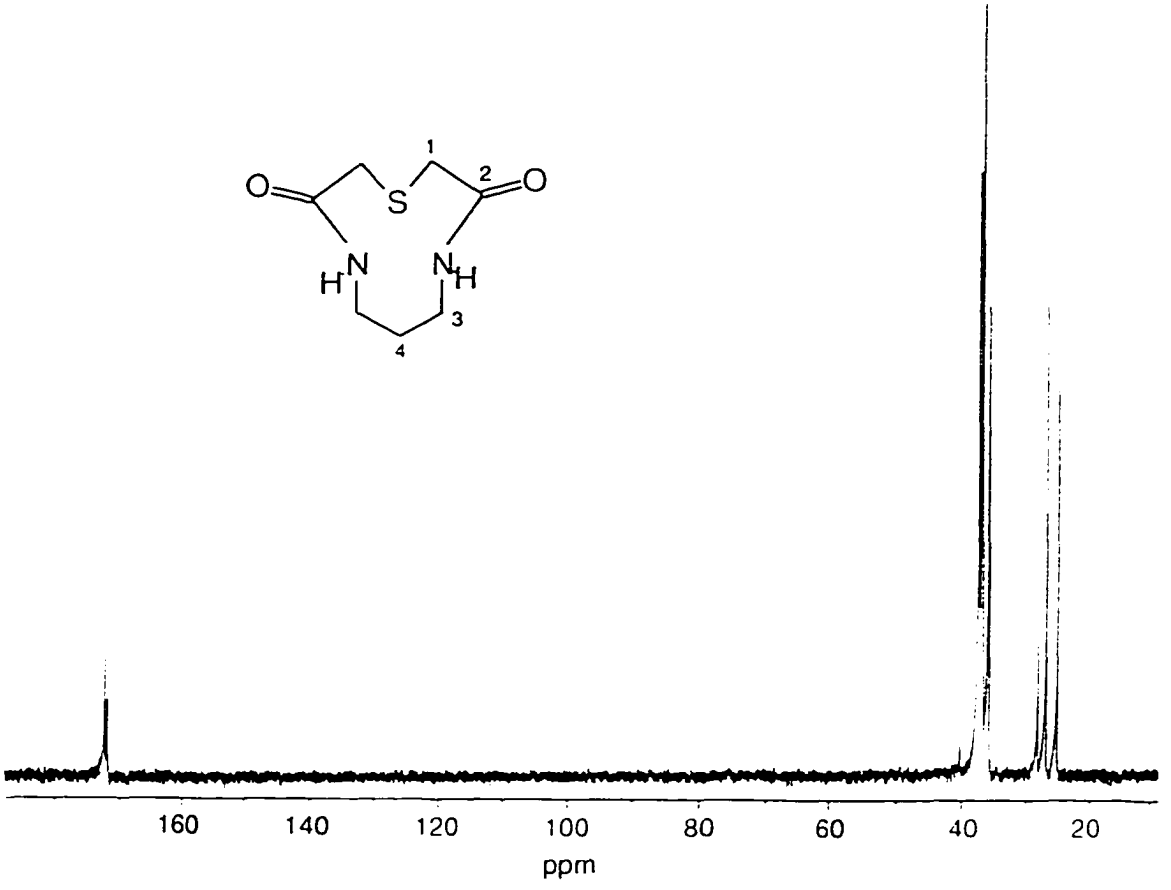

Figure 3.3(b). ^{13}C-NMR of crude [10]aneN_2S diamide **(23)** mixture from reaction of 2 equiv. diaminopropane with thiodigylcolic acid chloride.

After the borane reduction, most of the undesired products could be removed by vacuum distillation. The ^{13}C-NMR spectrum of the crude reduction mixture when potassium carbonate was used as the base is shown in figure 3.4(a), along with the spectrum recorded after removing an uncharacterizable product(s) by vacuum distillation. The ^{13}C-NMR spectra of the crude and vacuum distilled reduction mixtures from the 2:1 (amine : acid chloride) are shown in figures 3.5(a) and (b) respectively.

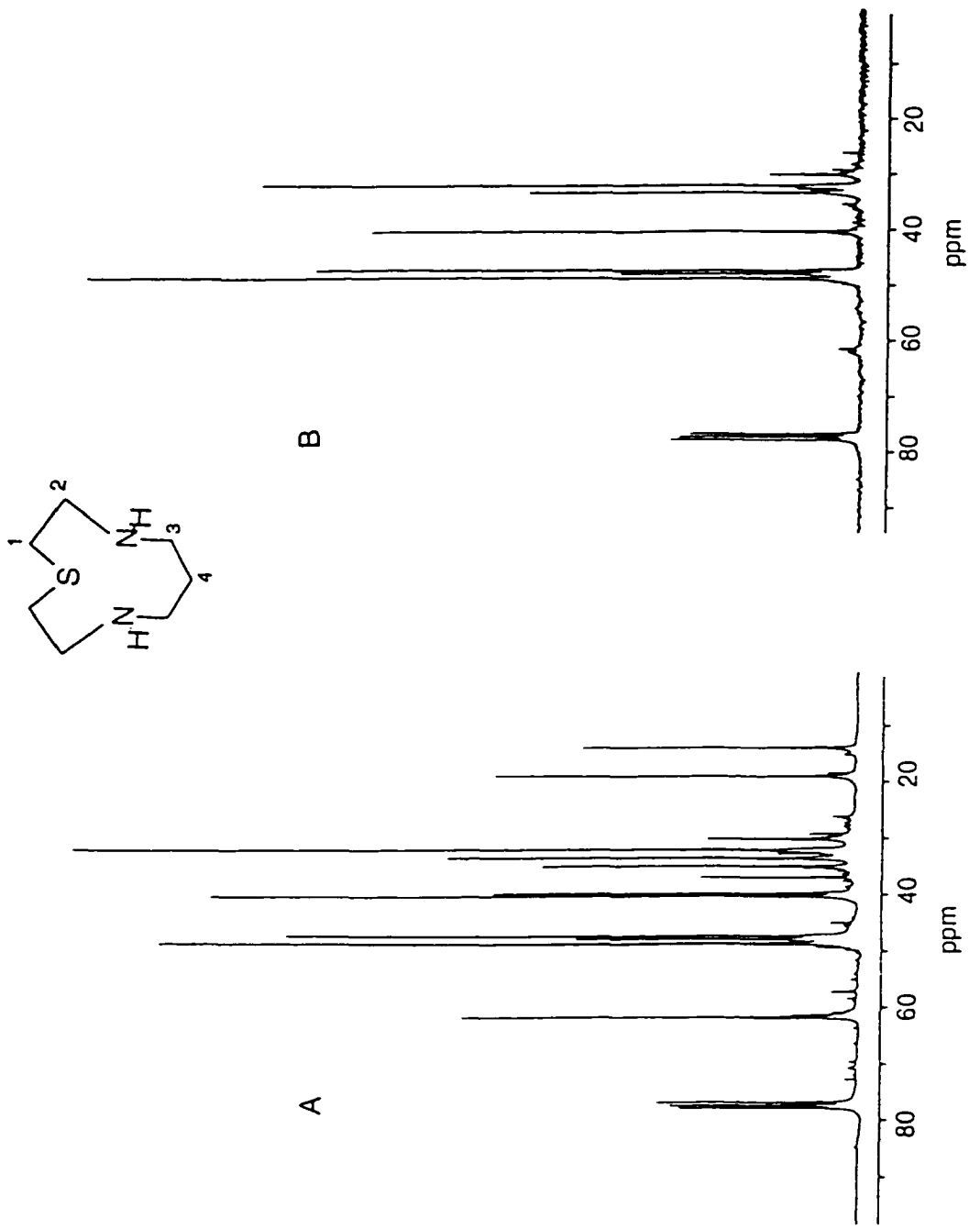

Figure 3.4. ^{13}C-NMR spectra of [10]aneN_2S **(20)** reduction mixture (K_2CO_3 method). A: crude mixture. B: same sample after vacuum distillation.

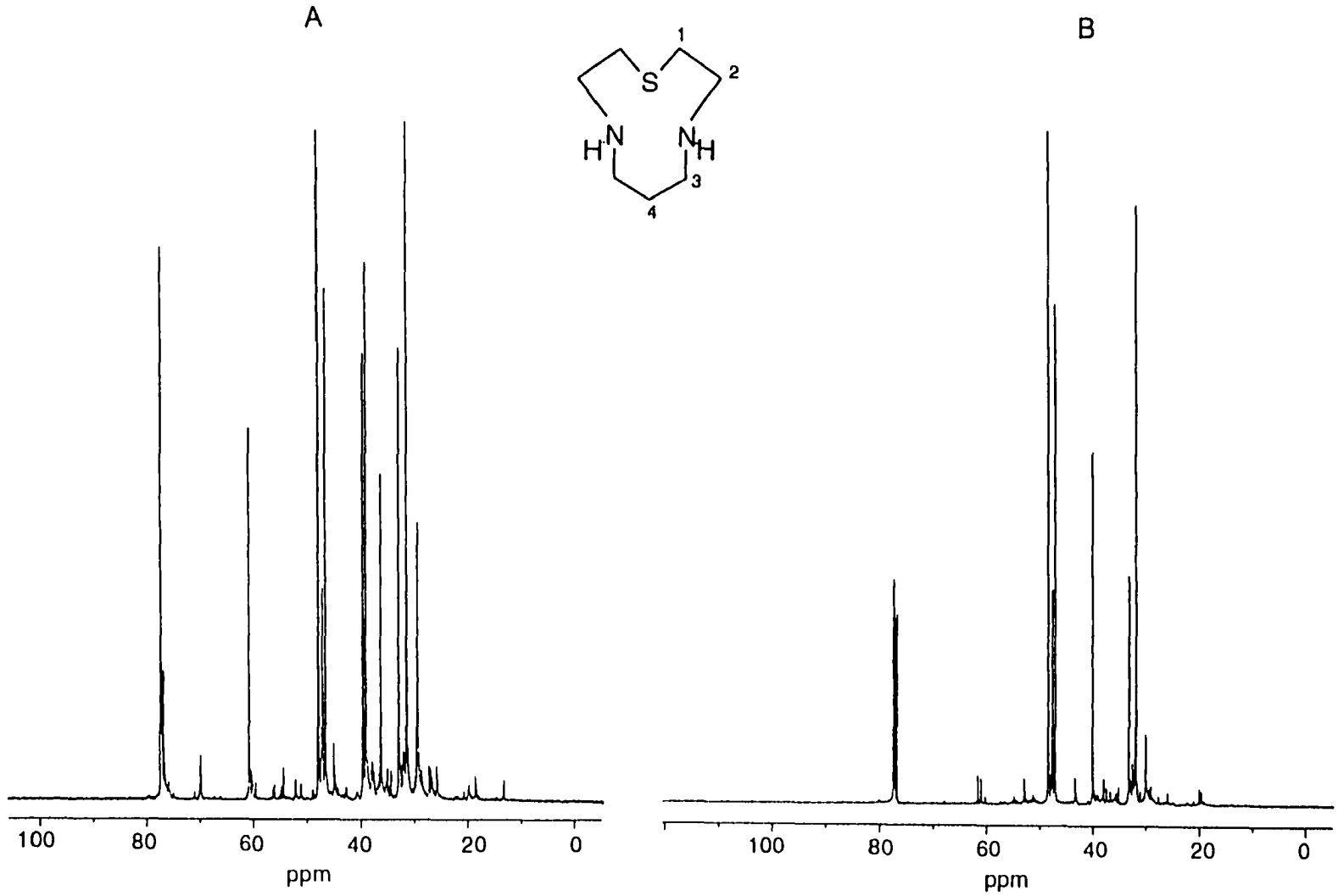

Figure 3.5. ^{13}C-NMR spectra of [10]aneN_2S **(20)** reduction mixture (2:1 method).

A: crude mixture. B: same sample after vacuum distillation.

ii) Attempts at purification of [10]aneN$_2$S (20) reaction mixture:

As can be seen in figures 3.4 and 3.5, the crude reduction mixtures were not acceptably purified by vacuum distillation. Further purification of these mixtures was achieved by synthesizing the corresponding metal complexes and chromatographing over sephadex CM-C25 cation-exchange packing. Initially, copper(II) was used as the coordinating metal, however, it was observed that the blue, six-coordinate $[Cu(\mathbf{20})_2]^{2+}$ complex converted into a green uncharacterizable form within minutes (or hours in some rare cases). The green material was relatively insoluble and did not separate as distinct, well-behaved bands when chromatographed over the sephadex. Usually, exposure of the blue complex to the sephadex column packing caused the complex to revert to the green form immediately. Exposure of the blue complex to heat also caused immediate conversion to the green form. Addition of base (NaOH), high salt concentrations or dissolution in ethanol were also observed to induce the conversion.

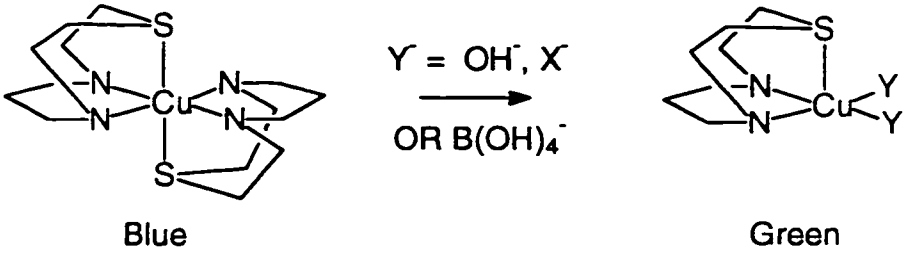

Figure 3.6. Displacement of [10]aneN$_2$S **(20)** from $[Cu(\mathbf{20})_2]^{2+}$ by coordinating anions.

It has been reported[126] that a green form of copper(II) complexation results when the copper to ligand ratios are non-stoichiometric. This situation can result when the coordinating amine ligands are not able to encapsulate the copper. In the case of cyclam, there are four amine donors locked by the macrocycle into a square planar arrangement around the copper(II) center. The metal is sufficiently encapsulated such that no degradation of the initial violet square planar complex is observed. In the case of [10]aneN_2S, the ligand can only coordinate in a facial tridentate geometry such that, given the fast self-exchange rate of copper(II), the copper can easily reorganize to bind in a different geometry. More specifically, it is believed that the copper(II) center is more stable if it loses one of the [10]aneN_2S ligands so that it can adopt a preferred five-coordinate geometry. The proposed mechanism is outlined in figure 3.6.

It was observed that the violet six-coordinate $[Ni(\mathbf{20})_2]^{2+}$ complex was robust enough to be easily chromatographed over sephadex CM-C25 packing. Two major bands were eluted using 0.1M $NaClO_4$. Both complexes were characterized by UV/VIS spectrophotometry and microanalysis. The nickel(II) was removed from each band with either Na_2S or NaCN and the free ligand extracted into chloroform. The free ligands were characterized by ^{1}H-NMR and ^{13}C-NMR spectroscopy, gas chromatography and mass spectroscopy.

The ^{13}C-NMR spectra of the two ligand products are shown in figures 3.7 and 3.8. The spectrum of the ligand obtained from the first band eluted off the column of sephadex contained four major product peaks (figure 3.7). A ^{13}C-DEPT experiment verified that all the peaks were methylene carbons, as expected for the product. The ^{1}H-NMR and ^{13}C-NMR chemical shifts were within experimental error of those already reported[109] for [10]aneN_2S. Mass spectroscopy gave the M+1 (161 m/e), M+29 (189 m/e) and M+41 (201 m/e) peaks expected for [10]aneN_2S. The UV/VIS and microanalytical data also corresponded to that reported for $[Ni(10aneN_2S)_2](ClO_4)_2$. The side product obtained is believed to be the 2:1 (diaminopropane to thiodiglycolic acid chloride) condensation product (**24**). The propyl chain is no longer symmetric in this product so there are five

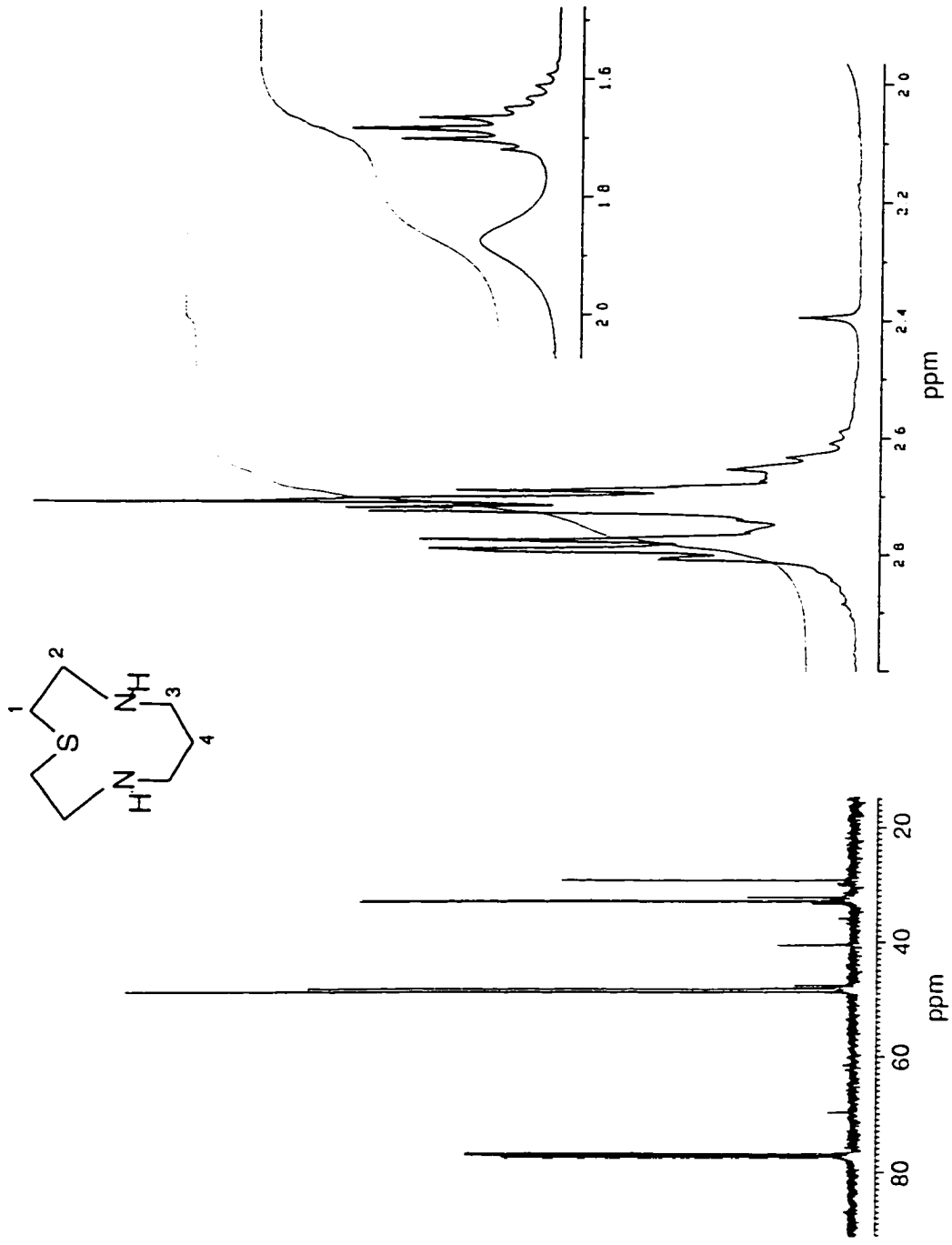

Figure 3.7. ^{13}C-NMR and ^{1}H-NMR spectra of [10]aneN_2S (**20**) after chromatography of nickel(II) complex over sephadex CM-C25 packing.

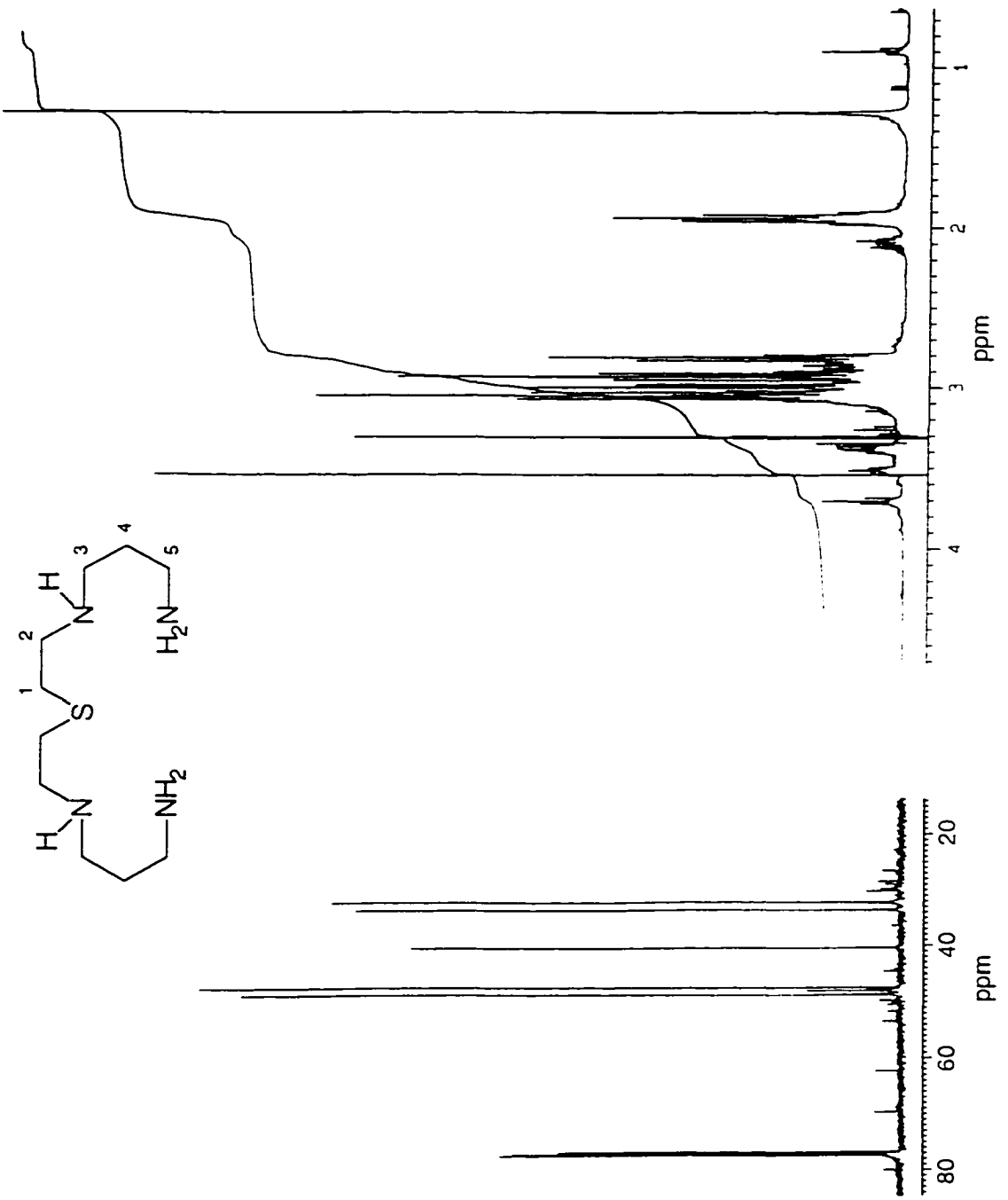

Figure 3.8. ^{13}C-NMR and ^{1}H-NMR spectra of [15]aneN$_4$S linear side product (**24**) after chromatography of nickel(II) complex over sephadex CM-C25 packing.

peaks of equal intensity in the ^{13}C-NMR spectrum (figure 3.8): 32.1, 33.5, 40.3, 47.3 and 48.6 ppm. The ^{1}H-NMR consisted of four triplets and one quintet as expected for such a side product. Mass spectroscopy gave the M+1 (235 m/e) and M+41 (275 m/e) peaks expected. Microanalysis of [Ni(**24**)]$(ClO_4)_2$ also supported this assignment.

As can be seen in the ^{13}C-NMR spectra in figures 3.7 and 3.8, the mixture of [10]aneN_2S and N_4S linear side product was not completely purified by the chromatography over sephadex. In fact, there is contamination of a small amount of each product with each other. This was presumably because the nickel(II) ion does not completely bind the various products in a well behaved (stoichiometrically integral metal-to-ligand ratios) fashion. Because the [10]aneN_2S ligand is only tridentate and therefore only partially encapsulates the metal center, complexes can form in which more than one product can bind to the nickel(II).

The most obvious method of purifying the free ligand mixture would be normal phase chromatography over silica gel. However, primary and secondary amine ligands are known to bind to silica gel such that chromatography is not possible. Silica gel is acidic, which causes the amine to precipitate out of the organic solvent used as the mobile phase. There have been some reports that chromatography over basic alumina avoids these problems. Attempts at chromatographing the [10]aneN_2S mixture over silica and basic alumina using a variety of solvents met with no success. More recently, there have been several reports in the literature[112] in which polyaza and crown ether macrocycles (containing secondary amines) were successfully separated by chromatography over silica gel and alumina by adding ammonium hydroxide to the eluent. The amounts of ammonium hydroxide used (5 - 40 %) were sufficient to prevent the amine from precipitating out, yet there was apparently not enough to deactivate the silica. These methods were tried with the [10]aneN_2S mixture. However, no effective separation occurred.

High performance liquid chromatography (HPLC) has been a very successful method of separating many types of mixtures.[119] Indeed, the [10]aneN_2S mixture was separated by reverse phase (C18) HPLC. The eluent was a mixture of

chloroform/acetonitrile (90 : 10 ratio which was slowly ramped up to a 60 : 40 ratio after loading the sample). Although the method was successful using an analytical HPLC column which can only separate small amounts (less than 10 mg), unsurmountable practical difficulties were encountered when trying to use a large scale preparative column.

Separation of amine mixtures was achieved by reverse phase chromatography over an octadecyl functionalized silica gel column packing (Aldrich) designed for medium pressures. Reverse phase chromatography allows one to use polar and/or aqueous solvents as the mobile phase such that precipitation of amines does not occur. Methanol/NH_4OH (80 : 20) was used as the eluent. The side product **24** and another side product, the semi-reduced monoamido [10]aneN_2S, were isolated in acceptable purity. No [10]aneN_2S eluted from the column which suggested that the amines still precipitated despite the use of a polar mobile phase.

Attempts at separating the mixture as the corresponding HBr salts by recrystallization and chromatography over DOWEX 50 X 8 cation-exchange packing, managed to only partially separate the mixture.

3.2(c). Synthesis of [10]aneN_2S and Boron complex using NEt_3 as base:

The reaction of diaminopropane with thiodiglycolic acid chloride using triethylamine as the base is reported separately because of the unusual nature of the side product produced by this reaction. There have been many reports in the literature of using triethylamine to neutralize the HCl generated by a cyclization reaction involving an acid chloride. One such report involves the cyclization of dimethyl cyclen with 3,3'-thiodipropionic acid chloride[97] which is a very similar reaction to the [10]aneN_2S synthesis.

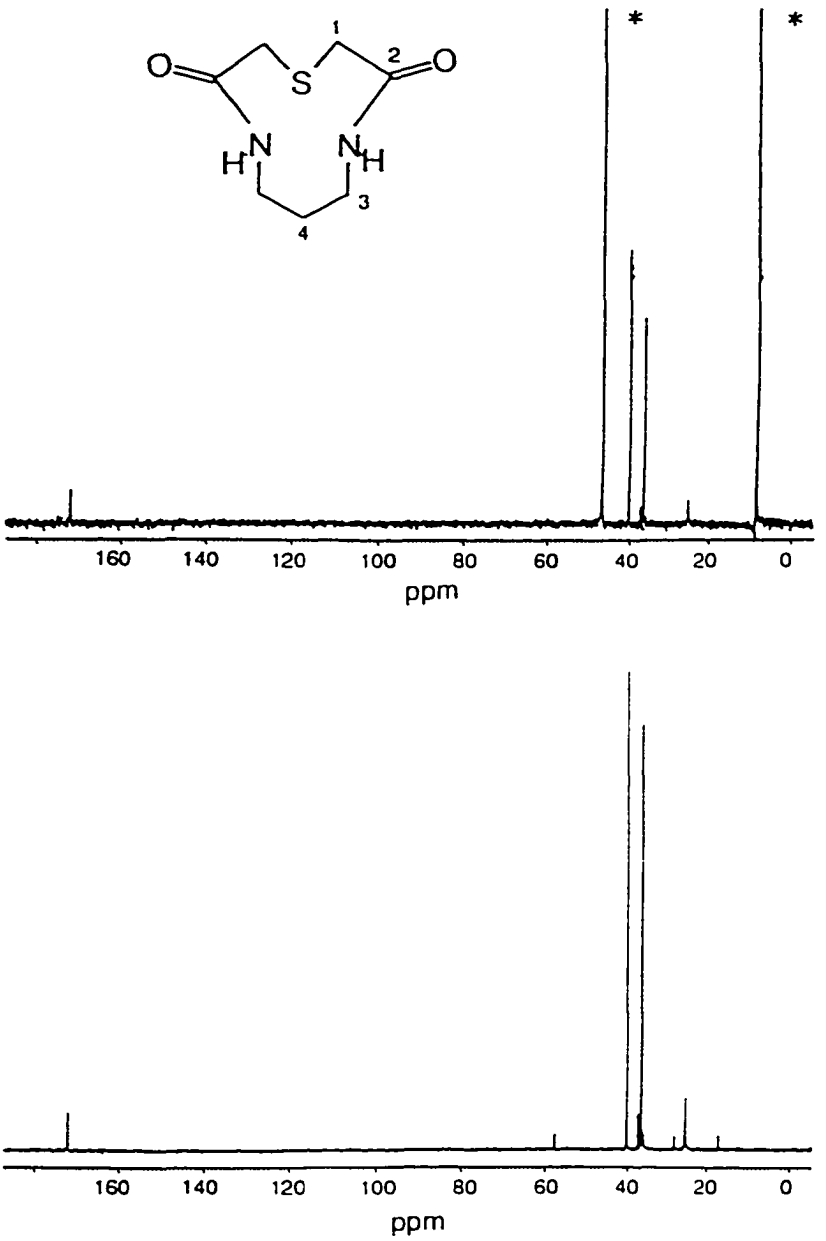

Figure 3.9. ^{13}C-NMR and ^{1}H-NMR spectra of [10]aneN_2S diamide **(23)** before (top) and after (bottom) purification by chromatography over DOWEX cation-exchange packing. * = triethylamine base used to neutralize HCl.

The synthetic procedure was identical to that described for the K_2CO_3 reaction (section 3.2(b)) except that 2.5 equivalents of triethylamine were added dropwise along with the diaminopropane (4.44 g, 0.06 mol) reactant, instead of adding K_2CO_3. Considerable brown polmeric solids were formed in the reaction and removed by filtration. It was interesting that so much polymer formed considering the fact that none formed during the 2:1 syntheses in which the base used was simply another equivalent of diaminopropane. The white solid (8.64g) isolated from the crude reaction filtrate was shown by ^{13}C-NMR (figure 3.9) to be pure [10]aneN_2S diamide and triethylamine. The triethylamine was removed by dissolving the mixture in 25 mL pH 2 - 3 deionized water and chromatographing over DOWEX 50 X 8 cation-exchange packing (see figure 3.9). The first 100 mL of eluent were collected and taken to dryness on a rotary evaporator then dried further in vacuo. ^{13}C-NMR (figure 3.9) of the resulting 3.32 g of white solid showed that all of the triethylamine had been removed by the DOWEX packing. The yield of [10]aneN_2S diamide **(23)** was 29%. It is also important to note that the yields quoted here are those found after the stirring conditions and reagent addition methods were improved. The stirring speeds were in the 1000 - 1200 rpm range.

With an acceptable yield of [10]aneN_2S diamide at hand, the diborane reduction was carried out. The same borane reduction procedure reported above for the K_2CO_3 methods was followed. This procedure was inherited from previous work in this laboratory[120] and was the same as that reported in the literature[97] for reductions of similar compounds. The ^{13}C-NMR spectrum of the resulting pale brown oil is shown in figure 3.10. Although there were four methylene peaks in the ^{13}C-NMR as expected, the pattern and chemical shifts did not correspond at all to the known spectrum for [10]aneN_2S **(20)**. Likewise, the ^{1}H-NMR spectrum showed two quintets at 1.4 ppm when only one should have been present and the triplets did not have the same chemical shift pattern expected for [10]aneN_2S. Although the product was quite pure, mass spectroscopy did not show any M+1, M+29, M+41 patterns such that the molecular weight remained undetermined. The IR spectrum did not show any unusual features other than the lack of strong NH

absorptions that would have been expected for the product. The NMR and IR spectra clearly indicated that the amide functions had been completely reduced. Also, the ligand must still have been intact because any degradation or cleavage would destroy the plane of symmetry in the ligand and would result in there being more than the minimum four peaks present in the NMR spectra. It was also observed that the product would not complex to copper(II) or nickel(II).

The synthesis was repeated. After refluxing the amide in 1M BH_3•THF, one fifth of the solution was worked-up immediately and characterized by NMR. Although not perfectly pure, the desired [10]aneN_2S product was present in good yield. When the rest of the reduction mixture was worked up one day later, the major product present was the same unidentified material as from the previous synthesis. It was therefore surmised that the properly reduced [10]aneN_2S ligand was forming but was coordinating the borane reagent too strongly for the HCl reflux to remove it. Coordination of boron would explain why the NMR patterns were different even though the ligand was still intact. It would also explain why the ligand could no longer coordinate transition metals.

To determine if such a boron coordinated species was present, ^{11}B-NMR spectra of the product samples were recorded. The spectra are displayed in figure 3.10. There was a significant peak at -0.1 ppm. If the boron coordinated ligand was properly hydrolyzed by the HCl reflux, then there should only be polyborate species present. The chemical shift of these species is known to be 21.5 ppm.[121] The spectra also showed that the samples were sometimes contaminated with these borate species, $B(OH)_4$, which carried through from the extraction of the ligand into chloroform. The anomolous peak at -0.1 ppm falls in the chemical shift range reported for nitrogen and sulphur chelated boron complexes.[121] There was also another form of the ligand observed immediately after work-up whose ^{11}B-NMR showed one peak at -9.0 ppm. These observations strongly suggest that the [10]aneN_2S ligand was chelating a boron atom in a tridentate fashion and that the hydrolysis conditions being used were either not strong enough to remove it, or were in fact somehow promoting the formation of such a complex.

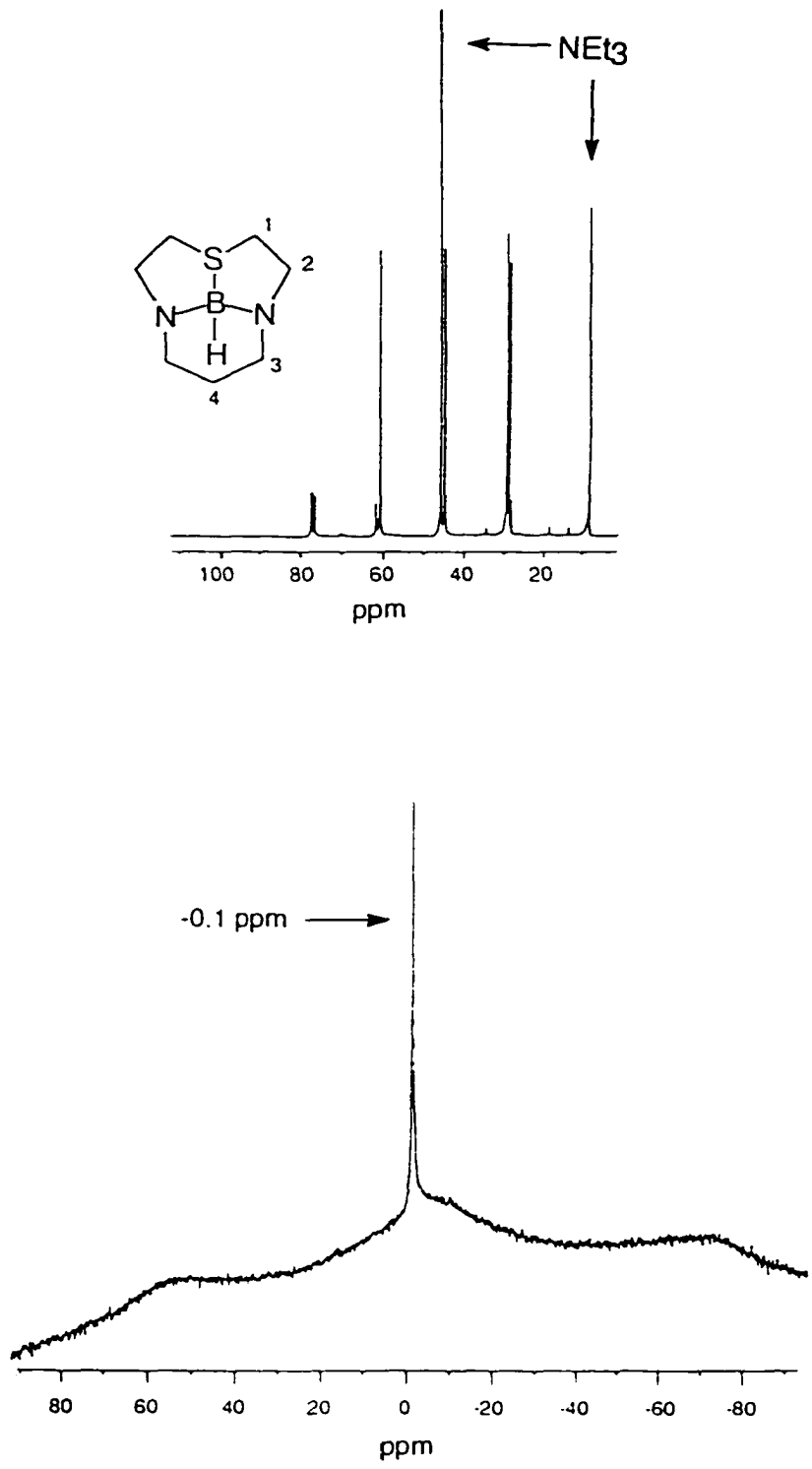

Figure 3.10. ^{13}C-NMR spectrum (top) and ^{11}B-NMR spectra (externally calibrated with BF_3 etherate) of 10aneN_2S reduction mixture.

The fact that the boron complex formed after the ligand had been properly reduced and the boron hydrolyzed off of it, suggested that it was the excess borane reagent that was involved. The original papers published by H. C. Brown et al[98] were consulted and it was found that the amounts of borane used in the current syntheses were in great excess of that used by Brown et al. They reported that the optimum stoichiometries for reductions of simple amines were: tertiary amides, 1 2/3 mol BH_3 per mole of amide; secondary amides, 2.0 mol BH_3 per mole amide; primary amides, 2 1/3 mol BH_3 per mole amide. Another important result reported was that the optimum length of time for reducing the amides was four hours. Presumably, current procedures reported in the literature were applying the "more is better" principle without determining if such was really necessary.

A report by Lehn et al[99] described the isolation of a *bis* BH_3 coordinated cryptand isolated after a borane reduction of the corresponding amide. This was not a case of boron being chelated by the ligand as proposed for the [10]aneN_2S coordinated product. The authors reported that the *bis*(amine-boron) complex was very stable and resisted acid hydrolysis. The authors found that it was necessary to use forcing conditions involving refluxing the amides in 20 mL of 6M $HCl_{(aq)}$ per gram of compound at 125 °C for three hours. Two condensors, one on top of the other, with glass wool at the juncture, were used to prevent the acid from frothing out. These conditions were tried on the boron coordinated [10]aneN_2S complex but the compound decomposed before significant amounts of the boron were removed.

The reduction of a pure sample of [10]aneN_2S diamide (**23**) was tried with four changes to the conditions. Firstly, as suggested by Brown et al, only 2.0 equivalents of BH_3•THF per mol of amide (4.0 mol BH_3•THF per mol of diamide (**23**)) were added for reflux. Secondly, the reflux was stopped and cooled on an ice bath after four hours instead of the usual eight hours. Thirdly, the excess borane was then immediately destroyed (**CAUTION**) by dropwise addition of water instead of ethanol. Finally, following the procedure reported by Lehn[99], 20 mL of 6N HCl per gram of **23** was used for the acid

hydroysis reflux instead of the 30% HCl in methanol used previously. This new procedure was successful and produced the intended reduced [10]aneN_2S in good yield and little or none of the boron complexed product. It was observed that if the BH_3•THF reflux was allowed to continue beyond four hours, the boron complex would start to form. Within two or three hours of additional refluxing, the boron complex would be the major product. These observations imply that the major factor involved was the length of time of the reflux.

It is interesting to note that no boron complex was obtained when the [10]aneN_2S diamide from the K_2CO_3 and 2:1 (amine to acid chloride) methods was reduced. The only notable difference at the point of reduction was that they contained the linear N_4S side product. That side product contained primary amines which must have somehow interacted with the borane to prevent it from coordinating the reduced [10]aneN_2S.

Mass spectroscopy (CI) of newly prepared mixtures of [10]aneN_2S with a small amount of the putative boron complex present has detected M+1 (171 m/e) and M+29 (199 m/e) peaks in addition to the [10]aneN_2S molecular ion peaks. The most reasonable structure possible that would give a molecular weight of 170 g/mol would be one in which there are no hydrogens on the amines and no substituents on the boron other than the [10]aneN_2S ligand. The molecular weight of [10]aneN_2S (without the amine hydrogens) plus the weight of the ^{11}Boron center adds to 169 g/mol, suggesting the presence of a hydrogen as well. In view of the nature of the amine-boron bonding present in this system, it would be necessary for the boron center to remain bonded to one hydrogen in order to maintain its desired valence.

In this case, the nitrogen donors of the macrocycle are not donating a lone pair into the empty p-orbital of a *tris*-coordinated boron center according to the classical amine-boron bonding scheme.[126] Instead, the nitrogens have each donated one of their three valence electrons (the other two valence electrons are participating in covalent bonds to the carbons) into a covalent bond with one valence electron from the boron. Since [10]aneN_2S has two nitrogen donors, two of the three valence electrons from the boron

are accounted for; however, the third boron electron can not bond to the thioether donor because, unlike nitrogen, the thioether can only donate an electron pair. To resolve this conflict and still remain electroneutral, the third valence electron of the boron must be involved in a covalent bond with hydrogen such that the complex is more appropriately viewed as a BN_2H center whose empty boron based molecular orbital is partially π-bonding with the thioether lone pair (the amine donors are probably partially π-bonding as well). This is the only chemically reasonable structure which can account for the observed molecular weight:

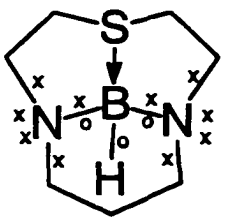

x = electrons from nitroger

o = electrons from boron

Only two reports of similar small macrocycles chelating boron have been found.[122] It was found that the reduction of the *p*-cyanobenzyl appended [12]aneN_3 diamide shown in scheme 3.3 with BH_3•THF gave not the expected tetramine, but the boron complex instead. The boron was efficiently bound in the plane of the triaza ring to form a robust neutral complex. The other report,[123] which included an X-ray crystal structure, shows that that exhaustive reaction of 1,5,9-triazacyclododecane with $B(OMe)_3$ results in a similar chelated boron complex.

Although it has been found in this work that the refluxing time is crucial, it is also believed that destroying the excess borane after the reflux with ethanol or methanol (as was done in the reduction of [12]aneN_3 reported by Parker[122]) predisposes the boron for coordination to the ligand. This is because the macrocycle can easily displace the alkoxide ligands from the resulting $B(OR)_3$ species. When the excess borane is destroyed with

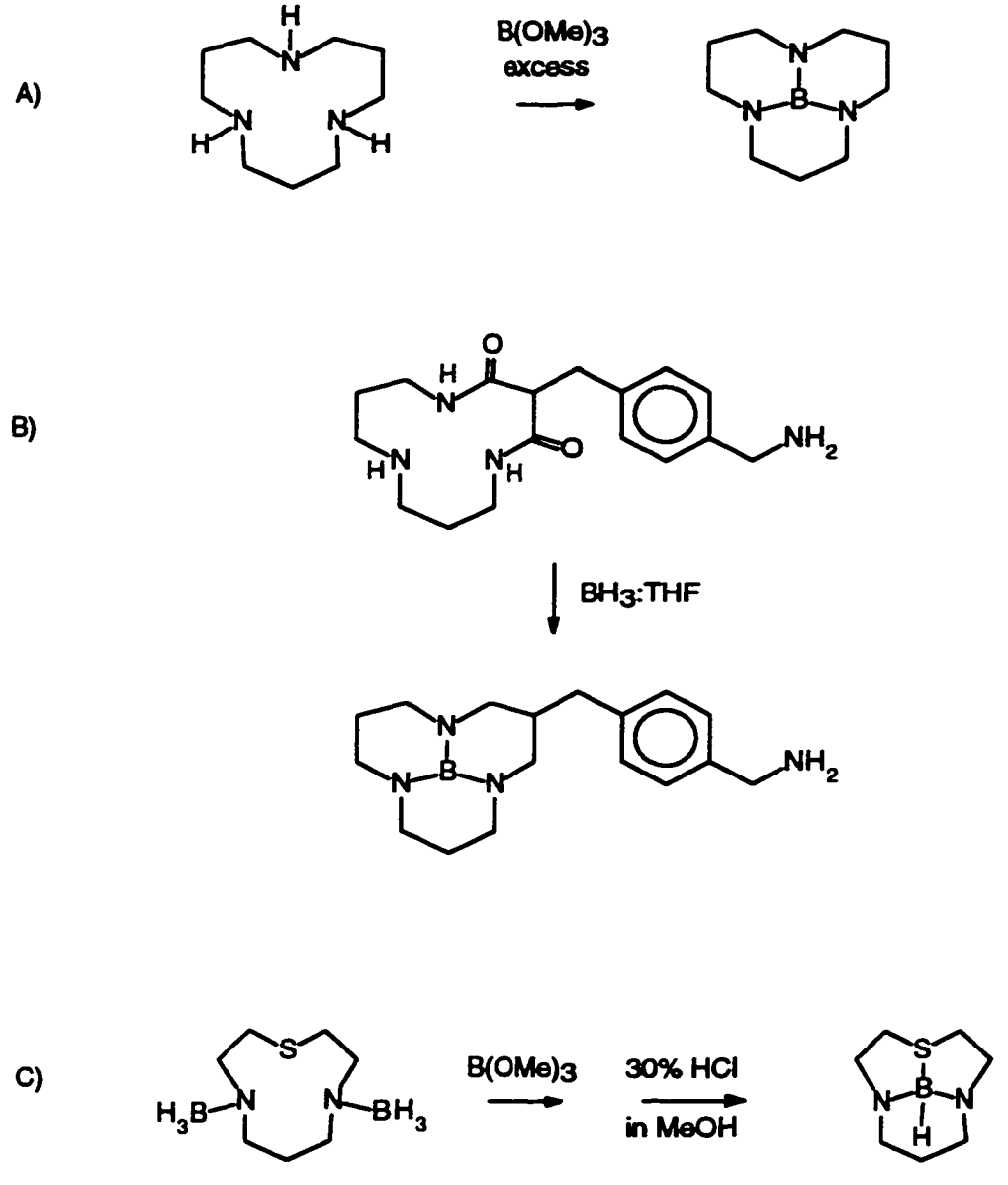

Scheme 3.3. A) Complexation of Boron with 1,5,9-triazacyclododecane ([12]aneN$_3$).[123]
B) Complexation of Boron with *p*-cyanobenzyl appended [12]aneN$_3$.[122]
C) Proposed formation of B([10]aneN$_2$S)H complex in the present study.

water, the resulting $B(OH)_3$ and polyborate species formed are not as easily coordinated by the macrocycle.

A report by Hancock[124] explains how the -N-CH_2-CH_2-CH_2-N- group is ideally suited for the coordination of small metals such as boron. One would naively expect that the propylenediamine chelate would prefer to coordinate larger metals than would an ethylenediamine group because it has a longer chain of methylene groups between the two chelating nitrogens. Instead, the conformational folding of the propylenediamine group causes the lone pairs of the two nitrogens to point to a focal point which is much closer than the ethylenediamine. Consequently, the propylenediamine chelate is actually most suited for coordination of central atoms which are smaller than copper(II), namely beryllium and boron.[124]

3.2(d). Modified Synthesis of [10]aneN_2S (20):

i) Cyclization to form [10]aneN_2S diamide (23) intermediate:

When the synthesis of [10]aneN_2S was initially conducted via the 2:1 (amine to acid chloride) method described in section 3.2(b), it was observed that the product yield depended on the stirring conditions. As with many cyclization reactions, it was found that as better high dilution conditions were used, more product was obtained. The details concerning the high dilution apparatus used in this work have been presented in section 8.1(c).

There were two products present in a 10:1 ratio. The major product was the 1:1 condensate, [10]aneN_2S diamide **(23)** , and the minor product was the proposed 2:2 condensate, [20]aneN_4S_2 tetraamide **(25)** (no polymer formation was observed). If the [10]aneN_2S diamide was contaminated with a significant amount (10 - 30%) of the 2:2 condensate, then pure [10]aneN_2S diamide was obtained by washing the sample with 50 mL methanol per gram of solid.

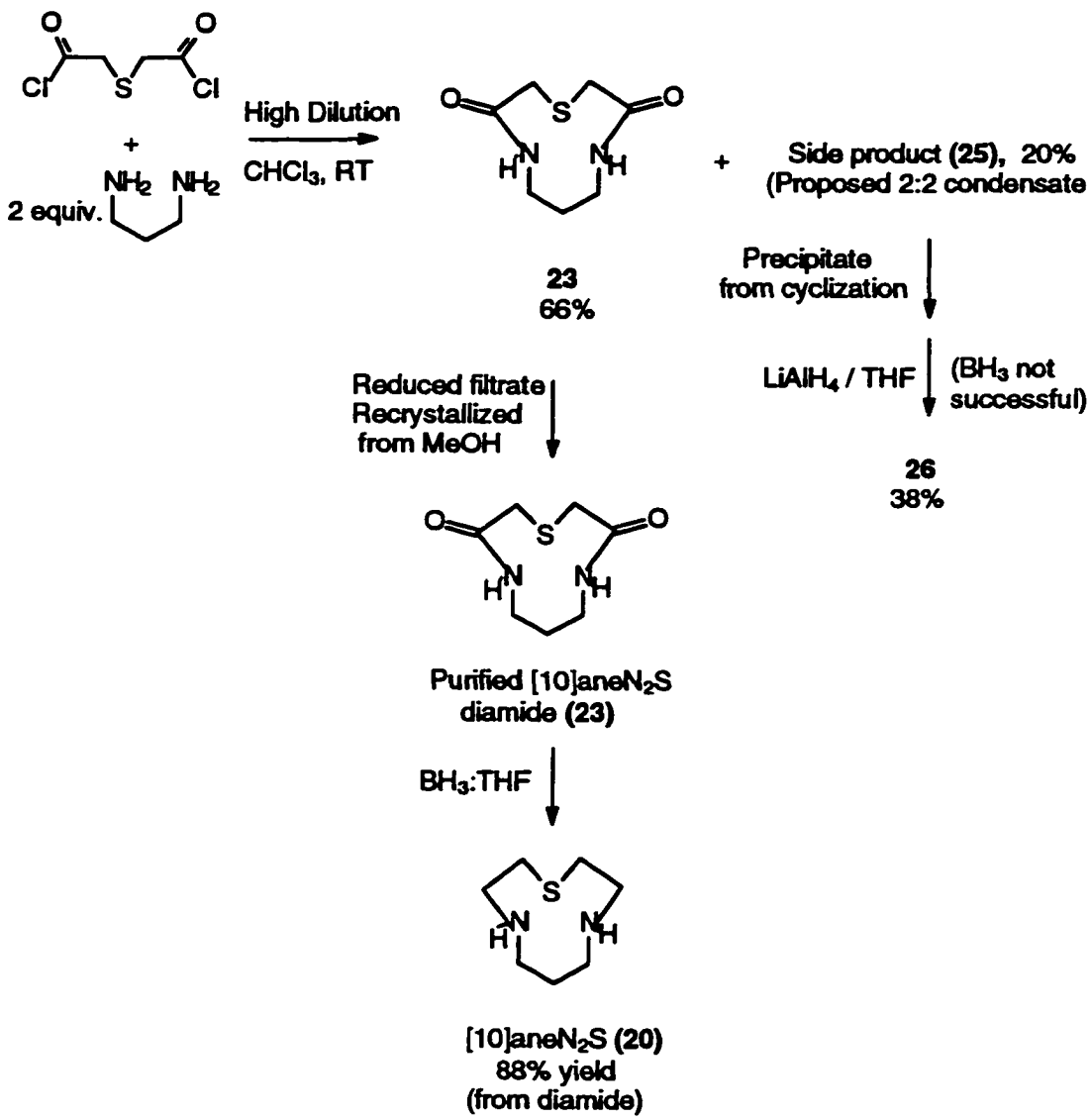

Scheme 3.4. Synthetic route to [10]aneN_2S (**20**) via improved 2:1 amine:base method.

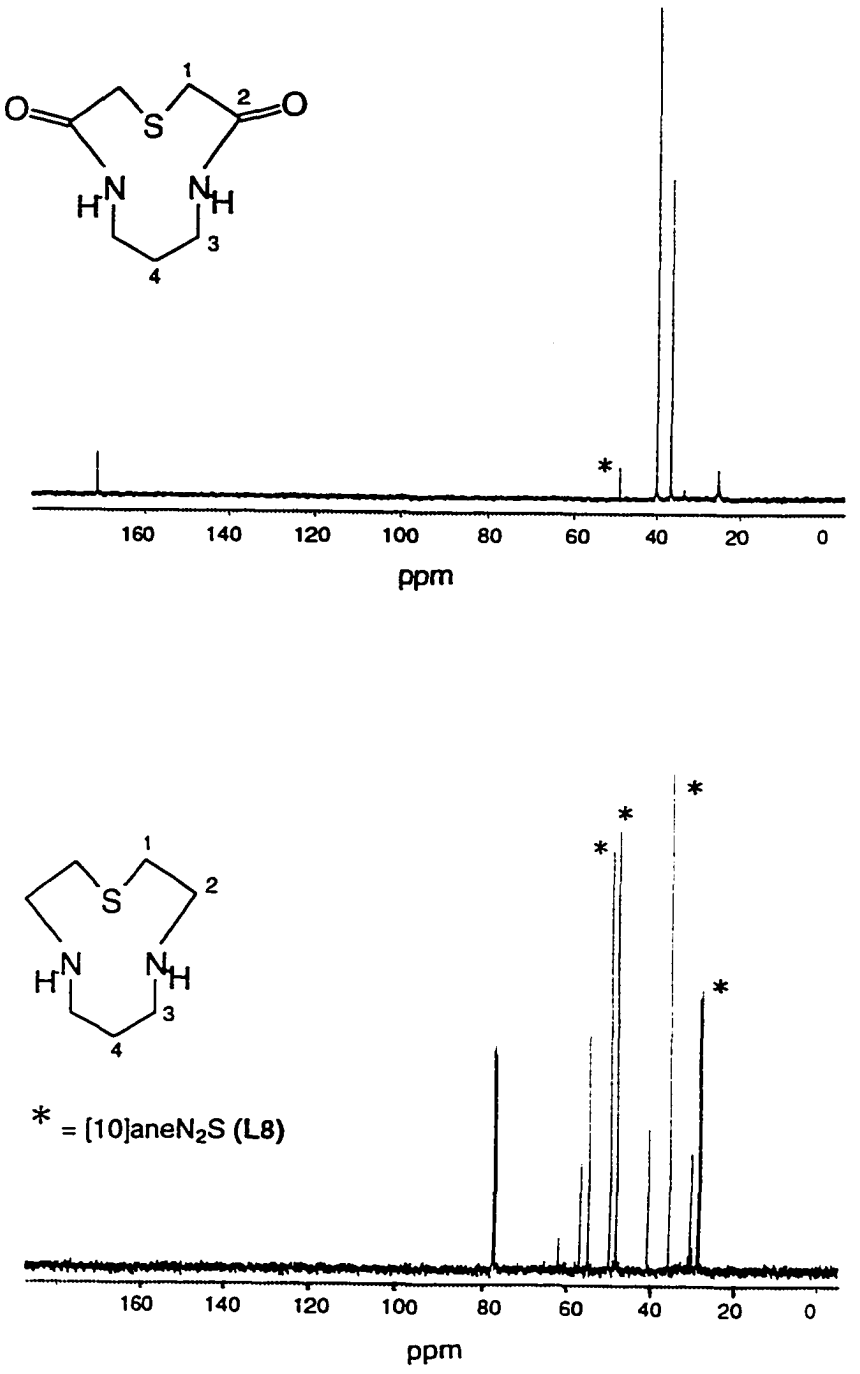

Figure 3.11. ^{13}C-NMR of [10]aneN_2S diamide **(23)** (top, * = methanol) and resulting [10]aneN_2S **(20)** crude reduction mixture showing "additional peaks" (bottom).

The most important aspect of the improved synthetic conditions was that the yield of [10]aneN_2S diamide from the cyclization reaction depended on the effectiveness of the stirring conditions. As described in section 8.1c, the optimum stirring conditions to date consist of adding both reagents via a syringe pump apparatus into a 5 litre round bottom flask containing special glass indents. The syringe pump apparatus ensures that both reagents are added slowly in exact equimolar amounts such that the desired stoichiometry is maintained at all times. The glass indents ensure that the solution mixes effectively. The most important variable affecting the effectiveness of the mixing was observed to be the stirring speed. Table 3.1 lists the yields obtained as the stirring speed was varied (all other factors such as type of flask and syringe pump mechanism were kept the same).

Table 3.1. Yield of [10]aneN_2S diamide as stirring speed is increased.

R.P.M.	YIELD
600 - 800	15% - 20%
1180	20% - 25%
1370	33%
1900	66%

Although the better stirring conditions resulted in similar improvements in the cyclization yield for the NEt_3 method (to 40%), the yields from the 2:1 amine to acid chloride method were still greater. For both methods, the cyclization yields were very reproducible. The yields of both reactions did not vary by more than 5% for a given set of reaction conditions and the reactions never failed despite having been performed over twenty times. Hence, the goal of finding a more reliable methodology than that of the tosylate method was achieved. The major factor responsible for this difference was that

the acid chloride methodology allows chloroform to be used as the solvent. The chloroform was easily and reproducibly prepared each time. The synthesis is also much less time consuming and more convenient than the tosylate methods.

Further evidence of the importance of stirring conditions for this reaction is provided by the fact that when the stirring speed was increased from 800 rpm to > 1100 rpm, the side product obtained was no longer the 2:1 (amine to acid chloride) N_4S linear diamine, but instead was the proposed 2:2 cyclic condensation product, [20]aneN_4S_2 tetraamide (**25**).

The effect of lower reaction temperature on the yield was studied and it was found that room temperature was optimum. The synthesis was tried with pyridine as the base but the reaction did not work as well.

ii) Borane reduction of [10]aneN_2S diamide (23) to produce [10]aneN_2S (20):

It has been observed[98] that diborane reductions give better yields when conducted on a smaller scale, therefore the reductions of [10]aneN_2S diamide samples were performed on 2 - 3g scales.

The presence of unwanted borate materials was monitored by ^{11}B-NMR spectroscopy. If borate species were present, they were removed by dissolving the oil in 20 mL pH >12 distilled water and chromatographing on DOWEX 1 X 8-400 anion exchange packing (column dimensions: 3.5 cm diam. X 8 cm) in the hydroxide bound form. The first 100 mL of eluent were collected and taken to dryness on a rotary evaporator then dried further in vacuo.

As can be see in figure 3.11, when the borane reduction was carried out on the pure [10]aneN_2S diamide, ^{13}C-NMR spectroscopy showed additional peaks implying the presence of additional species in the resulting product. These extra peaks were consistently produced at the same chemical shifts. Mass spectroscopy was unable to detect

any molecular ions other than that due to [10]aneN_2S. It was suspected that these peaks were not necessarily due to side products because subsequent derivatization (N-alkylation) of the sample with bromoethyl acetate and chloroacetyl chloride resulted in crude reaction samples that were more pure than the original [10]aneN_2S sample used for the reaction. Also, similar additional peaks were present in the NMR spectra of the [10]aneN_2S synthesized by the tosylate method[125]. Such observations suggested that the "extra" peaks were some other conformation or form of the intact [10]aneN_2S. The number and chemical shift pattern of these peaks were not consistent with such an explanation.

About the time the borane reduction procedure was changed to avoid the formation of the boron complex, it was noticed that the subsequent samples would not coordinate nickel(II). Upon addition of the nickel(II) perchlorate to aqueous or ethanolic solutions of the [10]aneN_2S, no violet coloured complex formed and a flocculate green precipitate formed which was presumably a mixture of nickel(II) hydroxo species. Surprisingly, the ligand sample did bind to copper(II) yielding a light blue solution. Previously, the copper(II) complex would convert to the green species mentioned above such that chromatography on sephadex CM-C25 was not feasible. Presently it was found that the blue $[Cu(10aneN_2S)_2](ClO_4)_2$ complex was robust enough to survive the chromatography. There was only one major band observed and removal of the copper(II) and characterization of the free ligand by ^{1}H-NMR and ^{13}C-NMR spectroscopy showed that the ligand had been obtained in the highest purity achieved (figure 3.12). It is interesting to note that additional, smaller triplet and quintet peaks previously observed in the ^{1}H-NMR spectra, which were present even when no additional peaks were present in the ^{13}C-NMR, were no longer present in the spectra of the more pure sample. Previously, these additional peaks were thought to be a consequence of 2nd order coupling effects, however, the lack of such peaks in the present spectra proves that such was not the case.

Although complexation of the [10]aneN_2S reduction sample to copper(II) allowed the isolation of the ligand in acceptable purity, the percent recovery was unacceptably low (<20%). Once again, it was desired to find a purification method which avoided forming a

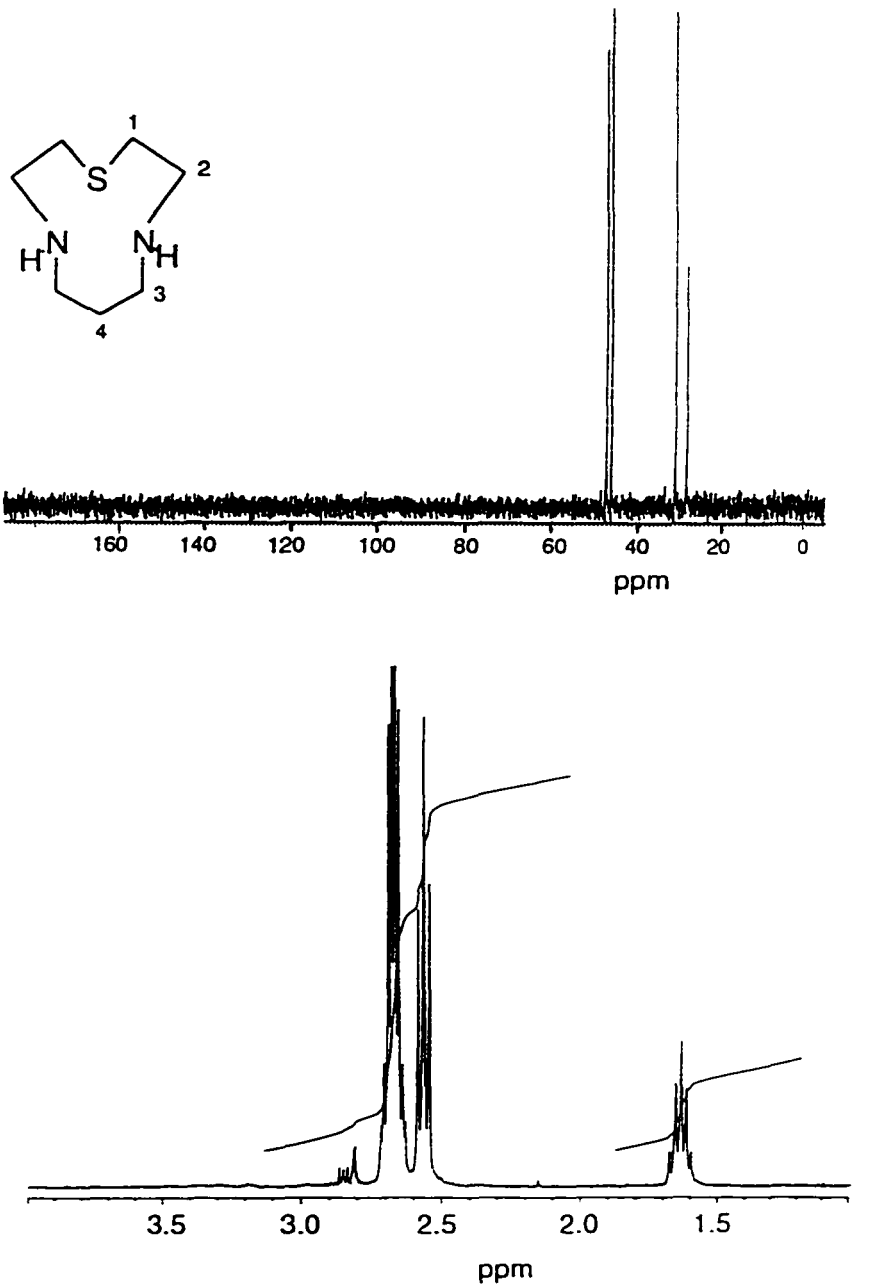

Figure 3.12. ^{13}C- and ^{1}H-NMR of [10]aneN_2S **(20)** free ligand purified as copper(II) complex over sephadex CM-C25 cation-exchange packing.

metal complex for reasons discussed above in section 3.2(b). The most obvious method of purifying the free ligand mixture would be chromatography on silica gel. As explained in section 3.2(b), the presence of secondary amine (NH) groups causes the ligand to stick to the silica and not travel. The best way to avoid such problems would be to derivatize the secondary amines into tertiary amines with a suitable protecting group. After chromatography, the protecting group can be removed and hopefully such a process would not lead to any side products. It was decided that tert-butoxycarbamate (t-BOC) would be the best protecting group to try. It forms stable carbamate derivatives with amines that are known[105] to be well behaved on silica gel and is hydrolyzed from the amine under relatively mild acidic conditions.

A sample of [10]aneN_2S where the NMR spectrum showed many addtional peaks was derivatized with di-*tert*-butyl dicarbonate (6 equiv.'s) in chloroform. As can be seen in figure 3.13, the ^{13}C-NMR spectrum of the derivatized material, before any purification was attempted, showed only one additional peak other than those of the derivatized [10]aneN_2S. The fact that the mixture "cleaned up" so well upon derivatization once again suggests that these additional peaks are in fact due the presence of some other form of the intact [10]aneN_2S ligand and not side products. When the derivatized sample was chromatographed on silica gel (10% MeOH in chloroform) using the chromatotron appartaus described in section 8.1, only two bands were eluted from the chromatotron plate. The first band was the excess di-*tert*-butyl dicarbonate, while the second band was the pure t-BOC derivatized [10]aneN_2S.

Cleavage of the t-BOC protecting group off of the [10]aneN_2S ligand was achieved by stirring at room temperature in 33% HBr in acetic acid (Fluka Chemicals) in the presence of 5 equivalents each of phenol and thiophenol for three hours. The phenols are necessary to prevent alkylation of the thioether groups.

The [10]aneN_2S free ligand was obtained in acceptable purity by this purification method and the recovery (ca. 60%) was acceptable also. The NMR spectra of the purified material are presented in figure 3.15. It has since been found that the subsequent

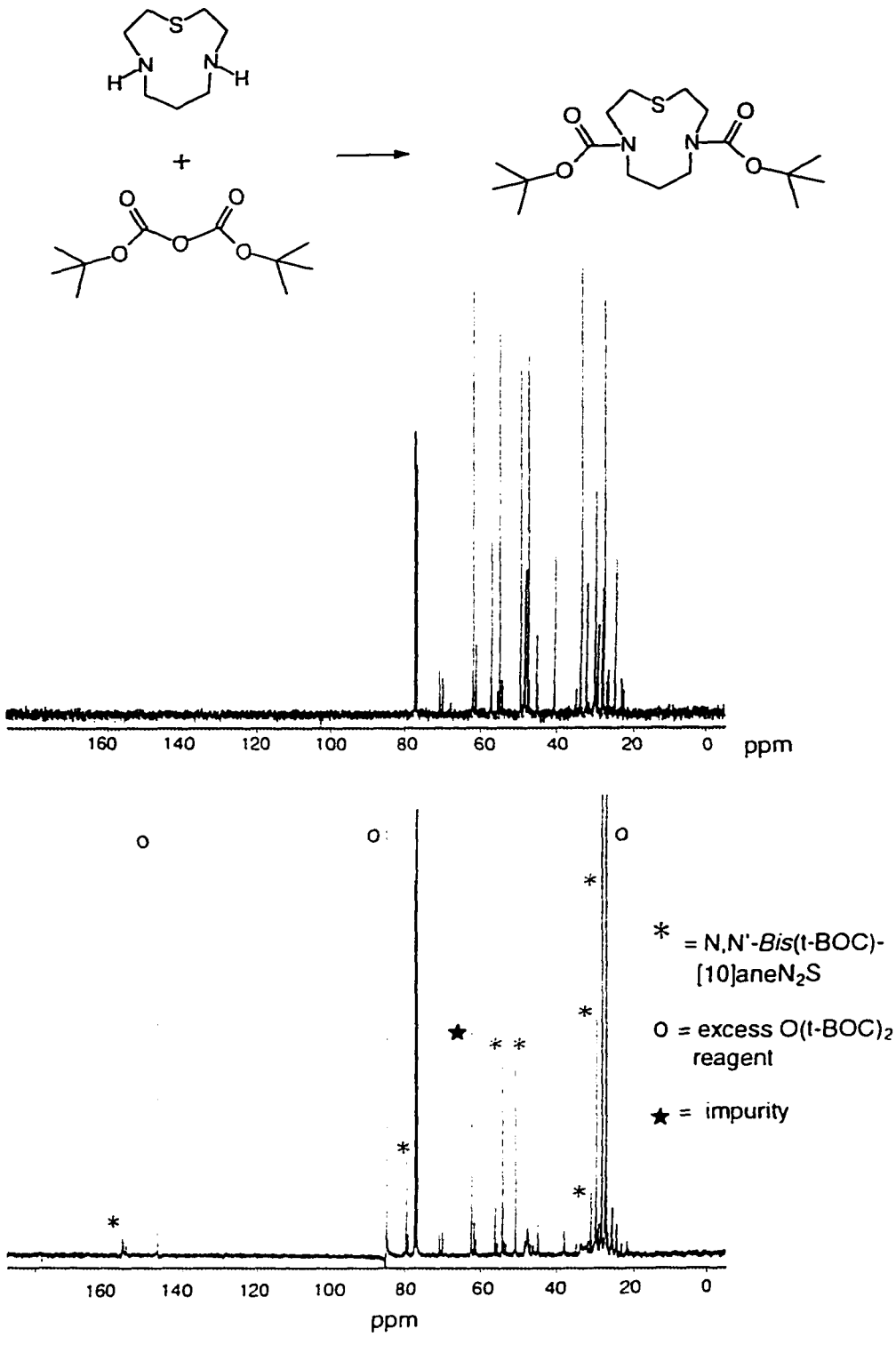

Figure 3.13. ^{13}C-NMR [10]aneN_2S before (top) and after (bottom) addition of t-BOC protecting group (no purification performed yet).

cyclization reaction with [10]aneN_2S to form the [10]aneN_4S bicycle diamide gives the same yield and purity regardless of whether or not the t-BOC purified sample is used, which once again implies that the addtional peaks present in the crude [10]aneN_2S reduction mixture are not side product ligands.

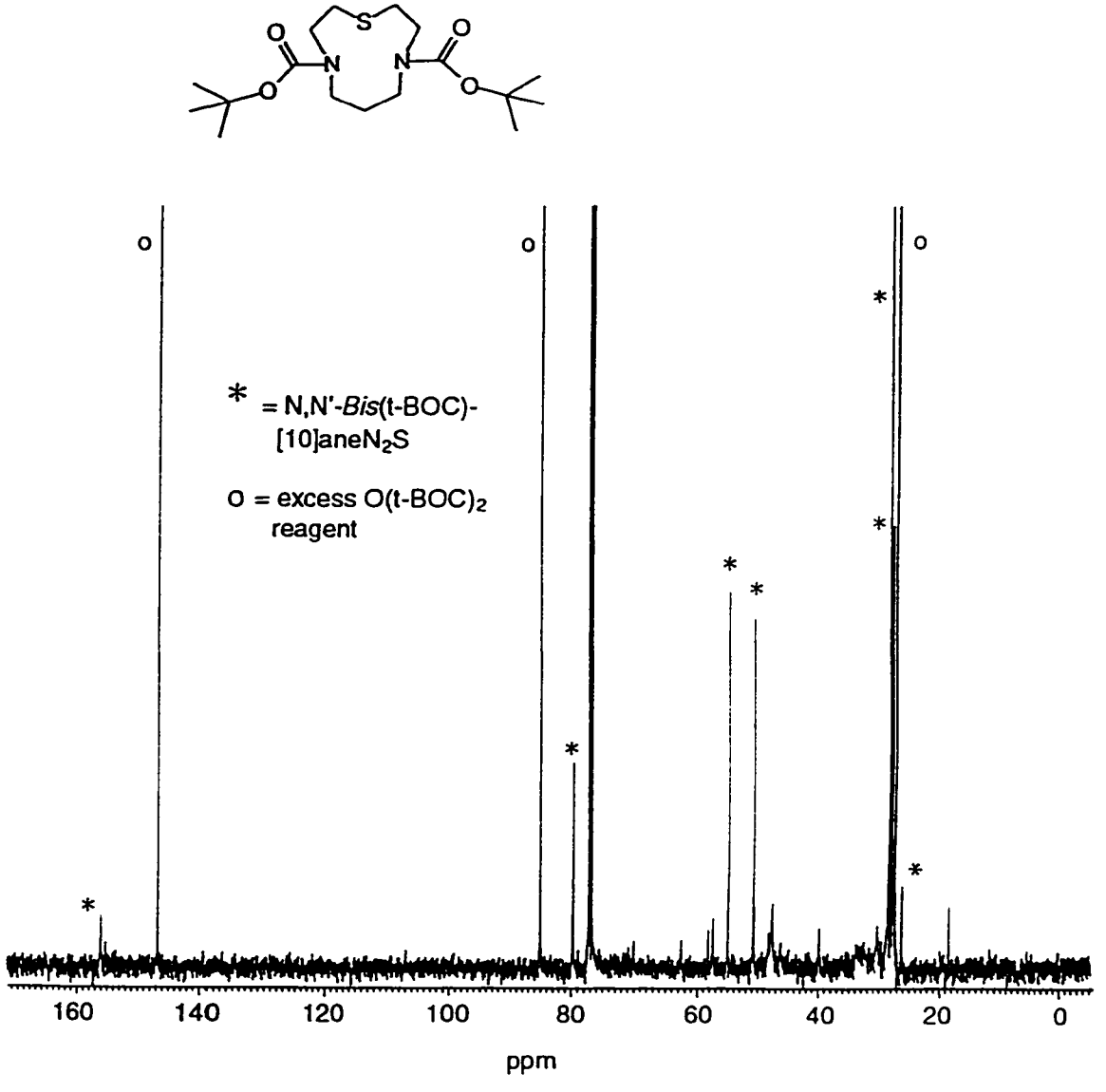

Figure 3.14. ^{13}C-NMR spectrum of purified t-BOC derivatized [10]aneN_2S.

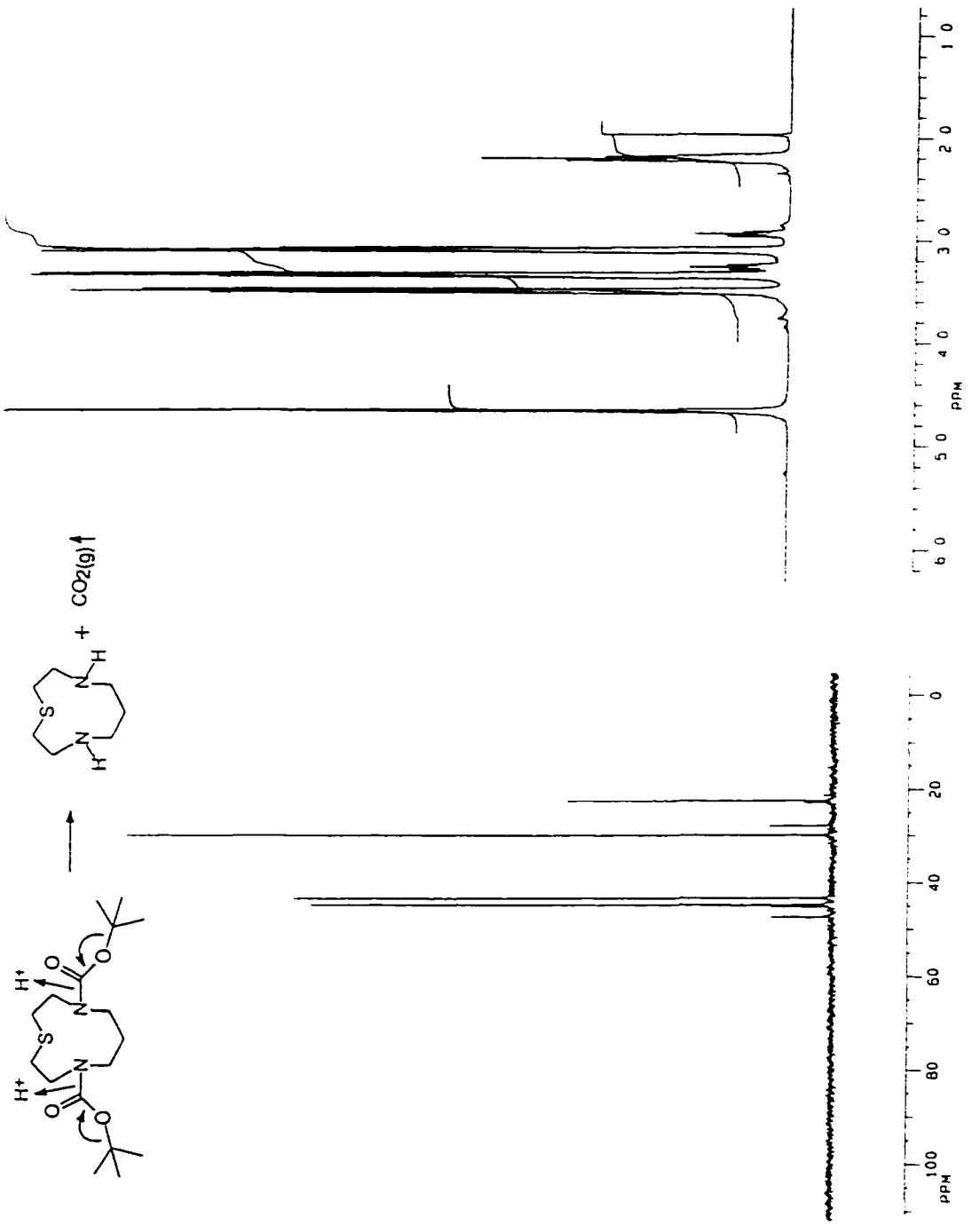

Figure 3.15. ^{13}C- and ^{1}H-NMR spectra of resulting [10]aneN_2S after hydrolysis of t-BOC derivative.

3.2(e) Characterization of side product of [10]aneN_2S (20) synthesis:

As mentioned in section 3.2(d), the reaction of diaminopropane with thiodigylcolic acid chloride via the improved 2:1 (amine to acid chloride) method produced a side product which, based on the ^{13}C-NMR and mass spectra, is proposed to be the 2:2 condensation product, [20]aneN_4S_2 tetraamide (**25**). As the stirring conditions were improved to maximize the yield of [10]aneN_2S diamide (**23**), the yield of **25** decreased from 30% to 18.6%. There were two sources of this side product. It was isolated from the filtrate residue by washing with methanol (50 mL per gram of solid). It was isolated from the precipitate by dissolving in pH 2 - 3 deionized water and passing down a column of DOWEX 50 X 8 cation-exchange packing. The precipitate contained a large amount of the diaminopropane hydrochloride salt (formed by the reaction) which bound to the cation-exchange packing. That the side product did not bind to the cation-exchange packing implies that there are no unreacted amine groups present which further supports the proposed structure. No [10]aneN_2S diamide material was observed in the precipitates.

As can be seen by the ^{13}C-NMR spectrum in figure 3.16, the putative [20]aneN_4S_2 (**26**) was not acceptibly purified by chromatography of the copper(II) complex. The smaller impurity peaks are believed to be caused by oxidation of the ligand as it passes through the sephadex. Although large multigram amounts of this side product have been prepared, the reduction reaction has only been performed twice on small amounts. If any further reductions are attempted, purification of the reduced ligand by derivatization with t-BOC followed by chromatography on silica gel should be attempted since this method was successful at purifying the 1:1 ([10]aneN_2S) product.

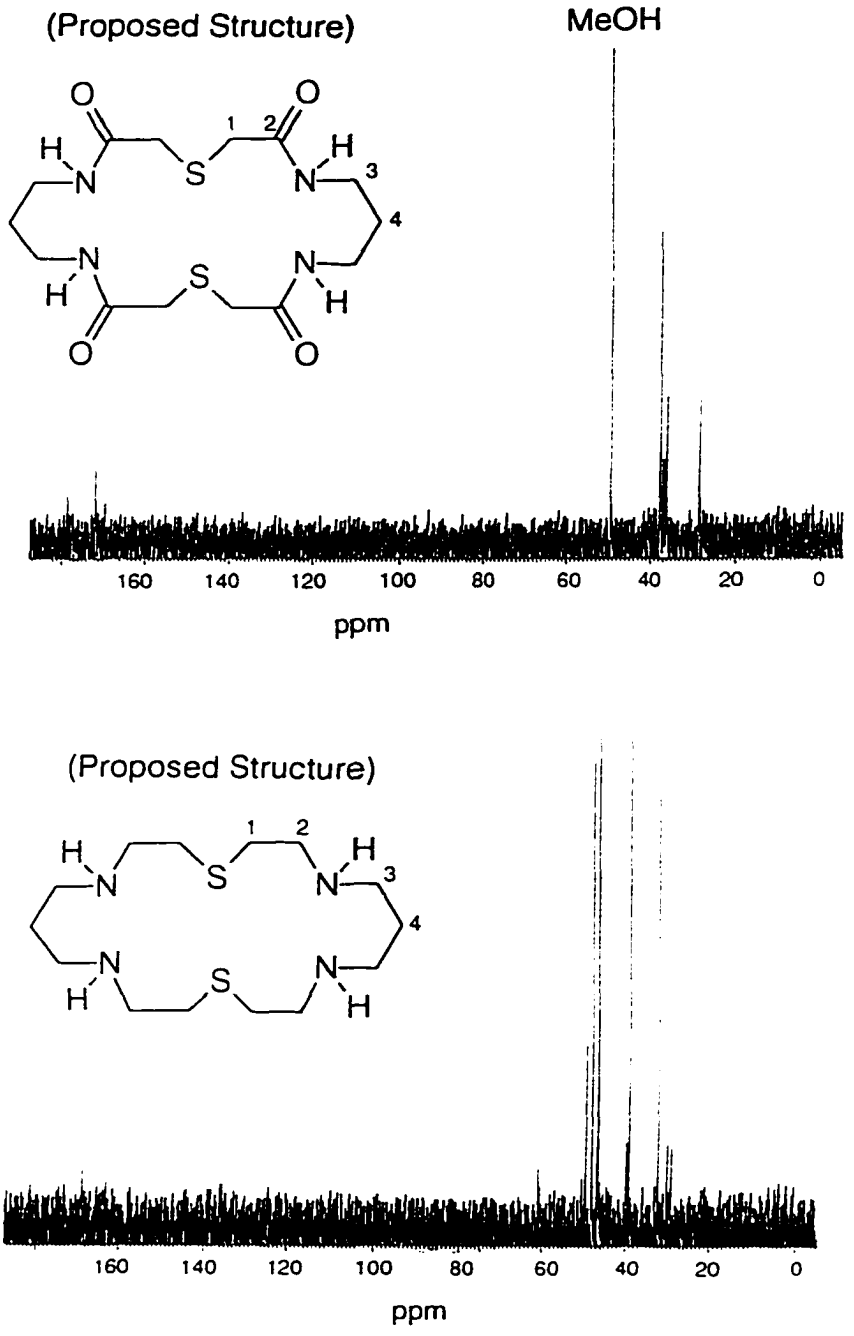

Figure 3.16. ^{13}C-NMR spectra of side product **25** (top) from improved [10]aneN_2S synthesis and reduction product **26** (bottom).

3.3. Development of synthetic routes to [10]aneN$_4$S bicycle (L3):

3.3(a) Discussion of synthetic routes to [10]aneN$_4$S bicycle (L3):

A major synthetic goal in this work was to establish a general synthetic route to the [10]ane isomer of the cyclam-based N_4S-bicyclic and N_4S_2-tricyclic ligand frameworks (figure 3.17). This ligand framework consists of the tetraazacyclotetradecane (cyclam) ligand fused to the tridentate [10]aneN_2S ligand. It can also be viewed as the isomer formed by linking the -CH_2-CH_2-S-CH_2-CH_2- bridge across the two adjacent propylene-linked 1, 11-nitrogens of the cyclam ring.

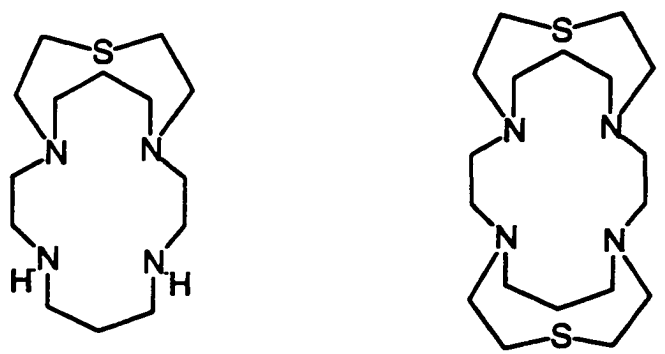

Figure 3.17. Structure of [10]ane N_4S bicycle and N_4S_2 tricycle.

Several bicyclic and tricyclic polyethers with the same general ligand framework have been reported in the literature.[83] Five general synthetic routes have been used in the synthesis of cylindrical macropolycyclic polyethers which are summarized[83] in figure 3.18. The specific reagents and conditions used in each pathway will of course vary for each specific synthesis. The initial cyclic starting material with two reactive sites, shown in figure 3.18, corresponds to using the [10]aneN_2S ligand.

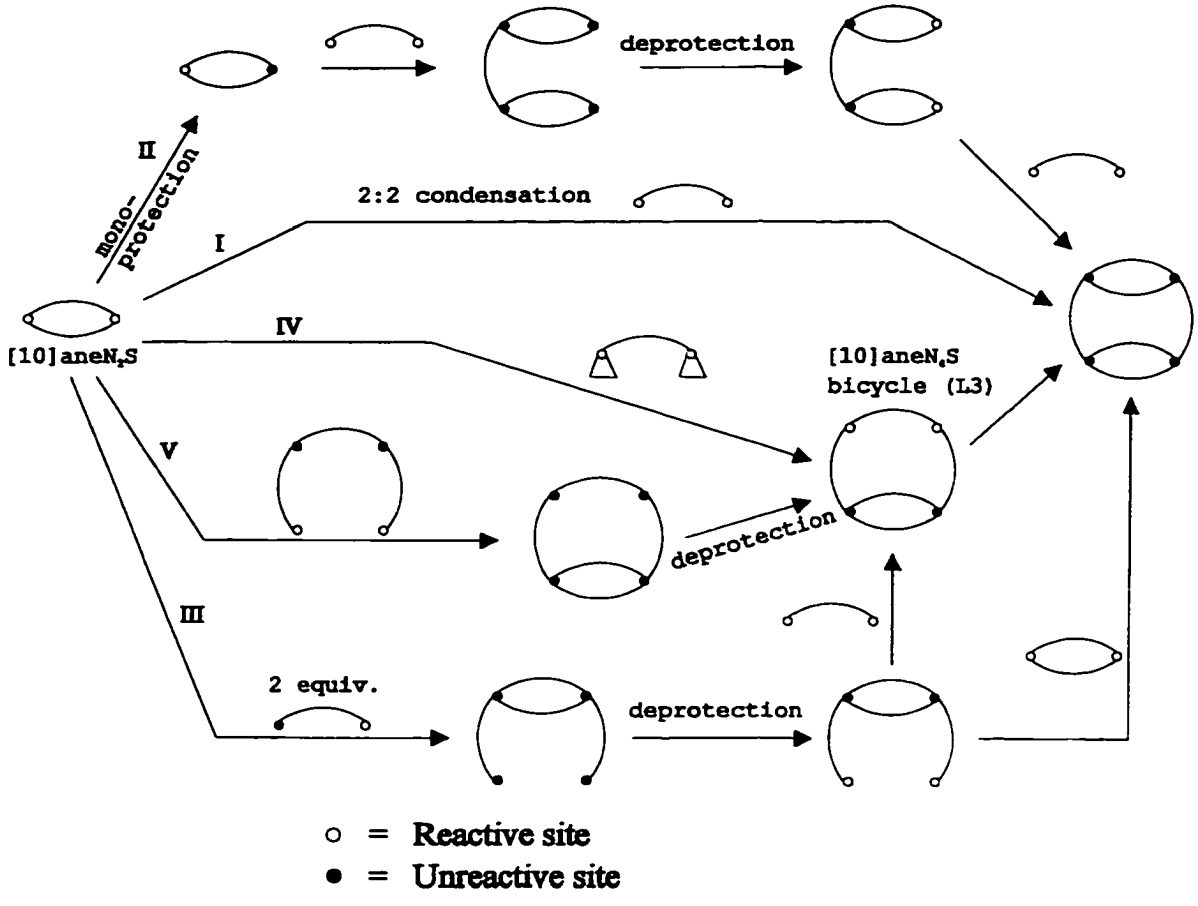

Figure 3.18. General synthetic strategies (I-V) for synthesis of cylindrical macrocyclic ligands.[83] Note that use of N-----N instead of [10]ane in the last step of route III would give the bicycle.

Route I allows the synthesis of symmetrical cylindrical macrotricyclic ligands containing the same macrocyclic and bridging units in one step. A direct methods (non-templated) synthesis of the N_4S_2-tricyclic ligand via this route was not attempted because the synthesis requires the 2:2 condensation product to form. As was shown for the synthesis of [10]aneN_2S and [20]aneN_4S_2, it is inevitable that both the 1:1 and 2:2 condensation products would form. The yield of 2:2 condensate would therefore be

inherently lower than desired due to the formation of the 1:1 product (and polymer). The starting material for the formation of tricycle via route I would be [10]aneN_2S itself which was difficult to prepare on a sufficiently large scale such that the amounts of 2:2 condensation product obtained would be acceptable. It would be better to conduct the synthesis stepwise via route III in the diagram to avoid the production of the 1:1 condensate.

Route I has been attempted as a copper(II) templated reaction between the [Cu([10]ane$N_2S)_2$]$(ClO_4)_2$ complex and dibromoethane and was found to produce only the 2:1 ([10]aneN_2S to ethylene) intermediate in very low yield (<5%). This copper(II) templated reaction suffered from two major problems. Firstly, as discussed in section 3.2(b), the blue [Cu([10]ane$N_2S)_2$]$(ClO_4)_2$ complex undergoes conversion into an uncharacterizable green form such that the properly 2:1 ([10]aneN_2S to copper(II)) coordinated species was not sufficiently stable to undergo the template reaction. Secondly, although there are many reports of transition metal templated cyclizations of linear tetraamines in which the two primary amines are coordinated about the metal in a *cis* geometry, there are no literature precedents for cyclizing across secondary amines to form tertiary amines.

Routes II and III have been used to construct cylindrical macrotricycles with the same or different macrocyclic units and the same or different bridging units by the successive construction of systems of increasing cyclic order. Route II allows the synthesis of a macrotricycle in which the two macromonocyclic components are the same. As a consequence, the N_4S_2-tricycle can be prepared by this route but not the N_4S-bicycle. The two bridges can be different but such is not required for the target ligands in this work. Route II was not attempted because the initial reaction requires the selective protection of one of the two identical amines of the [10]aneN_2S ligand. Reaction of one equivalent of a protecting group would lead to a mixture of several products.

Another important reason for not fully attempting routes I and II has to do with the fact that the synthesis of the [10]aneN_4S bicycle and [10]aneN_4S_2 tricycle target

ligands by these methods both require the cyclization of the [10]aneN_2S secondary nitrogens with a two-carbon bridge. The Richman and Atkins methodology cannot be used for cyclizations involving secondary amines. This is because the success of the reactivity requires that the reacting nitrogen nucleophiles be protected by tosylation. The tosyl substituent not only protects primary amines from reacting more than once but also stabilizes the formation of negative charge at the nitrogen centers such that they become strong nucleophiles without becoming too strongly basic. Without the tosylation, the deprotonated amines tend to react only as strong bases and promote deprotonation of any available hydrogens. The alternative to Richman and Atkins methodology is to react the neutral amine nucleophile with an acid chloride or ester to form an amide which cannot react further. Because the bridging species required to make the target ligands in this work are required to be two-carbon species, the resulting diamide intermediate is a "fused" diamide functionality, i.e. RNCOCONR, which could not be reduced to the desired diamine by conventional amide reduction methods.

Route IV in figure 3.18 is unique to the formation of crown ether macrocycles because it involves cyclization with epoxide electrophiles such that ether donors end up in the ring. The [10]aneN_4S bicyclic ligand system requires that these donors be nitrogen centers.

Route III was therefore the most attractive. The generalized strategy for synthesizing the [10]aneN_4S bicycle and [10]aneN_4S_2 tricycle ligands via route III is shown in scheme 3.5. Attempts at synthesizing **L3** by first adding α-chloro amido,[127] ethylbromoacetate, hydroxyethyl,[128] aminoethyl, and oxalyl chloride "arms" onto the secondary nitrogens of [10]aneN_2S (**23**) were each conducted (scheme 3.5). However, various synthetic difficulties (specific to each synthesis) were encountered that will not be discussed.

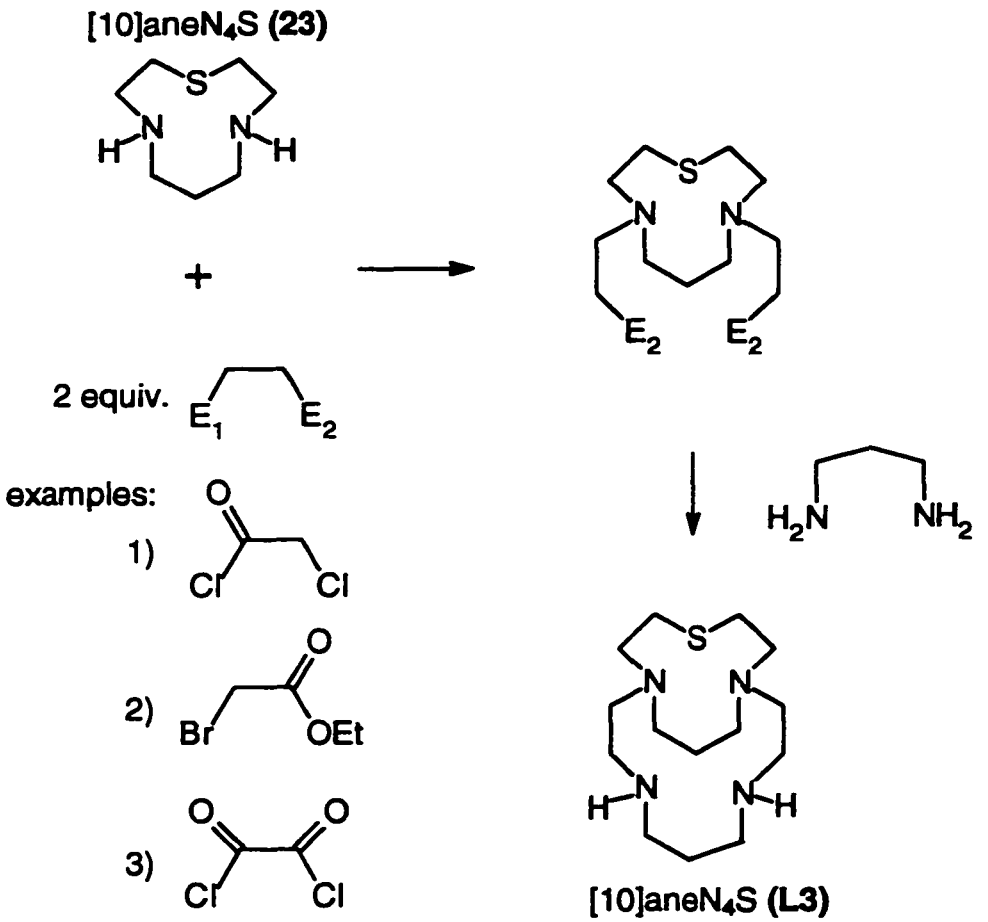

Scheme 3.5. Generalized synthetic strategy for route III (E = electrophile).

3.3(b). Synthesis of [10]aneN$_4$O bicycle (29):

Referring to figure 3.18, it can be seen that the synthesis of the [10]aneN$_4$X bicyclic and [10]aneN$_4$X$_2$ tricyclic ligand frameworks via route V was the only method that had not been attempted. Route V consists of reacting [10]aneN$_2$X (X = S, O, N) with N,N'-alkylated diaminopropane. The amine groups of the diaminopropane unit should be protected from reaction and the ends of the arms on each nitrogen must contain an

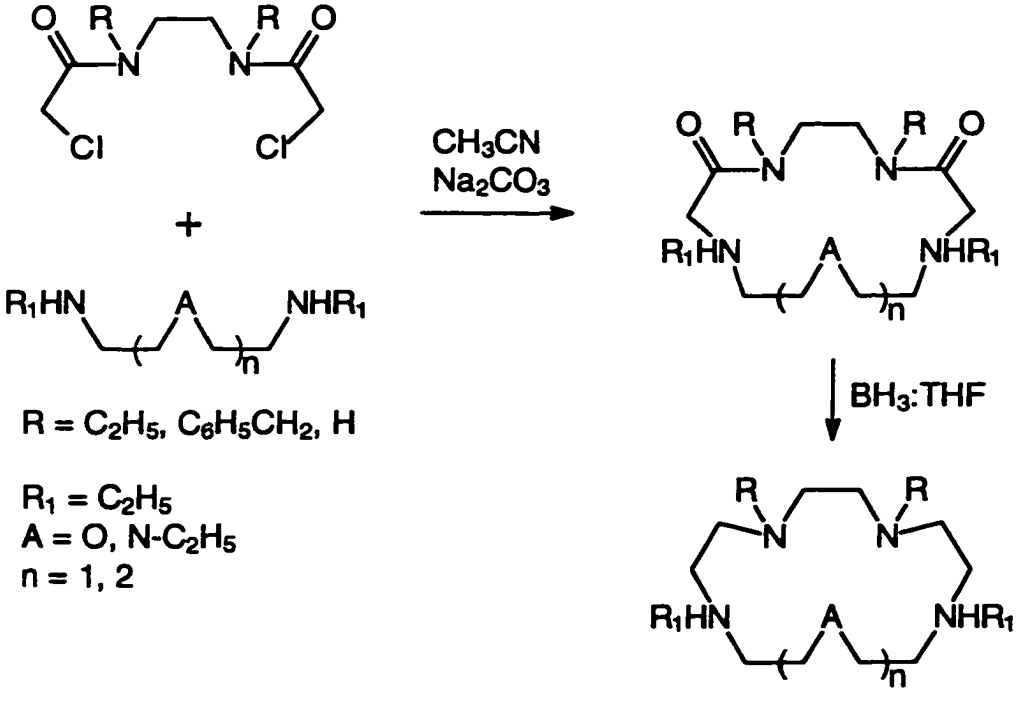

Scheme 3.6. Synthesis of macrocycles from *bis* α-chloro amide electrophiles.[129]

appropriate electrophile for a cyclization reaction. The bis α-chloro amide electrophiles reported by Bradshaw[129] are ideally suited for this purpose. Scheme 3.6 gives an example of the syntheses for which Bradshaw used the bis α-chloro amide electrophiles. As can be seen from scheme 3.6, Bradshaw used the linear bis α-chloro amide electrophiles, unlike

the route III synthesis reported in section 3.3(a) which used bis α-chloro amide arms appended to the two nitrogens of [10]aneN$_2$S. The synthetic difficulty encoutered was that the bis α-chloro amide arms reacted with each other to form an ene-dione bicyclic species. No such reactivity was reported by Bradshaw for the linear bis α-chloro amide reagents. The amides serve to orient the electrophiles for cyclization but do not orient them so closely that they react with each other. It was therefore decided to try the synthesis of the [10]aneN$_4$O bicycle using the synthetic route shown in scheme 3.7.

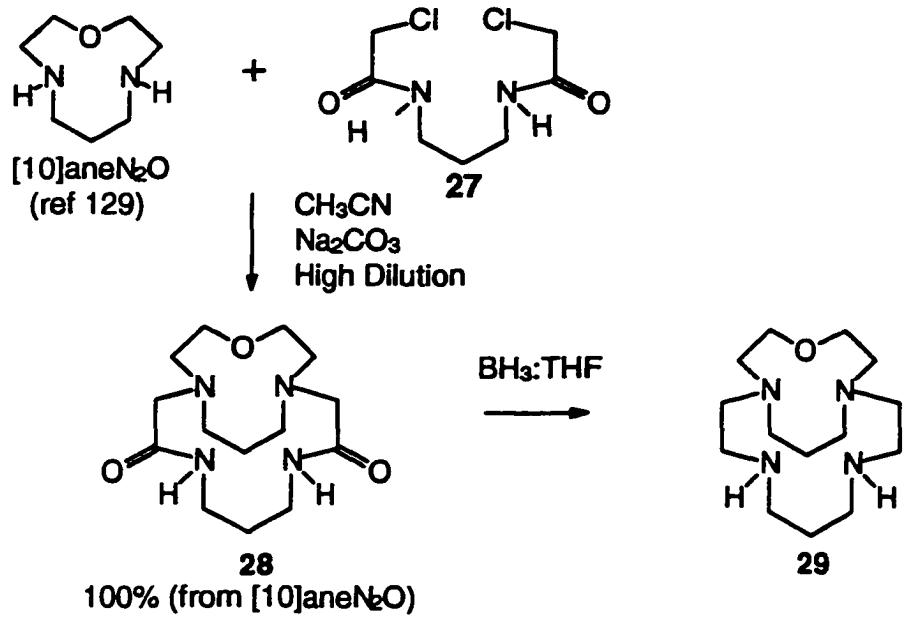

Scheme 3.7. Synthesis of [10]aneN$_4$O bicycle using Bradshaw reagent.

[10]aneN$_2$O was used as the starting material instead of [10]aneN$_2$S because the [10]aneN$_2$S was difficult to obtain in 100% purity as judged by NMR spectroscopy (see section 3.2(d)). [10]aneN$_2$O on the other hand had been synthesized by T. Rodopoulos[128] and was 100% pure. With such high purity, it would be easier to determine how well the

synthesis worked. The synthetic route was therefore first tested out in collaboration[128] on the [10]aneN_2O system.

The cyclization of [10]aneN_2O with N,N'-*bis*(α-chloro amido)diaminopropane (**27**) was very successful. Although the crude reaction mixture contained some unreacted **27**, no unreacted [10]aneN_2O or side products were observed (see figure 3.19). This result implied that all of the [10]aneN_2O had reacted to form product.

Bradshaw[129] attributed the relatively high cyclization yields for this type of reactivity to the possibility that the *bis*(α-chloro amido) reactant could associate by hydrogen bonding between the two amine hydrogens (from [10]aneN_2O in this case) and the two amide oxygen atoms. This association would place the the chlorine atoms and the amine groups in position to react, forming the cyclized *bis*-amide. Also, an internal hydrogen bond between one amide hydrogen and the other amide oxygen in the N,N'-

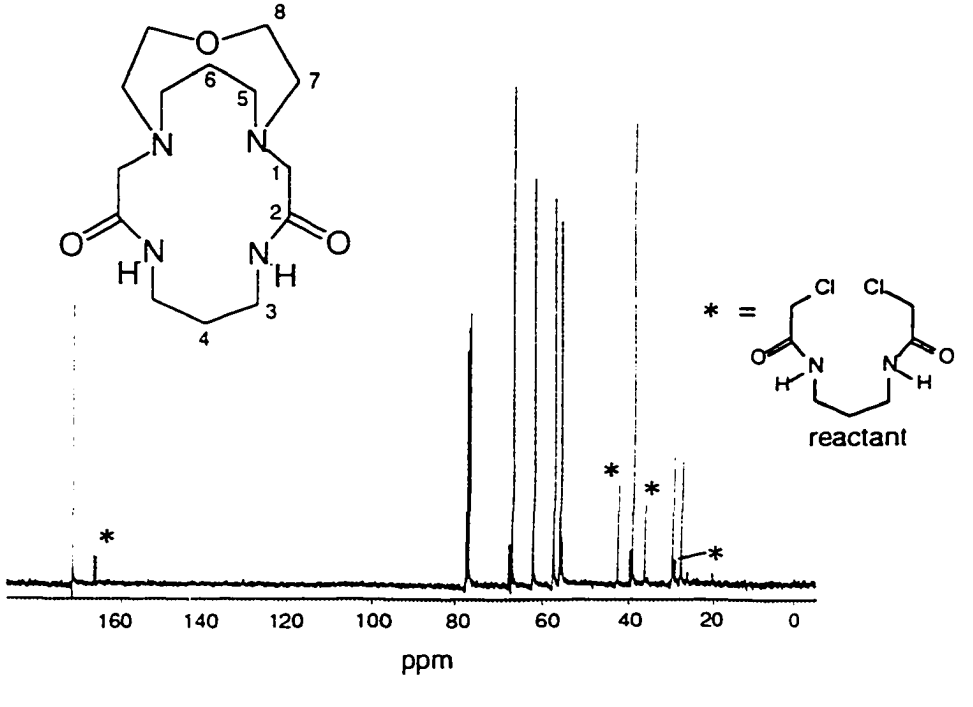

Figure 3.19. ^{13}C-NMR of [10]aneN_4O bicycle diamide crude reaction filtrate.

bis(α-chloro amido)diaminopropane reagent would serve to "pre-orient" the two chloride reaction sites in the "crab-like" form needed for the cyclization reaction. That such an internal hydrogen bond should occur is supported by the results of Hunter et al[80] which are discussed in section 2.1.

A crucial aspect of this reaction was the solubility of the N,N'-bis(α-chloro amido) reactant. The use of amides to protect the 1,11 amines from reaction was already tried with dioxocyclam (1,4,8,11-tetraazacyclotetradecane-5,7-dione). However, the synthesis

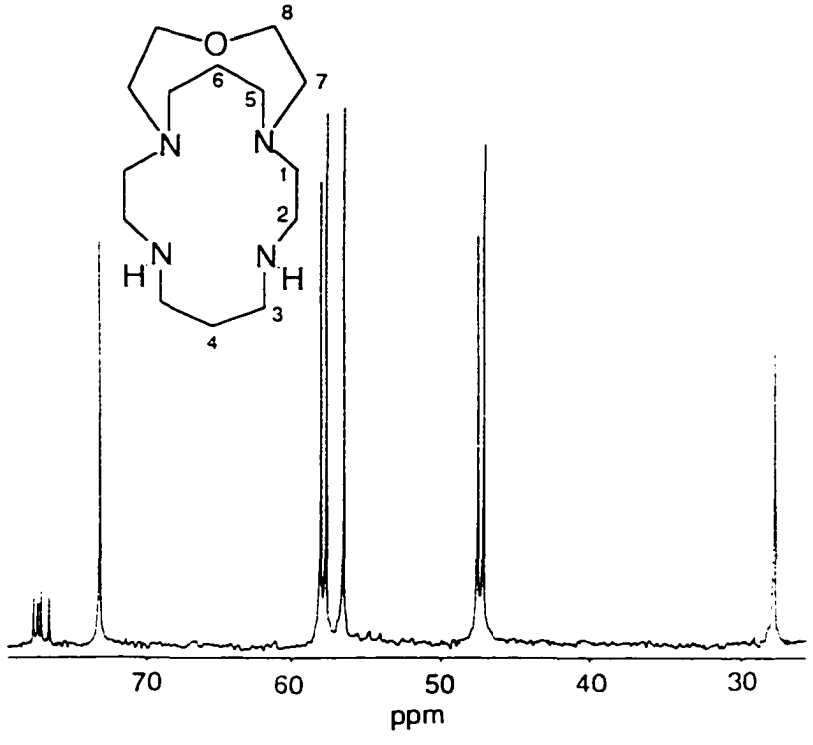

Figure 3.20. ^{13}C-NMR spectrum of [10]aneN$_4$O bicycle (**29**).

of the [10]aneN$_4$S bicycle by reacting dioxocyclam and thiodiglycolic acid could not be attempted because dioxocyclam was not soluble in organic solvents nor in acetonitrile. The N,N'-*bis*(α-chloro amido)diaminopropane reagent has a low but sufficient solubility (*ca.* 400 mg per 50 mL) such that it can be reacted in acetonitrile. Amides are generally

not very soluble in acetonitrile and chloroform. Although it was possible to dissolve the linear N,N'-*bis*(α-chloro amido)diaminopropane reagent in acetonitrile, dioxocyclam, which is essentially a cyclic version of N,N'-*bis*(α-chloro amido)diaminopropane, did not dissolve. The additional amines present in dioxocyclam should be readily soluble in acetonitrile such that it was presumbly the cyclic nature of dioxocyclam which lowered the solubility relative to the linear analogue.

3.4. Synthesis of [10]aneN$_4$S bicycle (L3):

The success of the synthesis of the [10]aneN$_4$O bicyclic ligand system by reacting the N,N'-bis(α-chloro amido)diaminopropane electrophile with [10]aneN$_2$O (section 3.3b), suggested that a similar synthesis should be attempted with [10]aneN$_2$S.

The cyclization of [10]aneN$_2$S (**20**) with N,N'-*bis*(α-chloro amido)diaminopropane (**27**) was successful. No side products were observed in the NMR spectra of the crude reaction filtrate (see figure 3.21). There was no unreacted [10]aneN$_2$S detected in the crude reaction filtrate nor the precipitate, which implied that all of the [10]aneN$_2$S had reacted to form product.

Unreacted N,N'-*bis*(α-chloro amido)diaminopropane (**27**) was, however, present in the solid residue from the crude reaction filtrate. Complexation of the solid residue with copper(II) perchlorate in water followed by chromatography over sephadex CM-C25 purified the [10]aneN$_4$S bicycle diamide (**30**) product. This was because the unreacted N,N'-*bis*(α-chloro amido)diaminopropane formed polymeric complexes with copper(II) such that it bound to the sephadex, whereas the [10]aneN$_4$S bicycle diamide must have formed a neutral [Cu(**30**)] complex due to the deprotonation of the two amide groups. The neutral complex therefore did not bind to the sephadex cation-exchange resin. NMR

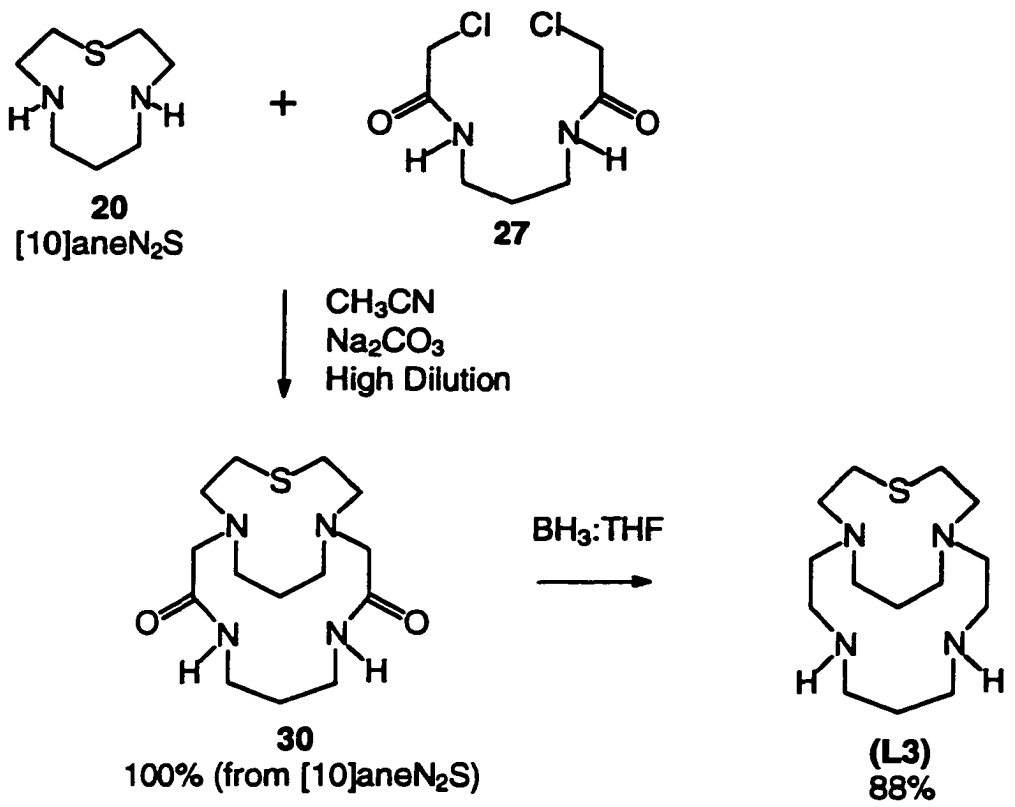

Scheme 3.8. Synthetic route to [10]aneN$_4$S bicycle (**L3**) from [10]aneN$_2$S (**20**).

spectroscopy indicated that the reactant (**27**) had been successfully removed such that the product (**30**) was better characterized than the crude hemi-cryptateN$_4$S bicyclic diamide (**16**) discussed in section 2.5(c). However, the elemental analysis gave lower %C and %N values than expected and higher %H. This is likely to be due to the presence of salts from the removal of the copper(II) ion from the complex using Na_2S and NaOH/HCl.

The discussion in section 3.2(d) regarding the purity of the [10]aneN$_2$S used in this work is relevant to the observations made in this synthesis. When the initial [10]aneN$_2$S reagent was impure, no side products were observed in the crude reaction mixture of the [10]aneN$_4$S bicycle (see figure 3.21). Curiously, when the t-BOC purified [10]aneN$_2$S

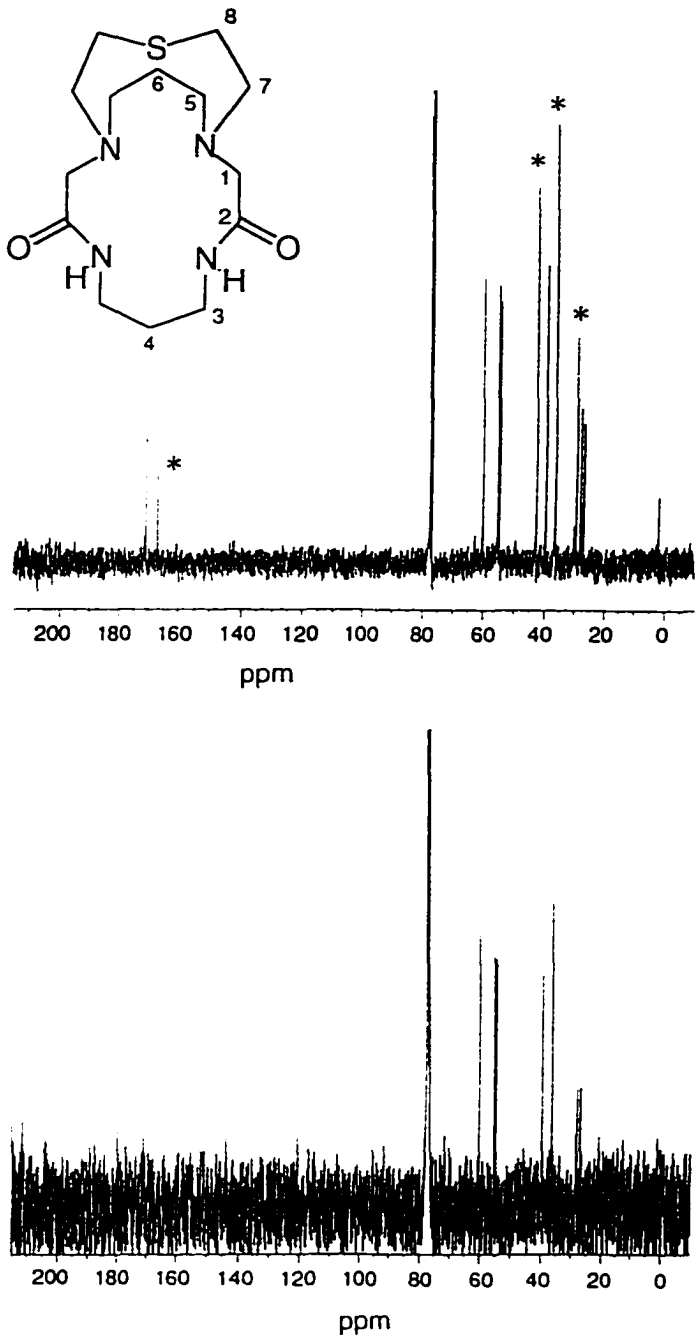

Figure 3.21. ^{13}C-NMR of crude acetonitrile filtrate (top) and purified (bottom) [10]aneN_4S bicycle diamide **(30)**. * = unreacted N,N'-bis(α-chloro amido)diaminopropane **(27)**.

sample (which was much more pure) was reacted, the resulting crude reaction filtrate was shown by ^{13}C-NMR spectroscopy to have at least 30% unreacted [10]aneN_2S and two forms of unreacted N,N'-*bis*(α-chloro amido)diaminopropane. This result supports the

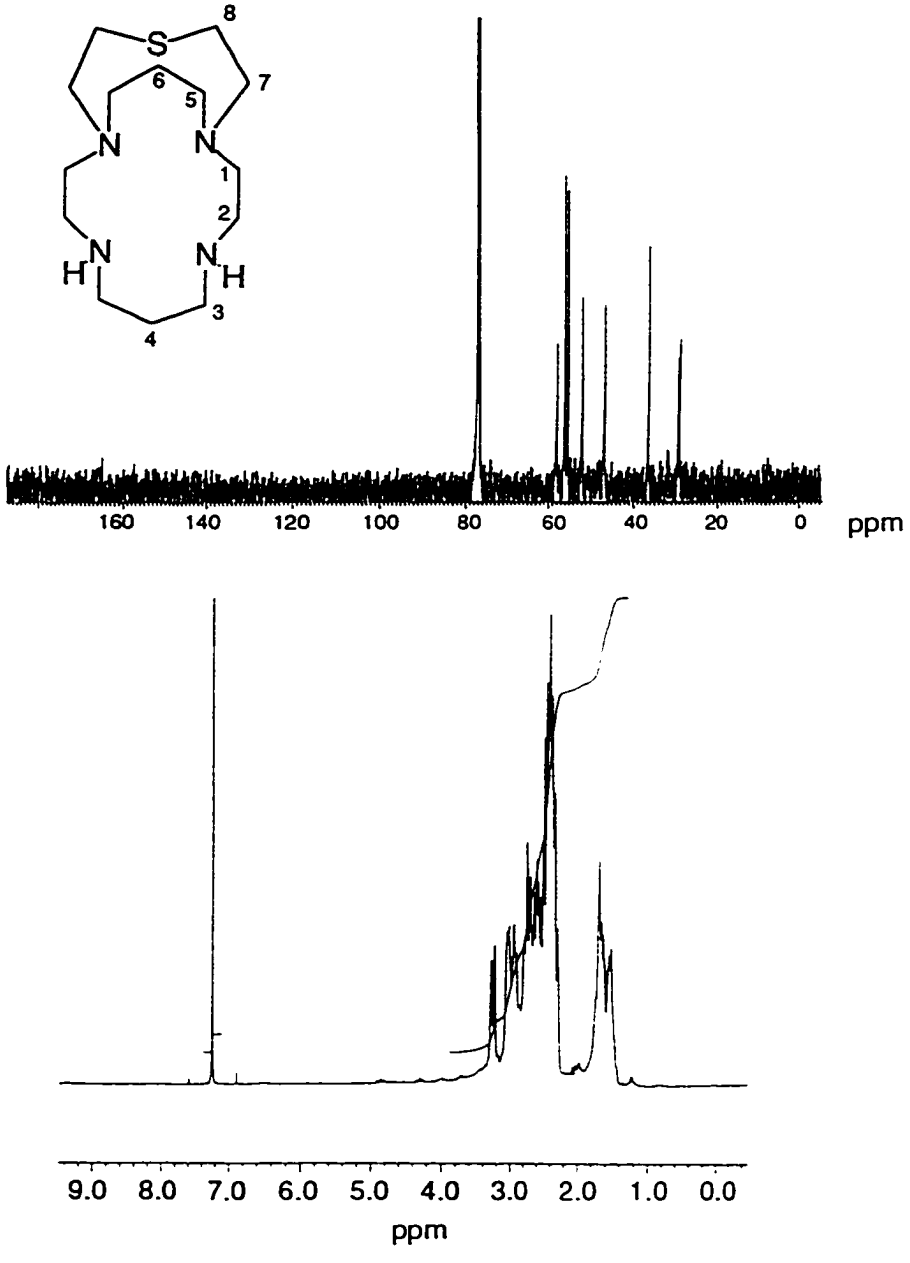

Figure 3.22. ^{13}C-NMR and ^{1}H-NMR spectra of purified [10]aneN_4S (L3) bicycle.

idea that the additional peaks seen in the NMR spectra of [10]aneN_2S are due to an intact form of the [10]aneN_2S ligand since the subsequent reaction with N,N'-*bis*(α-chloro amido)diaminopropane resulted in a crude reaction mixture of much higher purity than the original [10]aneN_2S reactant. Alkylation of the nitrogens of the putative [10]aneN_2S side product(s) appears to produce the same product species as alkylation of [10]aneN_2S itself.

An attempt at chromatographing the [10]aneN_4S bicycle diamide over silica gel (5% NH_4OH / 47.5%MeOH / 47.5% chloroform) resulted in only an uncharacterizable, somewhat decomposed, form of the ligand. It was also noticed that dissolution of the [10]aneN_2S bicycle diamide sample in methanol for 1.5 days resulted in similar decomposition. It is believed that these effects were a result of formation of sulphonium salts[130] by reaction of the product with the unreacted N,N'-*bis*(α-chloro amido)diaminopropane (see figure 3.23). In both cases, the sample had been dissolved in a polar solvent system which stablizes the formation of charged sulphonium salts. The subsequently synthesized [10]aneN_4S bicycle diamide samples were not dissolved in water or alcohols (except when complexed with copper(II) perchlorate).

Another interesting observation relating to the possibility of [10]aneN_2S having more than one conformation on the NMR time scale was that the initial ^{13}C-NMR spectrum of the column purified [10]aneN_4S bicycle also contained additional peaks. Purification of the other two isomers of the [10]aneN_4S bicycle by the same method produced samples that were NMR pure. As with [10]aneN_2S, no other molecular ions were detected in the mass spectrum. When the [10]aneN_4S bicycle ligand was further complexed to copper(II) perchlorate and chromatographed over sephadex CM-C25 cation-exchange packing a second time, the $[Cu(L3)]^{2+}$ product was the only compound observed and eluted. When the copper(II) was removed, the ^{13}C-NMR spectrum of the free ligand no longer contained the additional peaks.

As with [10]aneN_2S, it was first believed that the presence of additional peaks in the NMR spectra of the [10]aneN_4S bicycle was due to conformational effects. However, as with [10]aneN_2S, the fact that it was possible to purify the ligand further such that there

were no longer additional peaks in the NMR spectrum, suggested that conformational effects were not the cause. In the future, variable temperature NMR experiments should be performed to see if the additional peaks collapse at higher temperature.

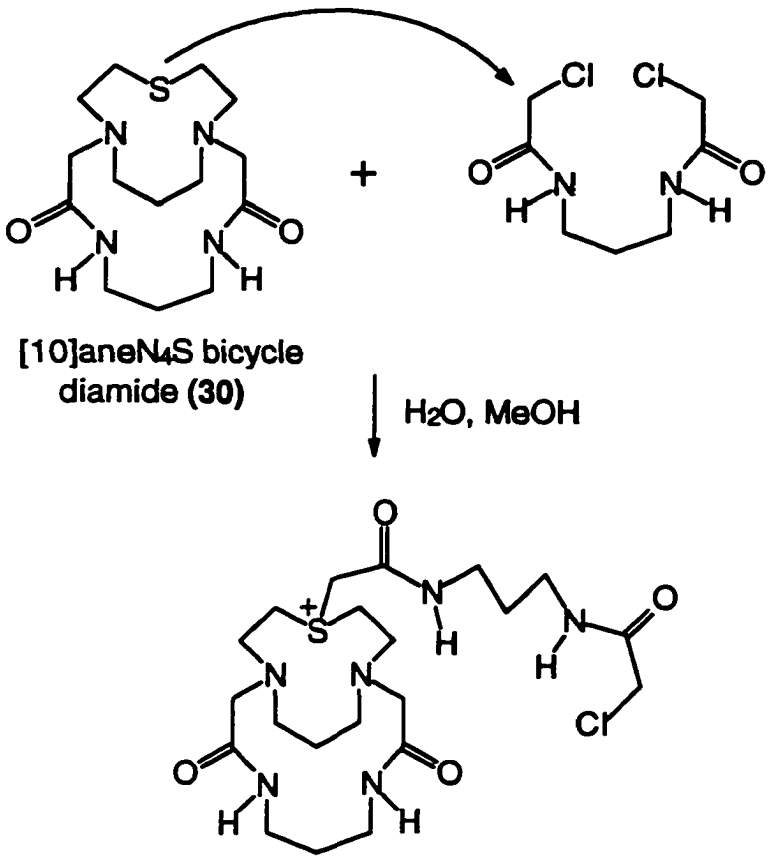

Figure 3.23. Proposed formation of sulphonium salts.

3.5. Ligand Rigidity Relative to ^{1}H-NMR Spectra of N_4S bicycles:

There is a growing interest[131] in the field of coordination chemistry concerning the effects of ligand rigidity on the chemistry of the coordinated metal atom. Highly flexible ligands allow too much dynamic variation in coordination geometry on the time scales of most chemical studies, such that only time averaged geometries can be considered. Rigid ligands bind the central metal in a more well-defined geometry so that the effect of a given geometry on the observed chemistry of the metal (e.g. redox potential, self-exchange rate, kinetic rates) can be determined. If the coordinating ligand is too rigid however, the metal will not be able to coordinate all of the ligand donors because energy is required to position the donors into the coordination sphere of the metal for bonding. Multidentate macrocyclic ligands are the most suitable ligands for these kinds of studies[72] since their metal complexes are kinetically inert with respect to metal dissociation, and the donor atoms are linked by the ligand backbone.

In order to design ligands which meet the criteria of being flexible enough to allow bonding of all donors yet rigid enough to provide a well-defined coordination geometry, it would be useful to develop methods of assessing the relative rigidity of various known ligands. The most useful technique for assessing ligand rigidity is ^{1}H-NMR spectroscopy. Here, the geminal and vicinal coupling constant data provide at least qualitative determinations of ligand conformation. The only reports[132] found in the literature in which ligand structure is assessed by ^{1}H-NMR spectroscopy involve analyses of the metal complexed ligand. Most multidentate macrocyclic ligands synthesized to date for the purpose of coordinating transition metals are flexible enough in their free ligand form in solution to produce dynamically averaged NMR spectra. Only upon coordination of the central metal does the ligand "lock" into one well-defined conformation. The coordination of the donor atoms renders them stereochemically rigid thereby forcing the ligand to accomodate the interactions by adopting the lowest energy conformation(s) suitable for coordination.

In this work, the ligands of interest are the N_4S bicycle structural isomers. These ligands consist of a cyclam (tetraazacyclotetradecane) ring fused to a [9]aneN_2S, diethyl sulphide or [10]aneN_2S ring. The parent [9]aneN_2S (figure 3.24), cyclam (figure 3.25) and [10]aneN_2S (figures 3.12, 3.15) moncyclic free ligands have ^{1}H-NMR spectra which show only first order couplings. The diamide analogues of these ligands, dioxocyclam and [10]aneN_2S diamide (figure 3.2) respectively, are much more rigid due to the planarity of the amides such that the ^{1}H-NMR spectra show second order couplings. The cause of the second order effects has always been considered to be due to the lack of free rotation of the methylene chains due to the cyclic structure of the ligand.

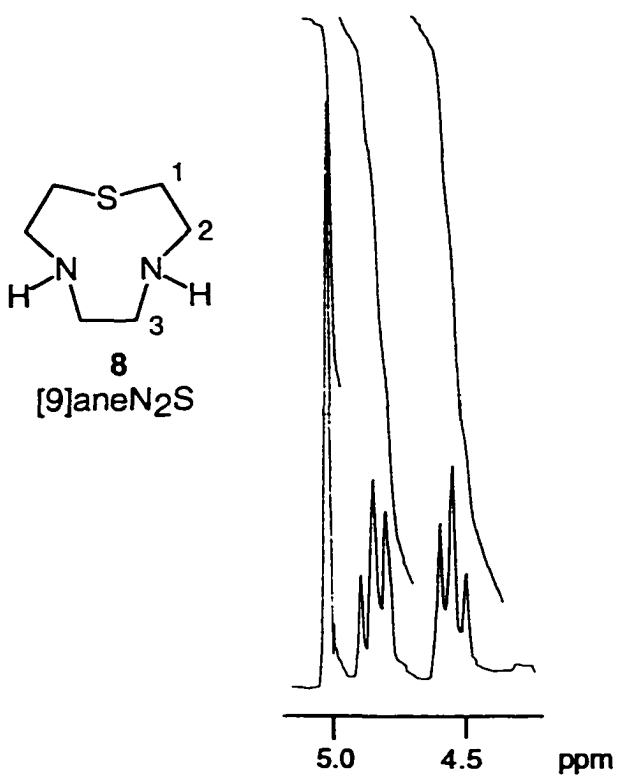

Figure 3.24. ^{1}H-NMR spectrum of [9]aneN_2S (8).

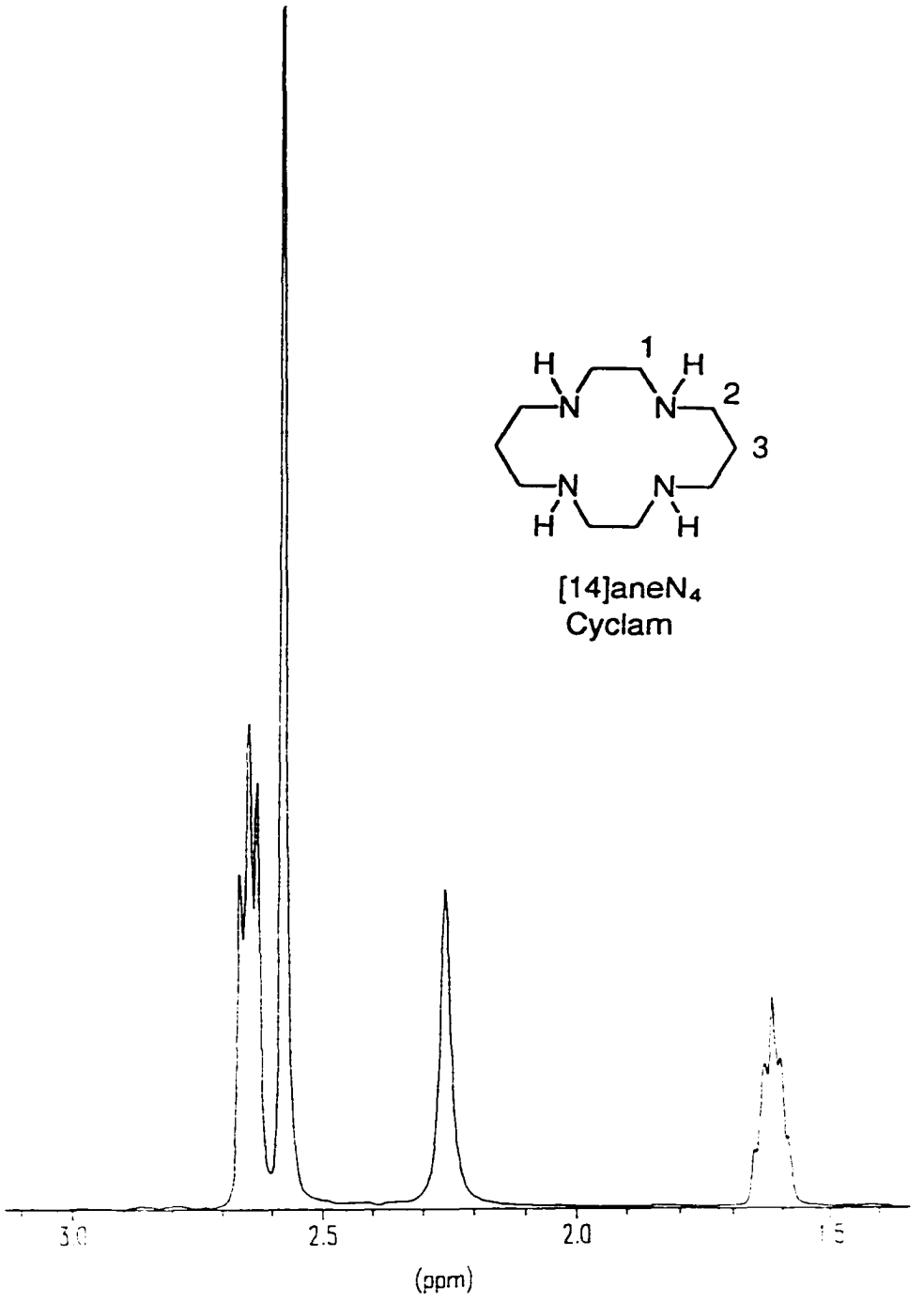

Figure 3.25. Room temperature ^{1}H-NMR spectrum of cyclam.

Lehn et al[99] reported the synthesis and properties of a series of diazapolyoxa-macrobicycles. Their ^{1}H-NMR spectra showed first order coupling at room temperature. The [2.2.2] ligand shown below has a C_3 symmetry axis through the bridgehead nitrogens such that the two protons on any given methylene carbon are equivalent by symmetry. It is therefore not necessary for free rotation to occur to average the signals to first order:

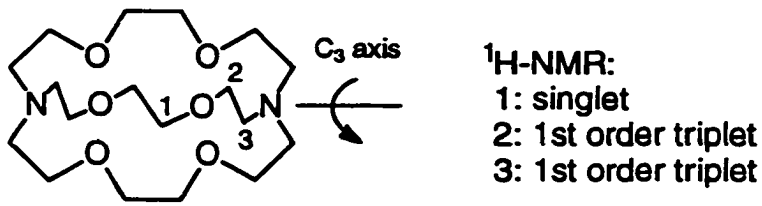

Lehn's [2.2.2] diaza polyether cryptand.[99]

Likewise, the two protons on any given methylene carbon of cyclam and [10]aneN_2S are also equivalent by symmetry due to the presence of the plane of symmetry in the plane of the macrocyclic ring.

The ^{1}H-NMR spectra showed second order coupling at low temperatures (< -80 °C). Such a result implies that the methylenes are not freely rotating at these temperatures. There are other molecular motions that can average the couplings but not enough to obtain first order behaviour. One of these motions must have been restricted at low temperature in order for the spectrum to show second order behaviour. Lehn et al[99] concluded that the molecular motion involved in the bicyclic cryptands was that of nitrogen inversion. Although linear secondary and tertiary amines are considered to be stereochemically non-rigid due to rapid inversion at the nitrogen centers,[114b] these macrobicyclic ligands were of sufficient rigidity to hinder the nitrogen inversions at low temperature.[99] As a result, each macrobicycle was reported to exist in solution at low temperature as an interconverting mixture of the three exo-exo, exo-endo and endo-endo isomers shown in figure 3.26. At room temperature the inversions were rapid on the NMR time scale. The energy barrier was reported to be 5 - 8 kcal/mole and the rate of

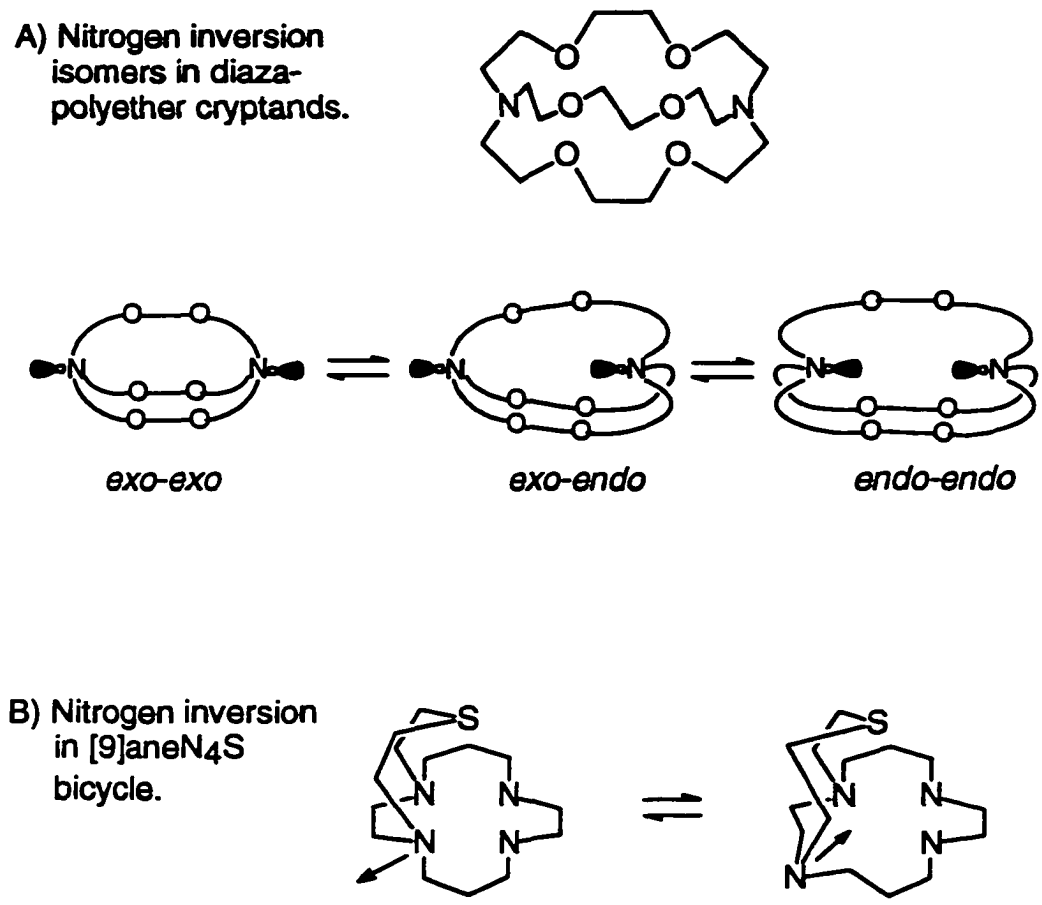

Figure 3.26. Pictorial representation of nitrogen inversion isomers.

interconversion at ambient temperature was > 10^3 sec^{-1}. This energy barrier is less than that reported[133] for amide groups which explains why the the ^{1}H-NMR of the diamide macrocycles are also second order.

Although the cyclic structure of Lehn's diaza polyether ligands can prevent free rotation of the methylene groups which link the various donor atoms, it is not possible to determine if free rotation was occurring, because the protons on each methylene are symmetrically equivalent. The symmetry prevents the two protons on a given methylene carbon from geminally coupling with each other. Molecular motions other than nitrogen

inversion were not reported by Lehn et al,[99] presumably because the macrobicyclic ligands reported in that work were relatively large such that there was enough freedom of motion in the methylene linkages.

Unlike the macrobicyclic ligands reported by Lehn[99] which were first order at room temperature, the N_4S bicyclic ligands synthesized in this work were observed to have very complicated second order coupling in their ambient temperature ^{1}H-NMR spectra (figure 3.27). This result implies that the methylene groups are not freely rotating on the NMR time scale. Also, the room temperature ^{1}H-NMR spectrum of the smaller 12-membered 4,10-dimethyl-1,4,7,10-tetraazabicyclo[5.5.2]tetradecane macrobicyclic cryptand reported by Micheloni et al[134] had a complex second order coupling pattern similar to the macrobicycles reported in this work:

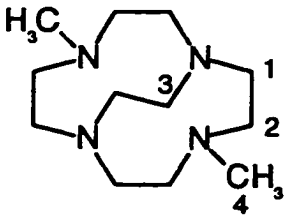

^{1}H-NMR:
1: 2nd order multiplet
2: 2nd order multiplet
3: singlet
4: singlet

The resonances labeled 1 and 2 above were assigned[134] by 2D-NMR techniques (^{1}H-^{1}H homonuclear and ^{1}H-^{13}C heteronuclear correlations) as the two unique methylenes of the cyclen ring. If these methylenes were averaging by free rotation at room temperature then they should only have produced first order (or at least deceptively simple second order coupling) like the cryptands synthesized by Lehn.[99]

This complexity is expected for the N_4S bicycles and Micheloni's N_4 bicycle because, unlike the diazapolyether cryptands, cyclam and [10]aneN_2S, the two protons on any given methylene carbon are not equivalent by symmetry. Each set of chemically unique methylenes will therefore contain geminal couplings giving rise to the observed complexities in the ^{1}H-NMR spectra.

It is necessary to assess the degree of rigidity implied by these spectra in order to determine how much more rigid the ligand is when complexed to a transition metal (e.g.

diamagnetic palladium(II)). The lack of symmetry provided the opportunity to obtain some qualitative information on the relative rigidity of the [9]aneN$_4$S bicycle since only molecular motions can simplify the couplings.

The variable temperature ^{1}H-NMR spectra of the [9]aneN$_4$S bicycle are presented in figure 3.27. It is not possible to interpret the multiplets between 2.2 and 3.1 ppm, but the two C-C$\underline{H_2}$-C resonances at 1.51 and 1.77 ppm are very illustrative. The fact that there are two such resonances at room temperature implies that the two C-C$\underline{H_2}$-C protons are not identical, as was expected from symmetry. One of these protons lies above the N_4 plane on the same side as the sulphur bridge while the other lies below the plane further from the bridge. There are two such methylene groups which are equivalent due to the plane of symmetry bisecting the [9]aneN$_4$S bicycle and perpendicular to the N_4 plane (this plane of symmetry is present in the ^{13}C-NMR). At higher temperature (> 40 °C) the two resonances collapse into one broad unresolved peak, indicating that the two methylene protons are starting to be averaged by molecular motion of some kind.

In addition to nitrogen inversion, there are three other molecular motions which could be slow on the NMR time scale at room temperature which became rapid enough to collapse the C-C$\underline{H_2}$-C methylene signal at 1.65 ppm. These motions are depicted for the [9]aneN$_4$S bicycle in figure 3.28. The first motion is that of free rotation. Although there is no rotamer in which the two methylene protons are equivalent by symmetry, rapid free rotation averages the environment of each proton such that the observed coupling is essentially first order. A relevant example is that of *cis*-1,5-cyclooctanediol:

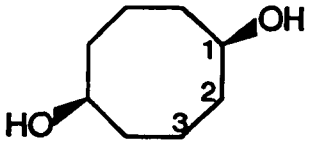

^{1}H-NMR:
1: 1st order quintet
2: 1st order quartet
3: 1st order quintet

This molecule has a cyclic structure with three methylenes bridging between the hydroxyl substituted carbons. The hydroxyl substituted carbons are chiral with both hydroxyl groups on the same side of the ring thus these carbons can be likened to being

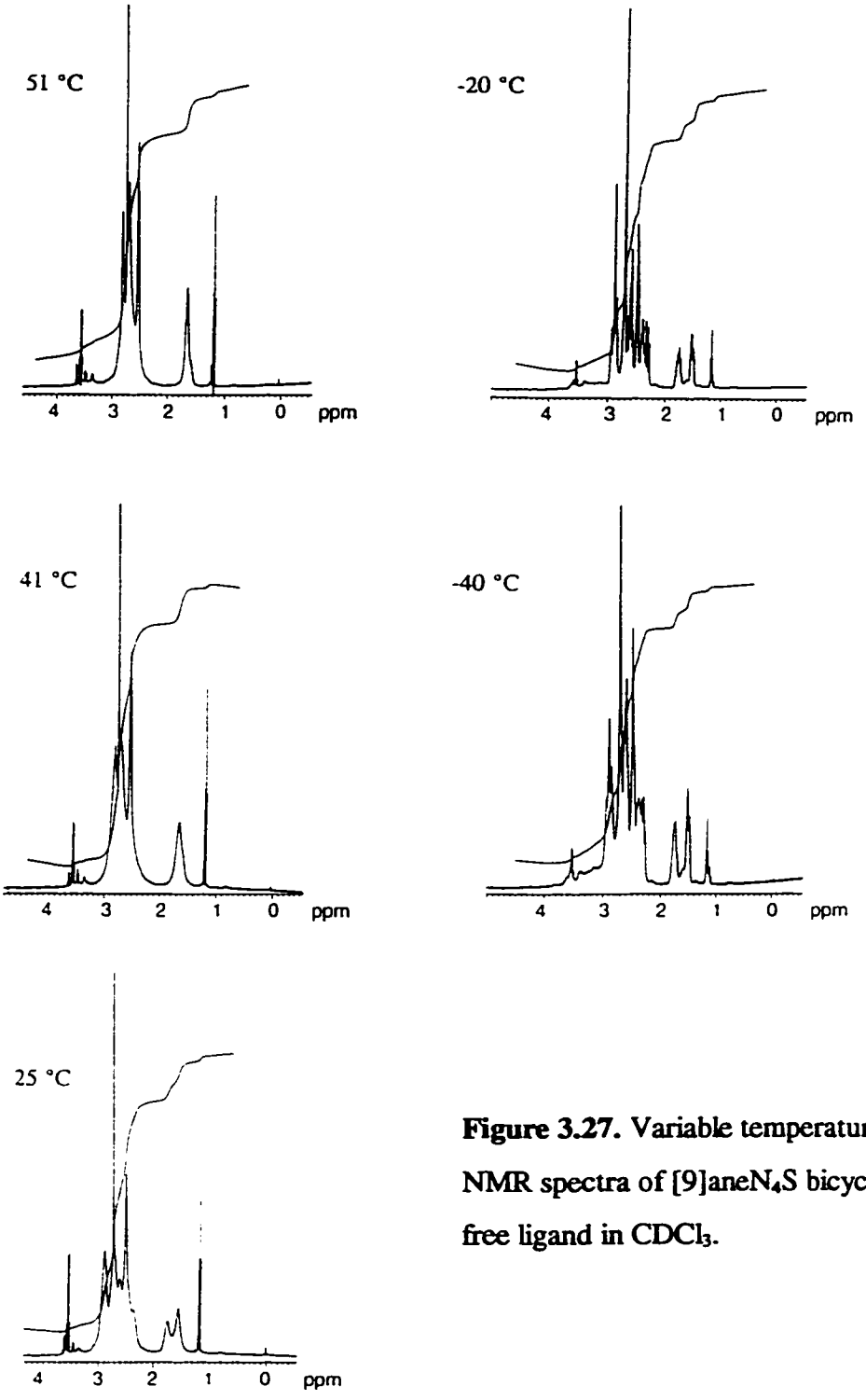

Figure 3.27. Variable temperature ^{1}H-NMR spectra of [9]aneN$_4$S bicycle (**L1**) free ligand in $CDCl_3$.

bridgeheads. The two protons on any given methylene carbon are therefore not equivalent by symmetry such that geminal coupling (2nd order) should occur. Instead, the splittings of the proton resonances of the two unique methylenes are first order (quartet and quintet). The "bridgehead" methine proton is also a first order quintet. Since there are no nitrogens present in this system, nitrogen inversion is not possible. It must be concluded that free rotation of the methylenes has averaged the couplings.

Although it is still possible that the second order coupling observed in the C-C$\underline{H_2}$-C methylene signal in the [9]aneN$_4$S bicycle spectrum could be due to hindered free rotation, it does not seem likely based on the fact that the spectra of similar ring systems (*cis*-1,5-cyclooctanediol, [2.2.2]-cryptand) are first order. The [9]aneN$_4$S bicycle can be viewed as having two bridgehead nitrogens in a 9-membered ring which are bridged by a 10-membered fragment. It is this 10-membered bridge which contains the two C-C$\underline{H_2}$-C methylene groups in question. The freely rotating bridges (first order couplings observed) in the diazapolyether cryptands are shorter (8-membered) than this 10-membered bridge and therefore should be more hindered.

In the absence of free rotation of the -CH$_2$-CH$_2$-CH$_2$- groups, it is still possible for this propylene fragment to average by flipping between alternative chair and boat conformations as depicted in figure 3.28(b). The energy barrier to this kind of molecular motion is much less than that of free rotation. A relevant example is that of cyclohexyl iodide. Experiments with this molecule and other substituted cyclohexanes[114c] have shown that such conformational inversions are very rapid on the NMR time scale at room temperature (half life < 10^{-5}). Also, the preceding arguments suggested that free rotation is occurring in the [9]aneN$_4$S bicycle such that conformational inversion must also be rapid on the NMR time scale.

The third type of molecular motion, depicted in figure 3.28(c), is that of homeomorphic isomerization. This motion is a result of the nature of the bicyclic and tricyclic ligand frameworks and refers to the interconversion of isomers that occurs when one of the bridging chains slips through the center of the ring that it bridges, effectively

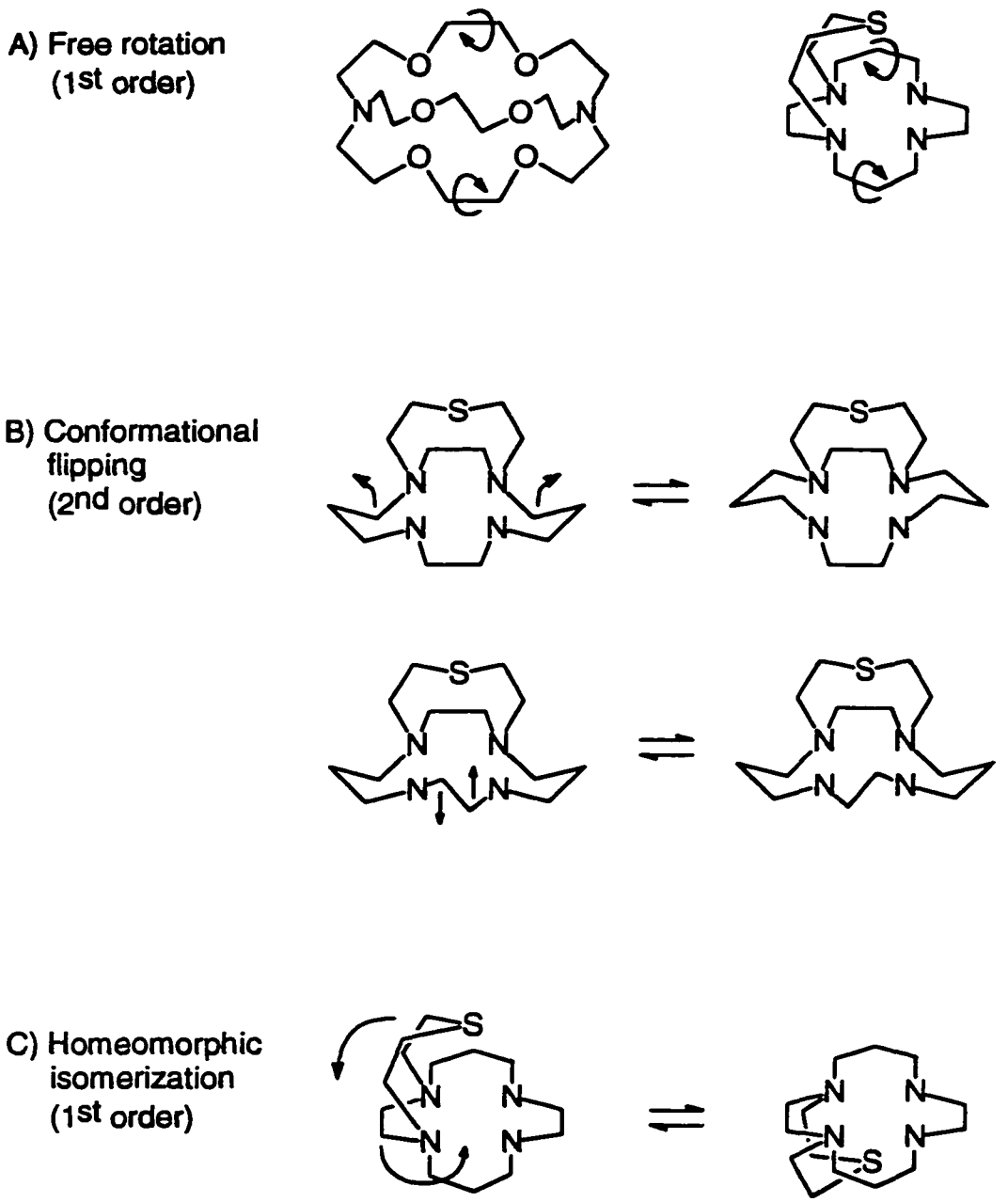

Figure 3.28. Molecular motions which can average the middle methylene signals.

turning the molecule inside out. Homeomorphic isomerization has been reported[135] for several bicyclic molecules with sp^3 carbon bridgehead atoms. Unlike the bicyclic systems with nitrogen bridgehead atoms, these carbon bridgehead atoms can not interconvert by stereochemical inversion. Interconversion of the in-in, in-out and out-out isomers therefore can only occur via homeomorphic isomerization as shown in figure 3.29.

The barriers to homeomorphic isomerization are much higher than the free rotation and conformational inversion motions discussed above. For example, an elegant NMR study of the interconversion of the in-out atropoisomers of a peptidic bicyclic molecule determined the energy barrier to homeomorphic isomerization to have a half-life of 158 hours. Although this system contained relatively rigid amide groups in the bridges which serve to slow the movements, homoemorphic isomerization is generally much slower such that it is unlikely to be responsible for the collapse of the C-$C\underline{H}_2$-C signals in the 40 °C ^{1}H-NMR of the [9]aneN_4S bicycle.

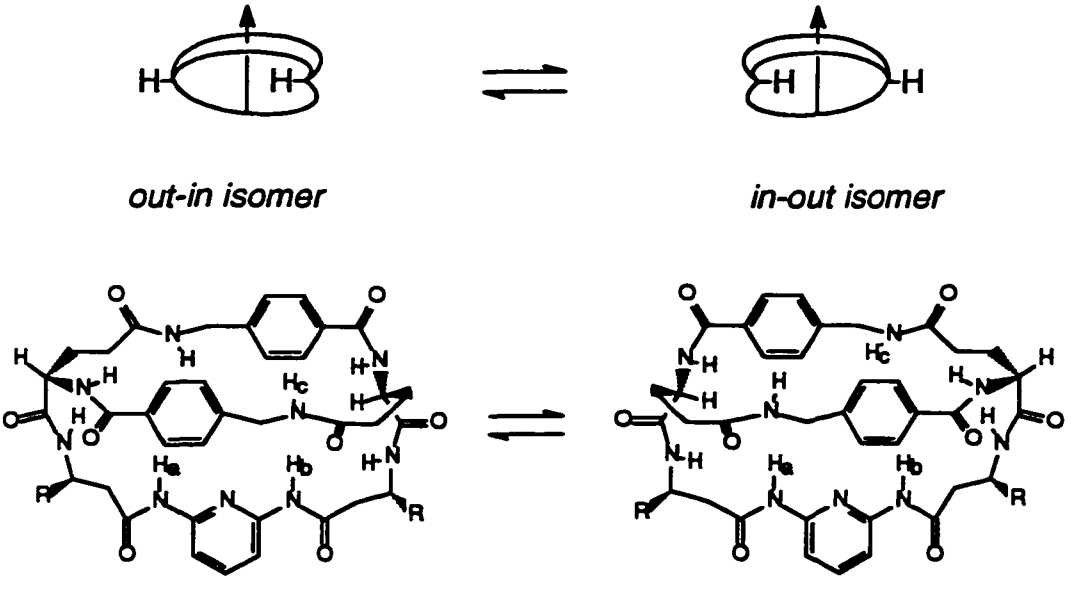

Figure 3.29. *Out-in* and *in-out* diastereomers which can only interconvert via homeomorphic isomerization.[135]

It is worthy of noting that the hemi-cryptateN_4S bicycle (**L2**) offers an opportunity to study homeomorphic isomerization. This is because the bicyclic topology of the ligand is chiral, as depicted below. The ligand was presumably synthesized as a racemic mixture. If one of the enantiomers were isolated, perhaps by forming the diastereomeric [Cu(**L2**)](*d*-tartrate) salt then removing the copper(II), the enantiomer could only racemize by homeomorphic isomerization. The racemization would have to be followed by polarimetry to determine the half-life.

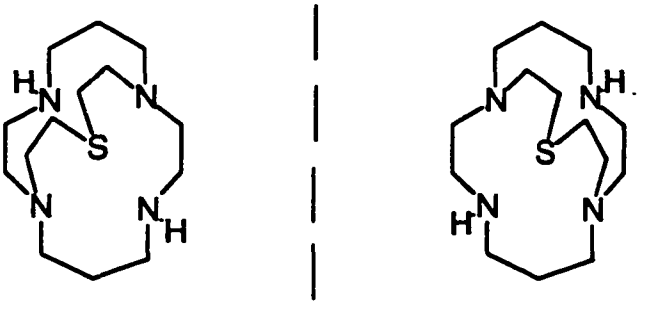

Figure 3.30. Enantiomers of hemi-cryptate N_4S bicycle.

In attempting to explain the source of these coupling effects in the [9]aneN_4S bicycle free ligand, it is necessary to consider that these ligands are much smaller versions of the macrobicycles reported by Lehn et al.[99] The nitrogen inversion processes discussed above (see figure 3.26) are therefore likely to be much slower in the [9]aneN_4S bicycle due to the shorter 3-membered and 5-membered linkages across the bridgehead nitrogens. Bicyclic structures with nitrogen bridgeheads can adopt only out-out structures when the rings are small (3- or 4-membered) or common sized (5- and 6-membered). In larger systems, out-in and eventually, in-in structures become possible and may be more stable.[136] Very little is known about the borderlines for these changes.

The effect of ligand strain on nitrogen inversion has been studied in detail for many small diazabicyclo alkanes. Several dynamic NMR studies[137] of N,N'-dialkylhexahydropyrimidines have shown that ring inversion ($\Delta G^{\ddagger} \approx 11$ kcal/mol) is a higher energy process than N-inversion ($\Delta G^{\ddagger} = 6$ -8 kcal/mol). The most relevant study found in the literature[138] followed the conformational inversions of the 1, (n+2)-diazabicyclo[n.3.1]alkane systems shown below. In these systems, where both processes necessarily involve concomitant torsions in the (n+3)-membered rings, higher barriers might be expected:

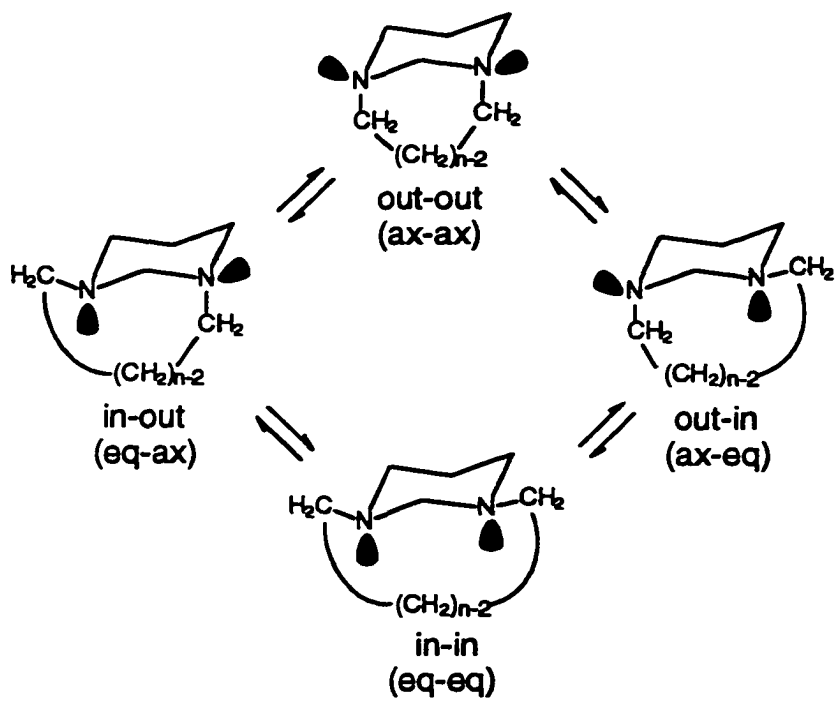

Figure 3.31. N-inversion isomers of 1, (n+2)-diazabicyclo[n.3.1]alkane systems.[138]

As with the middle methylene (C-C<u>H</u>$_2$-C) of the [9]aneN$_4$S bicycle, the aminal 1-carbon methylene group between the bridgehead nitrogens provided a good probe for the

study of the two basic processes of ring inversion and nitrogen inversion by dynamic NMR. The aminal N-C$\underline{H_2}$-N protons are geminally coupled such that geminal exchange provided a way of monitoring the molecular motions. This mutual exchange was found[138] to be in the slow exchange limit on the NMR time scale at ambient temperature for all members of the 1, (n+2)-diazabicyclo[n.3.1]alkane series that were studied (n = 0 to 5).

Photoelectron spectroscopy, was also used to distinguish N-inversion on these compounds. The energy barriers to molecular motions were modelled with empirical force field calculations (MM2) and semiempirical MO calculations. It was concluded that the borderline for changeover from out-out to in -out structures for the 1, (n+2)-diazabicyclo[n.3.1]alkane series of bicyclic molecules was at n = 4. In light of such a result, it is reasonable to propose that the reason the N-inversion barrier was much lower for the diazapolyether cryptands was because of the larger size which allowed the ligand to be more flexible at the bridgeheads than in Micheloni's[134] oxalyl bridged cyclen bicycle and the [9]aneN$_4$S bicycle reported in this work.

The results of Lehn's diazapolyether cryptands and Alder's diaza bicycles suggest that N-inversion is the cause of the 2nd order couplings in the [9]aneN$_4$S bicycle NMR spectrum but that ring inversion (chair-chair flipping) is probably slow on the NMR time scale at room temperature also and is certainly slow at low temperature. The presence of another slow exchange molecular motion on the NMR time scale such as ring inversion would explain why the low temperature spectra of the [9]aneN$_4$S bicycle did not freeze out into sharp subspectra.

It is probably not necessary to consider the N-inversion and ring inversion movements as separate from each other, especially as the bicycle becomes smaller, or has a 1-carbon bridge as in the case just described. Instead they should be considered to be concerted motions since inversion of the bridgehead nitrogen inevitably imparts torsional motion on the attached methylene linkages.

Molecular modelling (MM2 calculations) of the [9]aneN$_4$S bicycle was used to qualitatively assess the rigidity imposed by bridging the adjacent 1,12 nitrogen centers of

the cyclam ring. In order to obtain consistent and meaningful results, the crystallographic fractional atomic coordinates[90] were used as the initial structure.

After minimization to the molecular mechanics optimized structure, the energy of the [9]aneN$_4$S bicycle was 39.28 kcal/mol (optimization of cyclam gave 11.36 kcal/mol). To provide a more appropriate comparison, the -CH_2-CH_2-S-CH_2-CH_2- bridge of the [9]aneN$_4$S bicycle was disconnected at one of the S-CH_2 bonds then minimized. The energy of the optimized structure was 32.22 kcal/mol. The energy difference between the connected and disconnected structures is 7.06 kcal/mol which suggests that there is a significant but not large increase in strain associated with bridging the adjacent nitrogens. This strain energy is similar to that which is suggested by the ^{1}H-NMR observations, however, the error in such calculations is considered[139] to be +/- 5 kcal/mol such that this result is not reliable.

Chapter 4

Synthesis and Characterization of Copper(II) Complexes of N_4S Macrobicyclic Ligands

4.1. Introduction:

There is considerable interest in studying the coordination chemistry of copper-sulphur complexes, which has been motivated by the presence of sulphur coordination in metalloenzymes such as the "blue" copper proteins[140-143] and cytochrome c.[144,145] The blue copper proteins have attracted much interest because of their distinctive spectrochemical properties. For example, plastocyanin (in photosystem I) and Azurin (in bacteria) are blue coloured single copper proteins which function as electron transfer centers in biological redox chains.[145]

All members of the blue copper proteins contain a type I copper site which is characterized by an intense blue colour due to a S(Cys)→Cu(II) charge transfer absorption near 600nm ($\varepsilon \approx 5000\ M^{-1}\ cm^{-1}$) and a relatively small Cu(II) hyperfine interaction ($A_{//} \leq 90 \times 10^{-4}\ cm^{-1}$). The available X-ray crystal structures of several copper proteins with a type I site (see figure 4.1) reveal three strong ligands, a cysteine thiolate and two histidine imidazole residues, in a trigonal arrangement with relatively short bonds (≈ 2 Å) and a fourth, weaker methionine thioether axial ligand (≈ 3 . Å). The observed modulation of the Cu(II)/Cu(I) redox potential has been attributed[21] to the nature of the axial ligand(s) and the number and strength of the NH•••S-(Cys) hydrogen bonding interactions. For example, $E^{o_1}(Cu^{2+/1+}) = 276$ mV has been determined for *A. denitrificans* azurin whereas the value for *P. vulgaris* plastocyanin is 360 mV. In *A. denitrificans* azurin, the Cu-S(Met) bond is 0.02 Å longer than in poplar plastocyanin, and there is a carbonyl oxygen 3.1 Å away from the copper center, compared with 3.8 Å in plastocyanin. These differences in bond lengths are expected to stabilize copper(II) in azurin to a greater extent than in plastocyanin, and result in a lower E^{o_1} value for azurin.

It is again important to note that the intention of using macrocyclic complexes as models for the metalloenzymes is not to exactly reproduce the nature of the active site but rather to gain insight into certain salient features present. The oxidation/reduction behaviour of the series of [13-16]aneN_4 copper(II) complexes and their corresponding

open-chain analogues has been investigated.[146] Although the $Cu^{2+/3+}$ redox potentials were observed to depend on the structural features of the ligands, the various redox potentials (generally in the -0.8V to -1.2V range relative to ferrocene$^{0/+}$) do not correspond well with that observed in the blue copper proteins.

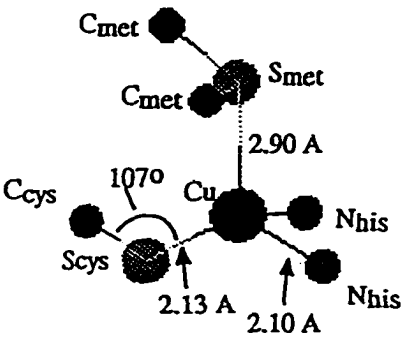

Figure 4.1. Pictorial representation of structure of the copper coordination environment of oxidized poplar plastocyanin.[142]

It has been well documented[84,147] that replacement of nitrogen donors with thioethers in both acyclic and cyclic ligands results in significant stabilization of copper(I). It has also been estimated[148] that the contribution, ΔE, of a sulphur donor to the half-wave reduction potential of copper(II) is *ca.* 140 mV, while that of a secondary amine donor is *ca.* -105 mV. Clearly, the nature of the donor is the dominant factor influencing the observed redox potentials.

As mentioned above, the redox properties of the copper blue proteins are not simply a reflection of sulphur coordination. Variation in the structural effects of the protein translate into "fine-tuning" of the copper(II) versus copper(I) stabilities. It is therefore of interest to investigate the effects of ligand structure for polyaza, polythiaaza and polythia complexes. For example, Hosken and Hancock[149] have reported the effect of

ligand rigidity on copper(II) stability for two analogous (with respect to donors) acyclic N_4 donor ligands. The authors reported that the presence of the rigid bispidine bridging group preorganizes the N,N'-*bis*(2-pyridylmethyl)-bispidine (DPB) ligand (shown in figure 4.2) relative to the analogous, but unreinforced, DPTN ligand. In fact, the extra stabilization provided by the DPTN ligand is considerably larger (4.8 log units) than the extra stabilization (3.3 log units) provided by the cherished macrocyclic effect of cyclam relative to 2,3,2-tet. Similar investigations[150] have been reported for nitrogen/sulphur mixed donor and polythioether ligands.

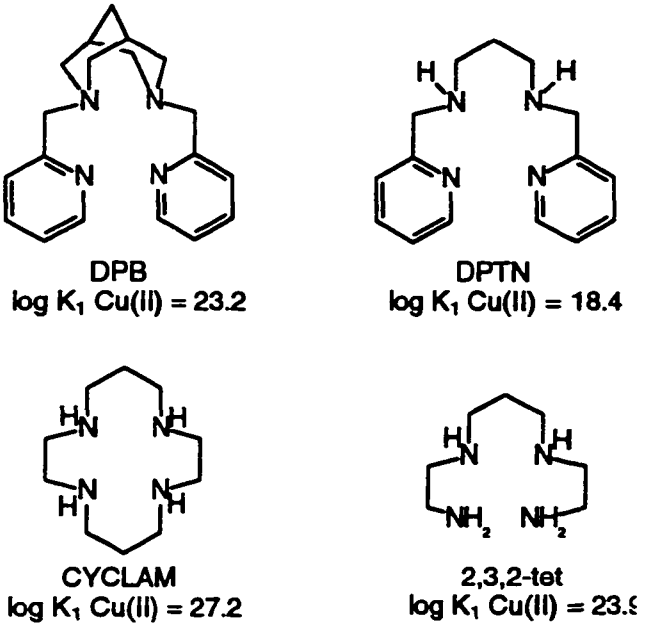

Figure 4.2. Comparison of copper(II) complex stabilities (log K_1) of acyclic preorganized DPB ligand versus that of cyclam.[149]

In light of the current interest in ligand rigidity effects upon copper complexes, an investigation of the properties of the copper complexes of the N_4S donor macrobicyclic ligands synthesized in the present study was conducted.

4.2. Synthesis of Copper(II) Complexes:

The syntheses of the three structurally isomeric copper(II) N_4S bicyclic complexes are reported in section 8.3 (compounds **31-33**). Only the characterization of the copper(II) complexes of the N_4S bicyclic target ligands (**L1-L3**) will be discussed:

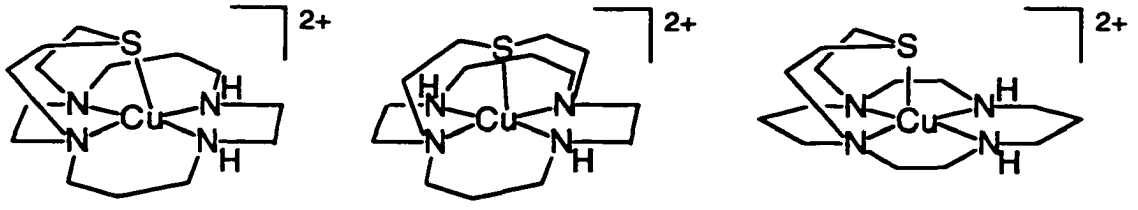

31
$[Cu(\mathbf{L1})](ClO_4)_2$

32
$[Cu(\mathbf{L2})](ClO_4)_2$

33
$[Cu(\mathbf{L3})](ClO_4)_2$

Each of the copper(II) complexes was prepared in satisfactory yield by addition of a stoichiometric amount of copper(II) perchlorate to the ligand. The complexes were purified from the copper(II) perchlorate and free ligand reactants by chromatography over sephadex CM-C25 cation-exchange packing. Typically, several recrystallizations must be performed in order to remove the considerable amount (~ 0.10 M) of $NaClO_4$ present after elution of the product complex. The yields reported in section 8.3 are that of the isolated complexes since loss of product occurs during recrystallization.

The synthesis of $[Cu([9]aneN_4S)](ClO_4)_2$ via a copper(II) templated condensation with glyoxal was previously reported by Fortier and McAuley[90] and is discussed in section 2.3. The preparation of the proposed monoamido complex, $[Cu(\mathbf{4\text{-}H})](ClO_4)$, is discussed in section 2.4. The microanalysis result for $[Cu(\mathbf{4\text{-}H})](ClO_4)_2$ gave unacceptably low C, H and N compositions. The amido complex is very hygroscopic and it was therefore difficult to remove all of the $NaClO_4$ by recrystallization.

Both the $[Cu([10]aneN_4S)](ClO_4)_2$ and $[Cu(hemi\text{-}cryptN_4S)](ClO_4)_2$ complexes were prepared in good yield and exhibited the exceptional acid stability already reported[90]

for [Cu([9]aneN$_4$S)](ClO$_4$)$_2$. The stability of each of these complexes is such that the only satisfactory method of removing the copper(II) center is to reflux with excess Na_2S wherein precipitation of CuS provides the driving force.

4.3. Proposed Ligand Structure Properties and Molecular Mechanics Modelling:

Although crystallographic studies have been performed on the copper(II), nickel(II), cobalt(III) and palladium(II) complexes of the [9]aneN$_4$S bicycle, and crystallography of the [Cu([10]aneN$_4$S)](ClO$_4$)$_2$ complex is in progress, it is also possible to gain insight into the comparative structural behaviour of the three N$_4$S bicycle isomers using MM2 molecular mechanics calculations.

It is of interest to assess the extent of ligand strain present upon coordination to the metal center. To achieve this goal, the fractional atomic coordinates of the [9]aneN$_4$S bicyclic ligand, without the copper atom, from the [Cu([9]aneN$_4$S)](ClO$_4$)$_2$ complex[90] were entered and the energy parameters calculated. These energy parameters represent the calculated energy of the ligand when it was in its coordinated, and therefore strained, conformation. The total energy of the structure was 69.5 kcal/mol. The structure was then minimized to obtain the lowest energy conformation of the free ligand (see figure 4.3). The total energy of the minimized structure was 39.3 kcal/mol, suggesting that the strain energy induced by coordination of the copper(II) center was *ca.* 30 kcal/mol. The largest contribution (*ca.* 20 kcal/mol) to this effect derived from the bond stretch term.

It is important to note that one of the major difficulties encountered in such calculations is that it is not possible to prove that the global minimum energy has been found. Indeed, the use of such calculations by experimental chemists often has led to erroneous predictions.[139] However, in this particular case, it is the energy difference which is of interest such that location of a lower energy minimum would only serve to increase the difference in (calculated) strain energy .

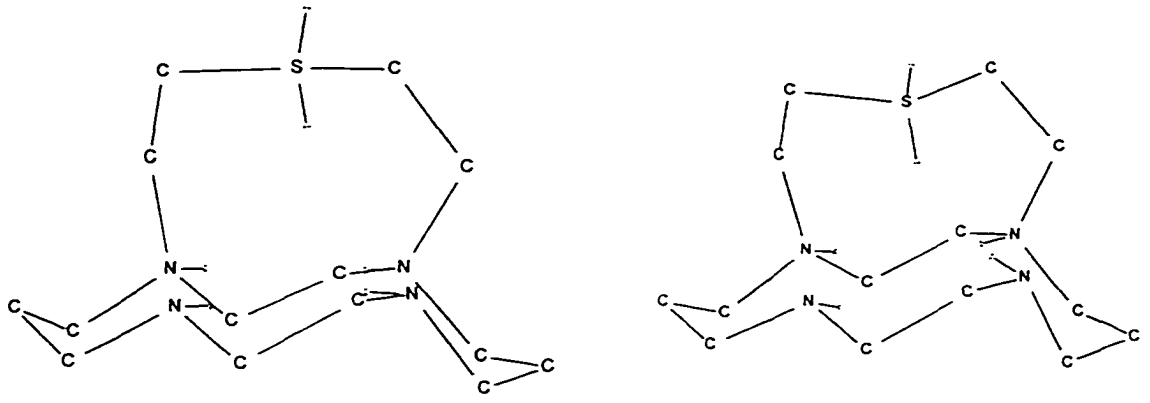

Figure 4.3. Representation of ligand strain energy associated with coordination (left) of copper(II) center in $[Cu([9]aneN_4S)](ClO_4)_2$ (using crystallographic coordinates for initial conformation) vs. minimized free ligand (right).

Calculation of the strain energy in this manner is analogous to the hole-size/strain energy calculations reported by Busch et al[151] and the magnitude (30 kcal/mol) calculated in the present study is greater then the the values calculated by Busch (2 - 10 kcal/mol) for the [14-15]aneN$_4$ complexes. Although the intention is to compare the strain energies calculated in this way for each of the three $[Cu(N_4S)](ClO_4)_2$ isomers, such a comparison can not be made until the crystallographic studies are completed.

In order to gain more insight into the coordinating ability of each N$_4$S-bicyclic ligand, molecular dynamics simulations were performed. Each of the three $[Cu(N_4S)](ClO_4)_2$ isomers were simulated using the cyrstallographic coordinates of the $[Cu([9]aneN_4S)](ClO_4)_2$ isomer as the initial coordinates. In the case of the hemi-cryptateN$_4$S and [10]aneN$_4$S bicycle isomers, two of the methylene groups in the sulphur bridge were disconnected from their bridehead nitrogen and re-connected to the appropriate nitrogen necessary to generate that isomer. This perturbation on the bridge conformation, as well as the effect of having the axial copper(II)-thioether bond length

equal to that of the $[Cu([9]aneN_4S)](ClO_4)_2$ isomer, was minimized by artificially "locking" the coordinates of each atom of the structure, except for those that had been moved, then performing a minimization to reposition them in their most stable coordinates.

It is of considerable interest to gain insight into the relative axial coordination abilities of the three isomers. In order to compare the constant temperature dynamics simulations for each of the three isomers, the coordinates of the four equatorial nitrogens, but not the axial thioether, first were artificially locked in their crystallographic coordinates. It is expected that the dynamics simulation would therefore only reflect the variation in metal-sulphur distances that each N_4S-bicyclic ligand prefers (with respect to energy) in the presence of N_4 equatorial coordination of the metal. It is important to note that, although the metal center has been labelled as copper in this simulation, the metal-nitrogen bonding requirements are not being accounted for (except for the fact that the metal and donors have been locked in the positions found in the crystal structure) such that the result gives the general tendency of where the ligand prefers to position the axial sulphur regardless of the nature of the metal. The simulation was performed in this manner to avoid the inherent error associated with application of molecular mechanics methods to transition metal complexes[152]. Considerable advances in adapting molecular mechanics techniques to give accurate predictions of the experimentally observed coordination numbers and geometries of copper(II) have been made[153] using the angular overlap model (AOM)[154] and cellular ligand field (CLF)[153] theories.

The results of the dynamics simulations are shown in figure 4.4. As expected for the $[Cu([9]aneN_4S)](ClO_4)_2$ isomer, there was a significant variation in axial sulphur distance. It was found that this distance was able to vary evenly within a *ca.* 2.3 Å - 4.4 Å range (figure 4.4(a)) without developing significant strain energies. There was no energy correlation with the axial distance within this range. Likewise, it was shown (figure 4.4(b)) that the $[Cu([10]aneN_4S)](ClO_4)_2$ isomer was able to vary the axial sulphur distance over a considerable (*ca.* 2.3 Å - 3.1 Å) range without developing significant strain energy. That

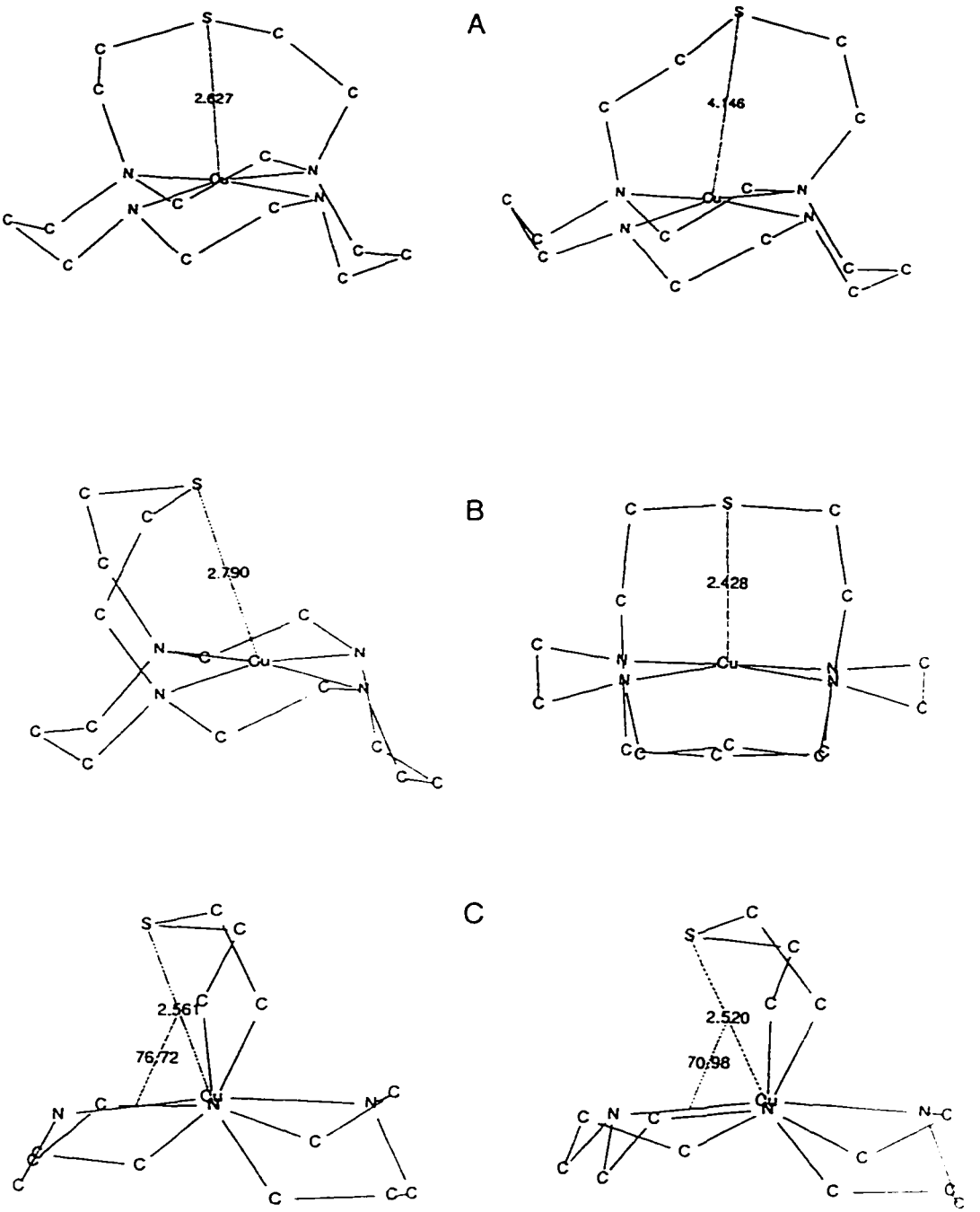

Figure 4.4. Molecular dynamics simulations of the three $[Cu(N_4S)](ClO_4)_2$ isomers showing Cu-S distances (Å): A) $[Cu([9]aneN_4S)](ClO_4)_2$ B) $[Cu([10]aneN_4S)](ClO_4)_2$ C) $[Cu(hemi\text{-}cryptN_4S)](ClO_4)_2$ Note: Cu-S-N bond angles shown also for this isomer

the upper limit of this range (3.1 Å) was less than that (4.4 Å) of the $[Cu([9]aneN_4S)](ClO_4)_2$ isomer, may be an indication that there is greater rigidity in the 10-membered ring.

The general conclusion from these molecular mechanics studies is that both the $[10]aneN_4S$ and $[9]aneN_4S$ bicyclic ligands are flexible with respect to accomodating the axial metal-sulphur bond distances required by the metal. This flexibility was also expected simply by considering that there is no obvious reason why bridging across adjacent nitrogens of the cyclam ring would significantly constrain movements of the sulphur bridge.

However, for the hemi-cryptateN_4S bicycle isomer, the bridging across the diagonally-opposed (*trans*) nitrogens will result in a ligand structure that is more rigid with respect to accomodating the axial bond length requirements of the metal center. Because the distance separation of the *trans* nitrogens is greater than that of the *cis*, it is expected that the ligand structure will result in a smaller variation in axial sulphur distance about the optimum free ligand value. This structural effect is represented pictorially in figure 4.5.

Figure 4.5(a) illustrates that, for the free ligand, the optimum axial distance of the sulphur above the cyclam plane will be a function of the matching of the sulphur bridge length with the macrocyclic hole-size of the cyclam ring. As the number of methylene linkages in the bridge increases, the optimum height of the sulphur increases also.

The resulting concerted motions of the bridge-sulphur and the bridgehead nitrogen donors are depicted in figure 4.5(b). It can be seen that a metal center that requires the axial bond length to be longer than the "natural" free ligand value, will "push" the sulphur upwards. However, in doing so, there is a concomitant pushing of the *trans* bridgehead nitrogens inwards towards the metal center due to the linkage of the sulphur bridge. This shortening of the hole-size will be resisted by the cyclam ring, as well as the metal center, such that significant strain energy must develop as the sulphur is raised further above its optimum (free ligand) axial distance. Conversely, the opposite effect exists for a metal

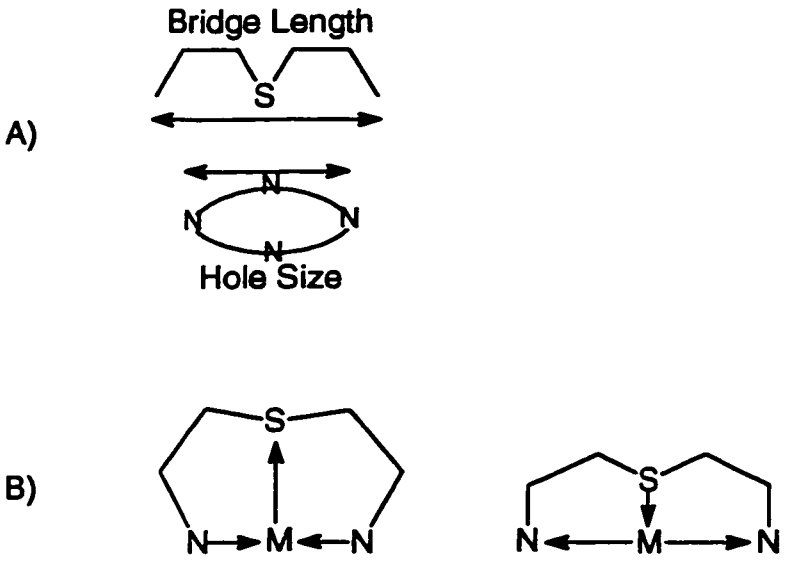

Figure 4.5. Pictorial representation of the concerted motions between the axial sulphur and equatorial bridehead nitrogen donors for hemi-cryptateN_4S complexes.

center that requires an axial bond length that is shorter than the optimum free ligand value. The "pulling" of the sulphur down towards the cyclam ring will, at some point, cause significant strain energy to develop due to lengthening of the cyclam ring hole-size.

Performing the same dynamics simulation (metal center and four nitrogen donors in fixed positions) as described above for the [9]aneN_4S bicycle and [10]aneN_4S bicycle isomers, provides an estimate of the upper and lower limits of the variation in axial sulphur distance caused by the nature of the *trans* linkage of the sulphur bridge in the hemi-cryptateN_4S isomer.

The results of this dynamics simulation are shown in figure 4.4(c). The sulphur was shown to vary within a 2.4 Å - 2.9 Å range without developing significant strain energies. This result suggests that metal centers requiring an axial bond distance that is greater than

this range will become significantly strained and possibly be forced to accept a shorter bond length. Likewise, a metal center requiring an axial bond distance that is shorter than this range will be significantly strained.

Another important result of the molecular mechanics calculation on the [Cu(hemi-cryptN$_4$S)]$^{2+}$ is that the optimum position of the thioether sulphur was displaced from the center of the N_4 donors, parallel to the plane of the cyclam ring. As can be seen in figure 4.4(c), the predicted dynamically averaged S-M-N(secondary NH) bond angles are approximately 75° and 120°. This result implies that the dihedral torsions in the methylene carbons of the sulphur bridge can not accomodate 90° bond angles between the equatorial and axial donors. Such a result was not unanticipated because it has been well documented[155] that SCCS fragments in crown thioether macrocycles are most stable in the *anti* conformation, rather than the expected *gauche* arrangement.

4.4. Electronic Spectroscopy of $[Cu(N_4S)](ClO_4)_2$ Complexes:

The UV/visible spectral data of the copper(II) complexes prepared in the present study are presented in table 4.1.

Table 4.1. UV/visible spectral data for copper(II) complexes in aqueous solution.

COMPLEX	N_4S: λ_{max}/nm (ε/$M^{-1}cm^{-1}$)
$[Cu([9]aneN_4S)](ClO_4)_2$ (data from ref 90)	d-d: 532 (143), 728 (37) UV: 281, (5400)
$[Cu([10]aneN_4S)](ClO_4)_2$	d-d: 533 (135), 743 (32) UV: 286 (4600)
$[Cu(hemi\text{-}cryptN_4S)](ClO_4)_2$	d-d: 603 (352) UV: 312 (4620), 282 (3200)
proposed [Cu(**4**)](ClO_4)	d-d: 579 (11)
proposed [Cu(**5**)]	d-d: 546 (54)

The UV/visible spectra of the three $[Cu([N_4S)](ClO_4)_2$ isomers are shown in figure 4.6. The absorption maxima of the d-d band of the $[Cu([9]aneN_4S)](ClO_4)_2$ and $[Cu([10]aneN_4S)](ClO_4)_2$ isomers are identical (532 nm) which suggests that any structural differences in the isomers must be insignificant with respect to perturbation of the ligand fields. This result agrees with the prediction that the $[9]aneN_4S$ and $[10]aneN_4S$ bicyclic ligands are both similar in structure and flexibility such that they do not alter the requirements of the copper(II) relative to each other.

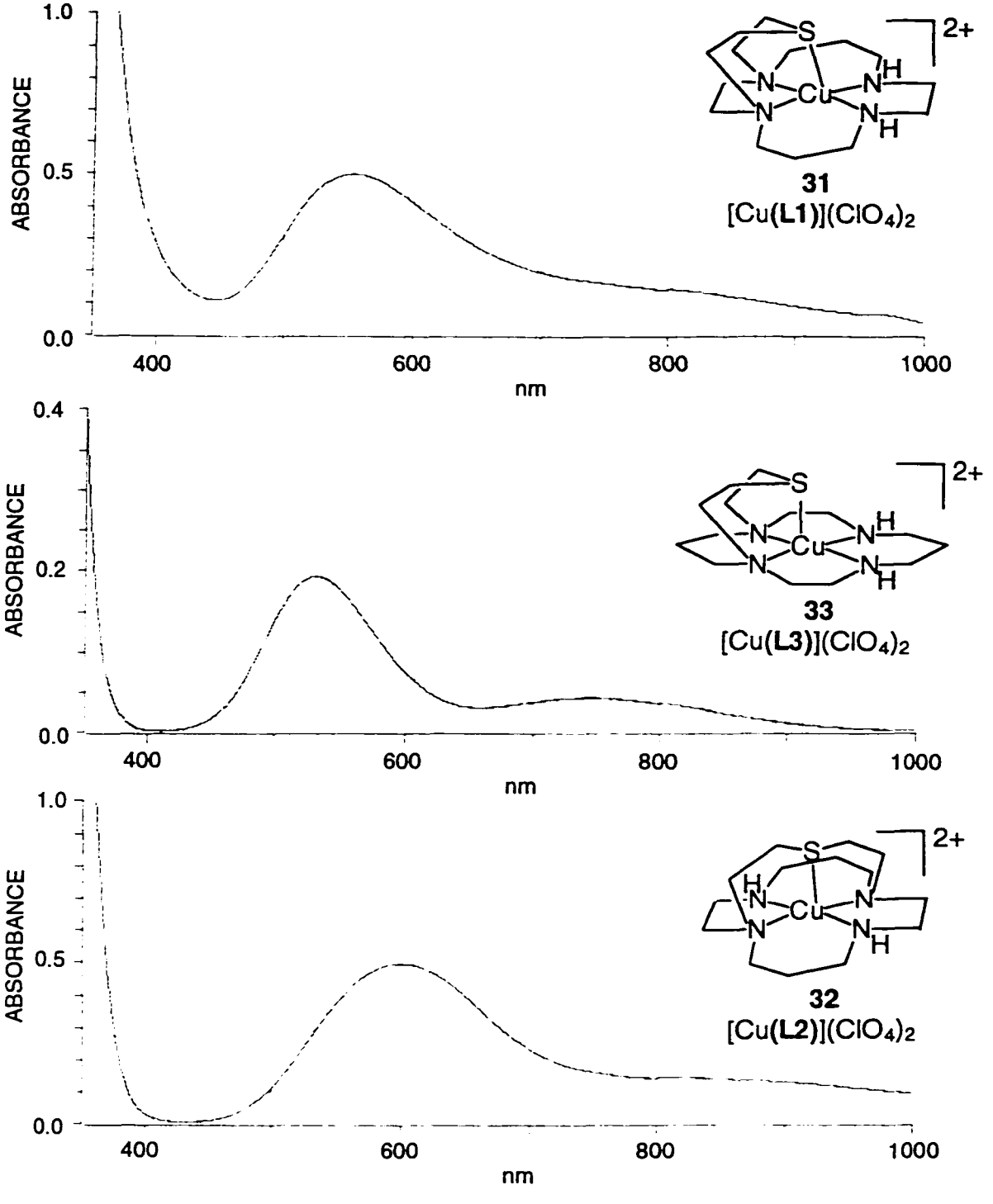

Figure 4.6. Visible spectra of the three $[Cu(N_4S)](ClO_4)_2$ isomers.

An X-ray crystal structure[90] of [Cu([9]aneN$_4$S)](ClO$_4$)$_2$ shows that the cyclam ring is in the trans-I configuration (NH hydrogens on same side of cyclam ring as sulphur bridge) and the copper(II) center lies 0.141Å above the N$_4$ plane, towards the apical sulphur. The geometry of this complex therefore is best described as square pyramidal.

The 603nm absorption maximum of the [Cu(hemi-cryptN$_4$S)](ClO$_4$)$_2$ isomer is in sharp contrast to that of the other two. This result indicates that the structural demands of the hemi-cryptateN$_4$S ligand differ significantly. There are several possible sources of the observed 70 nm shift.

One possibility is there is a contribution from the difference in coordination symmetry of the hemi-cryptateN$_4$S relative to the other two. The [9]aneN$_4$S and [10]aneN$_4$S isomers both coordinate with *cis*-tertiary and *cis*-secondary nitrogens whereas the hemi-cryptateN$_4$S ligand coordinates with *trans*-tertiary and *trans*-secondary nitrogens. Given that the both tertiary nitrogens are essentially identical and both secondary nitrogens are likewise essentially identical, the difference in *cis* vs. *trans* coordination is expected to have little or no effect on the relative absorption maxima. For example, no difference in absorption maxima was reported[156] for the copper(II) complexes of the (*cis* and *trans* coordination environments) two N$_2$(Imine)$_2$ tetraaza isomers shown below:

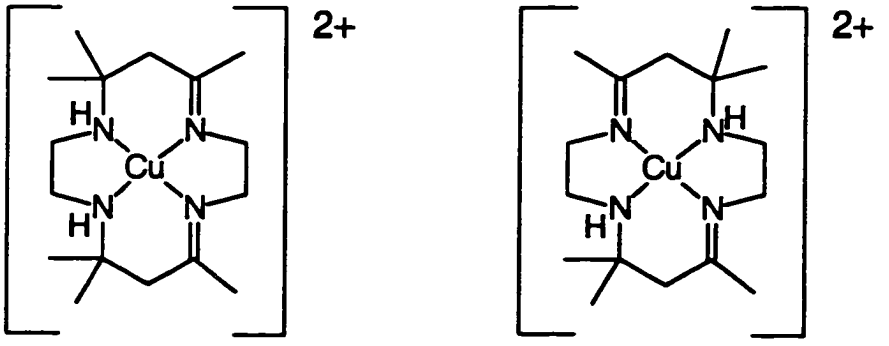

Because this symmetry effect is negligible, the shift in absorption maximum for the $[Cu(hemi\text{-}cryptN_4S)](ClO_4)_2$ complex must be due to structural effects of the ligand. There are two general effects which alter the ligand field experienced by the copper(II) center.

Firstly, the rigidity of this macrobicyclic ligand may be "pushing" certain donors towards the metal center and/or "pulling" other donors away (see figure 4.5). This effect may not alter the actual bond lengths, however, it would nonetheless alter the "apparent" ligand field experienced by the metal.

Secondly, the rigidity of the macrobicycle may be distorting the coordination geometry such that the donor-metal-donor bond angles are significantly different from those observed[90] in the $[Cu([9]aneN_4S)](ClO_4)_2$ X-ray structure. Such a significant distortion is predicted by the molecular mechanics calculation (section 4.3) which indicated that the methylene torsions of the sulphur bridge force the sulphur to be offset relative to the center of the cyclam ring. It is likely that both bond length and bond angle distortions are contributing to the observed shift.

It is interesting to note that the absorption maximum (603 nm) of $[Cu(hemi\text{-}cryptN_4S)](ClO_4)_2$ is similar to that observed in the copper blue proteins (section 4.1). Furthermore, the copper blue proteins have high absorption coefficients (*ca.* 5000 M^{-1} cm^{-1}), and the absorption coefficient of the $[Cu(hemi\text{-}cryptN_4S)](ClO_4)_2$ d-d transition is more than double that of the other two isomers.

The similarity of the absorption maximum to that of the copper blue proteins is not unusual for a sulphur-containing macrocycle. Indeed, it has been well documented[84] that the presence of sulphur donors in macrocyclic ligands generally results in such absorption shifts relative to their aza analogues.

That the blue absorption shift is present in the hemi-cryptateN_4S isomer and not in the [9]aneN_4S (and [10]aneN_4S) isomer is of interest because these isomers differ only with respect to relatively subtle structural features. The observation that the $[Cu([9]aneN_4S)](ClO_4)_2$ complex did not closely resemble other polythiaether macrocyclic

complexes was interpreted[90] to reflect a predominance of the cyclam ring. For example, coordination of an axial thiolate donor to copper(II)cyclam was reported[157] to result in only a weak (2.9 Å) interaction and no significant changes in structure or absorption maximum (520 nm) relative to copper(II)cyclam. However, such a predominance is not present in [Cu(hemi-cryptN$_4$S)](ClO$_4$)$_2$ because the expected shift in absorption maximum for sulphur was present.

For comparison to other N$_4$S macrobicyclic complexes, the only relevant precedent[26] is the copper(II) complex of 12,17-dimethyl-5-thia-1,9,12,17-tetraazabicyclo[7.5.5]nonadecane. This complex can be considered to be a "chelate ring arrangement" isomer of [Cu(hemi-cryptN$_4$S)](ClO$_4$)$_2$. Although an X-ray crystal structure was not reported for this copper(II) complex, the X-ray structure of the analogous 5-aza analogue was reported.[185] As can be seen in figure 4.7, this macrobicycle consists of linking a -CH$_2$CH$_2$CH$_2$NHCH$_2$CH$_2$CH$_2$- bridge across the diagonally opposed nitrogens of the 12-membered N$_4$ macrocycle cyclen, and therefore structurally resembles the hemi-cryptateN$_4$S macrobicycle. In this complex, the copper(II) center is positioned well above the N$_4$ ring towards the 5-aza donor (*trans*-basal N(1)-Cu-N(5) angle is 158.5° compared to 173.6° in [Cu([9]aneN$_4$S)](ClO$_4$)$_2$).

The absorption maximum (687 nm) of the corresponding 5-thia complex has a greater shift relative to that of [Cu([9]aneN$_4$S)](ClO$_4$)$_2$ than was observed for [Cu(hemi-cryptN$_4$S)](ClO$_4$)$_2$. It is possible that the similar structure of the hemi-cryptateN$_4$S bicycle has also forced the copper(II) center further out of the plane of the cyclam ring (compared to [Cu([9]aneN$_4$S)](ClO$_4$)$_2$) towards the sulphur and that this is the distortion responsible for the shift in absorption maximum between the [Cu([9]aneN$_4$S)](ClO$_4$)$_2$ and [Cu(hemi-cryptN$_4$S)](ClO$_4$)$_2$ isomers. However, in the diagonally bridged cyclen complexes, the bridge length is considerably greater than that present in the hemi-cryptateN$_4$S bicycle and the 12-membered tetraaza ring is significantly smaller than the cyclam ring present in the hemi-cryptateN$_4$S bicycle. These factors are expected to force the copper(II) well above

the cyclen ring in those complexes but are not expected to be operative in the [Cu(hemi-cryptN$_4$S)](ClO$_4$)$_2$ complex.

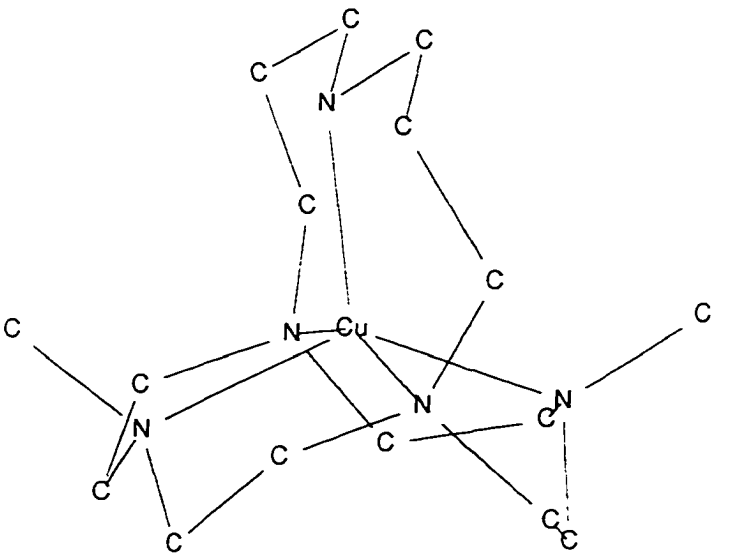

Figure 4.7. Pictorial representation of coordination geometry in (12,17-dimethyl-5-thia-1,9,12,17-tetraazabicyclo[7.5.5]nonadecane)copper diperchlorate.[185]

4.5. ESR Spectroscopy of Copper(II) Complexes:

The isotropic (room temperature, aqueous solution) esr spectra of the three $[Cu(N_4S)](ClO_4)_2$ isomers are presented in figure 4.8 and the data is shown in table 4.2. The esr spectrum of each complex is characteristic of square pyramidal or tetragonally-elongated octahedral geometry. The g_{iso} values are similar for each complex as expected, given the similarity of the identity and arrangement of donors present in each ligand. The ambient temperature solution ESR spectra show four hyperfine lines due to the interaction of the unpaired electron with the nuclear spin of the copper(II) nucleus ($^{63,65}Cu$; I=3/2).

Table 4.2. ESR spectral data for copper(II) complexes in aqueous solution at ambient temperature.

COMPLEX	g_{iso}	A_{iso}^{Cu} /gauss
$[Cu([9]aneN_4S)](ClO_4)_2$[a]	2.092	86
$[Cu([10]aneN_4S)](ClO_4)_2$	2.090	85.4
$[Cu(hemi\text{-}cryptN_4S)](ClO_4)_2$	2.089	80.4

[a]Values taken from ref. 90.

The $[Cu([9]aneN_4S)](ClO_4)_2$ complex was shown[90] to not coordinate either F^- or thiocyanate anions (based on the absence of further splitting of the ESR signal) even in the presence of a 250-500-fold excess of fluoride. It was therefore concluded that the complex remains five-coordinate as in the solid-state X-ray structure. In contrast, the $[Cu([15]aneN_4)]^{2+}$ complex was reported[158] to form six-coordinate complexes with thiocyanate.

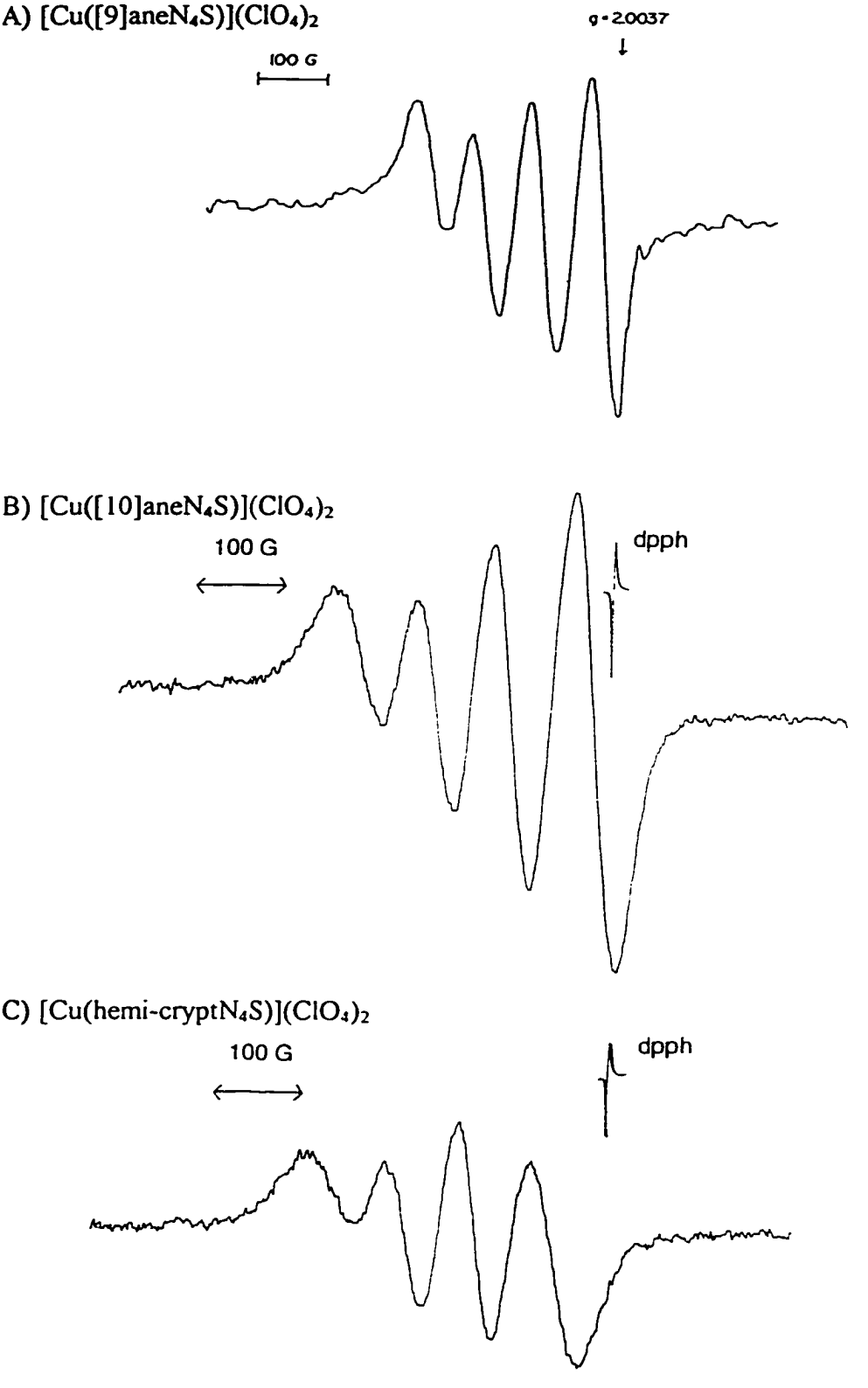

Figure 4.8. ESR spectra of the three $[Cu(N_4S)](ClO_4)_2$ isomers (H_2O, ambient temp.).

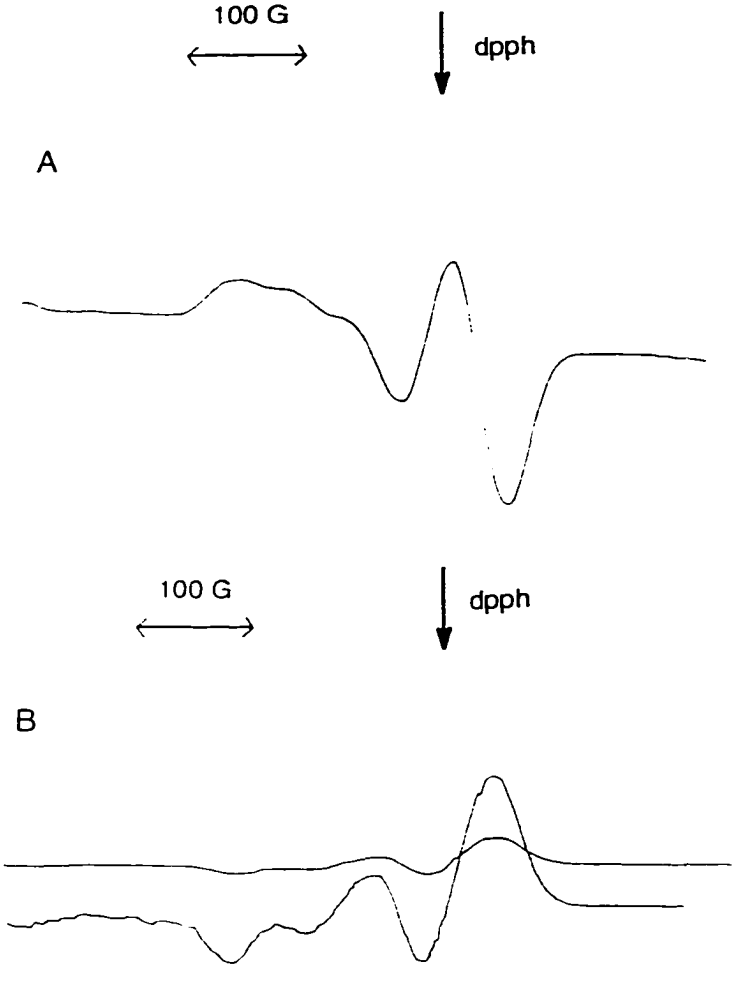

Figure 4.9. Frozen solution (DMF/CH_3CN 50:50, 77K) ESR spectra of A) $[Cu([10]aneN_4S)](ClO_4)_2$. B) $[Cu(hemi\text{-}cryptN_4S)](ClO_4)_2$.

It has been documented[159] that for polyaza copper(II) complexes, "N-shf coupling is observable only if the percentage of s-character contributed to the bonding molecular orbital by the nitrogen donors exceeds a critical value of 20% s". The nitrogen donors in the N_4S-bicyclic ligands are each sp^3 hybridized such that they are at or below this

detection limit. This effect explains why N-shf coupling is not observed in the ESR spectra of the present study.

The frozen solution (77K) ESR spectra of the $[Cu(hemi\text{-}cryptN_4S)](ClO_4)_2$ and $[Cu([10]aneN_4S)](ClO_4)_2$ complexes are presented in figure 4.9. These spectra are indicative of axial symmetry ($g_z \neq g_x = g_y$). The observed order of g values is that $g_{//} > g_\perp > g_e$ which is indicative[160] of a tetragonally elongated (Jahn Teller effect) geometry with the unpaired electron predominantly in the d_{x2-y2} orbital. Although the separation of the $g_{//}$ and $g_\perp$ regions was not sufficient for accurate determination of these values, they were observed to be similar to those reported for other polythiaaza copper(II) complexes[161].

4.6. Electrochemistry of Copper(II) Complexes:

Cyclic voltammetric scans (in acetonitrile solution using a standard three electrode configuration: platinum working/counter electrodes and Ag/Ag^+ reference) of the $[Cu([10]aneN_4S)](ClO_4)_2$ and $[Cu(hemi\text{-}cryptN_4S)](ClO_4)_2$ complexes did not produce electrochemically reversible oxidation or reduction waves (E_{pc}-$E_{pa} > 0.25$ V). That the $Cu^{2+/3+}$ couple was irreversible is expected because of the poorer σ-donor abilty of the axial sulphur relative to the aza and oxo analogues. However, previous investigation[90] of the $Cu^{2+/1+}$ redox for $[Cu([9]aneN_4S)](ClO_4)_2$ showed a reversible process at -0.935V relative to ferrocene. The π-acceptor ability of the axial donor is expected to stabilize the Cu^{1+} ion relative to the aza and oxo donors. A comparison[63] of the $[Cu(N_4X)](ClO_4)_2$ (X = NH, O, S) reduction potentials determined that the sulphur donor stabilized the copper(I) state by 0.190 V relative to the oxygen analogue.

Although the reduction waves were quasi-reversible such that comparison of the $E_{1/2}$ values is tenuous at best, the estimated $E_{1/2}$ values for both the $[Cu([10]aneN_4S)](ClO_4)_2$ and $[Cu(hemi\text{-}cryptN_4S)](ClO_4)_2$ complexes were in the -0.9 to -1.1 V range (vs. ferrocene$^{+/0}$) which corresponds to the that of the

$[Cu([9]aneN_4S)](ClO_4)_2$ isomer. These values are in sharp contrast to that observed for the various copper(II)-polythiother complexes. For example, the $E_{1/2}$ values for $[Cu([9]aneS_3)_2]^{2+/1+}$ and $[Cu([18]aneS_6)]^{2+/1+}$ are +0.854V and +0.964V (vs. NHE) respectively.[162,163] The $[Cu(N_4S)]^{1+}$ complexes are therefore strong reductants, but are still *ca.* 400-500 mV less reducing than the parent $[Cu(cyclam)]^{1+}$ complex.[164]

The quasi-reversible nature of the reductions in the present study is likely to have been caused by the known tendency of copper(I) to disproportionate, resulting in deposition of copper(0) on the working electrode. The redox wave of the ferrocene standard was less reversible after running the copper complexes. This difficulty has been overcome by other workers using either glassy carbon[164] or mercury drop[165] working electrodes.

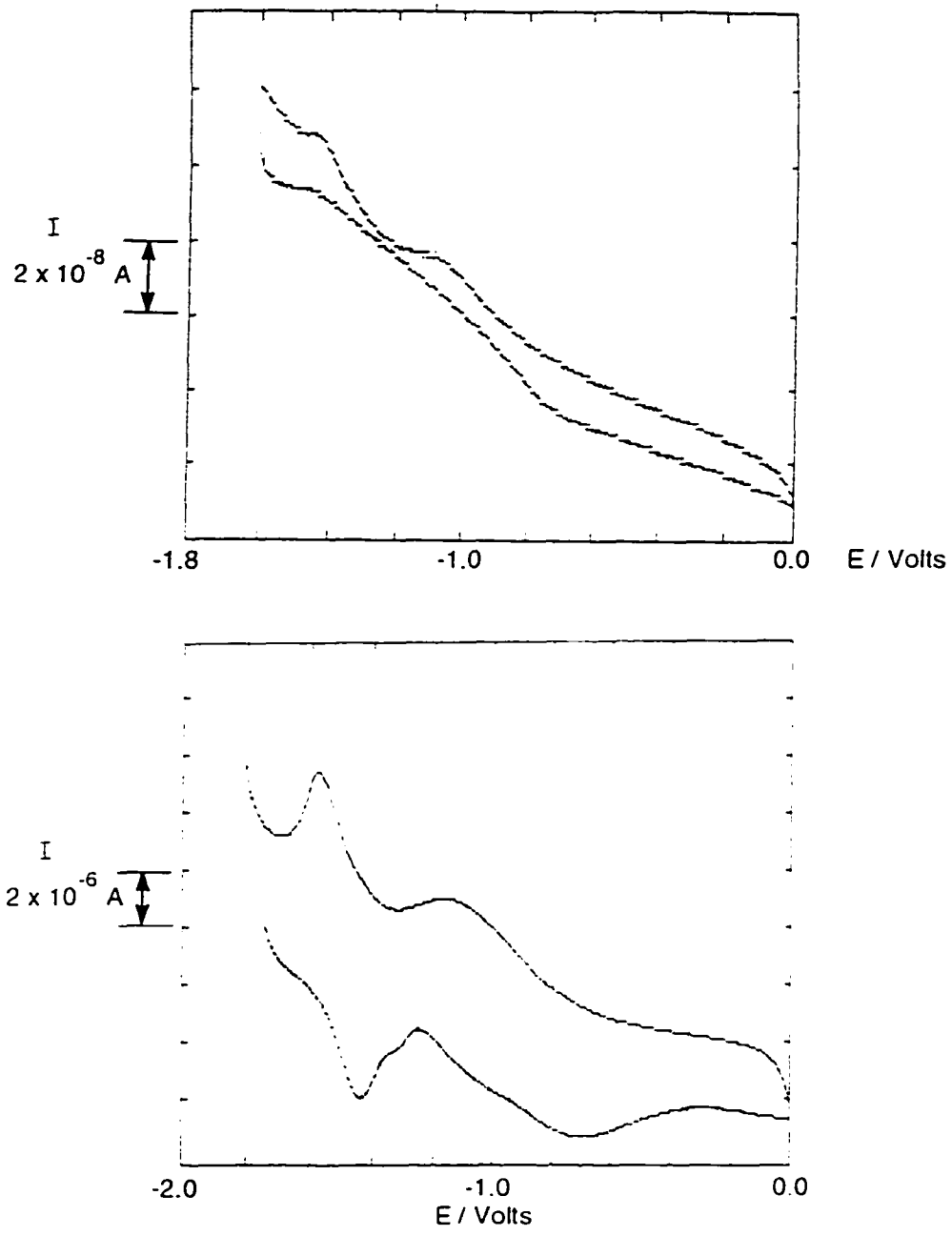

Figure 4.10. Cyclic voltammograms of [Cu(hemi-cryptN$_4$S)](ClO$_4$)$_2$ (top) and [Cu([10]aneN$_4$S)](ClO$_4$)$_2$ (bottom) in acetonitrile.

Chapter 5

Synthesis and Characterization of Nickel(II) Complexes of N_4S-donor Macrobicyclic Ligands

5.1. Introduction:

There is considerable interest in studying the coordination chemistry of macrocyclic nickel complexes which has been primarily motivated by the presence of nickel in metalloenzymes. Nickel is now recognized[21] as an essential trace element for bacteria, plants, animals and humans. The role of nickel in animal biochemistry is still not well defined. However, four bacterial enzymes have been found to be nickel dependent: urease, carbon monoxide dehydrogenase (CODH), hydrogenase (H_2-ase), and methyl-S-coenzyme-M methylreductase (MCR) which employs a nickel-containing prosthetic group (factor 430). The nickel environment is different in each enzyme but the nickel centers are believed to reside in the active sites and to be intimately involved in their catalytic cycles.

In the case of urease[166], whose biological function is the hydrolysis of the metabolic end product urea (at 10^{14} times the uncatalyzed rate), the active site consists of two nickel atoms 3.5 Å apart bridged by the carboxylate side chain of an unusual carbamate-derivatized lysine residue. This enzyme exploits the established Lewis acid property of nickel(II).

With the exception of urease, whose X-ray crystal structure was recently determined at 2.0Å resolution[166], these enzymes have not been characterized by X-ray crystallography. Despite the great amount of spectroscopic and physiochemical data available for these enzymes, the nature and role of the nickel centers remain unclear. This continuing uncertainty has inspired considerable interest in the coordination chemistry of nickel.

The other three nickel-containing enzymes are unusual with respect to the known coordination chemistry of nickel in that they contain redox active nickel centers that can cycle between the +3, +2, and/or +1 oxidation states.[167] The nickel centers are coordinated in thiolate-rich or tetrapyrrole ligand environments that were previously not considered to favour such metal-centered redox processes in nickel complexes.

For example, methyl-S-coenzyme-M methylreductase (MCR) is one of the components of the enzyme system responsible for the conversion of carbon dioxide to methane, through a series of four two-electron reduction steps, in the metabolism of methanogenic bacteria.[168]

The active site in MCR (factor 430) contains the nickel-tetrapyrrole complex shown figure 5.1. The tetrapyrrole ligand is unique compared to its heme analogues in that it is the most reduced macrocycle known to exist in biology and is a mono-anionic ligand. This enzyme catalyses the formation of methane from $H_3CSCH_2CH_2SO_3^-$ (methyl coenzyme M) during the final methane evolution step during CO_2 metabolism.[169] The overall reaction is the reductive demethylation of 2-(methyl-thio)ethanesulphonic acid (CH_3-S-CoM) with a reducing equivalent from the novel coenzyme, 7-(mercaptohepatanoyl)-L-threonine-O^3-phosphate (HS-HTP). The balanced equation is:

$$CH_3\text{-S-CoM} + \text{HS-HTP} \Rightarrow CH_4 + \text{CoM-S-S-HTP}$$

The proposed mechanism of methane formation involves a CH_3-F430M intermediate as depicted below for studies[170] of the interaction of native F430 with CD_3. This is the most interesting step of the metabolic pathway from a chemical perspective because such a methane yielding reaction is unique in biology.

The question of why nature has developed a highly saturated corphinoid to accomodate the nickel ion rather than other metals appears to have been answered by the observation[171] of a nickel(I)-ESR signal in intact cells. This observation suggests that the nickel(II) center has been reduced, explaining the observed unusual reactivity of the coenzyme.

In the absence of accurate X-ray data, EXAFS experiments[172] have indicated that native F430 is a six-coordinate pseudo-octahedral nickel center exhibiting long Ni-N bond distances of *ca.* 2.1Å with two axial ligands (which are presumed to be water, despite no

evidence thereof). Another interesting feature[169] of F430 is that extrusion of the coenzyme results in epimerization of the C12,C13 backbone carbons. This epimer has been shown to

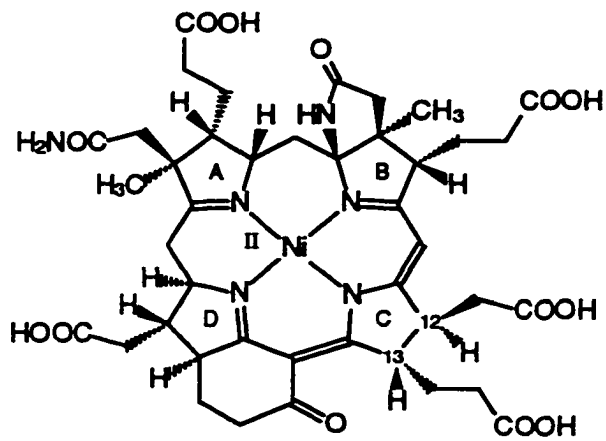

Native Coenzyme F430
(12,13 = epimeric carbons)

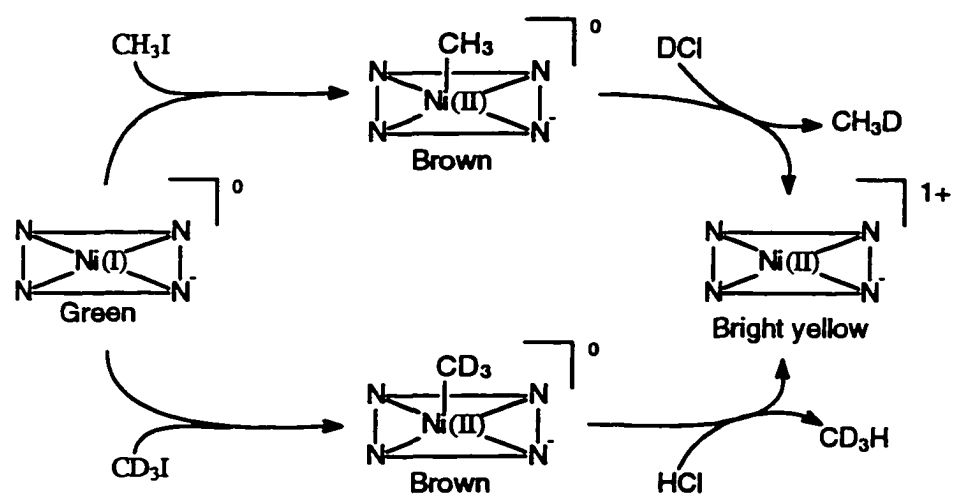

Figure 5.1. Structure of native coenzyme F430 (top) and proposed catalytic formation of methylnickel(II) derivative as an intermediate in biological pathway (bottom).[169]

have shorter (1.89Å) Ni-N bond lengths due to formation of a "ruffled" (S_4 symmetry, rather than planar) macrocyclic ring structure. This di-epimer is therefore likely to result in N_4 square planar coordination and it has been observed that axial ligands bind less strongly.

Corden and co-workers[168] have reported that the nickel(II) complex of the macrocyclic [16]aneN_5-14,16-dionato(2-) ligand (see figure 5.2) converts methyl-coenzyme M to methane and coenzyme M in a stoichiometric process. The addition of an oxidant such as I_2 or $NaClO_3$ made the reaction catalytic. That aqueous solutions of nickel(II) acetate, nickel(II) tetraethylenepentamine and nickel(II) 1,4,8,11-tetraazacyclotetradecane-5,7-dionato(2-) do not effect such reactivity suggets that the [16]aneN_5-dionato(2-) complex is unique in its ability to activate nickel(II) in this way. The authors attributed the reactivity to the observation that the $Ni^{2+/3+}$ redox couple of this complex (0.48V vs. NHE) is one of the lowest reported in the literature (see sections 1.3(e) and 1.4 regarding stabilization of nickel(III)).

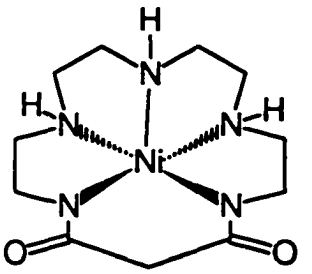

[Ni(L)]

$$LNi(II) + CH_2\text{-}S\text{-}CoM \rightleftharpoons LNi(II)S(CH_3)CoM$$

$$H_2O + LNi(II)S(CH_3)CoM \longrightarrow LNi(III)\text{-}S\text{-}CoM + CH_4 + OH^-$$

$$LNi(III)\text{-}S\text{-}CoM + OH^- \longrightarrow 1/2\ O_2 + LNi(II) + HS\text{-}CoM$$

$$LNi(II) + HS\text{-}CoM \rightleftharpoons LNi(II)S(H)CoM$$

$$1/4\ O_2 + HS\text{-}CoM \longrightarrow 1/2\ H_2O + 1/2\ (CoM\text{-}S\text{-}S\text{-}CoM)$$

$$CH_3\text{-}S\text{-}CoM + 1/2\ H_2O \longrightarrow CH_4 + 1/4\ O_2 + 1/2\ (CoM\text{-}S\text{-}S\text{-}Co$$

$$HS\text{-}CoM + I_2 \longrightarrow 2HI + 1/2\ (CoM\text{-}S\text{-}S\text{-}CoM)$$

Figure 5.2. Structure of Ni[1,4,7,10,13-pentaazacyclohexadecane-14,16-dionato(2-)] and proposed mechanism of substrate cleavage.[168]

Considerable progress has been made in stabilizing nickel(I) by Suh and co-workers.[173] These workers have synthesized structurally reinforced macrotricyclic analogues of cyclam (see below) which stabilize nickel(I) ($Ni^{2+/1+}$ redox couples in the -1.3 to -1.4 V range) and have reported[173] X-ray crystal structures of these complexes. The nickel(I) ion has a tetrahedrally distorted square planar geometry in these complexes.

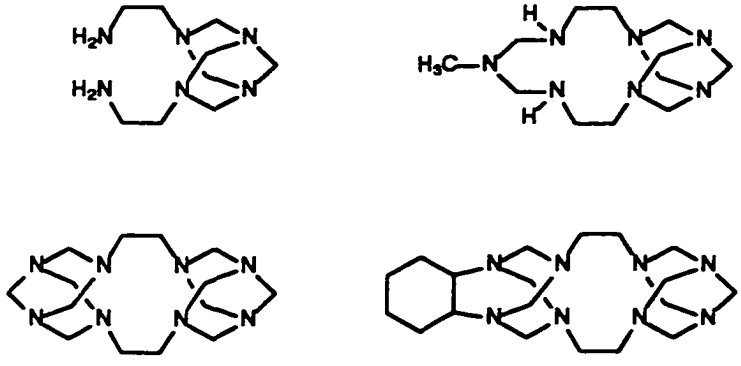

Structurally reinforced analogues of [14]aneN$_4$ (cyclam) used to stabilize Nickel(I).[173]

Although there have been numerous studies of nickel complexes of tetracoordinate ligands which stabilize the square planar low spin d^8 nickel(II) ion, there is considerable interest in synthesizing pentacoordinate ligands for the purpose of inducing the high-spin octahedral nickel(II) ion such that its spectroscopic, kinetic and electrochemical properties can be readily investigated. To date, few such ligands have been prepared[90], presumably because of synthetic difficulties. As mentioned in section 1.4, incorporation of additional donors in monocyclic ligands[174] has not resulted in significant stabilization of the octahedral geometry because these ligands are not preoriented for such coordination. The strategy[175] of attaching pendant arm donors to the macrocyclic ring to impose octahedral geometry results only in coordination of axial donors that are acid labile due to the lack of rigidity of the backbone linkage to the pendant donor.

The N_4S-macrobicyclic ligands have been shown[90] to overcome these difficulties and result in stable octahedral coordination wherein the five macrobicyclic donors are inert with respect to dissociation of the donors, while the sixth (axial) donor site is available for reactivity studies. It is therefore of interest to compare the spectroscopic and electrochemical properties of the nickel(II) complexes of the N_4S-macrobicyclic ligands synthesized in the present study.

5.2. Synthesis of Nickel(II) Complexes of N_4S-macrobicyclic Ligands:

The syntheses of the various nickel(II) complexes have been reported in section 8.3 (compounds **34-36**). Only the characterization of the N_4S bicyclic ligands (**L1-L3**) will be presented:

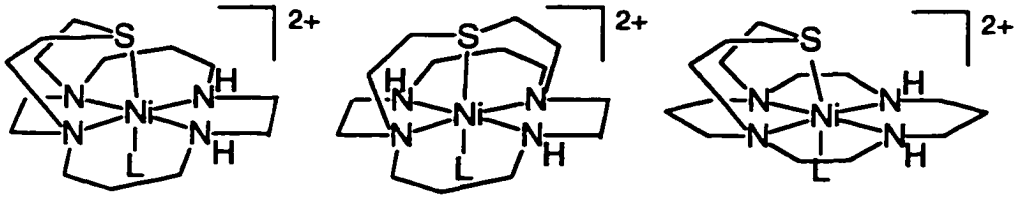

34
$[Ni(\mathbf{L1})(L)](ClO_4)_2$
(L = solvent)

35
$[Ni(\mathbf{L2})(L)](ClO_4)_2$
(L = solvent)

36
$[Ni(\mathbf{L3})(L)](ClO_4)_2$
(L = solvent)

The synthesis of $[Ni([9]aneN_4S)(solv)](ClO_4)_2$ was achieved in satisfactory yield and purity according to the previously published procedure reported by Fortier and McAuley.[90]

The [Ni(hemi-cryptN$_4$S)(solv)](ClO$_4$)$_2$ complex was prepared in satisfactory yield by reacting nickel(II) perchlorate and the hemi-cryptN$_4$S bicyclic free ligand (purified as copper(II) complex) in a 1:1 stoichiometric ratio in aqueous solution. Unlike the synthesis of the copper(II) complex, addition of several drops of 0.1M NaOH was usually required before the violet colour of the complex formed. The experimental carbon composition was 31.91%, whereas that expected for [Ni(hemi-cryptN$_4$S)](ClO$_4$)$_2$ is 30.91%. The carbon composition expected for the formulation [Ni(hemi-cryptN$_4$S)](ClO$_4$)$_2$ • 1/2EtOH is 31.77% which fits the experimental results and therefore suggests the presence of ethanol in the crystal lattice. As with the [Ni([9]aneN$_4$S)(solv)](ClO$_4$)$_2$ isomer, the microanalysis indicates that there is no water or anion coordinating in the sixth site in the dry solid state since such coordination would lower the expected carbon composition even further.

Attempts at synthesizing the [Ni([10]aneN$_4$S)(solv)](ClO$_4$)$_2$ under similar conditions in aqueous solution failed to produce any colour. Reaction of the free ligand (**L3**) with nickel(II) chloride and nickel(II) acetate failed as well. Only the reaction of excess (~2-4 equiv.) nickel(II) acetate with the free ligand (**L3**) in dry non-aqueous solvent produced the violet coloured complex. The isolated yield was very low compared to that of the other isomers, such that the synthesis must be attempted again on a larger scale in order to properly characterize and study the complex. The same result was found[128] for the synthesis of the analogous [Ni([10]aneN$_4$O)(solv)]$^{2+}$ complex. There is no obvious reason why this particular isomer of the N$_4$S bicycle (and N$_4$O bicycle) can not bind nickel(II) perchlorate in water, given that the other two isomers did so.

5.3. Electronic Spectroscopy of $[Ni(N_4S)](ClO_4)_2$ Complexes:

The UV/visible spectral data of the nickel(II) complexes prepared in the present study are presented in table 5.1. The spectra are shown in figure 5.3.

Table 5.1. UV/visible spectral data for nickel(II) complexes in aqueous solution.

COMPLEX	N_4S: λ_{max}/nm (ε/$M^{-1}cm^{-1}$)
$[Ni([9]aneN_4S)(OH_2)](ClO_4)_2$	d-d: 331(sh), 504 (14), 845 (sh), 945 (sh), 1040 (16) UV: 261 (1900), 330 (sh)
$[Ni([10]aneN_4S)(OH_2)](acetate)_2$	d-d: 335(13), 400 (sh), 513 (8), 841 (~ 4) 904 (8), 1016 (sh), 1050 (6) UV: 208 (1800), 262 (sh)
$[Ni(hemi\text{-}cryptN_4S)(L)](ClO_4)_2$	d-d: 355 (sh), 544 (18), 817 (~ 5), 916 (6), 1080 (10) UV: < 200nm
$[Ni(4\text{-}H)(L)](ClO_4)$ (presumed complex)	d-d: 530 (12), 670 (sh), 910 (brd)

Each of the $[Ni(N_4S)](ClO_4)_2$ isomers displays d-d absorption patterns which are indicative of sexicoordinate pseudo-octahedral or tetragonal geometries. An X-ray crystal structure[90] of $[Ni([9]aneN_4S)](ClO_4)_2$ contained a weakly bound perchlorate (Ni-O, 2.563Å) in the sixth available coordination site. Presumably, in solution, there is a water molecule in this site. As with the copper(II) complexes, the nickel(II) complexes exhibit exceptional kinetic stability, even in strongly acidic solutions.

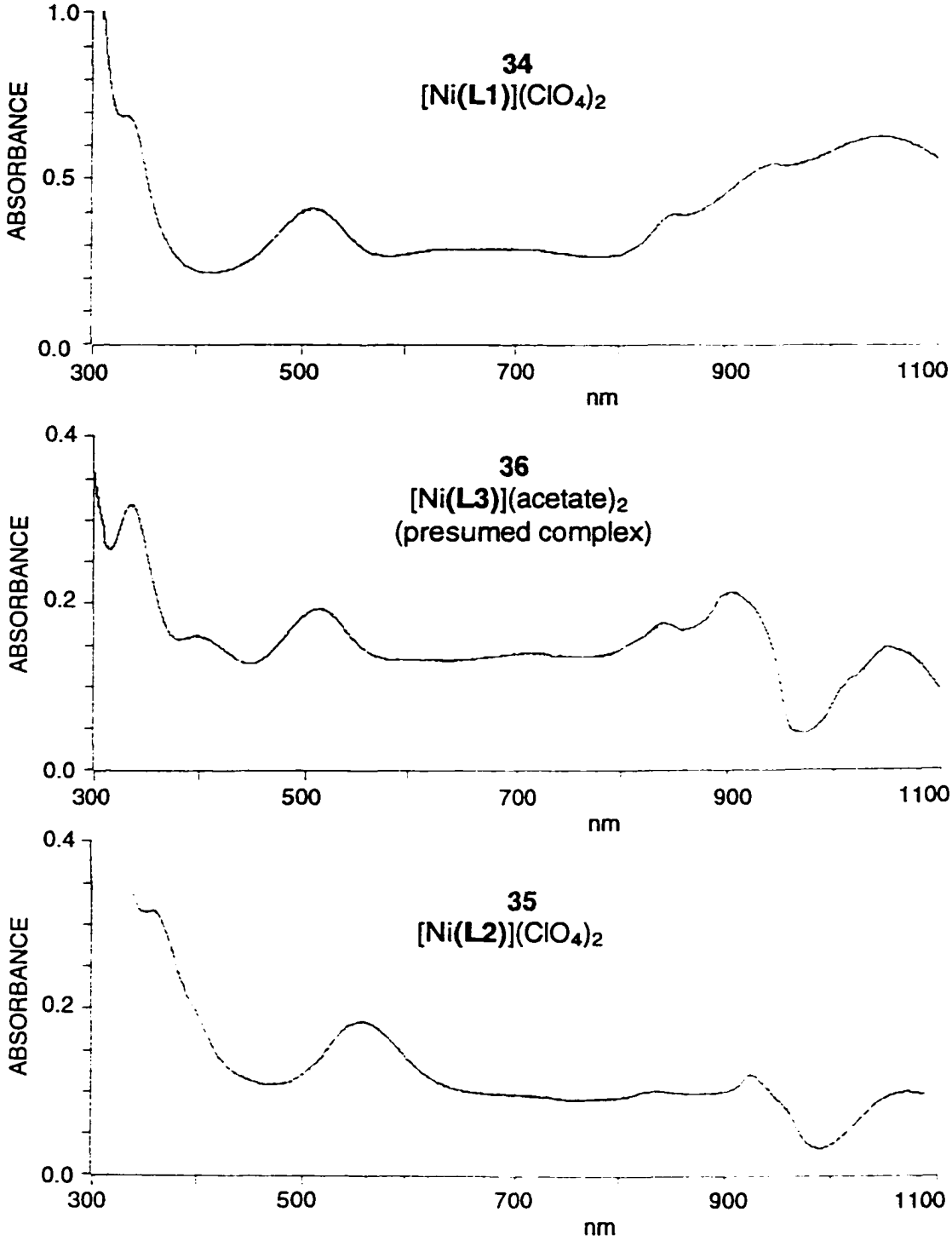

Figure 5.3. Visible spectra of the three $[Ni(N_4S)(OH_2)](ClO_4)_2$ isomers.

The UV/visible spectral data of octahedral transition metal complexes are amenable to more detailed analysis using the ligand field model.[176] Early applications of the ligand field model were dominated by cobalt(III) and chromium(III) due to the relatively great number of examples available. Since then, the development of tetradentate macrocyclic ligands, which present a constant set of four equatorial donors while the axial donor is varied, has generated interest in application of the ligand field model to tetragonal (D_{4h}) nickel(II) complexes. This is because their UV/visible spectra often contain sufficient data (three or more distinguishable band envolopes) to fix unique values for the ligand field parameters.[177]

Assignment of the bands observed in the UV/visible spectrum can provide more information than the transition energies alone. Assignments often are complicated by the large bandwidths obtained from solution spectra, as was observed in the spectra of the present study. Ideally, assignments should be based on single crystal measurements using polarized light, preferably at cryogenic temperatures. However, such data require considerable skill, special apparatus and knowledge of the crystal structure is desirable. Lever[178] has argued that high quality and chemically useful data often can be obtained with ordinary light from un-oriented single crystals if such spectra are obtained at low temperatures. These data can be collected in a conventional spectrometer using a simple cryostat. If the ligand field distortion results in a sufficient difference between the axial and equatorial ligand fields, a resolved spectrum can be obtained with relatively little effort.

The strain energy correlation study by Busch[179] (discussed in section 1.4) used such single-crystal/polarized light spectra for the series of monocyclic tetraaza macrocycles. Busch also performed Gaussian analyses using a non-linear least-squares computer program.[180]

Busch[179] noted that the solid state and chloroform solution spectra were essentially identical. It was therefore considered worthwhile to determine the equivalent ligand field values of the three $[Ni(N_4S)](ClO_4)_2$ isomers in the present study. Although the spectral

data are those of the room temperature solution studies, the bands are sufficiently discernible for such a calculation. It must, however, be cautioned that the results of such a calculation will be of less accuracy than those reported by Busch.

The tetragonal ligand field model[180,181] used was an extension of the first-order global crystal field model developed by Wentworth and Piper[182] for tetragonally distorted (D_{4h} site symmetry) cobalt(III) complexes. The relevant ligand field splitting diagram and equations used to model the splitting of the $^3T_{2g}$ excited state upon descent in symmetry to D_{4h} are shown in figure 5.4.

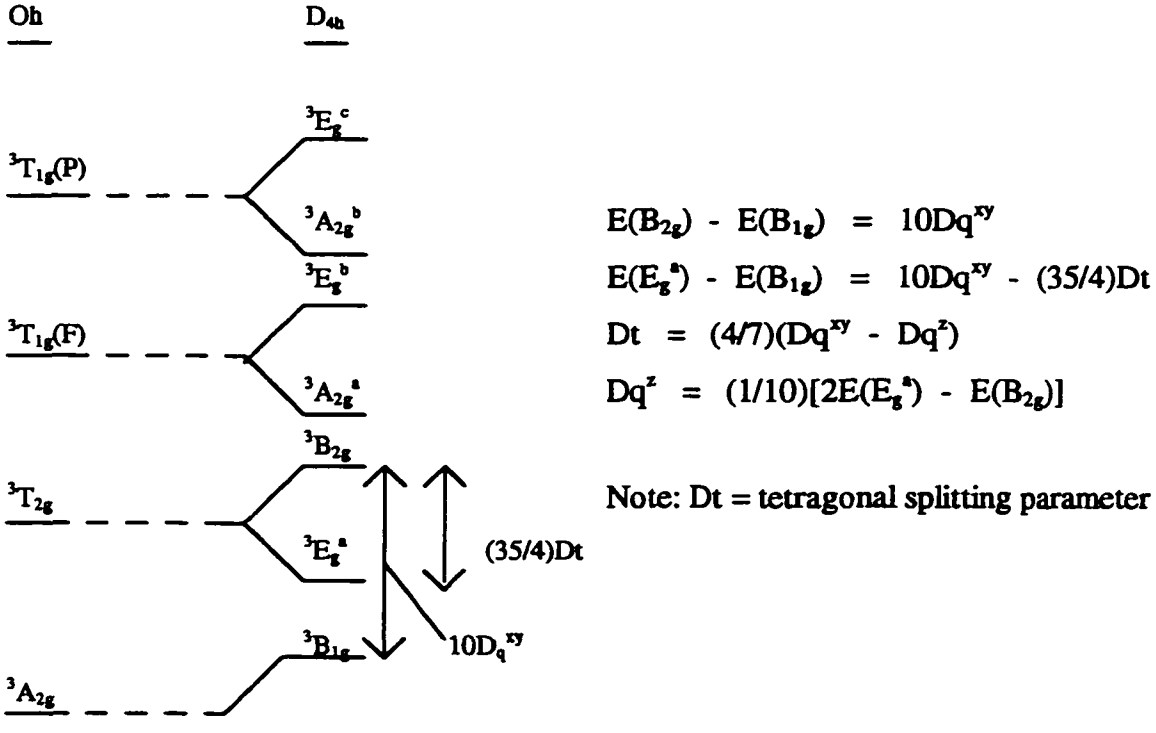

Figure 5.4. Ligand field splitting diagram for nickel(II) in O_h and D_{4h} symmetry with equations used to calculate Dq^{xy} and Dq^z parameters form UV/visible data.

This calculation is limited because it does not account for effects such as configuration interaction, spin-orbit coupling, local σ- and π-bonding effects and lower symmetry. More "complete" models have been developed by Drago and Rowly[177] (weak field approach) and Lever[183] (strong field model), however these calculations require that the experimental values of the five band energies be used for iterative solution methods. Busch[179] used these calculations where possible, but noted that, in the cases where all the bands could not be resolved, the simpler calculation[177], which only requires two d-d transition energies (figure 5.4) was less accurate but still meaningful.

A further limitation in application of the tetragonal ligand field model to the $[Ni(N_4S)](ClO_4)_2$ complexes of the present study is that the axial donors are not identical such that the effect of lower than D_{4h} site symmetry is expected to be significant. Despite these limitations, it is believed that the result of the calculation can at least identify the relative equatorial and axial ligand field trends for the three $[Ni(N_4S)](ClO_4)_2$ isomers, given their similarity and that the trend can be seen in the reported spectral absorption maxima for each isomer. For example, Busch noted[179] that the presence of lower than D_{4h} site symmetry in the $Ni([13\text{-}16]aneN_4)(X)_2$ (X = halide) complexes usually produced only a small effect. Hence, the deviations caused by not accounting for such effects can be regarded as "error" in the calculation.

The similarity of the Dq^{xy} and Dq^{z} values calculated for the $[Ni([9]aneN_4S)](ClO_4)_2$ and $[Ni([10]aneN_4S)](ClO_4)_2$ isomers to those calculated by Busch[179] for the $Ni([14]aneN_4)(X)_2$ (X = halide) series suggests that the error caused by the presence of C_{4v}, rather than D_{4h} symmetry is small enough that the values are at least qualitatively meaningful. It simply must be considered that deviations in these values are just as likely to be derived from symmetry distortions as from changes in ligand field strengths.

Table 5.2. Dq^{xy} (in cm^{-1}) and Dq^{z} (in cm^{-1}) ligand field strength values calculated from UV/visible spectral data (calculations shown in appendix I).

COMPLEX	Dq^{xy}	Dq^{z}
$[Ni([9]aneN_4S)(OH_2)](ClO_4)_2$ [a]	1180	740
$[Ni([10]aneN_4S)(OH_2)](ClO_4)_2$ [a]	1190	720
$[Ni(hemi\text{-}cryptN_4S)(OH_2)](ClO_4)_2$ [a]	1220	630
$[Ni([7.12]bicycloN_5)(Br)](ClO_4)$ [b]	1100	470
$Ni([14]aneN_4)(Cl)_2$ [c]	1480	379
$Ni([14]aneN_4)(Br)_2$ [c]	1487	287
$Ni([14]aneN_4)(N_3)_2$ [c]	1445	661
$Ni([15]aneN_4)(Cl)_2$ [c]	1242	589
$Ni([15]aneN_4)(Br)_2$ [c]	1283	452

[a]This work. [b]From reference 185: [7.12]bicycloN$_5$ = 12,17-Dimethyl-1,5,9,12,17-pentaazabicyclo[7.5.5]nonadecane. [c]From reference 179.

With this in mind, a comparison of the values for each isomer will be considered (see table 5.2). That the Dq^{xy} values for each $[Ni(N_4S)](ClO_4)_2$ isomer are similar (within expected error limits) suggests that there are no significant differences in the N_4 equatorial cyclam ring in each complex. This result is important because it implies that the displacement of the nickel(II) center out of the plane of the cyclam ring is relatively small and similar for each isomer. That the Dq^{xy} values (1180, 1190, 1220 cm^{-1}) of each isomer are all lower than the *ca.* 1480 cm^{-1} calculated for the $Ni([14]aneN_4)(X)_2$ (X = halide) complexes, implies that the equatorial ligand field of the cyclam ring is weaker in the bicyclic complexes. Such an effect could be caused by a small displacement of the nickel(II) center out of the N_4 plane. Indeed, the nickel center was found[90] to lie 0.111 Å

above the N_4 plane, towards the sulphur, in the X-ray crystal structure of $[Ni([9]aneN_4S)](ClO_4)_2$. However, the weaker ligand field strengths are more likely to be due to the presence of the weaker tertiary amine donors in the bicyclic ligands.

It is interesting to note that the Dq^{xy} values correspond well with the "ideal" value (1200 cm^{-1}) calculated by Busch[70] for unrestricted planar N_4 coordination. That the $[Ni(hemi\text{-}cryptN_4S)](ClO_4)_2$ value (1220 cm^{-1}) is slightly higher than that of $[Ni([9]aneN_4S)](ClO_4)_2$ and $[Ni([10]aneN_4S)](ClO_4)_2$ complexes suggests that the nickel(II) may be sitting closer to the N_4 plane or that the hemi-cryptateN_4S bicycle has a stronger in-plane donation from the cyclam ring. However, the difference in Dq^{xy} values is 30 cm^{-1}, which may not be of sufficient magnitude relative to the expected error for an interpretation to be necessarily meaningful.

The Dq^z values of $[Ni([9]aneN_4S)](ClO_4)_2$ and $[Ni([10]aneN_4S)](ClO_4)_2$, 740 and 720 cm^{-1} respectively, are reasonable for the presence of the neutral thioether/aquo axial donors as compared to $Ni([14]aneN_4)(SCN)_2$ (876 cm^{-1}).[179] That there is a significant difference between these two isomers is of interest. The results of the corresponding copper(II) complexes, together with the flexibility and similarity of structure (both bicycles contain adjacently bridged nitrogens) of the ligands, are such that significant differences in ligand field and/or geometry, relative to each other, are not expected. Preliminary X-ray crystal data collected on the $[Ni([10]aneN_4O)](ClO_4)_2$ complex[128] shows the ligand to be complexed in the trans-III geometry, rather than the trans-I geometry found for the [9]aneN$_4$O and [9]aneN$_4$S bicycle complexes.

If a trans-III geometry was also present in the case of $[Ni([10]aneN_4S)](ClO_4)_2$, the large difference in Dq^z values could be explained by the differing structure/strain properties and steric influences on the axial donors expected[71] for these two different configurations. For example, Barefield et al[184] and Moore et al[32] have reported that the nickel(II) complex of 1,4,8,11-tetramethyl-1,4,8,11-tetraazacyclotetradecane (tetramethyl cyclam, TMC) can be synthesized in two different configurations which do not

interconvert in solution. These are the trans-III $[Ni(TMC)(solvent)_2]^{2+}$ and trans-I $[Ni(TMC)(solvent)]^{2+}$ complexes in which the steric repulsions of the trans-I form resulted in only *mono*(solvento) coordination for that isomer. It is of considerable interest to determine if the nature of the bridging present in the three N_4S-bicyclic ligands, which forces two of the four nitrogens to be present in a certain configuration, results in only the trans-I configuration (all substituents on same side of cyclam ring) or configurations unique to each isomer (in solution, as well as the solid state).

That the Dq^z value for the $[Ni(hemi\text{-}cryptN_4S)](ClO_4)_2$ complex is relatively low (630 cm^{-1}) is almost certainly a reflection of distorted geometry/symmetry, rather than axial ligand field strength. This result is well supported by application of the same ligand field calculation to the reported UV/visible values[185] for the $[Ni([7.12]bicycloN_5)(Br)]^{1+}$ (L = 12,17-dimethyl-1,5,9,12,17-pentaazabicyclo[7.5.5]nonadecane) complex. This ligand can be considered as a "chelate ring arrangement" isomer of the N_4S-bicyclic ligands in the present study. As can be seen in figure 4.7, the 12-membered tetraaza ring is too small for planar coordination of the metal center and the bridge is longer than in the present study. The nickel(II) ion therefore is expected to coordinate well above the 12-membered ring, towards the apical nitrogen donor. Table 5.2 shows that, as with $[Ni(hemi\text{-}cryptN_4S)](ClO_4)_2$ (Dq^z = 73 cm^{-1}), the Dq^z value (470 cm^{-1}) of this complex is also unusually low such that it can not be attributed to a ligand field effect alone.

Although the hemi-cryptateN_4S macrobicycle is a diagonally bridged structure like the [7.12]bicycloN$_5$ ligand, the larger tetraaza ring (cyclam) and shorter bridge would not be expected to result in similar positioning of nickel(II) ion out of the N_4 plane. This expectation is supported by the observation that the $[Ni([7.12]bicycloN_5)(Br)](ClO_4)$ complex has a lower Dq^{xy} value (1100 cm^{-1}), whereas that of $[Ni(hemi\text{-}cryptN_4S)](ClO_4)_2$ (1220 cm^{-1}) is greater than in the $[Ni([9]aneN_4S)](ClO_4)_2$ and $[Ni([10]aneN_4S)](ClO_4)_2$ isomers. Presumably, the distortion responsible for the low Dq^z value in $[Ni(hemi\text{-}cryptN_4S)](ClO_4)_2$ involves displacement of the axial sulphur donor (significantly altered

N-M-S bond angles), as was predicted by the molecular mechanics calculations (section 4.3).

5.4. Electrochemistry of Nickel(II) Complexes:

Complexation of nickel(II) by tetraaza macrocyclic ligands has been shown[186] to stabilize substantially the less common nickel(III) oxidation state as compared to to the solvated cation or to complexes of acyclic ligands. This interesting behaviour is derived from two general properties unique to the cyclic ligands: (i) formation of strong in-plane metal-nitrogen interactions, which raise the energy of the essentially metallic character antibonding orbital from which the electron is removed (thermodynamic effect); (ii) trapping of the strongly oxidizing nickel(III) cation in a closed framework, which reduces its tendency to react with solvent (kinetic effect).

Mostly because of the kinetic stability, the $Ni^{2+/3+}$ redox couple in macrocyclic complexes generally produces electrochemically reversible or quasi-reversible responses[39,187]. The $E_{1/2}$ values obtained from voltammetric investigations therefore approach E° values and reflect the thermodynamic stability of the trivalent state for nickel in each complex.

The overall oxidation-reduction behaviour of macrocyclic nickel complexes is a composite function of such ligand features as the nature of the donors, the degree and type of ligand unsaturation, macrocyclic ring size, the number and position of ring substituents, charge type, and coordination number. It is therefore necessary to study careful, systematic variations in the ligand features in order to assess the magnitude of each such contribution.

The greatest contribution to stability involves the nature of the donor atoms presented by the macrocycle.[147,148] Busch and coworkers[39] have correlated the $Ni^{2+/3+}$

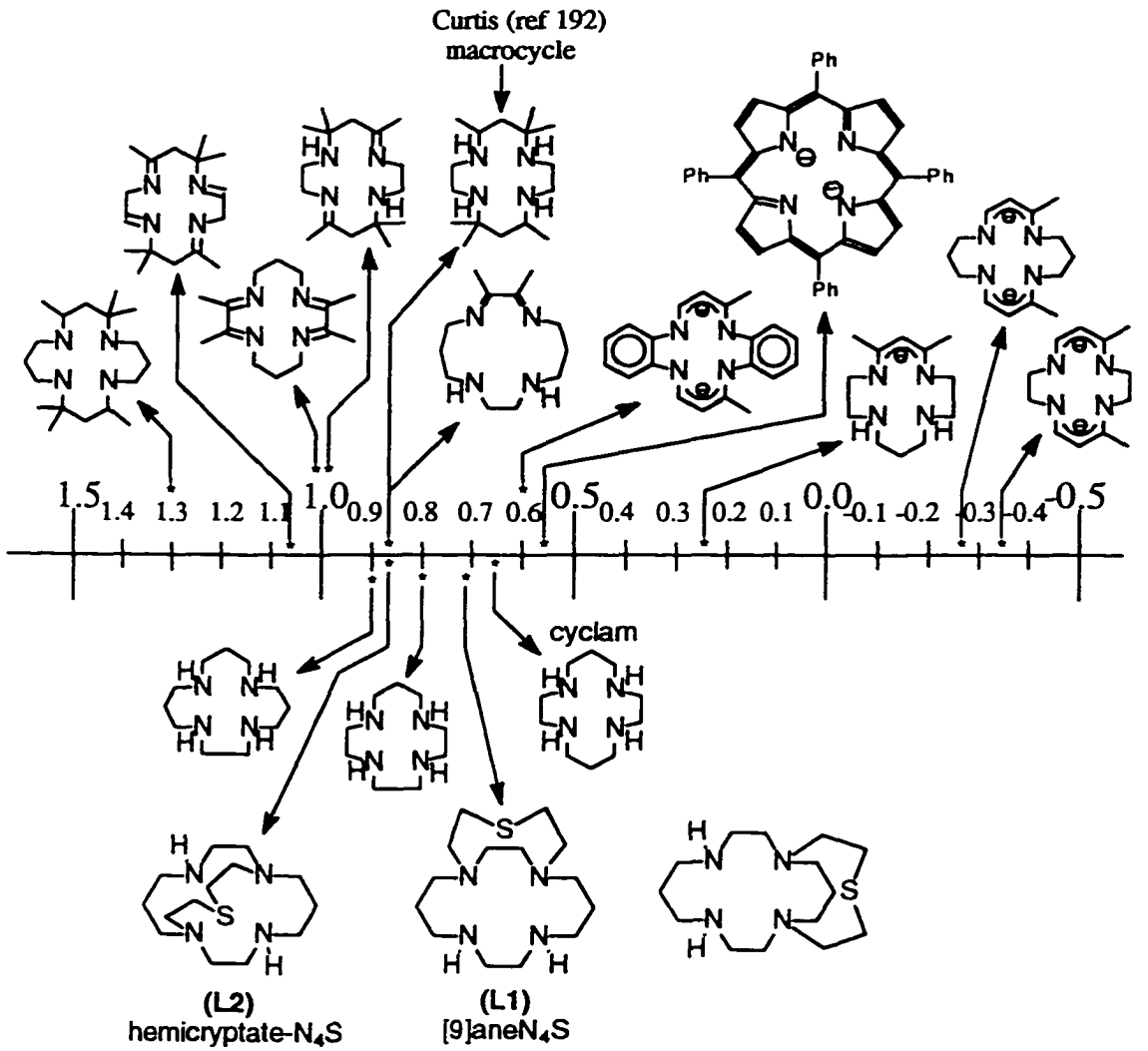

Figure 5.5. Comparison of $E_{1/2}$ values (vs. $Ag/AgNO_3$) of nickel(II)-tetraaza macrocyclic complexes.[39]

redox potentials of a large number of low-spin square planar tetraaza macrocyclic complexes. In that study, it was determined that three factors increase the $Ni^{2+/3+}$ redox potential: the presence of a larger macrocyclic ring, the presence of axial methyl groups in the six-membered chelate rings and the presence of ligand unsaturation. Anionic ligands decrease the $Ni^{2+/3+}$ redox potential. The various complexes studied are depicted in figure 5.5. In the absence of donor effects, the effect of increasing the ring size from 14- to 16-members produced a 0.3 V increase.

Another interesting result shown in figure 5.5 is that the $Ni^{2+/3+}$ redox potential (0.88 V in figure) of the reduced Curtis tetraaza macrocycle[186] (ms- and rac-(5,12)-7,7,14,14-Me_6-1,4,8,11-tetraazacyclotetradecane) is 200 mV greater than that of cyclam. Both ligands are 14-membered and the Curtis macrocycle differs from cyclam only in the presence of methyl substituents on the carbon atoms in the six-membered chelate rings. This result may be a demonstration of the effect of ligand rigidity derived from chelate conformational strain. As mentioned in section 1.4, Hancock[71] has argued that the source of rigidity effects derives mostly from chelate conformational preferences rather than from ligand strain, which was favoured by Busch. However, Busch[39] has pointed out that the methyl substituents in the Curtis macrocycle are likely to have appreciable non-bonding interactions with the axially coordinated solvent ligands in the nickel(III) complex such that the observed destabilization can be attributed to steric strain effects.

An investigation of the relative $Ni^{2+/3+}$ redox potentials of the three $[Ni(N_4S)](ClO_4)_2$ isomers in the present study offers the novel opportunity to assess the effect of ligand strain, rather than chelate strain, because features such as donor type, donor arrangement, ligand charge and the number and type of chelate rings do not vary in these complexes. The isomers only vary with respect to ring size and therefore any differences in redox potential can be attributed to the inherent ring strain effects. Furthermore, these macrobicyclic ligands induce sexicoordinate high-spin octahedral

geometries such that the effects of conversion from tetracoordinate square planar nickel(II) to sexicoordinate octahedral nickel(III) are not present.

Each of the $[Ni([9]aneN_4S)](ClO_4)_2$ and $[Ni(hemi\text{-}cryptN_4S)(solv)](ClO_4)_2$ isomers displayed electrochemically reversible oxidations, independent of scan rate (E_{pc}-E_{pa} = 65 - 70 mV, $i_{pc} = i_{pa}$ within error) . The cyclic voltammograms are presented in figure 5.6 and the $E_{1/2}$ values in table 5.3. Although the $E_{1/2}$ value has not yet been determined for the $[Ni([10]aneN_4S)](ClO_4)_2$ complex, the values of the corresponding oxygen analogues have been determined to be 0.760 V[127] and 0.750 V[100] for $[Ni([9]aneN_4O)](ClO_4)_2$ and $[Ni([10]aneN_4O)](ClO_4)_2$ complexes respectively. The two values are equal within experimental error and it is therefore expected that the $E_{1/2}$ value of $[Ni([10]aneN_4S)](ClO_4)_2$ will be similar to that of $[Ni([9]aneN_4S)](ClO_4)_2$.

Table 5.3. Half-wave, $E_{1/2}$, values for $Ni^{2+/3+}$ redox couple of the $[Ni(N_4S)](ClO_4)_2$ complexes.

COMPLEX	$E_{1/2}$ /V[a]
$[Ni([9]aneN_4S)(L)](ClO_4)_2$	0.709
$[Ni([10]aneN_4S)(L)](ClO_4)_2$	----
$[Ni(hemi\text{-}cryptN_4S)(L)](ClO_4)_2$	0.878
$[Ni(4\text{-}H)](ClO_4)$[b]	0.326

L = solv. [a]Potential vs. ferrocene$^{0/+}$ in 0.1M $(Et)_4NClO_4$ deaereated acetonitrile (scan rates = 200 mV/s) using platinum working and counter electrodes and $Ag/AgNO_3$ reference. [b](4) = 15-thia-1,5,8,12-tetraazabicyclo[10.5.2]nonadeca-6-one.

The $E_{1/2}$ value of the [Ni(hemi-cryptN$_4$S)](ClO$_4$)$_2$ isomer was observed to be 170 mV higher than that of [Ni([9]aneN$_4$S)](ClO$_4$)$_2$. In order to minimize the variation in error for a given electrochemical set-up ($E_{1/2}$ values can vary +/- 15 mV, even when referenced to ferrocene$^{0/+}$, depending on the nature of the solvent, electrolyte and electrodes), the potential was measured immediately after the [Ni([9]aneN$_4$S)](ClO$_4$)$_2$ complex using the same electrolyte solution and set-up. The potential of the ferrocene$^{0/+}$ couple (0.134 V) did not change before and after running the [Ni([9]aneN$_4$S)](ClO$_4$)$_2$ and [Ni(hemi-cryptN$_4$S)](ClO$_4$)$_2$ samples.

That the $E_{1/2}$ value of [Ni(hemi-cryptN$_4$S)](ClO$_4$)$_2$ is 170 mV higher is a significant result. This implies that the relatively subtle difference in structure of the hemi-cryptateN$_4$S bicycle translates into a significant destabilization of the nickel(II) to nickel(III) oxidation relative to the [9]aneN$_4$S bicycle. This structural effect can be attributed directly to a ring strain effect, rather than a chelate effect, and is similar in magnitude to the effect (*ca.* 300 mV) of increasing ring size in the [14-16]aneN$_4$ series studied by Busch[39].

It is not possible to determine the nature of the structural destabilization in the [Ni(hemi-cryptN$_4$S)](ClO$_4$)$_2$ complex in any more detail. The contributions of each donor to the overall observed potential are additive, such that this structurally derived weakening of the composite σ-donation strength of the ligand can not be assigned to particular donors. The source of the decreased σ-donation strength is likely to be due to rigidity in the sulphur bridge because the N$_4$S-bicycle isomers differ only with respect to the nature of the bridge linkage. As mentioned in section 4.2, the results of the molecular dynamics simulations of the three isomers suggest that the hemi-cryptateN$_4$S ligand will develop significantly increased ring strain (more so than the other two isomers) as the apical sulphur donor is "pulled" closer than *ca.* 2.4Å towards the metal center. This prediction can readily explain why the $E_{1/2}$ value of $Ni^{2+/3+}$ redox couple should be higher because, although the axial bond length requirement of the nickel(II) center is expected to be *ca.*

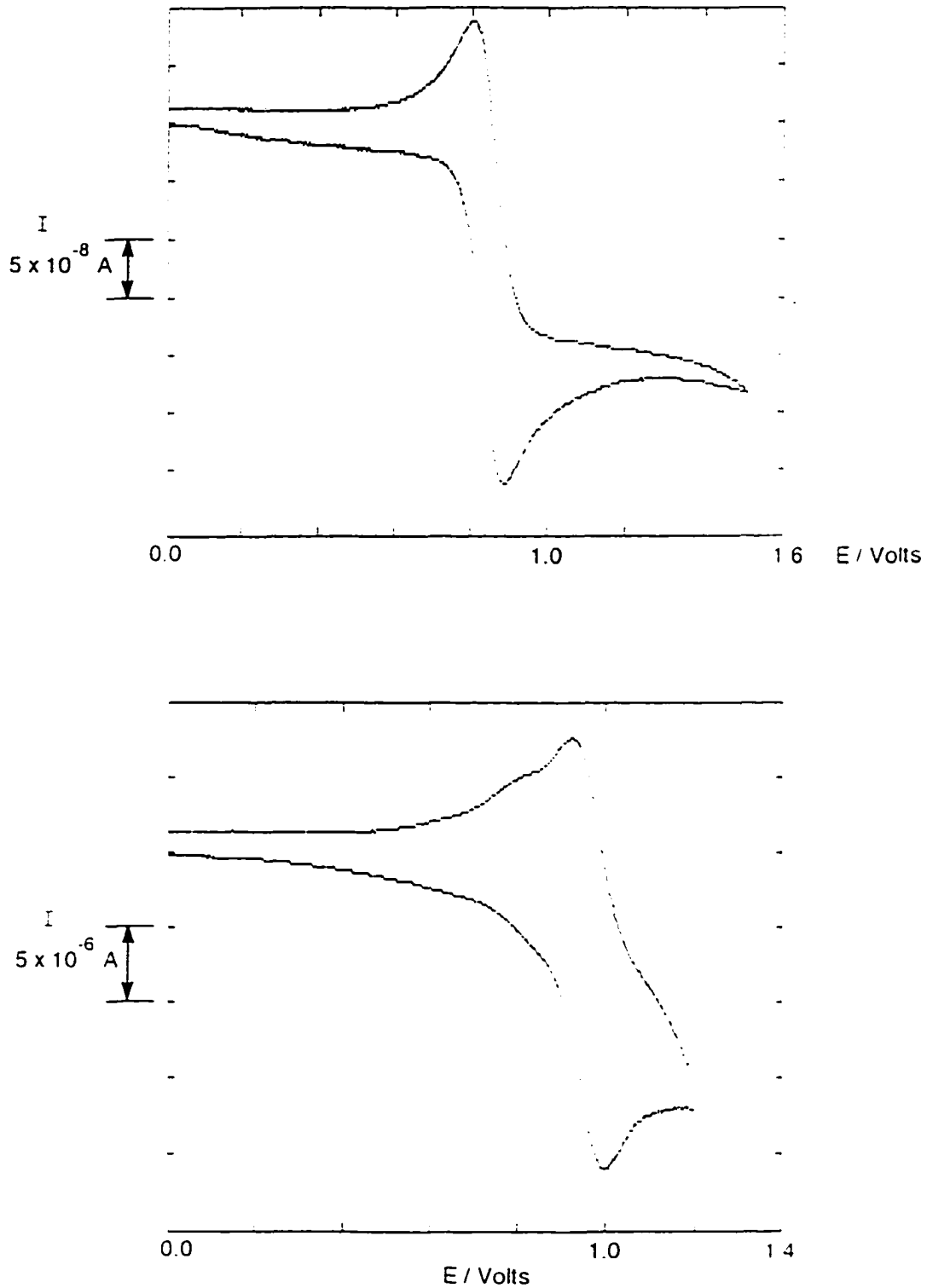

Figure 5.6. Cyclic voltammetric traces for oxidation of [Ni([9]aneN$_4$S)](ClO$_4$)$_2$ (top) and [Ni(hemi-cryptN$_4$S)](ClO$_4$)$_2$ (bottom).

2.4Å (based on the $[Ni([9]aneN_4S)](ClO_4)_2$ X-ray structure) which would not develop significant strain, the corresponding axial bond length requirement of the nickel(III) center produced in the oxidation would be shorter (*ca.* 1.9Å[188]), such that the ligand is not able to stabilize the nickel(III) center as well as the more flexible $[9]aneN_4S$ bicycle.

The nature of the cyclic voltammetric experiment is such that, even under electrochemically and chemically reversible conditions, the $E_{1/2}$ potentials depend on the nature of the solvent, electrolyte and electrodes used in each experiment. For this reason, the absolute value of $E_{1/2}$ can not be equated directly with $E^{o'}$. However, it is meaningful to compare the difference in $E_{1/2}$ values, $\Delta E_{1/2}$, observed for two different complexes such that this $\Delta E_{1/2}$ can be equated to the thermodynamic value, $\Delta G^{o'}$. In this experiment, the complexes must be measured under identical conditions so that the dependence of each redox potential on the conditions (solvent/electrolyte effects and electrochemical potential at the particular electrode used) is effectively cancelled out.

Given that these criteria have been satisfied for the $[Ni([9]aneN_4S)](ClO_4)_2$ and $[Ni(hemi\text{-}cryptN_4S)](ClO_4)_2$ isomers, it is interesting to note that application of the reversible free energy equation[189] gives:

$$\Delta\Delta G^{o'} = nF\Delta E^{o'} = (1)(96{,}487 \text{ coulombs/mol})(0.170 \text{ V}) = 3.9 \text{ kcal/mol}$$

where $\Delta\Delta G^{o'}$ represents the difference in stabilization energy for the $Ni^{2+/3+}$ redox couple between the two isomers. Application of this simple thermodynamic relationship does not account for differences such as outer-sphere solvent reorganization due to the change in charge at the metal center. However, it is believed that such effects should be similar for each isomer and therefore will not contribute significantly to the energy difference.

Busch[39,190] has calculated that the strain energy aquired by $[16]aneN_4$ upon coordination of low-spin square planar nickel(II) is 8.79 kcal/mol as compared to 2.40 kcal/mol for $[14]aneN_4$ (cyclam). The strain energy present in the $[9]aneN_4S$ bicyclic ligand upon coordination of copper(II) was calculated (section 4.3) to be 30 kcal/mol. These values can be explained by the expectation that strain effects present in the N_4S-

bicycle isomers are as likely to result in donor influences which oppose each other as influences which are additive. This effect would explain why the net stabilization energies observed in the electrochemistry are only a small fraction, 3.9 kcal / 30 kcal in this case, of the overall strain energy present in the ligands.

Chapter 6

Synthesis and Characterization of Cobalt(III) and Palladium(II) Complexes of [9]aneN$_4$S macrobicyclic Ligand

6.1. Introduction:

It is of interest to study the complexation properties resulting from coordination of transition metals other than the copper(II) and nickel(II) complexes reported in chapters 4 and 5. There have been numerous reports of cobalt(III)-amine complexation due its well-established[126] low-spin d^6 octahedral coordination chemistry and relatively inert substitution reactions.[43,46] There are also numerous reports[9] of complexation of cobalt(II) and cobalt(III) with macrocyclic polyaza ligands.

The importance of ligand rigidity effects such as ring strain are underscored by the occurrence of the 16-membered porphyrin ligand in heme proteins and the 15-membered corrin ring coordinating cobalt(III) in vitamin B_{12}.[21,22] It is believed that nature has exploited the shorter ring size in order to accomodate the shorter bond length requirements of cobalt(III). The cyclic nature of the heme and corrin ligands is one of several interesting features associated with these specialized natural ligands. The presence of fused rings, ligand charges, and highly conjugated π-bonding in these systems hinders attempts at delineating the contributions of each effect. Model studies in which these features are varied systematically therefore can provide valuable insight.

With this in mind, Busch[191] has correlated the ligand field parameters and kinetic substitution rates of the $[Co([13\text{-}16]aneN_4)(X)_2]^+$ series of complexes. In the absence of charge and π-bonding effects, deviations in this series can be attributed to strain effects. Table 1.6 shows the correlations of equatorial ligand field strength (Dq^{xy}) with ring size. In contrast with the ligand field correlation with ring size for nickel(II), which indicated that the natural hole-size of $[15]aneN_4$ matches nickel(II) best, it was found[70] (table 1.6) that $[14]aneN_4$ (cyclam) matches the bonding requirements of cobalt(III) best. Table 6.1 shows the correlation of aquation rate constants for the cobalt(III) complexes with ring size.

Table 6.1. Correlation of aquation rates with ring size for cobalt(III) complexes, *trans*-[Co([13-16]aneN$_4$)(Cl)$_2$]$^+$, of tetraaza macrocyclic ligands.[70]

Ligand	k_1 /s^{-1} (25 °C)
[13]aneN$_4$	6.76 x 10^{-4}
[14]aneN$_4$[a]	1.1 x 10^{-6}
[15]aneN$_4$	9.92 x 10^{-3}
[16]aneN$_4$	2.57

[a]Data obtained from Poon, C. K.; Tobe, M. L. *J. Chem. Soc. A*, **1967**, p. 2069.

Table 6.1 shows that the effect of ring size on aquation rate is large, spanning a range of more than five orders of magnitude, from 1.1 x 10^{-6} s^{-1} to 2.6 s^{-1} for [Co([14]aneN$_4$)(Cl)$_2$]$^+$ to [Co([16]aneN$_4$)(Cl)$_2$]$^+$ respectively. That the rate increases sharply with ring size contradicts the predicted trend based on the ligand field parameters which show that [14]aneN$_4$ has the highest ligand field strength and therefore should have the strongest labilizing *cis*-effect on the dissociative axial substitution reaction. In fact, *trans*[Co([14]aneN$_4$)(Cl)$_2$]$^+$ aquates more slowly than the well-studied acyclic analogue, *trans*-[Co(en)$_2$Cl$_2$]$^+$ (3.2 x 10^{-5} s^{-1}).[192]

Busch attributed this trend to the likely possibility that there is a five-coordinate transition state in the substitution reaction. It was proposed that the ring strain induced in the ground state equatorially coordinated tetraaza ligand by the cobalt(III) center is relieved by displacement of the cobalt(III) ion above the N$_4$ plane in the transition state (see figure 6.1). Busch noted a linear correlation of the calculated strain energy with ln(k_1) for these aquation reactions.

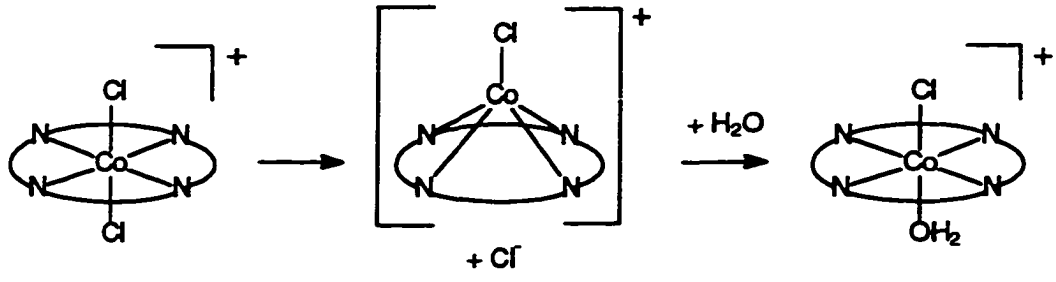

Figure 6.1. Proposed[70] mechanism of cobalt(III) aquation reaction.

Another interesting systematic variation of tetraazamacrocyclic ligand structure was reported by Lippard.[193] In this study, the ring size of the tropocoronand ligand shown in figure 6.2 was sequentially increased and the structures of the resulting [Co(Cl)(TC-n,m)] complexes were determined by X-ray crystallography. The presence of the two cycloheptatriene rings bridging adjacent nitrogen donors lends more rigidity than in the corresponding saturated aliphatic tetraaza ligands studied by Busch.

As is depicted in figure 6.2, the series of [Co(Cl)(TC-n,m)] complexes, in which the lengths (n and m) of the two saturated aliphatic bridges are sequentially increased by one member, have substantially different coordination geometries. The structure of the 14-membered [Co(Cl)(TC-3,3)] complex (left) is square pyramidal with identical *trans*-basal N-Co-N bond angles of 163.3°. The geometry of the 15-membered [Co(Cl)(TC-3,4)] complex (middle) is best described as intermediate between square planar and trigonal bipyramidal with N-Co-N bond angles of 171.5° and 142.1°. Finally, the 16-membered [Co(Cl)(TC-4,4)] complex (right) adopts a nearly perfect trigonal bipyramidal coordination geometry with the chloride in the equatorial plane. The latter two complexes displayed no solution NMR spectra at ambient temperature, which is indicative of paramagnetic behviour. Magnetic susceptibility measurements on the trigonal bipyramidal [Co(Cl)(TC-4,4)] complex in the temperature range of 300 K to 50 K, revealed a

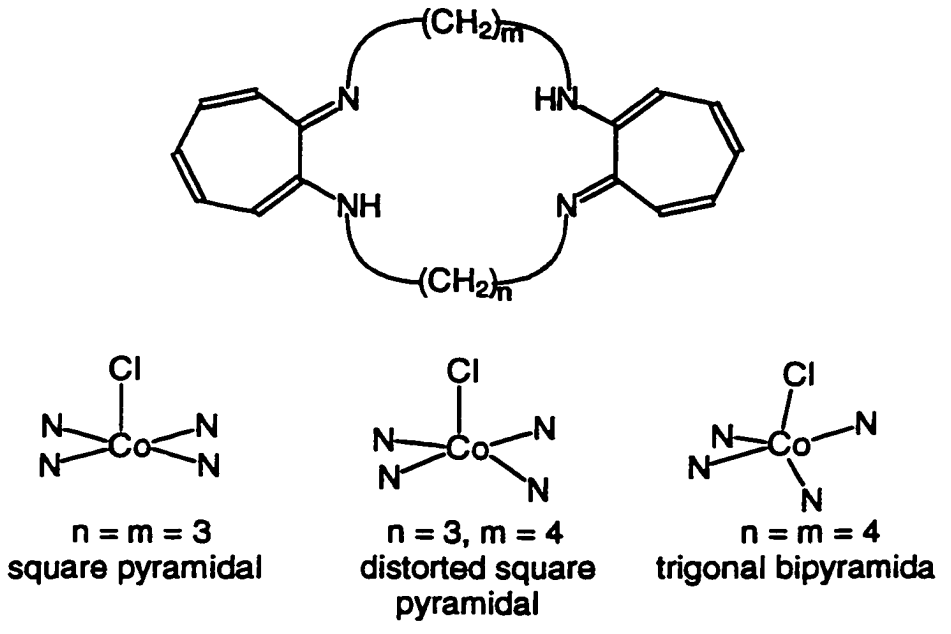

Figure 6.2. Correlation of coordination geometry of [Co(Cl)(TC-n,m)] (TC = tropocoronand tetraaza macrocyclic ligand system) complexes with sequential increases in the lengths, n and m, of the saturated aliphatic linkages.[193]

magnetic moment of 3.0 μ_B, corresponding to the presence of two unpaired electrons. Below 50 K, the magnetic moment was 1.1 μ_B.

It is therfore of interest to synthesize and characterize the cobalt(III) complex of the [9]aneN_4S macrobicycle prepared in the present study in order to determine if the rigidity of bicyclic structure, shown in section 3.7 to be significantly greater than that of the parent [9]aneN_2S and [14]aneN_4 rings, will result in geometry distortions or reactivities that can be attributed to ligand strain effects.

Coordination of the pentacoordinate [9]aneN_4S bicyclic ligand induces square pyramidal or octahedral geometries such that this ligand system is well-suited for complexation of the low-spin d^6 octahedral cobalt(III) ion. However, it was also

considered that coordination of this ligand to the classical low-spin d^8 square planar palladium(II) ion would be of interest in order to determine if the presence of the axial sulphur donor would aid in the stabilization of the less common d^7 palladium(III) ion.

6.2. Synthesis of Cobalt(III) and Palladium(II) Complexes of [9]aneN$_4$S macrobicycle:

The syntheses of the $[Co([9]aneN_4S)(X^{n-})]^{(3-n)+}$ (X = OH_2, Cl^-) complexes (section 8.3) were each carried out by bubbling oxygen through an aqueous solution of the [9]aneN$_4$S free ligand (**L1**) with one equivalent of hexaaquo cobalt(II) for 30 h. The solution first turned dark green upon addition of the reactants, presumably due to coordination of the cobalt(II) ion. Over the course of 1-2 h. the solution turned a dark red, implying the presence of oxidation to cobalt(III). It was found that it was necessary to use an oxygen gas cylinder, rather than the fumehood air line, as the source to avoid decompostion and side products. It was also found that exposure to strongly acidic and basic solutions accelerated decompostion.

The complexes crystallized readily from aqueous and acetonitrile solutions. Recrystallization from acetonitrile solution gave the acetonitrile coordinated $[Co([9]aneN_4S)(NCCH_3)]^{3+}$ complex. Only the isolated yields are quoted in section 8.3 which were relatively low after repeated recrystallization of each sample to obtain X-ray quality crystals. The microanalytical results agreed well with that expected. The IR and ^{13}C-NMR spectra of $[Co([9]aneN_4S)(OH_2)]^{3+}$ are shown figure 6.3.

The syntheses of the $[Pd([9]aneN_4S)]^{2+}$ and $[Pd([9]aneN_2S)_2]^{2+}$ complexes (section 8.3) each resulted in X-ray quality crystalline samples. Microanalytical data showed the complexes to be pure. The IR and ^{13}C-NMR spectra of the $[Pd([9]aneN_4S)]^{3+}$ complex are shown in figure 6.4.

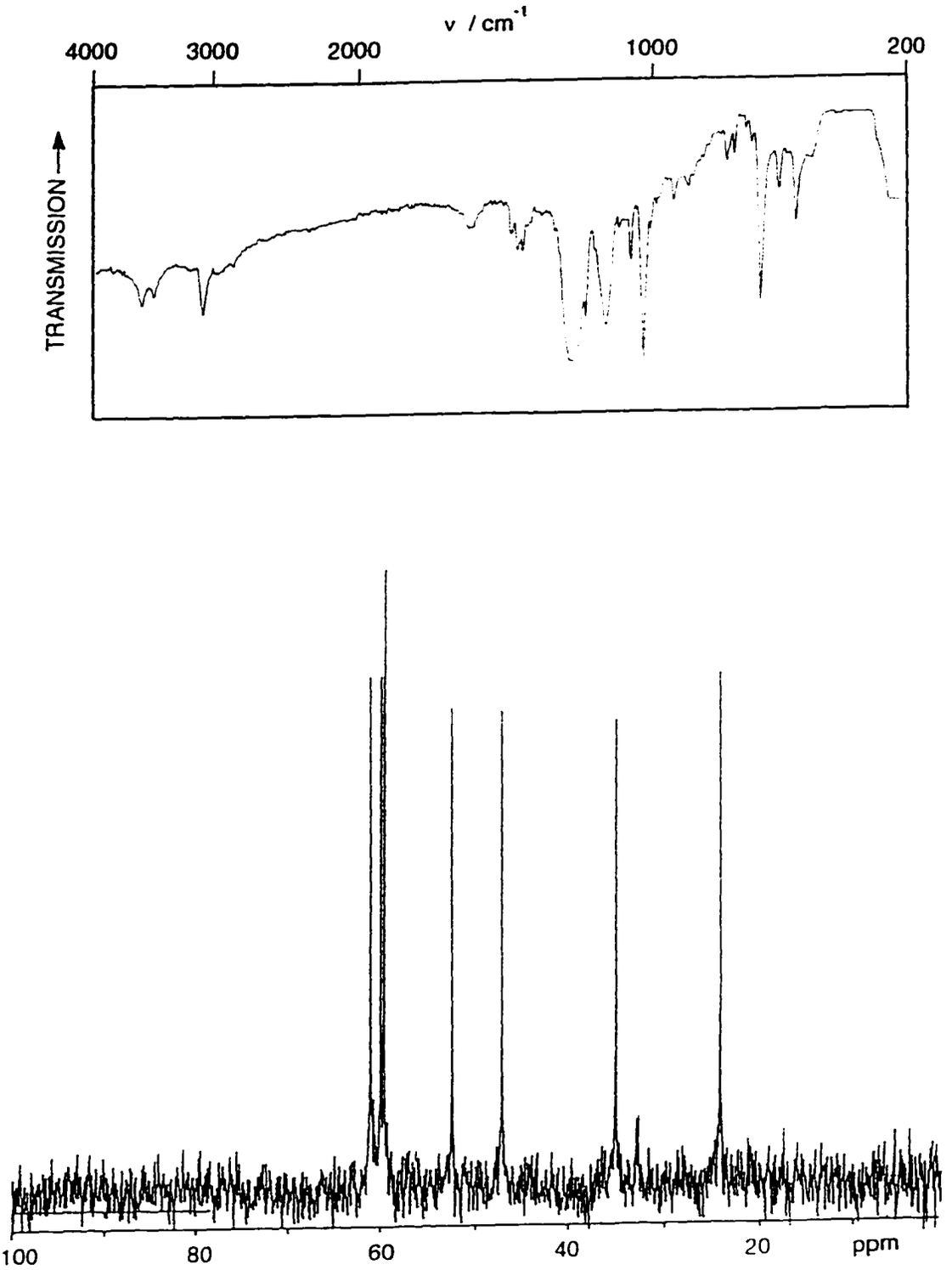

Figure 6.3. IR and ^{13}C-NMR spectra of $[Co([9]aneN_4S)(OH_2)](ClO_4)_2$ dihydrate.

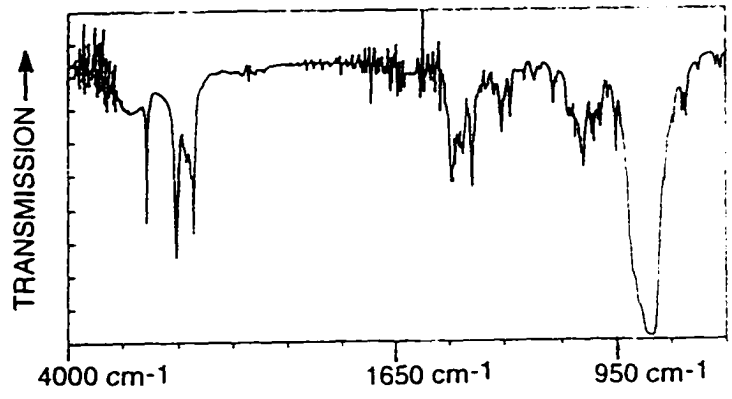

Infrared Spectrum of $[Pd([9]aneN_4S)](PF_6)_2$ (KBr powder).

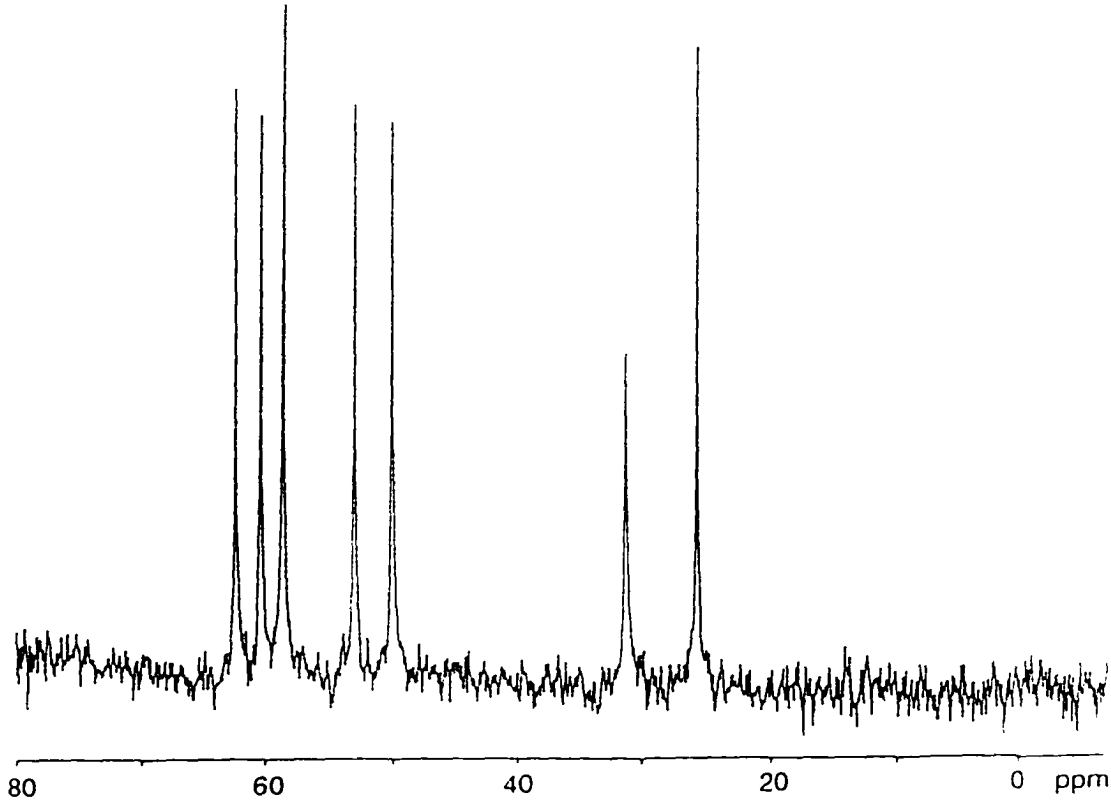

Figure 6.4. ^{13}C-NMR spectrum of $[Pd([9]aneN_4S)](PF_6)_2$ in D_2O.

6.3. Molecular Structures and Strain Energy Calculations:

6.3(a) $[Co([9]aneN_4S)(NCCH_3)](ClO_4)_2$:

The structure of the $[Co([9]aneN_4S)(NCCH_3)](ClO_4)_3$ complex is shown in figures 6.5(a) and (b), and selected bond lengths and angles are listed in table 6.2. The experimental parameters are listed in table 6.3 and the fractional atomic coordinates in table 6.4. All atoms were refined anisotropically except for the hydrogens. The refinement converged with a maximum shift/e.s.d. of 0.103 on the final cycle, and a maximum peak of 0.2 $eÅ^{-3}$, with an R-value of 0.086.

The ligand arrangement is similar to that in the copper(II) and nickel(II) X-ray structures[90] with the cyclam ring adopting a trans-I configuration. A molecular mechanics study by Billo and Connolly[31] on cyclam has shown that, of the five possible *trans* configurations (shown in figure 1.5), the trans-III configuration has the lowest energy. The trans-I configuration has the least relative strain energy of the remaining configurations for octahedral and planar geometries, and is close (2.5 kcal/mol) to the trans-(III) strain energy such that the presence of *ca.* 15% trans-I coordinated cyclam was used to explain the observed NMR spectrum of the nickel(II) complex. As can be seen in figure 6.5(b), the six-membered chelate rings are both in the lowest energy chair conformation and the five-membered chelates are both in the lowest energy gauche arrangement.

The four nitrogens of the cyclam ring form a plane with a mean deviation of 0.0055Å and trans basal N-M-N bond angles of 176.7° and 175.7°. The cobalt atom is displaced only 0.025Å above the N_4 plane and therefore can be considered virtually coplanar in comparison to the displacements of 0.141Å and 0.111Å for the nickel(II) and copper(II) complexes respectively.[90] According to molecular mechanics calculations performed by Hancock and coworkers[71], the ideal position for a metal ion coordinated to

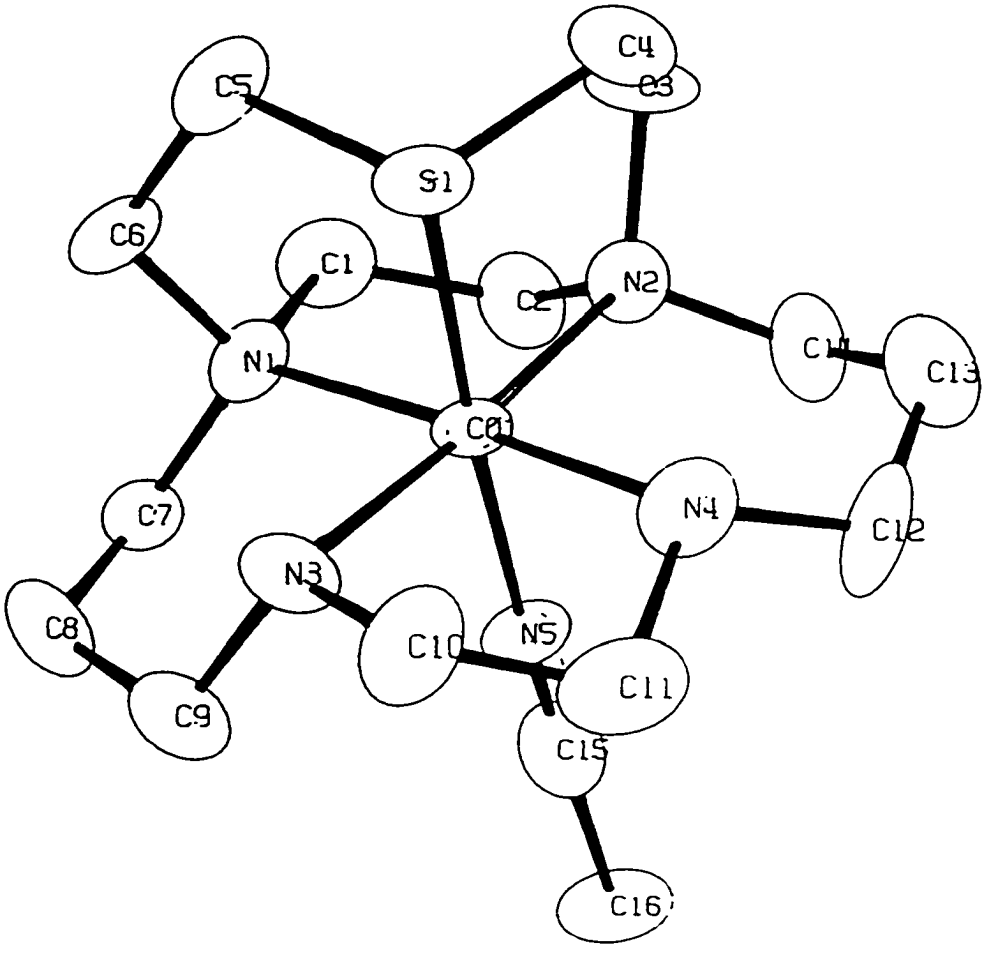

Figure 6.5(a). Ortep diagram (front view) of $[Co([9]aneN_4S)(NCCH_3)](ClO_4)_3$ complex cation with atomic labelling for non-hydrogen atoms.

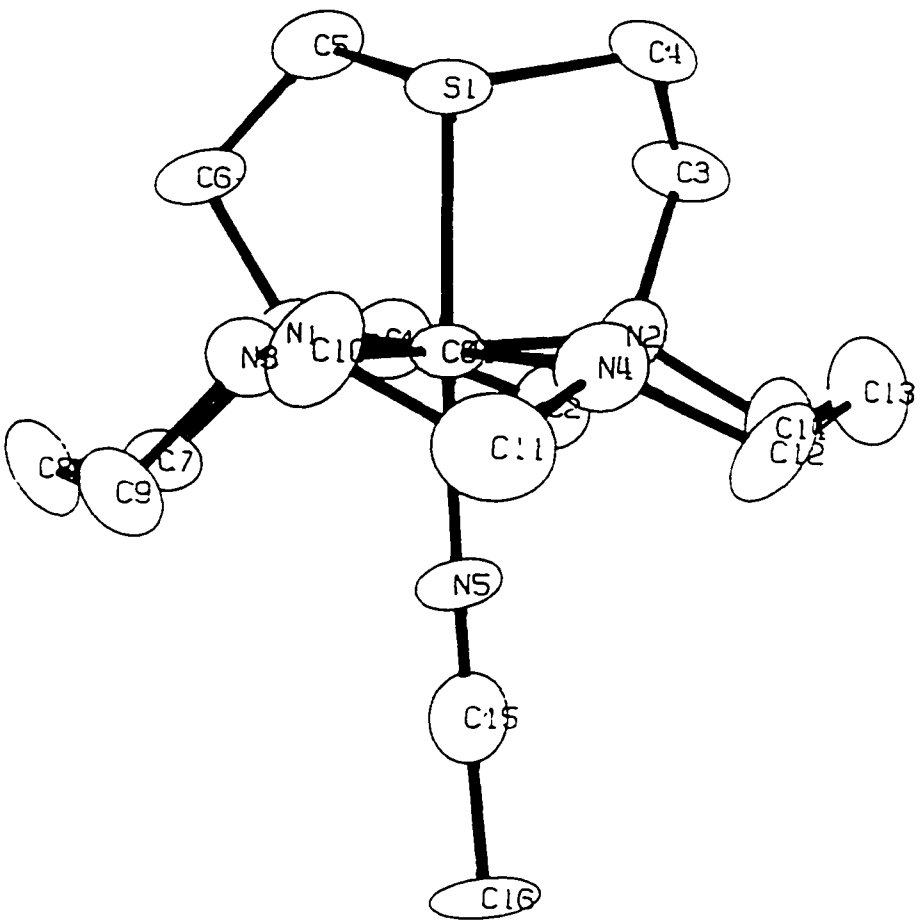

Figure 6.5(b). Ortep diagram (side view) of $[Co([9]aneN_4S)(NCCH_3)](ClO_4)_3$ complex cation with atomic labelling for non-hydrogen atoms.

Table 6.2(a). Interatomic distances (Å)[a] for $[Co([9]aneN_4S)(NCCH_3)](ClO_4)_3$.

Interatomic distances (Å).

Atoms	Distance	Atoms	Distance
S(1) -Co(1)	2.206(2)	C(1) -N(1)	1.522(12)
N(1) -Co(1)	2.014(7)	C(6) -N(1)	1.525(11)
N(2) -Co(1)	2.016(7)	C(7) -N(1)	1.511(11)
N(3) -Co(1)	1.991(7)	C(2) -N(2)	1.518(12)
N(4) -Co(1)	1.986(8)	C(3) -N(2)	1.557(11)
N(5) -Co(1)	1.966(7)	C(14) -N(2)	1.473(12)
O(1) -Cl(1)	1.346(12)	C(9) -N(3)	1.468(12)
O(2) -Cl(1)	1.330(11)	C(10) -N(3)	1.517(12)
O(3) -Cl(1)	1.299(11)	C(11) -N(4)	1.483(13)
O(4) -Cl(1)	1.308(18)	C(12) -N(4)	1.509(13)
O(5) -Cl(2)	1.425(10)	C(15) -N(5)	1.129(11)
O(6) -Cl(2)	1.415(10)	C(2) -C(1)	1.520(14)
O(7) -Cl(2)	1.414(10)	C(4) -C(3)	1.544(15)
O(8) -Cl(2)	1.345(11)	C(6) -C(5)	1.516(13)
O(9) -Cl(3)	1.421(9)	C(8) -C(7)	1.510(15)
O(10) -Cl(3)	1.348(11)	C(9) -C(8)	1.529(15)
O(11) -Cl(3)	1.313(14)	C(11) -C(10)	1.530(15)
O(12) -Cl(3)	1.265(15)	C(13) -C(12)	1.505(17)
C(4) -S(1)	1.817(10)	C(14) -C(13)	1.512(15)
C(5) -S(1)	1.816(10)	C(16) -C(15)	1.465(13)

[a]Estimated standard deviations are given in parentheses.

Table 6.2(b). Bond angles (deg)[a] for $[Co([9]aneN_4S)(NCCH_3)](ClO_4)_3$.

Atoms			Angle	Atoms			Angle
N(1)	-Co(1)	-S(1)	89.1(2)	C(5)	-S(1)	-C(4)	102.4(5)
N(2)	-Co(1)	-S(1)	90.1(2)	C(1)	-N(1)	-Co(1)	108.1(5)
N(2)	-Co(1)	-N(1)	88.0(3)	C(6)	-N(1)	-Co(1)	110.5(5)
N(3)	-Co(1)	-S(1)	88.1(2)	C(6)	-N(1)	-C(1)	108.1(7)
N(3)	-Co(1)	-N(1)	89.2(3)	C(7)	-N(1)	-Co(1)	112.2(5)
N(3)	-Co(1)	-N(2)	176.7(3)	C(7)	-N(1)	-C(1)	109.4(7)
N(4)	-Co(1)	-S(1)	89.6(2)	C(7)	-N(1)	-C(6)	108.5(7)
N(4)	-Co(1)	-N(1)	175.7(3)	C(2)	-N(2)	-Co(1)	102.3(5)
N(4)	-Co(1)	-N(2)	96.1(3)	C(3)	-N(2)	-Co(1)	113.3(6)
N(4)	-Co(1)	-N(3)	86.7(3)	C(3)	-N(2)	-C(2)	108.3(7)
N(5)	-Co(1)	-S(1)	176.7(2)	C(14)	-N(2)	-Co(1)	115.7(6)
N(5)	-Co(1)	-N(1)	94.1(3)	C(14)	-N(2)	-C(2)	107.9(7)
N(5)	-Co(1)	-N(2)	89.5(3)	C(14)	-N(2)	-C(3)	108.8(7)
N(5)	-Co(1)	-N(3)	92.5(3)	C(9)	-N(3)	-Co(1)	115.5(6)
N(5)	-Co(1)	-N(4)	87.2(3)	C(10)	-N(3)	-Co(1)	107.8(6)
O(2)	-Cl(1)	-O(1)	103.8(8)	C(10)	-N(3)	-C(9)	114.9(8)
O(3)	-Cl(1)	-O(1)	129.4(14)	C(11)	-N(4)	-Co(1)	106.6(6)
O(3)	-Cl(1)	-O(2)	119.5(13)	C(12)	-N(4)	-Co(1)	118.6(6)
O(4)	-Cl(1)	-O(1)	93.3(15)	C(12)	-N(4)	-C(11)	111.2(8)
O(4)	-Cl(1)	-O(2)	102.9(15)	C(15)	-N(5)	-Co(1)	176.2(8)
O(4)	-Cl(1)	-O(3)	100.7(9)	C(2)	-C(1)	-N(1)	110.0(7)
O(6)	-Cl(2)	-O(5)	102.4(8)	C(1)	-C(2)	-N(2)	110.0(7)
O(7)	-Cl(2)	-O(5)	111.8(8)	C(4)	-C(3)	-N(2)	111.5(8)
O(7)	-Cl(2)	-O(6)	107.6(8)	C(3)	-C(4)	-S(1)	109.4(6)
O(8)	-Cl(2)	-O(5)	111.5(9)	C(6)	-C(5)	-S(1)	108.8(6)
O(8)	-Cl(2)	-O(6)	111.4(10)	C(5)	-C(6)	-N(1)	112.1(8)
O(8)	-Cl(2)	-O(7)	111.8(8)	C(8)	-C(7)	-N(1)	114.3(8)
O(10)	-Cl(3)	-O(9)	113.1(6)	C(9)	-C(8)	-C(7)	116.2(8)
O(11)	-Cl(3)	-O(9)	109.5(9)	C(8)	-C(9)	-N(3)	111.8(8)
O(11)	-Cl(3)	-O(10)	106.9(12)	C(11)	-C(10)	-N(3)	107.4(8)
O(12)	-Cl(3)	-O(9)	109.0(9)	C(10)	-C(11)	-N(4)	106.1(8)
O(12)	-Cl(3)	-O(10)	112.0(14)	C(13)	-C(12)	-N(4)	113.7(9)
O(12)	-Cl(3)	-O(11)	106.0(18)	C(14)	-C(13)	-C(12)	112.8(9)
C(4)	-S(1)	-Co(1)	98.5(3)	C(13)	-C(14)	-N(2)	114.8(8)
C(5)	-S(1)	-Co(1)	100.6(3)	C(16)	-C(15)	-N(5)	176.8(11)

[a]Estimated standard deviations are given in parentheses.

Table 6.3. Crystallographic data of $[Co([9]aneN_4S)(NCCH_3)](ClO_4)_3$.

Molecular formula:	$Co_1S_1N_5C_{16}H_{31}Cl_3O_{12}$	
Molecular weight:	682.8	
Crystal colour:	dark red	
Crystal System:	monoclinic	
Space group:	P $2_1/n$ (No. 14)	
Unit cell dimensions:	a = 10.720(3)Å	α = 90°
	b = 17.822(5)Å	β = 91.09(3)°
	c = 13.914(5)Å	γ = 90°
Unit cell volume:	2657.8 Å	
Z:	4	
Density (g/cm^3):	1.701	
Radiation:	Mo 0.71069	
2θ range (deg):	0° - 50°	
No. of reflections used:	4677	
Residual electron density ($e/Å^3$):	0.2	
Final R, R_w values:	0.0869, 0.0934	

Table 6.4. Fractional atomic coordinates and temperature parameters for $[Co([9]aneN_4S)(NCCH_3)](ClO_4)_3$.

Atom	x/a	y/b	z/c	Ueq
Co(1)	18990(9)	15416(6)	26758(8)	283(3)
Cl(1)	69371(23)	35930(17)	25416(19)	565(9)
Cl(2)	17029(26)	39121(14)	25416(19)	555(9)
Cl(3)	18199(24)	38667(14)	1430(23)	559(9)
S(1)	3269(20)	23415(12)	26421(17)	376(7)
O(1)	6106(14)	3632(12)	3253(9)	223(11)
O(2)	6267(13)	3343(11)	1795(9)	187(9)
O(3)	8128(10)	3457(7)	2588(18)	236(14)
O(4)	6940(15)	4320(10)	2409(25)	356(23)
O(5)	3012(10)	3772(7)	4910(8)	113(5)
O(6)	1321(13)	3645(7)	3989(9)	131(6)
O(7)	1434(12)	4689(5)	4937(10)	124(5)
O(8)	1137(16)	3535(7)	5611(11)	162(8)
O(9)	1428(9)	3106(5)	209(8)	100(4)
O(10)	3052(9)	3958(6)	320(12)	130(6)
O(11)	1232(18)	4272(10)	780(21)	281(15)
O(12)	1492(26	4124(11)	-669(17)	293(15)
N(1)	1397(7)	1223(4)	4002(5)	38(2)
N(2)	769(7)	730(4)	2147(6)	41(2)
N(3)	2947(7)	2350(4)	3261(6)	43(3)
N(4)	2441(7)	1927(4)	1412(6)	45(3)
N(5)	3314(7)	840(4)	2628(5)	39(2)
C(1)	597(9)	520(5)	3906(7)	47(3)
C(2)	814(9)	147(5)	2942(7)	47(3)
c(3)	-609(8)	990(6)	2004(8)	52(4)
c(4)	-694(9)	1842(6)	1805(7)	52(3)
c(5)	-378(10)	2142(6)	3791(7)	49(3)
c(6)	616(9)	1834(5)	4470(7)	45(3)
c(7)	2512(8)	1060(6)	4647(7)	44(3)
c(8)	3351(10)	1727(7)	4832(8)	62(4)
c(9)	3914(9)	2095(6)	3946(7)	51(3)
c(10)	3414(10)	2842(6)	2454(8)	53(4)
c(11)	3631(10)	2333(6)	1588(8)	56(4)
c(12)	2549(13)	1381(7)	588(8)	66(4)
c(13)	1409(11)	900(7)	432(8)	62(4)
c(14)	1184(10)	368(5)	1258(7)	50(3)
c(15)	4137(9)	450(5)	2551(7)	46(3)
c(16)	5247(10)	-19(7)	2437(9)	65(4)

Coordinates x 10^4. Temperature parameters x 10^3.
Ueq = the equivalent isotropic temperature parameter
Ueq = 1/3 $\Sigma_i\Sigma_j U_{ij} a_i^* a_j^* (a_i \bullet a_j)$

[a]Estimated standard deviations are given in parentheses.

the trans-I configuration of cyclam is 0.06Å out of the N_4 plane. The sulphur donor is coordinated axially with no significant deviation (1.1°) of the cobalt-sulphur vector from the perpendicular to the N_4 plane. The M-S vector deviates 8.2° and 6.5° from the perpendicular to the N_4 plane in the copper(II) and nickel(II) complexes respectively. Thus, the coordination geometry is more strictly octahedral for the cobalt(III) complex reflecting the preference of the low-spin d^6 ion for octahedral geometry.

The Co-N bond distances are slightly longer (2.014Å and 2.016Å) for the tertiary amines than the secondary amines (1.991Å and 1.986Å). These values closely match those observed[194] (2.025Å and 1.991Å) in the X-ray structure of the cobalt(III) complex with the hexaamine ligand 1,4,7-*tris*(3-aminopropyl)-1,4,7-triazacyclononane. Correlation of a large number of experimental X-ray data[195] suggests that the average cobalt(III)-nitrogen bond length lies between 1.93Å and 2.03Å, consistent with that observed in the present study. The calculated[31] ideal M-N bond distance for cyclam in the trans-I configuration is 2.01Å which is also consistent with the present structure. That the bond distance requirements of cobalt(III) match the ideal M-N distance of the cyclam ring suggests that there should not be significant strain associated with coordination of the cyclam ring in the ion $[Co([9]aneN_4S)(NCCH_3)]^{3+}$.

As expected, the axial Co-S bond distance (2.206Å) is considerably shorter than that of the copper(II) and nickel(II) complexes (2.549Å and 2.385Å respectively). That the Co-S vector is essentially perpendicular to the N_4 plane is of interest because the greater deviations observed in the copper(II) and nickel(II) complexes are thought to be caused by an inability of the nonane ring to reach over and fully encapsulate the axial site. The strict octahedral coordination of the $[Co([9]aneN_4S)(NCCH_3)]^{3+}$ complex therefore provides an opportunity to assess the degree of ligand strain induced by such coordination. This can be achieved by performing the ligand strain calculation described in section 4.3 wherein the fractional atomic coordinates of the $[9]aneN_4S$ ligand are used as the initial structure then the minimum energy of the free ligand is calculated by the use of MM2 calculations. The energy difference between the initial (coordinated) ligand and the final minimized free

ligand is a prediction of the amount of strain induced in the ligand by coordination of the metal center.

The initial and final [9]aneN$_4$S structures are shown in figure 6.6. As expected, the most discernable movements upon minimization involve the orientation of the nitrogen donors. The calculated energies of the initial (coordinated) and final (minimized) structures are 72.09 kcal/mol and 39.28 kcal/mol respectively giving an energy difference of 32.8 kcal/mol. The corresponding calculation for the copper(II) complex resulted in energies of 69.5 kcal/mol (coordinated) and 39.3 kcal/mol (minimized) and an energy difference of 30.2 kcal/mol. These calculations suggest that the additional ligand strain imposed by positioning the axial sulphur donor perpendicular (and closer) to the ring, is only 2.6 kcal/mol, which is probably not significant in comparison to the solution energies present at room temperature.

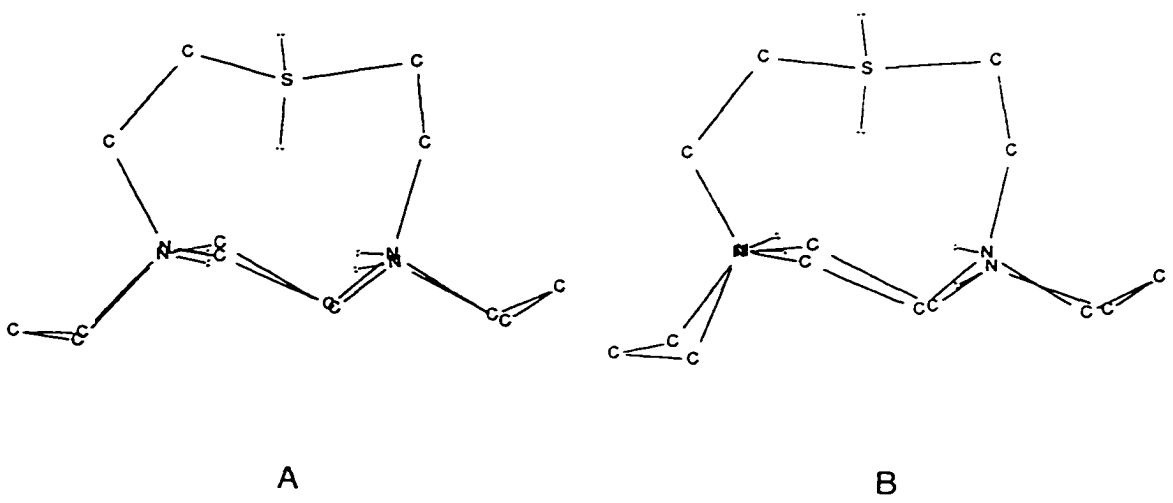

Figure 6.6. A) Conformation of [9]aneN$_4$S bicyclic ligand when complexed to cobalt(III) (using crystallographic coordinates). B) conformation of same ligand after molecular mechanics (MM2) energy minimization.

6.3(b). $[Pd([9]aneN_4S)](PF_6)_2$ and $[Pd([9]aneN_2S)_2](Cl)_2$:

The structure of the $[Pd([9]aneN_4S)](PF_6)_2$ complex is shown in figure 6.7 and selected bond lengths and angles are listed in table 6.5. The experimental parameters are listed in table 6.6 and the fractional atomic coordinates in table 6.7. All atoms were refined anisotropically except for the hydrogens. The refinement converged with a maximum shift/e.s.d. of 0.01 on the final cycle, and a maximum peak of 0.2 $eÅ^{-3}$, with an R-value of 0.065.

The ligand arrangement is similar to that in the cobalt(III) X-ray structure with the cyclam ring adopting the trans-I configuration. As with the cobalt(III) complex, the six-membered chelate rings are both in the lowest energy chair conformation and the five-membered chelates are both in the lowest energy gauche arrangement (figure 6.7).

The four nitrogens of the cyclam ring form a plane with a mean deviation of 0.0062Å and trans basal N-M-N bond angles of 176.1° and 175.4°. The palladium atom is displaced only 0.027Å above the N_4 plane and therefore can be considered coplanar (the displacements are 0.141Å and 0.111Å for the nickel(II) and copper(II) complexes respectively)[90]. The Pd-N bond distances are slightly longer (2.068Å and 2.088Å) for the tertiary amines than the secondary amines (2.063Å and 2.064Å) and both sets of distances are *ca.* 0.07Å greater than those observed in the cobalt(III) complex. The Pd-N bond lengths are consistent with those of the $[Pd([14]aneN_4)]^{2+}$ (2.055Å and 2.062Å)[196], $[Pd([9]aneN_3)_2]^{2+}$ (2.068Å and 2.050Å)[197] and $[Pd([9]aneNS_2)_2]^{2+}$ (2.081Å)[198] complexes. These similarities suggest that there is not significant distortion associated with coordination of the cyclam ring in $[Pd([9]aneN_4S)(NCCH_3)]^{3+}$.

The sulphur donor is positioned axially above the palladium, however, the palladium-sulphur vector deviates 16° from the perpendicular to the N_4 plane. This deviation is considerably greater than that of the copper(II) and nickel(II) complexes (8.2° and 6.5° respectively). The Pd-S distance is 2.87Å, which is consistent with but shorter than the distances reported for $[Pd([9]aneNS_2)](BF_4)_2$ (3.011Å)[198], $[Pd([9]aneS_3)_2](PF_6)_2$

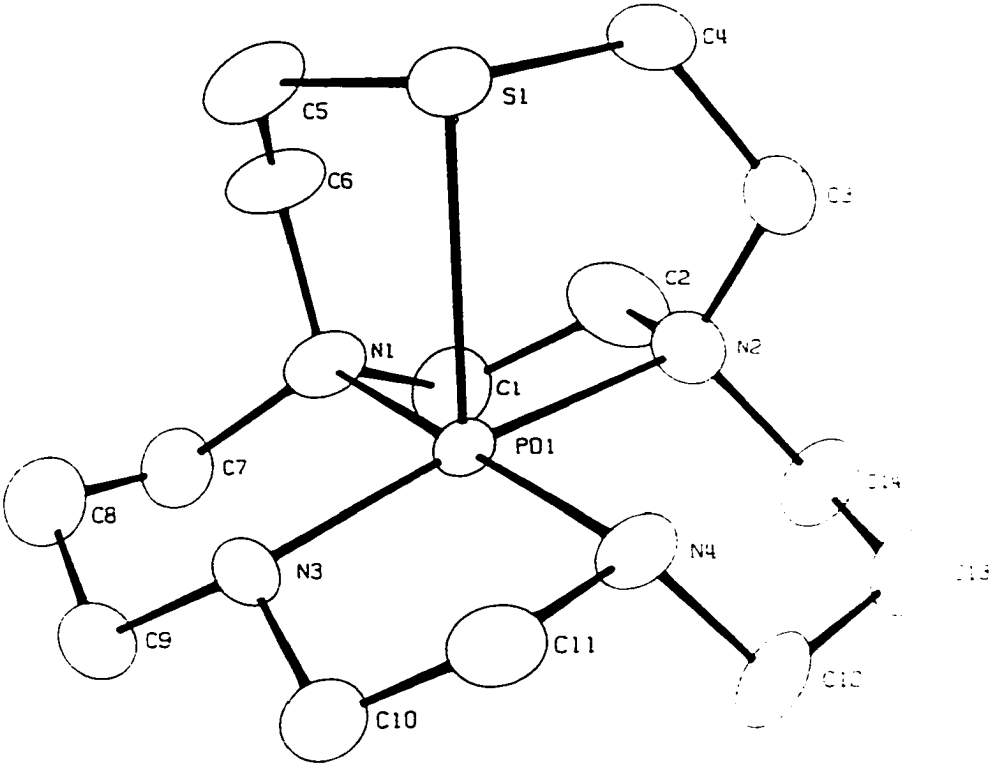

Figure 6.7. Ortep diagram of $[Pd([9]aneN_4S)](PF_6)_2$ complex cation with atomic labelling for non-hydrogen atoms.

Table 6.5(a). Interatomic distances (Å)[a] for $[Pd([9]aneN_4S)](PF_6)_2$

	Pd1···S1 2.875(3)		
Pd1-N1	2.068(9)	N1-C1	1.523(14)
Pd1-N2	2.088(9)	N1-C6	1.534(13)
Pd1-N3	2.063(8)	N1-C7	1.504(14)
Pd1-N4	2.064(8)	N2-C2	1.473(14)
S1-C4	1.819(12)	N2-C2	1.473(14)
S1-C5	1.845(14)	N2-C3	1.496(14)
P1-F1	1.553(8)	N2-C14	1.498(14)
P1-F2	1.552(8)	N3-C9	1.524(14)
P1-F3	1.478(11)	N3-C10	1.459(14)
P1-F4	1.537(8)	N4-C11	1.508(13)
P1-F5	1.525(9)	N4-C12	1.484(13)
P1-F6	1.503(12)	C1-C2	1.495(16)
P2-F7	1.558(8)	C3-C4	1.553(16)
P2-F8	1.549(8)	C5-C6	1.547(17)
P2-F9	1.492(10)	C7-C8	1.506(19)
P2-F10	1.525(8)	C8-C9	1.528(18)
P2-F11	1.556(8)	C10-C11	1.493(16)
P2-F12	1.481(10)	C12-C13	1.533(16)
		C13-C14	1.579(16)

[a]Estimated standard deviations are given in parentheses.

Table 6.5(b). Bond angles (deg)[a] for $[Pd([9]aneN_4S)](PF_6)_2$

		N1-Pd1-S1	86.9(3)
		N2-Pd1-S1	82.3(3)
		N3-Pd1-S1	102.0(2)
		N4-Pd1-S1	96.3(2)
		C4-S1-Pd1	88.5(4)
		C5-S1-Pd1	83.2(4)
N1-Pd1-N2	84.6(4)	Pd1-N3-C10	106.0(7)
N1-Pd1-N3	97.1(4)	C9-N3-C10	110.4(9)
N1-Pd1-N4	176.1(3)	Pd1-N4-C11	107.1(6)
N2-Pd1-N3	175.4(3)	Pd1-N4-C12	111.0(6)
N2-Pd1-N4	93.5(4)	C11-N4-C12	112.5(8)
N3-Pd1-N4	84.5(3)	N1-C1-C2	107.6(10)
C4-S1-C5	104.6(7)	N2-C2-C1	112.9(9)
Pd1-N1-C1	101.8(6)	N2-C3-C4	114.0(9)
Pd1-N1-C6	113.4(7)	S1-C4-C3	114.1(8)
Pd1-N1-C7	114.3(8)	S1-C5-C6	118.3(10)
C1-N1-C6	110.1(10)	N1-C6-C5	119.2(10)
C1-N1-C7	106.4(10)	N1-C7-C8	114.8(11)
C6-N1-C7	110.3(9)	C7-C8-C9	114.0(11)
Pd1-N2-C2	107.3(7)	N3-C9-C8	109.8(9)
Pd1-N2-C3	111.2(6)	N3-C10-C11	108.6(9)
Pd1-N2-C14	109.2(7)	N4-C11-C10	109.3(9)
C2-N2-C3	112.3(9)	N4-C12-C13	108.8(10)
C2-N2-C14	108.2(10)	C12-C13-C14	118.4(9)
C3-N2-C14	108.5(9)	N2-C14-C13	115.7(9)
Pd1-N3-C9	118.9(7)		

[a]Estimated standard deviations are given in parentheses.

Table 6.6. Crystallographic data of $[Pd([9]aneN_4S)](PF_6)_2$

Molecular formula:	$Pd_1S_1N_4C_{14}H_{30}P_2F_{12}$	
Molecular weight:	598.8	
Crystal colour:	yellow	
Crystal System:	orthorhombic	
Space group:	Pbca (No. 61)	
Unit cell dimensions:	a = 14.806(5)Å	α = 90°
	b = 15.083(6)Å	β = 90°
	c = 21.796(7)Å	γ = 90°
Unit cell volume:	4867.4 Å	
Z:	8	
Density (g/cm^3):	1.828	
Radiation:	Mo 0.71069	
2θ range (deg):	0° - 50°	
No. of reflections used:	4282	
Residual electron density ($e/Å^3$):	0.2	
Final R, R_w values:	0.065, 0.067	

Table 6.7. Fractional atomic coordinates for [Pd([9]aneN$_4$S)](PF$_6$)$_2$

Atom	x/a	y/b	z/c
Pd1	0.41094(3)	0.25877(3)	0.39319(2)
S1	0.59480(19)	0.19800(20)	0.38870(14)
P1	0.09350(19)	0.29150(23)	0.38880(12)
P2	0.18340(20)	0.48520(19)	0.15030(14)
F1	-0.00690(50)	0.26300(64)	0.38230(46)
F2	0.09660(53)	0.24460(68)	0.45220(39)
F3	0.06690(107)	0.37330(78)	0.42140(68)
F4	0.19530(54)	0.31010(90)	0.39320(38)
F5	0.08900(63)	0.33690(89)	0.32640(44)
F6	0.11410(82)	0.20650(86)	0.35550(57)
F7	0.23560(64)	0.51030(60)	0.09070(44)
F8	0.11830(71)	0.43720(85)	0.10560(44)
F9	0.23780(107)	0.40210(79)	0.15260(44)
F10	0.12750(85)	0.46620(68)	0.20750(39)
F11	0.25330(63)	0.52780(78)	0.19470(50)
F12	0.13820(121)	0.57280(85)	0.14750(44)
N1	0.39950(60)	0.21600(69)	0.30340(39)
N2	0.38670(60)	0.12620(53)	0.41540(44)
N3	0.42510(53)	0.39210(50)	0.37440(41)
N4	0.41330(56)	0.29870(56)	0.48380(36)
C1	0.32990(82)	0.14220(76)	0.30920(51)
C2	0.36180(103)	0.08020(78)	0.35820(66)
C3	0.46700(82)	0.08520(72)	0.44590(56)
C4	0.55430(82)	0.08710(76)	0.40640(60)
C5	0.57880(85)	0.20950(109)	0.30510(60)
C6	0.48790(82)	0.17910(98)	0.27710(59)
C7	0.35980(85)	0.28350(101)	0.26030(53)
C8	0.40560(89)	0.37270(109)	0.26130(60)
C9	0.38090(80)	0.42970(82)	0.31680(56)
C10	0.39290(80)	0.43880(73)	0.42870(60)
C11	0.43390(78)	0.39660(71)	0.48410(53)
C12	0.32680(85)	0.27750(86)	0.51480(50)
C13	0.31750(78)	0.17650(76)	0.51960(50)
C14	0.30810(76)	0.12100(79)	0.45850(59)

[a]Estimated standard deviations are given in parentheses.

(2.952Å)[199], and [Pd(py_2[9]aneN_2S)](BF_4)$_2$ (2.92Å)[200]. The crystal field stabilization energy (CFSE) for square planar geometry is considerable for the d^8 palladium(II) ion such that higher coordination numbers are rare. Equatorial Pd-S bond lengths typically are in the range 2.2 to 2.4Å, consistent with a bonding interaction, however, the axial distances clearly are longer than that expected for a "true" bonding interaction.

It is therefore of interest to consider if the axial dispostion of the sulphur donor in [Pd([9]aneN_4S)](PF_6)$_2$ is the result of a relatively weak interaction of the palladium(II) center or if it results from the structural forces present in the [9]aneN_4S bicyclic ligand. The 16° deviation of the Pd-S vector from the N_4 plane and the coplanarity of the palladium(II) atom with the N4 plane, are indicative of only a weak interaction at best.

More insight into the rigidity of the thioether bridge in the [9]aneN_4S bicyclic ligand can be gained by calculating (using the MM2 molecular mechanics method described above for the cobalt(III) complex) and comparing the ligand strain induced by coordination of the palladium(II) ion. The initial (coordinated) and final (free ligand) structures are shown in figure 6.8. Consistent with that of the cobalt(III) calculation, the most discernible movements occurred at the nitrogen donors. As with the cobalt(III) complex, the difference in orientation of the secondary amine donors was much greater than that seen for the tertiary amines. This may be an indication that the rigidity of the N_2S nonane ring serves to orient the tertiary nitrogens favourably for coordination of their lone pair electrons. The calculated energies of the coordinated and minimized free ligand structures are 70.9 kcal/mol and 39.2 kcal/mol respectively, giving an energy difference of 31.7 kcal/mol. The corresponding energy difference for the d^6 octahedral cobalt(III) complex is 32.8 kcal/mol which suggests that the energy required to position the sulphur donor perpendicular (and closer) to the N_4 plane is relatively insignificant (< 1.5 kcal/mol).

As can be seen in the X-ray structure of [Pd([9]aneN_2S)$_2$](Cl)$_2$ (figure 6.9), the sulphur atom is oriented away from the axial coordination site of the palladium. The orientation is in sharp contrast to that observed[198] in the X-ray structure of [Pd([9]aneNS_2)$_2$](BF_4)$_2$ which shows primary N_2S_2 coordination and axial orientations

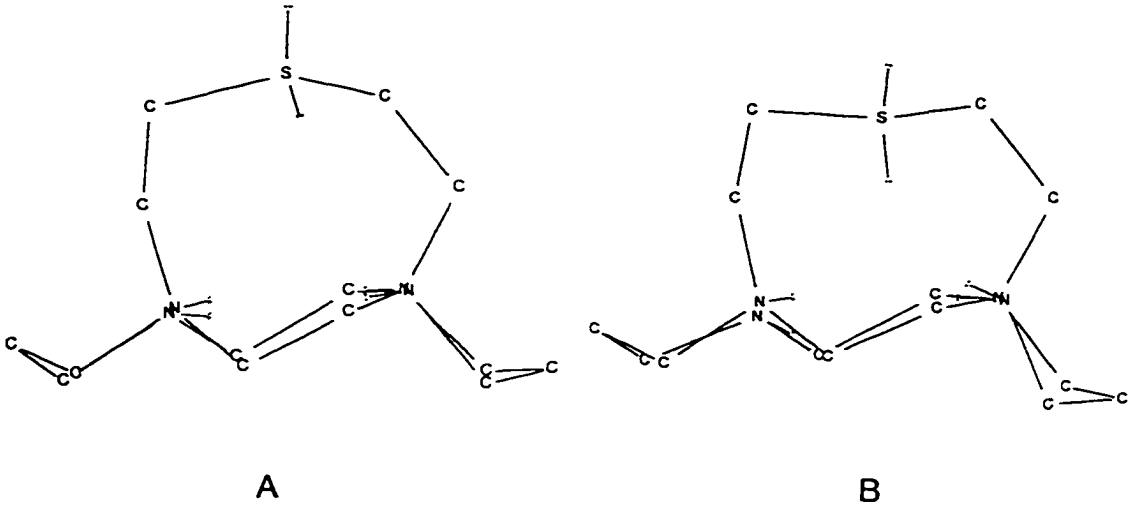

A B

Figure 6.8. A) Conformation of [9]aneN$_4$S bicyclic ligand when complexed to palladium(II) (using crystallographic coordinates). B) conformation of same ligand after molecular mechanics (MM2) energy minimization.

(3.011Å) of the two non-coordinated sulphur donors. These results indicate that the N_2S nonane ring does not necessarily orient the sulphur axially above the palladium center. It is therefore believed that, in the absence of a strong metal-sulphur interaction, the dominant forces positioning the sulphur bridge are most likely to be that of crystal-packing. The nature of the crystal environment will favour orientation of the sulphur bridge towards or away from the center of the N_4 plane.

The energy barrier to flipping between these two orientations was calculated by MM2 molecular mechanics methods to be *ca.* 5 kcal/mol for the [9]aneN$_4$S-bicycle (free ligand), which suggests that interconversion of the two orientations should be slow in solution. The presence of crystal-packing forces could further increase this barrier in the solid state. It should be noted that, regardless of which forces are responsible, the axial orientation of the sulphur allows for the possibility of an interaction with the palladium(II) center.

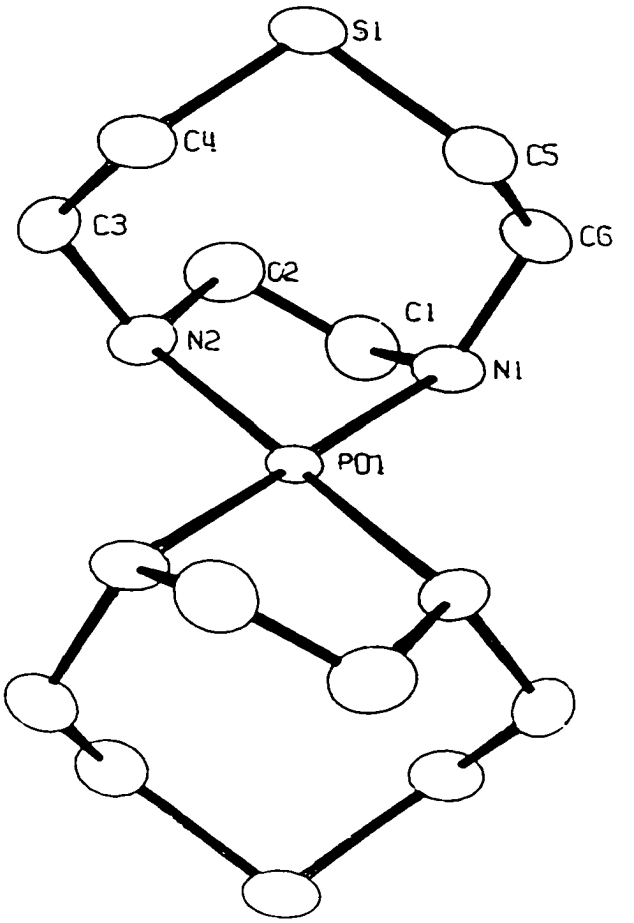

Figure 6.9. Ortep diagram of $[Pd([9]aneN_2S)_2](Cl)_2$ complex cation with atomic labelling for non-hydrogen atoms.

Table 6.8. Interatomic distances (Å)[a] and bond angles (deg)[a] for $[Pd([9]aneN_2S)_2](Cl)_2$

Atoms	Distance
N(1) -Pd(1)	2.045(9)
N(2) -Pd(1)	2.054(8)
C(4) -S(1)	1.816(10)
C(5) -S(1)	1.841(11)
C(1) -N(1)	1.487(12)
C(6) -N(1)	1.508(12)
C(2) -N(2)	1.515(14)
C(3) -N(2)	1.499(12)
C(2) -C(1)	1.485(16)
C(4) -C(3)	1.517(13)
C(6) -C(5)	1.507(13)

Atoms	Angle
N(2) -Pd(1) -N(1)	82.9(3)
C(5) -S(1) -C(4)	105.4(4)
C(1) -N(1) -Pd(1)	105.6(6)
C(6) -N(1) -Pd(1)	116.5(6)
C(6) -N(1) -C(1)	115.0(8)
C(2) -N(2) -Pd(1)	110.6(7)
C(3) -N(2) -Pd(1)	115.6(6)
C(3) -N(2) -C(2)	110.0(7)
C(2) -C(1) -N(1)	109.1(8)
C(1) -C(2) -N(2)	109.3(9)
C(4) -C(3) -N(2)	114.4(8)
C(3) -C(4) -S(1)	118.2(7)
C(6) -C(5) -S(1)	118.6(7)
C(5) -C(6) -N(1)	117.1(8)

[a]Estimated standard deviations are given in parentheses.

Table 6.9. Crystallographic data of $[Pd([9]aneN_2S)_2](Cl)_2$ monohydrate.

Molecular formula:	$Pd_1S_2N_4C_{12}H_{30}Cl_2O_1$	
Molecular weight:	487.82	
Crystal colour:	pale yellow	
Crystal System:	monoclinic	
Space group:	C 2/c (No. 15)	
Unit cell dimensions:	a = 16.515(1)Å	α = 90°
	b = 7.785(1)Å	β = 106.38(1)°
	c = 15.291(2)Å	γ = 90°
Unit cell volume:	1886.2 Å	
Z:	8 (1/2 molecules)	
Density (g/cm^3):	1.713	
Radiation:	Cu 1.542	
2θ range (deg):	0° - 50°	
No. of reflections used:	1891	
Residual electron density ($e/Å^3$):	0.1	
Final R, R_w values:	0.098, 0.094	

Table 6.10. Fractional atomic coordinates and temperature parameters for $[Pd([9]aneN_2S)_2](Cl)_2$

Atom	x/a	y/b	z/c	Ueq
Pd(1)	25000(10)	25000(10)	0(10)	182(3)
Cl(1)	35086(18)	2542(38)	27816(19)	464(10)
S(1)	11752(15)	-16308(32)	-3136(19)	356(8)
O(1)	0(1)	2777(22)	2500(1)	86(9)
N(1)	1579(5)	2614(9)	654(6)	28(3)
N(2)	1486(5)	2275(10)	-1138(6)	26(2)
C(1)	841(6)	3429(15)	-4(7)	38(3)
C(2)	666(7)	2524(12)	-893(9)	37(4)
C(3)	1449(6)	649(12)	-1673(7)	32(3)
C(4)	1757(6)	-934(12)	-1097(7)	32(3)
C(5)	1731(6)	-669(12)	792(7)	32(3)
C(6)	1389(7)	968(13)	1077(7)	36(3)

Estimated standard deviations are given in parentheses.

Coordinates x 10^4. Temperature parameters x 10^3.
Ueq = the equivalent isotropic temperature parameter
Ueq = 1/3 $\Sigma_i\Sigma_j U_{ij} a_i^* a_j^* (a_i \bullet a_j)$

6.3(c). Coordination properties of thioether donors:

Given the importance of sulphur coordination in natural metalloenzymes, it is of interest to consider the structural consequences and electronic nature of metal-sulphur bonding. For example, homoleptic polythioether macrocyclic ligands such as [9]aneS$_3$ and [18]aneS$_6$ have been shown[201] to result in low-spin complexes of cobalt(II) (magnetic moment of $[Co([18]aneS_6)]^{2+}$ = 1.8 μ_B). The presence of a low-spin electronic configuration is unexpected because the ligand field exerted by such thioethers is comparable to that of ammonia[202], and $[Co(NH_3)_6]^{2+}$ is high-spin. This effect has been rationalized by proposing that delocalization of t_{2g} electron density onto the sulphur donor (probably into the S-C σ^* orbitals[203]) reduces the electron-electron repulsions , and therefore the spin-pairing energy, of the t_{2g} electrons. Hence, the low-spin state ultimately derives from the π-acidity of thioethers.

The presence of covalent π-bonding interactions in metal-sulphur coordination is not adequately accounted for in simple Valence Shell Electron Pair Repulsion (i.e. Lewis structure) arguments nor is it in relatively sophisticated ligand field models. It is therefore necessary to perform molecular orbital (MO) calculations to predict the structural and electronic features.

Ab initio MO calculations have been reported for ruthenium(II)/(III)-thioether bonds by Jesperson and co-workers.[204] Their interest was to gain a better understanding the dependency of Ru(II)→Ru(III) metal-to-metal charge transfer (intervalence) absorption bands (seen in near IR) of mixed-valence $(NH_3)_5Ru^{II/III}$-thioether complexes upon the inner-sphere reorganization energies. The AB initio calculations were performed on simple, crystallograpically characterized, monomeric $(NH_3)_5Ru^{II/III}$-thioether complexes The results of the calculations, particularly those performed on the thioether free ligands appear to be generally applicable to other metal-thioether complexes such as those of the present study.

For example, ab initio calculations on the dimethyl sulphide ligand molecular orbitals, and on the $[(NH_3)5Ru^{III}S(CH_3)_2]^{3+}$ cation fragment were conducted.[204] The symmetries of the three highest-lying occupied molecular orbitals in $S(CH_3)_2$ and the amplitude contour maps calculated for $[(NH_3)5Ru^{III}S(CH_3)_2]^{3+}$ are depicted in figure 6.10.

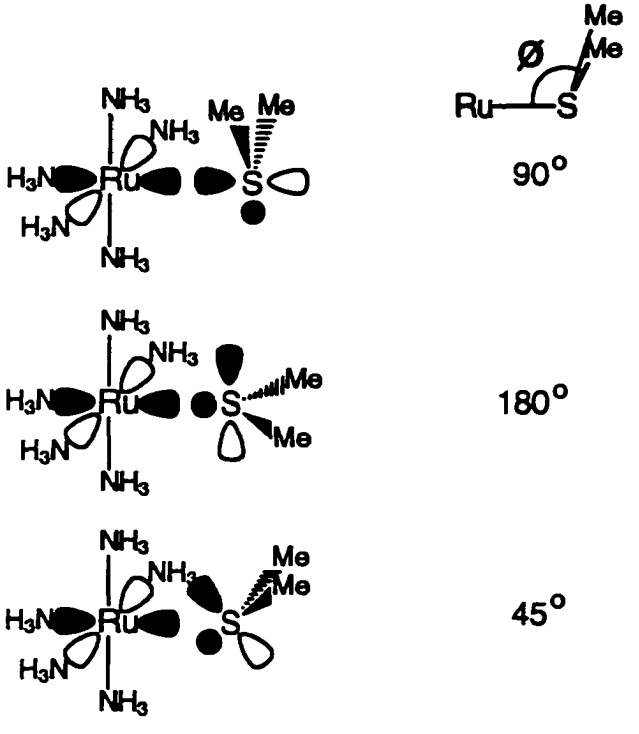

Figure 6.10. Symmetry of bonding molecular orbitals calculated for $[(NH_3)5Ru^{III}S(CH_3)_2]^{3+}$ in three different orientations with respect to Ru-S-X tilt angle (X = is a point on the CSC bisector).[204]

The calculations indicated that the most favourable electronic bonding interaction is achieved when the tilt angle between the Ru-S vector and the plane defined by the thioether ligand, $S(C)_2$, is 90°. Figure 6.10 shows the symmetry of the Ru-S bonding interactions for tilt angles of 90° (top), 180° (middle) and an intermediate angle (bottom). The authors argued that the observation of a 123° tilt angle in the X-ray structure[204] of $[(NH_3)5Ru^{III}S(CH_3)_2]^{3+}$, instead of the optimum 90° angle predicted for the electronic interaction, was merely a result of the inevitable steric hindrance between the sulphur substituents and the *cis* amine ligands.

It is therefore of interest to compare the C-S-M bond angles in the crystal structures of the metal-[9]aneN_4S bicycle complexes in order to gain insight into the nature of the metal-sulphur bonding. The cyclic structure in which the sulphur substituent carbons are linked to the nitrogen donors avoids steric hindrance perturbations such that the true bond angle preference of the thioether donor may be realized. Furthermore, the molecular mechanics calculations described above indicate that the strain energies associated with positioning and orienting the sulphur donor are negligible such that the geometrical preferences of the metal-sulphur interaction should be accomodated.

The C4-S-M and C5-S-M bond angles for each complex are listed in table 6.11. As predicted by the ab initio calculations, the bond angles are all significantly less than the 106° to 114° C-N-M bond angles observed for the σ-donating amines. The angles vary only within a 88° to 101° range which is close to the predicted tilt angle of 90° and therefore lends support to the ab initio calculations.

Within this range, there is also a consistent trend of increasing angle as the coordination geometry approaches true octahedral bonding. Thus, the C-S-M bond angles (88° and 92.6°) of the copper(II) complex, whose geometry deviates the most from true octahedral geometry, are closest to the predicted 90°. The bond angles (92.3° and 96.3°) in the nickel(II) complex, in which the coordination geometry is closer to octahedral than the copper(II) complex, are slightly increased and those (100.6° and 98.5°) of the strictly octahedral cobalt(III) complex are significantly increased, but still much less than that of

Table 6.11. C-S-M bond angles observed in X-ray structures of $[M([9]aneN_4S)]^{2+/3+}$ complexes.

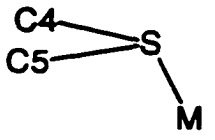

COMPLEX CATION	C5-S-M (deg)	C4-S-M (deg)
$[Cu([9]aneN_4S)]^{2+}$ (ref 90)	88	92.6
$[Ni([9]aneN_4S)]^{2+}$ (ref 90)	92.3	96.3
$[Co([9]aneN_4S)(NCCH_3)]^{3+}$	100.6	98.5
$[Pd([9]aneN_4S)]^{2+}$	83.2	88.5

the amine donors. The C-S-M bond angles in the palladium(II) complex, in which the lack of a strong M-S bonding interaction resulted in the largest deviation (16°) of the M-S vector from the perpendicular to the N_4 plane, are significantly less than those of the other three complexes. This trend can be explained by the expectation that the torsional strain of the methylene carbons in the sulphur bridge should perturb the C-S-M bonding angles greatest as the metal positions the sulphur closer to octahedral geometry (i.e. M-S vector colinear with the perpendicular to N_4 plane).

6.4. Solution Studies of $[Co([9]aneN_4S)(OH_2)](ClO_4)_2$:

6.4(a). Electronic Spectroscopy:

The aqueous UV/visible sprectrum of $[Co([9]aneN_4S)(OH_2)](ClO_4)_3$ is presented in figure 6.11. The chloride and thiocyanate axially substituted derivatives have also been prepared. There are two distinct d-d absorptions present in the spectra of each complex, one in the 500 - 570 nm region and a high energy band in the 340 - 380 nm region.

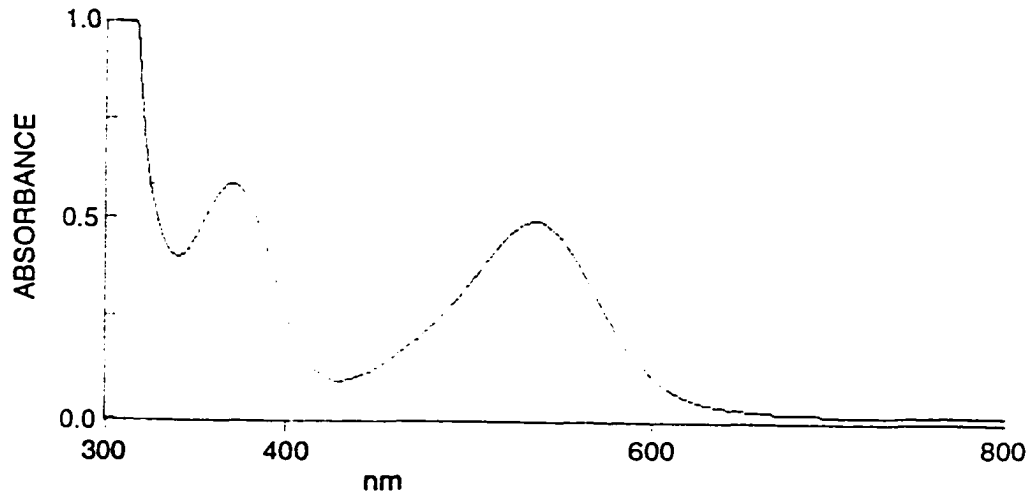

Figure 6.11. UV/visible spectrum of $[Co([9]aneN_4S)(OH_2)](ClO_4)_3$ in aqueous solution (pH 2.5).

The ligand field splitting energy diagram for a low-spin d^6 ion in O_h and D_{4h} symmetry is shown in figure 6.12. Two spin-allowed d-d transitions are expected for true octahedral complexes ($^1T_{1g} \leftarrow {}^1A_{1g}$ and $^1T_{2g} \leftarrow {}^1A_{1g}$); however, when the symmetry is

lowered to D_{4h}, each of the octahedral states, $^1T_{1g}$ and $^1T_{2g}$, splits into two states.[176] Hence, more than two bands are expected. In practise, usually three bands are observed: $^1E_g^a \leftarrow {}^1A_{1g}$, $^1A_{2g} \leftarrow {}^1A_{1g}$ and $(^1E_g^b + {}^1B_{2g}) \leftarrow {}^1A_{1g}$. In the complexes of the present study, the latter transition is of highest energy and is obscured by the more intense charge-transfer absorptions present in the UV region.

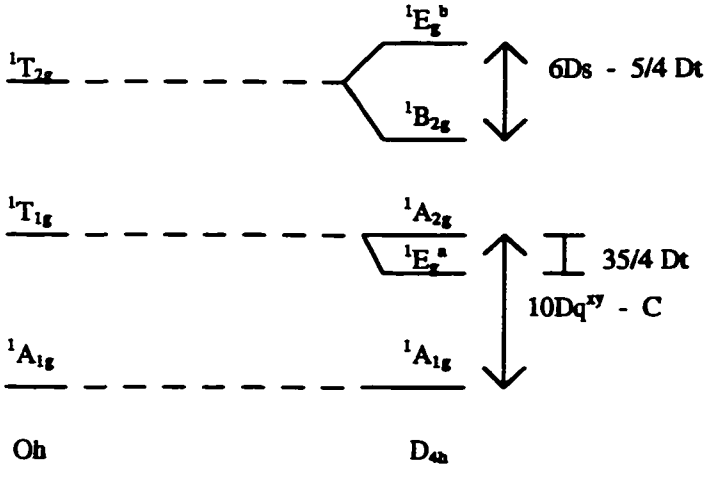

$$10Dq^{xy} = E(^1A_{2g} \leftarrow {}^1A_{1g}) + C$$

$$D_t = -(4/35)[E(^1E_g^a \leftarrow {}^1A_{1g}) - E(^1A_{2g} \leftarrow {}^1A_{1g})]$$

$$Dq^z = Dq^{xy} - (7/4)D_t$$

Figure 6.12. Energy level diagrams for a low-spin d^6 Ion in O_h and D_{4h} symmetry (above) and ligand field equations (bottom) used to calculate Dq^{xy} and Dq^z parameters from electronic spectrum of $[Co([9]aneN_4S)(OH_2)](ClO_4)_3$.

The ligand field strength parameters Dq^{xy} and Dq^z can be calculated[182] for D_{4h} site symmetry according to the equations shown in figure 6.12. The value of C is roughly constant and usually assumed[182] to be 3800 cm^{-1}. Dq^{xy} and Dq^z are the ligand field

parameters for the equatorial (xy plane) and axial (z axis) donors respectively. In order to apply the above equations, D_{4h} symmetry must be assumed. This assumption obviously does not hold for the $[Co([9]aneN_4S)(X^{n-})]^{(3-n)+}$ complexes since the nature of the two axial donors differs (therefore C_{4v} site symmetry is present). However, other cobalt(III) macrocyclic complexes which lack true D_{4h} symmetry have been usefully treated by this model.[205] The coordination geometry present in the X-ray structure of $[Co([9]aneN_4S)(OH_2)](ClO_4)_3$ was not distorted significantly from the 90° *cis* N-M-N bond angles expected for true octahedral coordination. For these reasons, together with the observation that the d-d absorption bands displayed in the UV/visible spectra are well resolved, the results of such a calculation are considered meaningful. The calculated values are presented in table 6.12 along with those of the $[Co([14\text{-}16]aneN_4)(Cl)_2]^{1+}$ series reported by Busch et al.[191]

Table 6.12. Absorption maxima and calculated Dq^{xy} (in cm^{-1}) and Dq^{z} (in cm^{-1}) ligand field (D_{4h}) strength values for $[Co([9]aneN_4S)(X^{n-})]^{(3-n)+}$ complexes at low pH (1 to 3).

COMPLEX[a]	λ_{max} /nm (ε /M^{-1} cm^{-1})	Dq^{xy}	Dq^{z}
$[Co([9]aneN_4S)(OH_2)]^{3+}$	532 (184), 365 (216)	3127	1392
$[Co([9]aneN_4S)(Cl)]^{2+}$	564 (70.5), 377 (101)	3025	1281
$[Co([9]aneN_4S)(NCS)]^{3+}$	523 (305), 351 (446)	3237	1347
$[Co([14]aneN_4)(Cl)_2]^{1+}$	617 (35), 458 (24)	2562	1437
$[Co([15]aneN_4)(Cl)_2]^{1+}$	640 (27), 490 (38)	2421	1465
$[Co([16]aneN_4)(Cl)_2]^{1+}$	662 (41), 510 (35)	2341	1441

[a]Data for the $[Co([14\text{-}16]aneN_4)(Cl)_2]^{1+}$ complexes taken from reference 191.

The $[Co([9]aneN_4S)(X^{n-})]^{(3-n)+}$ complexes each have significantly higher equatorial ligand field values than that of the $[Co([14\text{-}16]aneN_4)(Cl)_2]^{1+}$ complexes, consistent with the expectation that axial coordination of two anionic ligands decreases the ligand field exerted by the N_4 plane. Busch reported[191] that, for the $[Co([14]aneN_4)(NCS)_2]^{1+}$ complex, all but one broad band was masked by charge-transfer absorptions. However, it is interesting to note that the absorption maximum of that band was 521 nm, which is very similar to that (523 nm) of the $[Co([9]aneN_4S)(NCS)]^{2+}$ complex. This result suggests that the thioether donor in the $[9]aneN_4S$ bicyclic ligand is comparable to coordination of thiocyanate.

The axial ligand field values for the $[Co([9]aneN_4S)(X^{n-})]^{(3-n)+}$ complexes are lower than that of the $[Co([14\text{-}16]aneN_4)(Cl)_2]^{1+}$ complexes, which is again consistent with the expectation that the neutral thioether donor in the $[9]aneN_4S$ bicyclic ligand is weaker than the chloride donors. The Dq^z value of the thiocyanate complex is greater than that of the chloride complex, consistent with that reported for the $[Co([14\text{-}16]aneN_4)(Cl)_2]^{1+}$ and $[Co([14\text{-}16]aneN_4)(NCS)_2]^{1+}$ complexes. It has been noted[191] that these ligand field parameters are not constant for the same donor in different complexes and that there exists a marked dependence of the Dq^{xy} and Dq^z values on each other in the various complexes studied. For this reason, further interpretation of these values would not be meaningful.

6.4(b). Acid-Base Properties of $[Co([9]aneN_4S)(X^{n-})]^{(3-n)+}$ Complexes:

The d-d absorption maxima of $[Co([9]aneN_4S)(OH_2)](ClO_4)_3$ were observed to be pH dependent, implying the presence of an acid/base process. The pH dependency was observed for the chloride and thiocyanate axially substituted complexes as well. Spectrophotometric titrations of the $[Co([9]aneN_4S)(OH_2)](ClO_4)_3$ and $[Co([9]aneN_4S)(Cl)](ClO_4)_2$ complexes are shown in figures 6.13(a) and 6.13(b) respectively.

The changes in absorbance spectra were reversible with relativley well-resolved isosbestic points, which implies that there is an acid-base functionality present in the

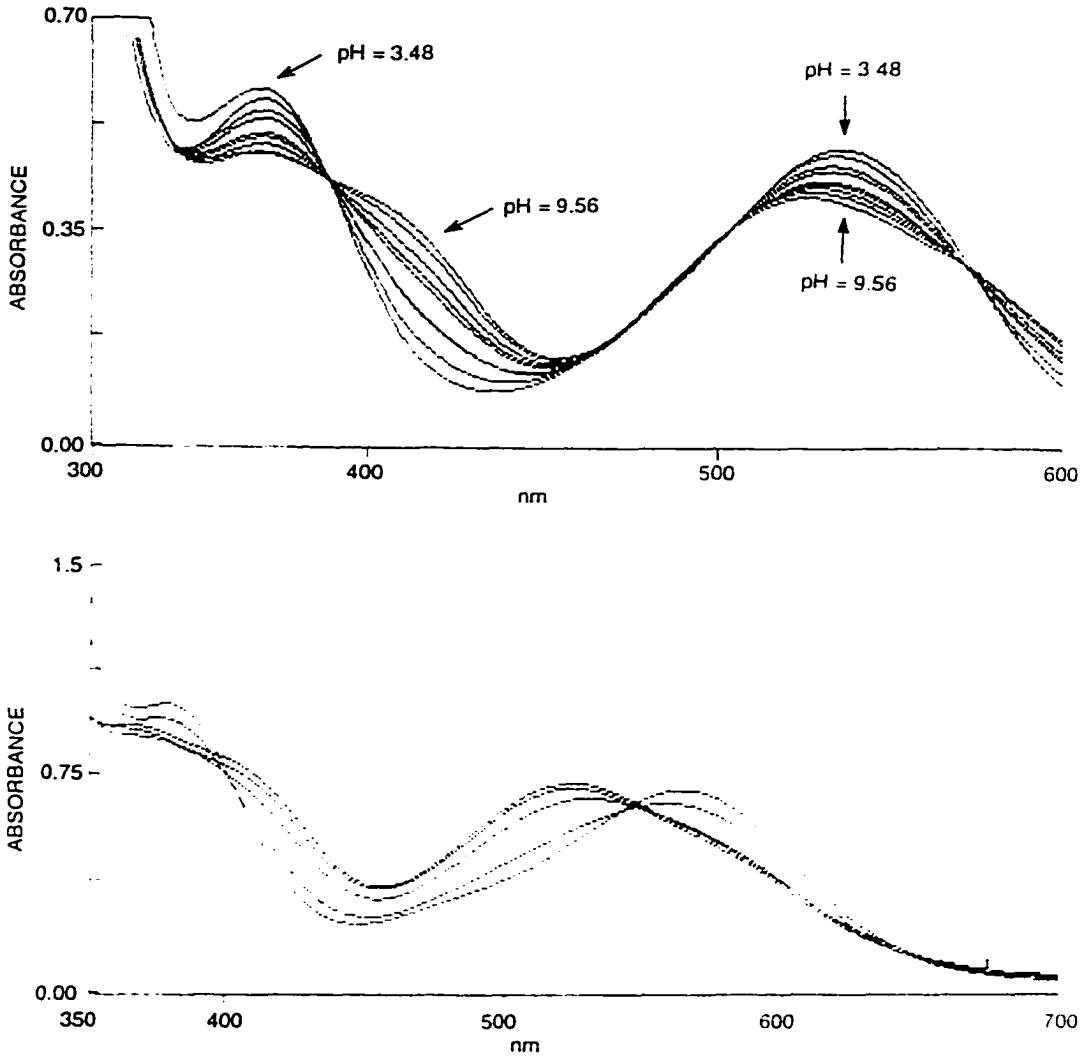

Figure 6.13. Representative traces from spectrophotometric titrations ($HClO_4$ and NaOH as titrants) of aqueous solutions of $[Co([9]aneN_4S)(OH_2)](ClO_4)_3$ (A) and $[Co([9]aneN_4S)(Cl)](Cl)_2$ (B).

complex. The pKa values obtained from the titrations were *ca.* 6.0 and 6.3 for the $[Co([9]aneN_4S)(OH_2)](ClO_4)_3$ and $[Co([9]aneN_4S)(Cl)](Cl)_2$ respectively (figure 6.14). The pKa values were difficult to quantify due to the presence of an additional acid-base process at low pH (< 2.5) which is believed[100] to correspond to protonation of one of the amines. The nature of the higher pH acid-base process deserves discussion.

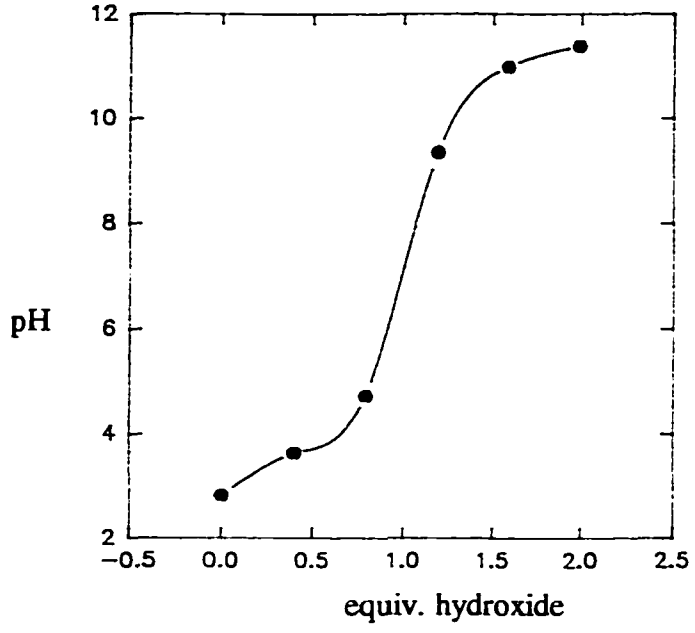

Figure 6.14. Titration of $[Co([9]aneN_4S)(OH_2)](ClO_4)_3$ in aqueous solution.

It is well documented[46] that coordination of water generally results in a marked increase in acidity. The most relevant example to the present cobalt(III) complex is that of $[Co(NH_3)_5(OH_2)]^{3+}$, which has a pKa of 6.1 associated with the presence of the aquo ligand[206]. This is a marked increase relative to free H_2O which has a pKa of 15.8. However, for the $[Co([9]aneN_4S)(X^{n-})]^{(3-n)+}$ complexes, the occurrence of the acid-base process in the chloro- and thiocycanato-substituted complexes indicates that it is not necessarily dissociation of axially bound water.

An interesting and relevant example involves the occurrence of an acid-base process with a similar pKa in the $[Ni^{III}([14]aneN_4)(solv)_2]^{3+}$ ([14]aneN$_4$ = cyclam) ion[207]. The nickel(III) ion is stable in acidic solution when coordinated by cyclam, and has a green colour resulting from the tail in the visible region of a strong charge-transfer band (ligand to metal) centered at 310 nm. The solution stability substantially decreases with increasing pH. In particular, if the solution is made definitively alkaline (e.g. 1M NaOH), the strong green colour disappears instantaneously and a much less intense yellow-orange colour forms, due to decomposition to the nickel(II) species.

Barefield and co-workers[208] noted that, if the solution is made only slightly basic, a violet transient colour forms, which lasts for less than 1 sec. before formation of the yellow-orange nickel(II) species. The violet transient species formed in water, pyridine and triethylamine solvents which implied that it was not an effect of axially coordinated solvent. On the basis of flow experiments performed in the cavity of an ESR spectrometer, Barefield[208] ascribed the transient violet species to a nickel(II)-ligand radical complex whose formation was promoted by the presence of base.

Subsequent studies by Ferraudi et al[209] on radiolytically generated nickel(III) macrocyclic complexes showed that the transient species was an authentic nickel(III) species. Meyerstein[210] carried out pulse radiolysis investigations on solutions of varying pH of the same complexes and characterized a "clean and reversible acid dissociation process" with a pKa value of 3.45. The authors assumed that the acid dissociation corresponded to deprotonation of one of the axially bound water molecules of the nickel(III) tetraazamacrocyclic complex.

Recently, Fabrizzi and co-workers[211] obtained the UV/visible spectrum of the transient violet species using a diode array fast data acquisition spectrophotometer equipped with a rapid mixing device. On the basis of the results of this investigation, and comparison to the unambiguous characterization of a metal-promoted deprotonation of the secondary amine groups of the fully saturated [9]aneN$_3$ (1,4,7-triazacyclononane) macrocycle in the $[Fe^{III}([9]aneN_3)_2]^{3+}$ complex (pKa = 11.4; deprotonated iron(III)

complex is kinetically stable) reported by Wieghardt[211], Fabrizzi concluded that the transient violet species corresponds to deprotonation of the coordinated secondary amine donors.

The deprotonation of coordinated secondary amines appears to be a relatively general feature of M(III)-polyaza macrocycle complexes. This is in sharp contrast to the analogous M(II)-polyaza macrocycle complexes involving the same ligands. These observations imply that the presence of the higher charge in the M(III) complexes promotes such deprotonation. It is therefore believed that the acid-base process occurring in the $[Co([9]aneN_4S)(X^{n-})]^{(3-n)+}$ complexes of the present study is very likely to be deprotonation of a secondary amine as well.

Further support of this proposal lies in the pattern of the UV/visible absorption spectra of the $[Co([9]aneN_4S)(X^{n-})]^{(3-n)+}$ complexes in basic solution. Referring to figures 6.13(a) and (b), it can be seen that the shifts in absorption maxima of the higher energy $^1A_{2g} \leftarrow {}^1A_{1g}$ d-d transition upon addition of base are not particularly significant. However, the band is clearly split into two absorption features upon addition of base which is indicative of a significant symmetry distortion. Since this d-d transition is affected most by the equatorial (xy) donors, it is reasonable to attribute the symmetry distortion to changes in the equatorial donor(s). This is consistent with the presence of a deprotonated amine donor because such amido donors are believed[212,40-42] to have significant π-bonding interactions with the metal center. The presence of a π-bonding interaction splits the ground state electronic configuration[176], and results in new absorptions of similar energy.

It is for this reason that the calculations of the ligand field parameters were performed on the acidic solution spectral data (pH 2-3). The UV/visible spectra of $[Co(en)_3]^{3+}$ in neutral and basic solution were reported by Goodall and Hardy.[213] These workers reported the pKa of deprotonation of the secondary amines to be 15.2, which is consistent with other pKa values reported for chelating amine complexes.[214] It is the pKa of the present $[Co([9]aneN_4S)(X^{n-})]^{(3-n)+}$ complexes, and of the corresponding N_4O[100] and N_5[133] complexes, that is unusual. The similarity of the $[Co([9]aneN_4S)(OH_2)](ClO_4)_3$

spectra (above and below the pKa of *ca* 3.8) to the $[Co(en)_3]^{3+}$ spectra (above and below the pKa of 15.2) suggests that a similar process is occurring. It is somewhat surprising that the acid-base properties of other cobalt(III)-polyaza macrocyclic complexes have not been reported. Comparison of the pKa values (of $[Co([14]aneN_4)(OH_2)](ClO_4)_3$ for example) would give considerable insight into the present observations and those of the nickel(III) and iron(III) complexes with $[14]aneN_4$.

6.4(c). Kinetic Aspects of $[Co([9]aneN_4S)(OH_2)](ClO_4)_3$ Substitution:

Although the amount of $[Co([9]aneN_4S)(OH_2)](ClO_4)_3$ prepared (< 40 mg) was insufficent for a thorough kinetic study, a limited study of the kinetic behaviour was conducted. The anation reactions of $[Co([9]aneN_4S)(OH_2)](ClO_4)_3$ with chloride and thiocyanate were investigated in 0.1M, 0.05M, 0.01M and pH 5.5 aqueous solutions of 1M ionic strength, adjusted by addition of the appropriate amounts of standardized $HClO_4$ and $LiClO_4$ solutions in each case. Each kinetic run was performed in duplicate and the k_{obs} values were averaged.

Figure 6.15 shows the spectral changes upon anation with thiocyanate ion. The anations were performed under pseudo-first order conditions (> 10 fold excess of chloride and thiocyanate). For each acid strength, the substitution rates were determined in the presence of 5, 10, 20 and 50 x 10^{-3} M concentrations of chloride and thiocycanate (concentration of $[Co([9]aneN_4S)(OH_2)](ClO_4)_3 = 2.18 \times 10^{-4}$M).

The most salient feature of the anation reactions was the pH dependency. The dependence of k_{obs} (SCN^- anation) on pH is shown in figures 6.16(a) and (b). The chloride substitutions showed similar pH dependence. There appear to be two distinct kinetic mechanisms operating above and below pH ≈ 1.5, which is consistent with the observation of the low pH acid-base process discussed above. At low pH (< 2), k_{obs} shows significant

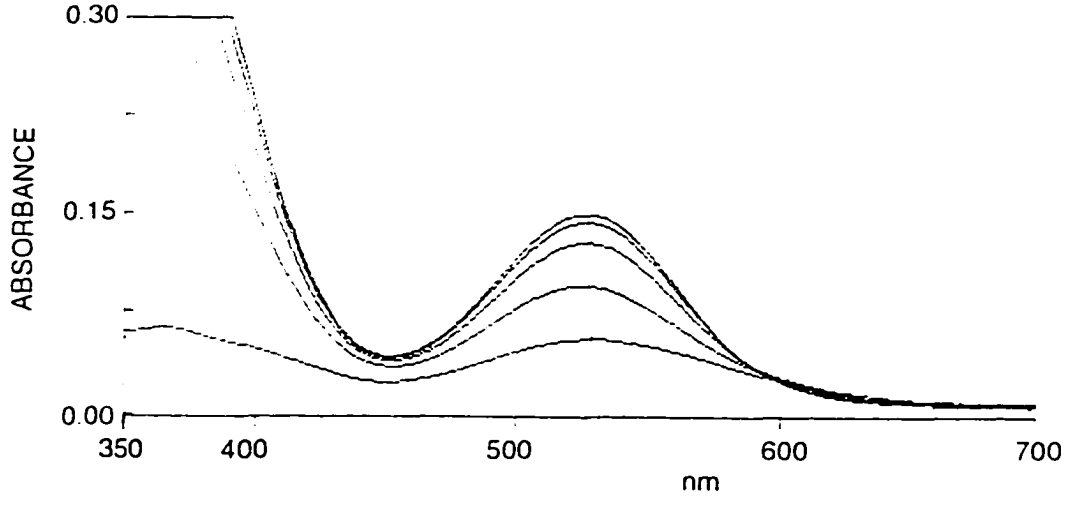

Figure 6.15. UV/visible spectral changes upon anation of $[Co([9]aneN_4S)(OH_2)](ClO_4)_3$ with thiocyanate ion.

dependence on the concentration of chloride and thiocyanate, implying the presence of an I_A mechanism. At higher pH (> 2), k_{obs} is clearly independent of chloride and thiocyanate concentration, implying the presence of a dissociative mechanism. As the pH was raised from pH 1.3 to pH 2, there was a four-fold increase in k_{obs}. At pH 5.5 there was a further ten-fold increase in k_{obs}.

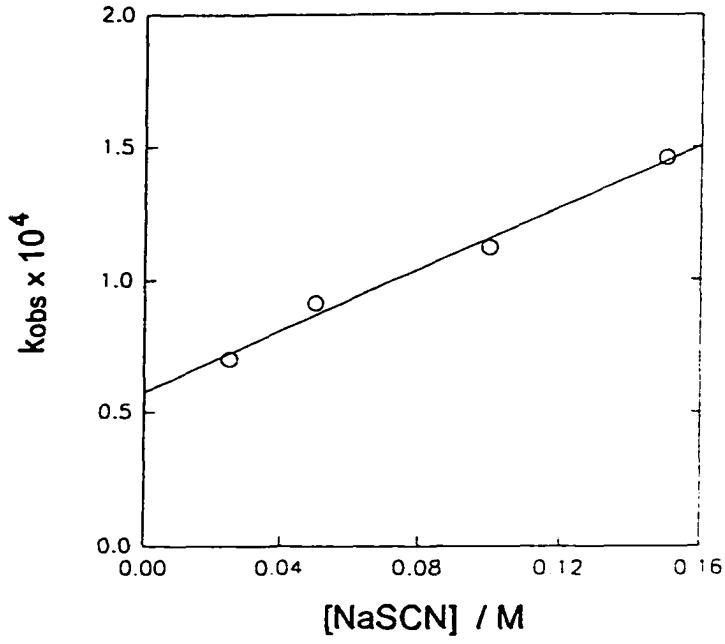

A) Plot of k_{obs} vs. [NaSCN] at $[H^+]$ = 0.05 M and ionic strength = 1.0 M

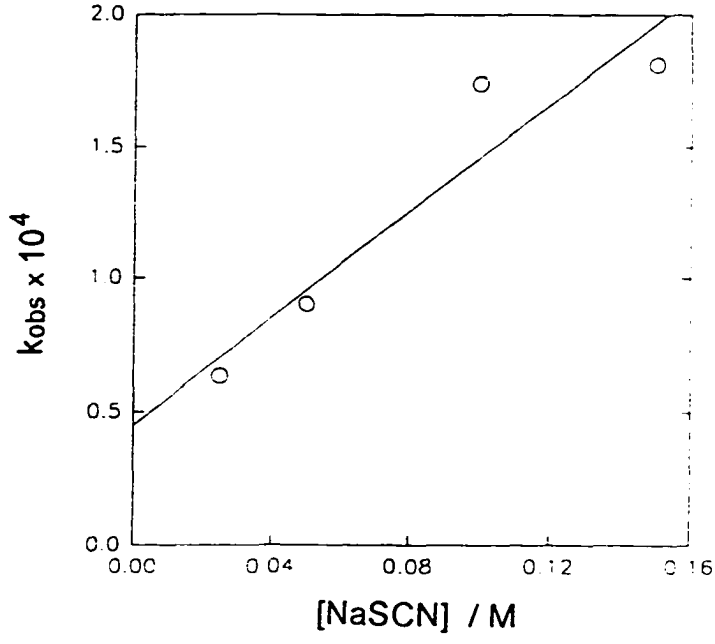

B) Plot of k_{obs} vs. [NaSCN] at $[H^+]$ = 0.10 M and ionic strength = 1.0 M

Figure 6.16(a). Dependence of k_{obs} on $[SCN^-]$ at acidic pH;
T = 25°C, λ = 525 nm, salt = $LiClO_4$.

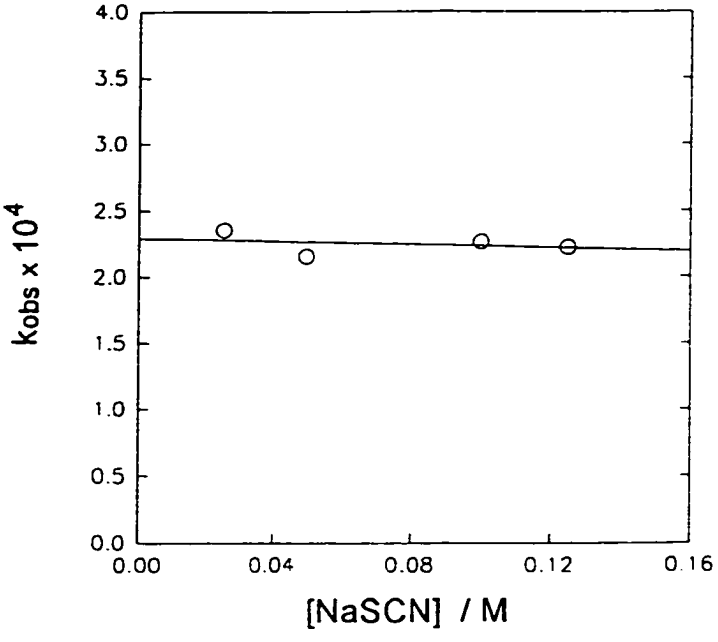

Plot of k_{obs} vs. [NaSCN] at $[H^+]$ = 0.01 M and ionic strength = 1.0 M

Figure 6.16(b). Dependence of k_{obs} on $[SCN^-]$ as pH approaches.neutral; T = 25°C, λ = 525 nm, salt = $LiClO_4$.

Although the results of this kinetic study are too limited in scope to propose intimate rate laws and mechanisms, the pH dependence is consistent with the results of a more comprehensive kinetic study performed on the $[Co([9]aneN_5)(OH_2)](ClO_4)_3$ complex by Cameron et al[215,133] in the present laboratory. Figure 6.17 shows the kinetic titration plot for the $[Co([9]aneN_5)(OH_2)](ClO_4)_3$ anation with thiocyanate ion obtained in that study.

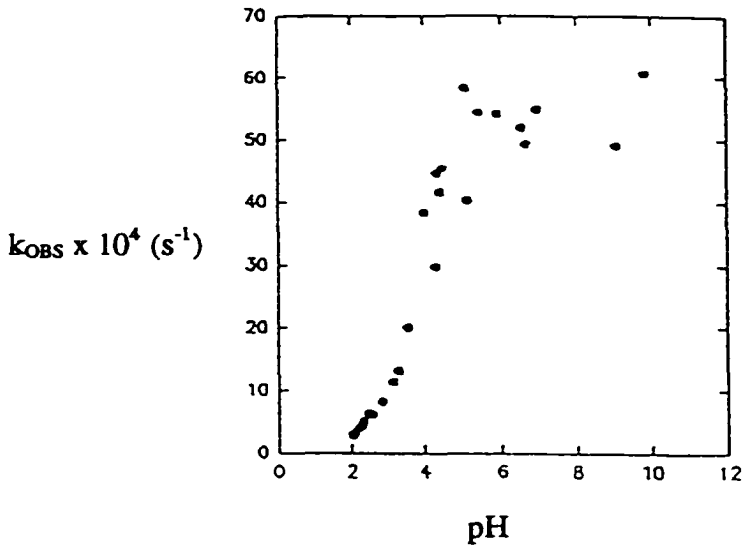

Figure 6.17. Kinetic titration plot for $[Co([9]aneN_5)(OH_2)](ClO_4)_3$ anation with thiocyanate (T = 50°C, λ = 320 nm). Reproduced with permission of the author.[133a]

There is a similar marked increase in k_{obs} as the pH is raised from 2 to 6 (figure 6.17). The authors attribute the pH dependence to an internal conjugate base mechanism involving an amino-hydroxo/aminato-aqua tautomerism. Such a mechanism has been proposed[215] for azide-anation of *mer*-$Co(dien)(dapo)(OH_2)^{3+}$ where dien = N-(2-aminoethyl)ethane-1,2-diamine and dapo = 1,3-diaminopropan-2-ol. The results of that study are summarized in figure 6.18.

Finally, it should be noted that the rates of thiocyanate anation of the $[Co([9]aneN_4S)(OH_2)](ClO_4)_3$ and $[Co([9]aneN_5)(OH_2)](ClO_4)_3$ complexes are approximately one order of magnitude greater than that of the monodentate $[Co(NH_3)_5(OH_2)](ClO_4)_3$[216] and bidentate *trans*$[Co(en)_2(Cl)_2](ClO_4)$[192] complexes. It was anticipated that the inclusion of an axial donor in the substitution inert $[9]aneN_4S$ bicyclic ligand (and $[9]aneN_5$) might lead to a greater substitution rate than was observed.

The aquation rates of the $[Co([13\text{-}16]aneN_4)(Cl)_2^+$ series reported by Busch[70] (see section 6.1) displayed a minimum at $[Co([14]aneN_4)(Cl)_2^+$ and increased by five orders of magnitude as the ring size increased to 16-members. The aquation rates were correlated

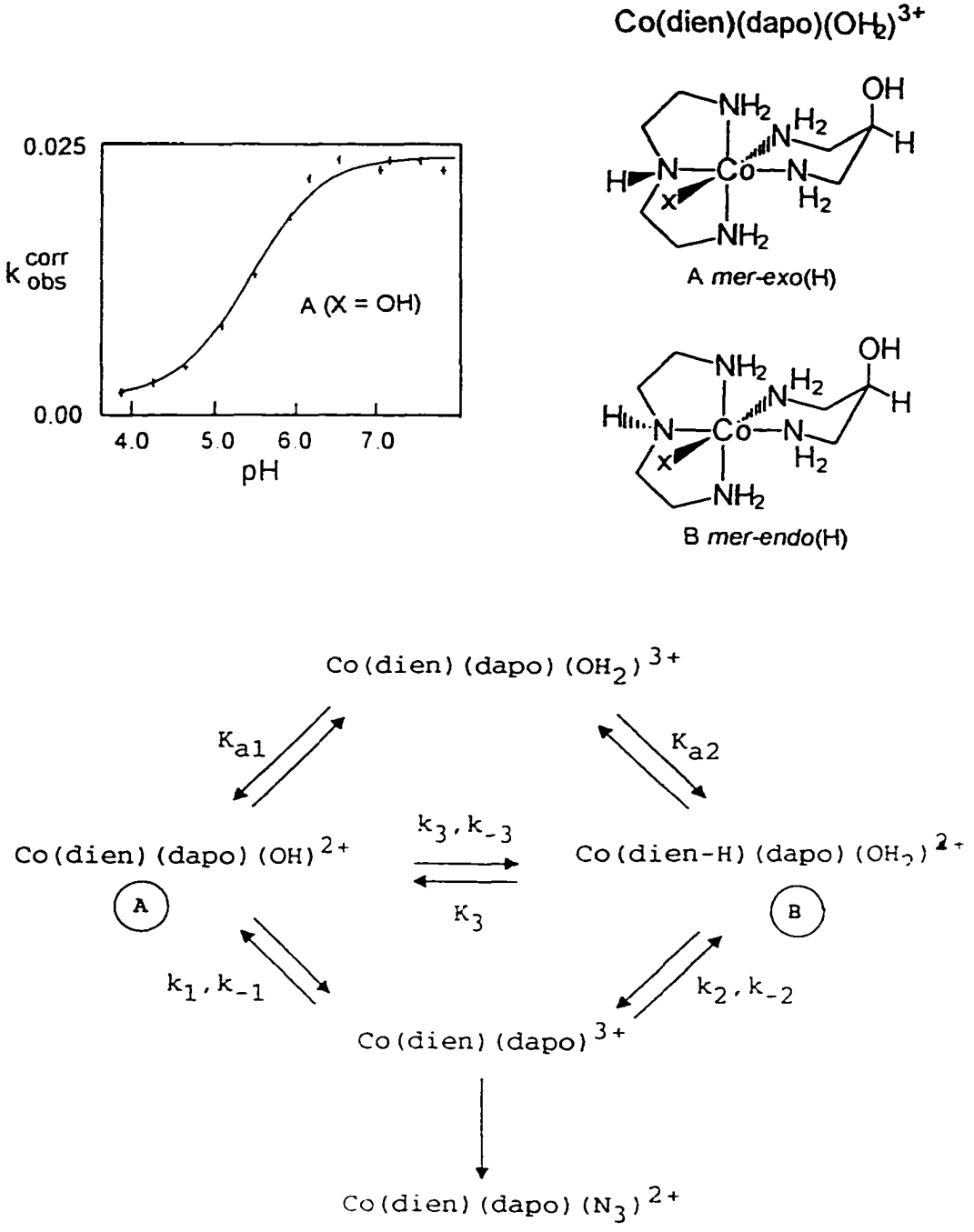

Figure 6.18. Kinetic titration plot and proposed mechanism for azide anation of $Co(dien)(dapo)(OH_2)^{3+}$. Reproduced with permission of author.[133a]

with the calculated ligand strain energies for coordination of cobalt(III). Busch suggested that these results were a reflection of relief of ligand strain in an intermediate of reduced coordination number (see figure 6.1). The nature of the intermediate in cobalt(III) substitutions is still speculative at best[41,216].

It is therefore interesting to note that the presence of a trigonal bipyramidal five-coordinate intermediate, as opposed to square pyramidal, could explain the results of the macrocyclic complexes. This is because square planar N_4 coordination is most favoured by [14]aneN_4 (cyclam) (due to the ideal matching of Co-N bond lengths to the "natural" hole size of the ligand) and is the least able to accomodate trigonal bipyramidal coordination. As the ring size is increased, the ability of the tetraaza macrocycle to fold and accomodate trigonal bipyrimidal geometries increases, leading to enhanced aquation rates.

The [9]aneN_4S bicyclic ligand (and [9]aneN_5) ligand of the present study would be even less able to accomodate trigonal bipyramidal coordination than the parent N_4 cyclam ring due to the bridging of adjacent nitrogens.

6.5. Solution Studies of [Pd([9]aneN_4S)]$(PF_6)_2$:

[Pd([9]aneN_4S)]$(PF_6)_2$ is a pale yellow crystalline material that dissolves readily to give a yellow aqueous and alcohol solutions. The UV/visible spectrum (see figure 6.19) consists of a high energy absorption with λ_{max} = 292 nm (ε = 312 M^{-1} cm^{-1}) and another absorption at higher frequency (λ_{max} = 234 nm, ε = 362 M^{-1} cm^{-1}). Oxidation with a stoichiometric deficiency of nitrosonium ion ($NO^+BF_4^-$) in neutral media results in a more intense green colour but no discernable peaks in the UV/visible spectrum. The oxidized species decomposed back to the corresponding palladium(II) complex within minutes at room temperature. Reduction of [Pd([9]aneN_4S)]$(PF_6)_2$ with sodium borohydride yielded a dark insoluble powder which oxidized back to palladium(II) upon addition of NO^+.

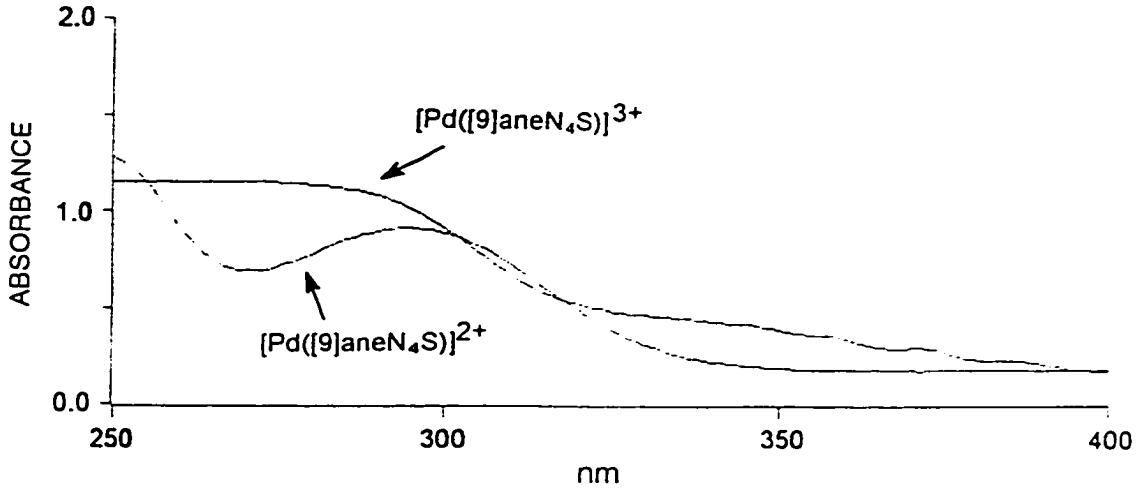

Figure 6.19. UV/visible spectra of $[Pd([9]aneN_4S)](PF_6)_2$ complex and $[Pd([9]aneN_4S)]^{3+}$ complex cation.

An electrochemical investigation of $[Pd([9]aneN_4S)](PF_6)_2$ in acetonitrile (0.1M (*tert*-butyl)$_4$N(ClO_4)) gave an electrochemically quasi-reversible (chemically reversible) (E_{ox} - E_r = 83 mV) oxidation wave at 0.815 V vs. ferrocene$^{0/+}$ and a barely distinguishable irreversible feature at *ca.* 0.15 V (figure 6.20). These results are consistent with the values reported[198] for $[Pd([9]aneNS_2)](BF_4)_2$. In that study, the oxidations occurred at $E_{1/2}$ = 0.43 V (E_{ox} - E_r = 140 mV) and 0.84 V (E_{ox} - E_r = 130 mV) vs. ferrocene$^{0/+}$ (0.1M NBu_4PF_6 in acetonitrile) for the $Pd^{2+/3+}$ and $Pd^{3+/4+}$ couples respectively. The assignments of the oxidations were made unambiguously by electronic spectroelectrochemistry. As can be seen in figure 6.20, two chemically irreversible reduction waves occurred at -0.16 V and -1.3 V corresponding to the $Pd^{2+/1+}$ and $Pd^{1+/0}$ couples respectively.

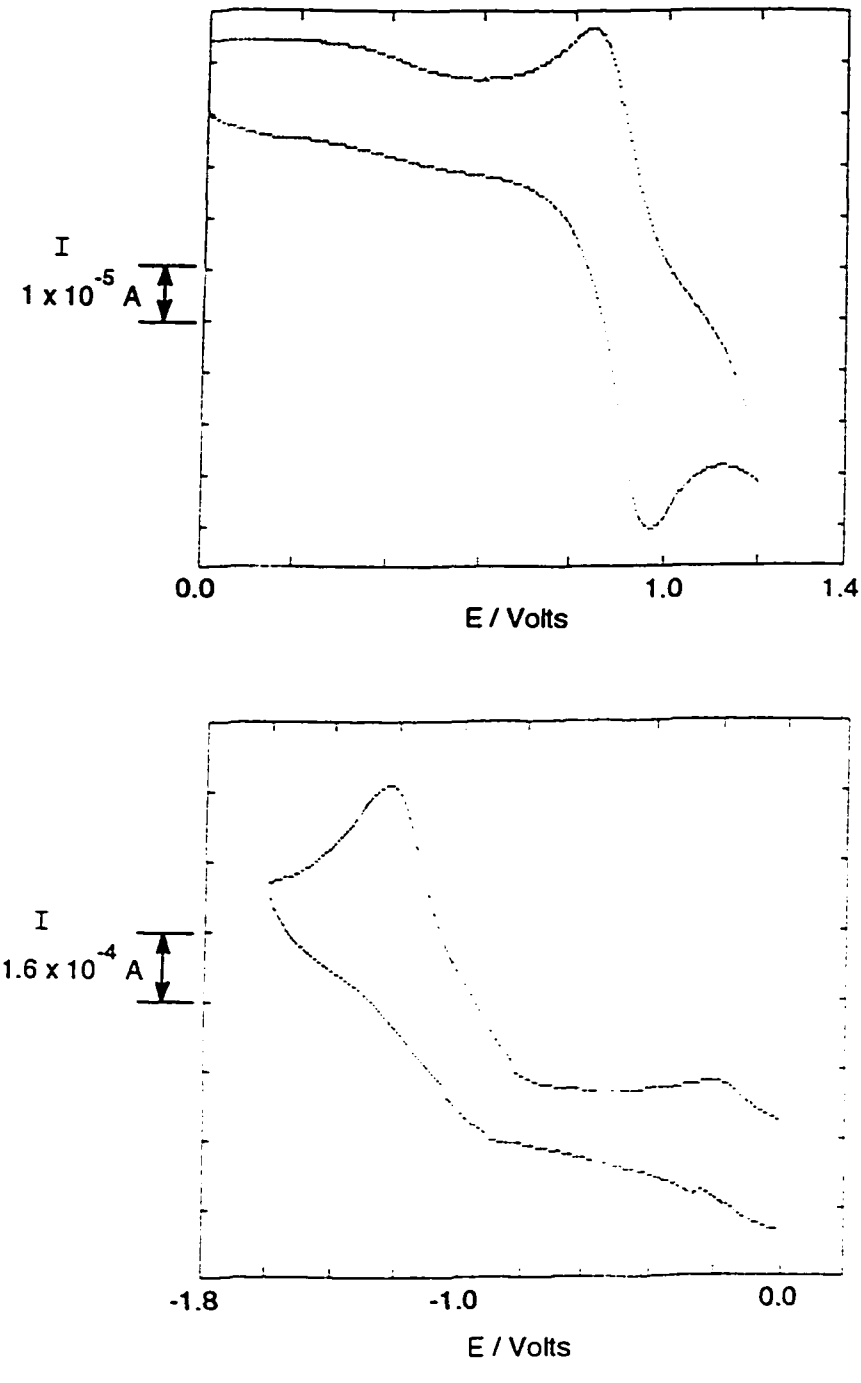

Figure 6.20. Cyclic voltammetric traces for oxidation (top) and reduction (bottom) of $[Pd([9]aneN_4S)](PF_6)_2$ complex in acetonitrile (0.1M $(t\text{-butyl})_4NClO_4$).

NMR studies:

As mentioned in section 6.3, the X-ray structure of $[Pd([9]aneN_4S)](PF_6)_2$ shows that the axially disposed sulphur donor lies 2.87Å away from the palladium(II) center, suggesting the presence of a long range interaction. A similar interaction was proposed[217] for the axial sulphur donors (2.954Å and 3.000Å) in $[Pd([18]aneN_2S_4)]^{2+}$ ([18]$aneN_2S_4$ = 1,4,10,13-tetrathia-7,16-diazacyclooctadecane). These proposed interactions in the solid state might simply be due to crystal packing forces and the lessened vibrational motions present in the solid. It is therefore of considerable interest to determine whether these interactions are present in solution.

It is also of interest to consider if the disposition of the sulphur donor in solution is controlled by the conformational rigidity of the coordinated macrocycle or by a metal-donor electronic interaction. These low-spin d^8 palladium(II) complexes are diamagnetic at room temperature such that the relative rigidity of coordinated ligand can be probed by NMR studies. For example, such studies can determine whether or not the sulphur bridge of $[Pd([9]aneN_4S)](PF_6)_2$ is fluxional in solution, as shown below:

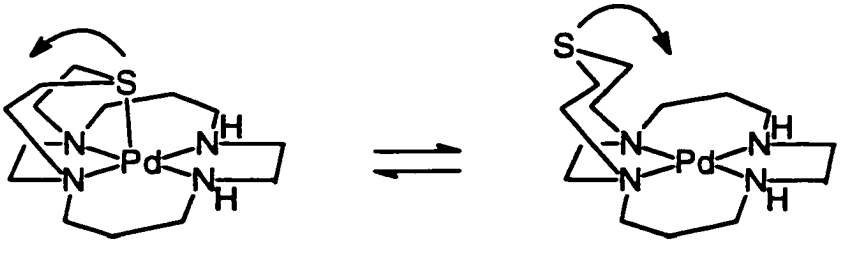

The room temperature ^{1}H-NMR spectrum of $[Pd([9]aneN_4S)](PF_6)_2$ is shown in figure 6.21. As expected, the signals are much more resolved than those of the free ligand (see section 3.5, figure 3.27) due to the rigidity and absence of nitrogen inversions imposed by coordination of the metal center. Comparison to the ^{1}H-NMR spectra of $[Pd([14]aneN_4)](Cl)_2$ and $[Ni([14]aneN_4)](ClO_4)_2$ shows a greater degree of splitting of

the methylene proton resonances associated with the [14]aneN$_4$ (cyclam) ring in [Pd([9]aneN$_4$S)](PF$_6$)$_2$. The presence of the sulphur bridge has resulted in greater rigidity, consistent with the spectra of the corresponding [9]aneN$_4$S bicycle and cyclam free ligands (section 3.7).

Analysis of the ^{1}H-^{13}C HETCORR and ^{1}H-^{1}H COSY spectra of [Pd([9]aneN$_4$S)](PF$_6$)$_2$ has aided in the assignments of the resonances (see figures 6.22 and 6.23). It can be seen that the methylene carbon bonded to sulphur donor (32.6 ppm) corresponds to the only broadened resonances in the ^{1}H-NMR spectrum at 3.2 ppm. The other proton resonances (centered at 3.05 ppm) of the CH$_2$-S methylene group do not appear similarly broadened, however, there is too much overlap of resonances to be certain. The other methylene carbon in the thia-amino chelate (54.0 ppm), which is bonded to the bridgehead nitrogen, is associated with the well-resolved proton resonances centered at 2.95 ppm and 2.69 ppm.

These qualitative observations suggest that, although the methylene group of the thia-amino chelate (sulphur bridge) adjacent to the bridgehead nitrogen is restricted from fluxional movements, the methylene group adjacent to the sulphur donor is undergoing limited torsional movements in solution at room temperature. It should be noted that the broadened proton resonances associated with this methylene show significant splittings that are not present in the free ligand resonances assigned to this methylene group. Such a result suggests that there is at least a partial restriction of movement of this methylene group that is not present in the free ligand. It may be that the acetonitrile solvent is competing with the sulphur by weakly interacting with the palladium(II) center, thereby disrupting the palladium-sulphur interaction.

The VT ^{1}H-NMR spectra of [Pd([9]aneN$_4$S)](PF$_6$)$_2$ in deuterated methanol are presented in figure 6.24. The broadening of the CH$_2$-S methylene group seen in acetonitrile solvent is not observed in methanol, implying the presence of a solvent effect.

No changes or fluxionality were observed up to 40 °C, implying that the ligand remains rigidly coordinated as expected. It is most interesting to consider the low

temperature spectra. At 0 °C, the resonances begin to broaden, consistent with the presence of a fluxional process, however, as the temperature is lowered to -90 °C, no sharpening of the resonances occurs. Instead, the spectrum broadens further. These low temperature spectra strongly resemble that expected for a paramagnetic complex. This result suggests that, as the temperature is lowered, a significant interaction with the axially positioned sulphur donor is occuring.

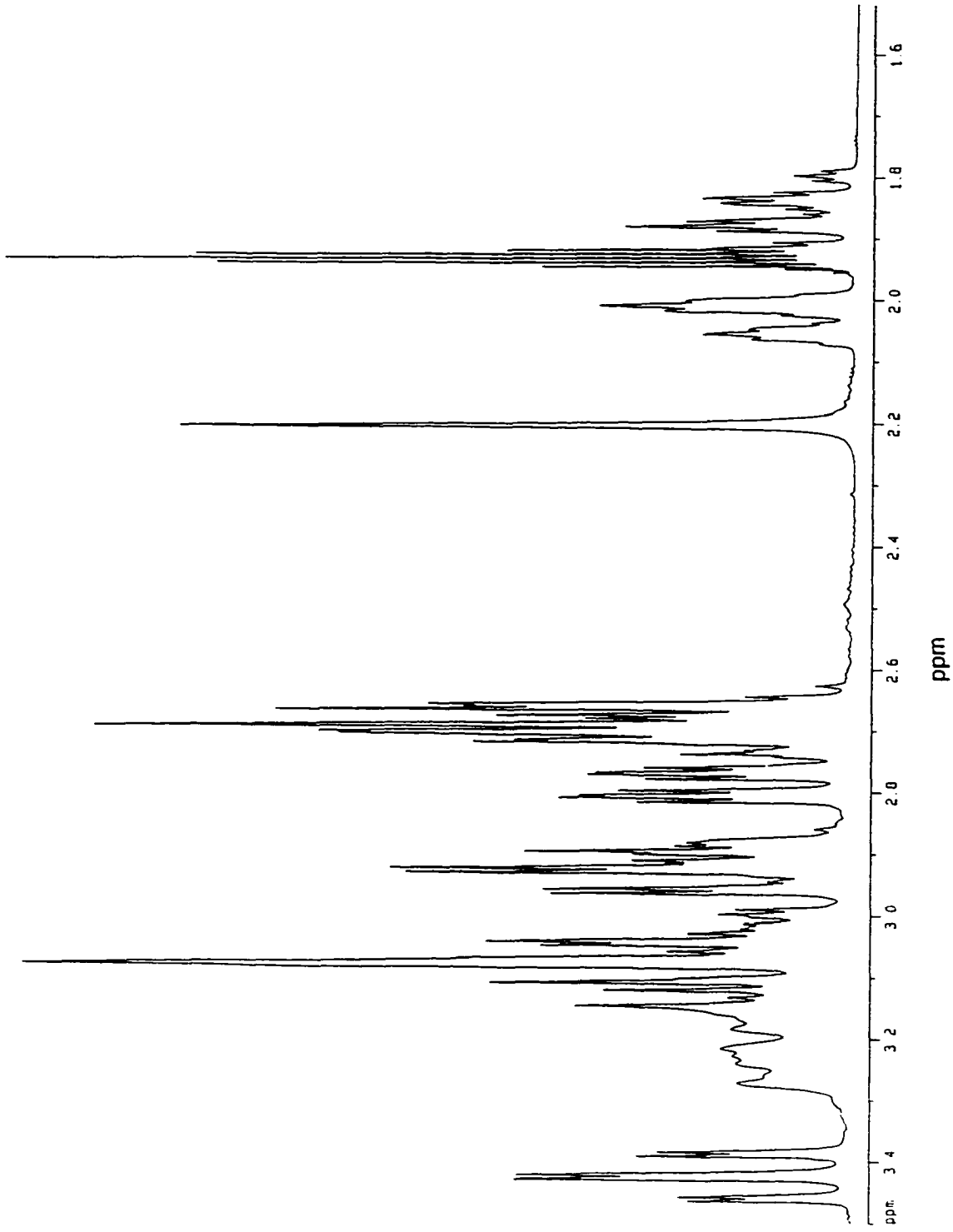

Figure 6.21. ^{1}H-NMR spectrum of [Pd([9]aneN$_4$S)](PF$_6$)$_2$ (RT, CD$_3$CN)

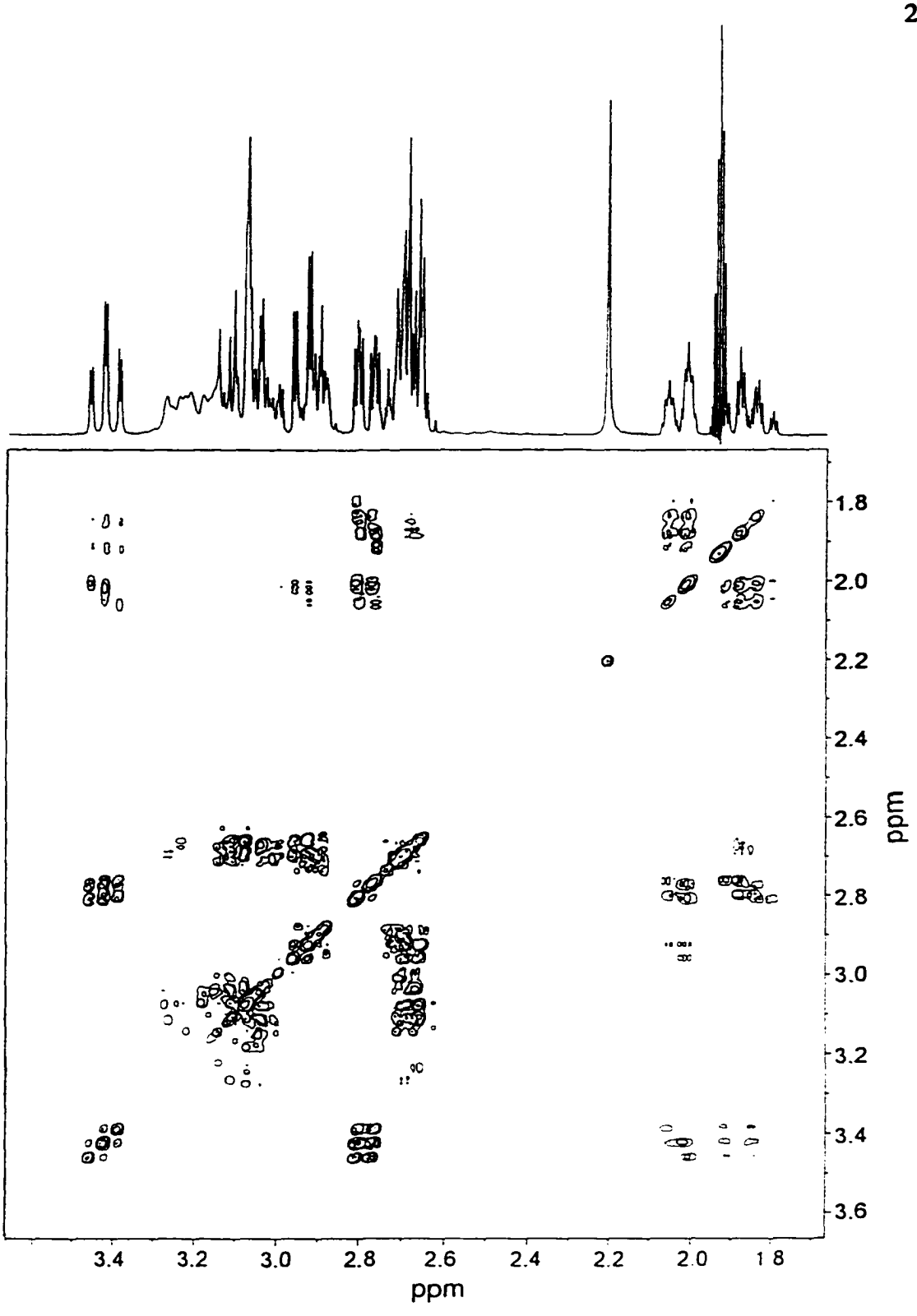

Figure 6.22. ^{1}H-^{1}H COSY spectrum of $[Pd([9]aneN_4S)](PF_6)_2$ (RT, CD_3CN)

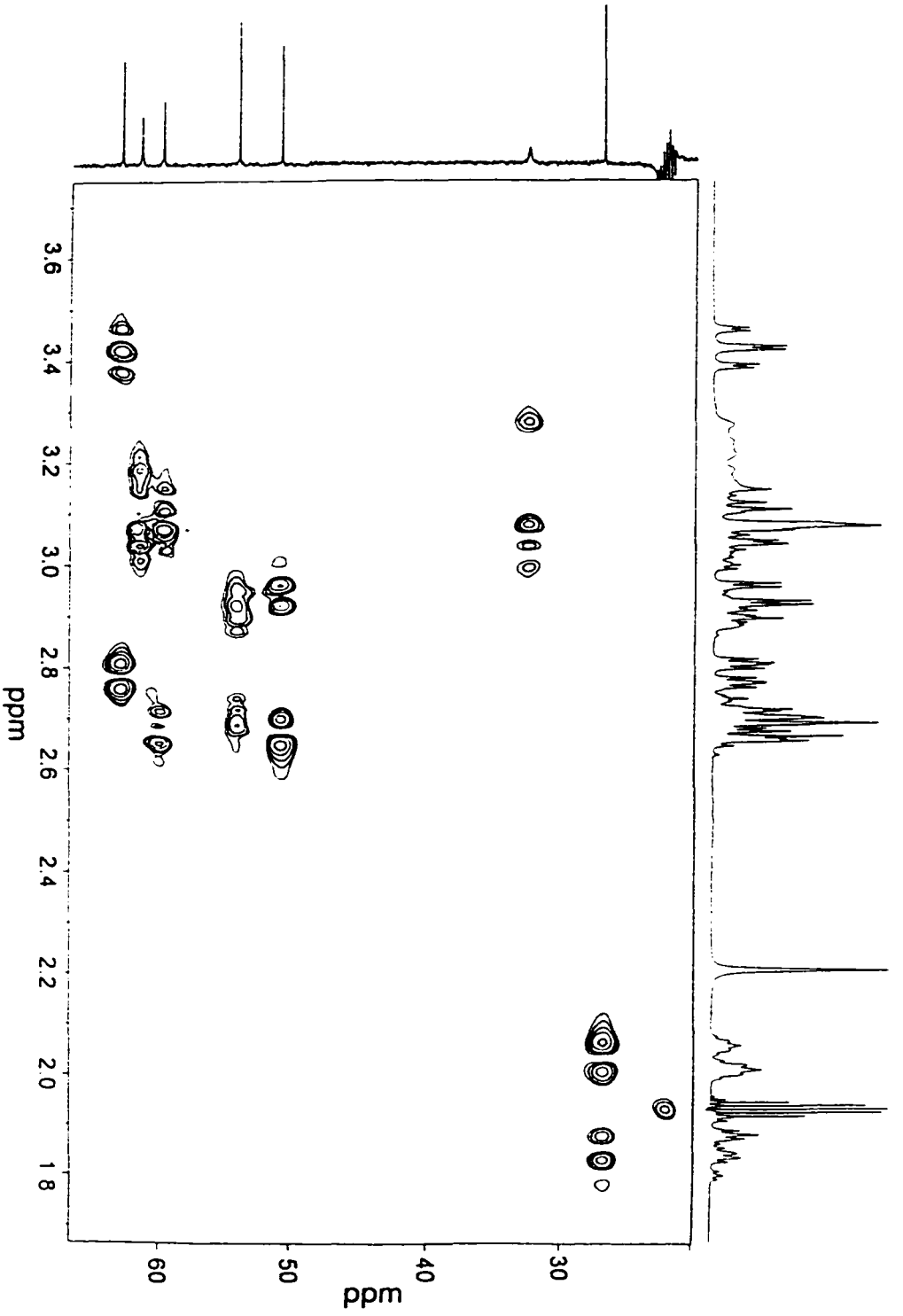

Figure 6.23. ^{1}H-^{13}C HETCORR spectrum of $[Pd([9]aneN_4S)](PF_6)_2$ (RT, CD_3CN)

Figure 6.24. Variable temperature ^{1}H-NMR spectra of [Pd([9]aneN$_4$S)](PF$_6$)$_2$ (CD$_3$OD)

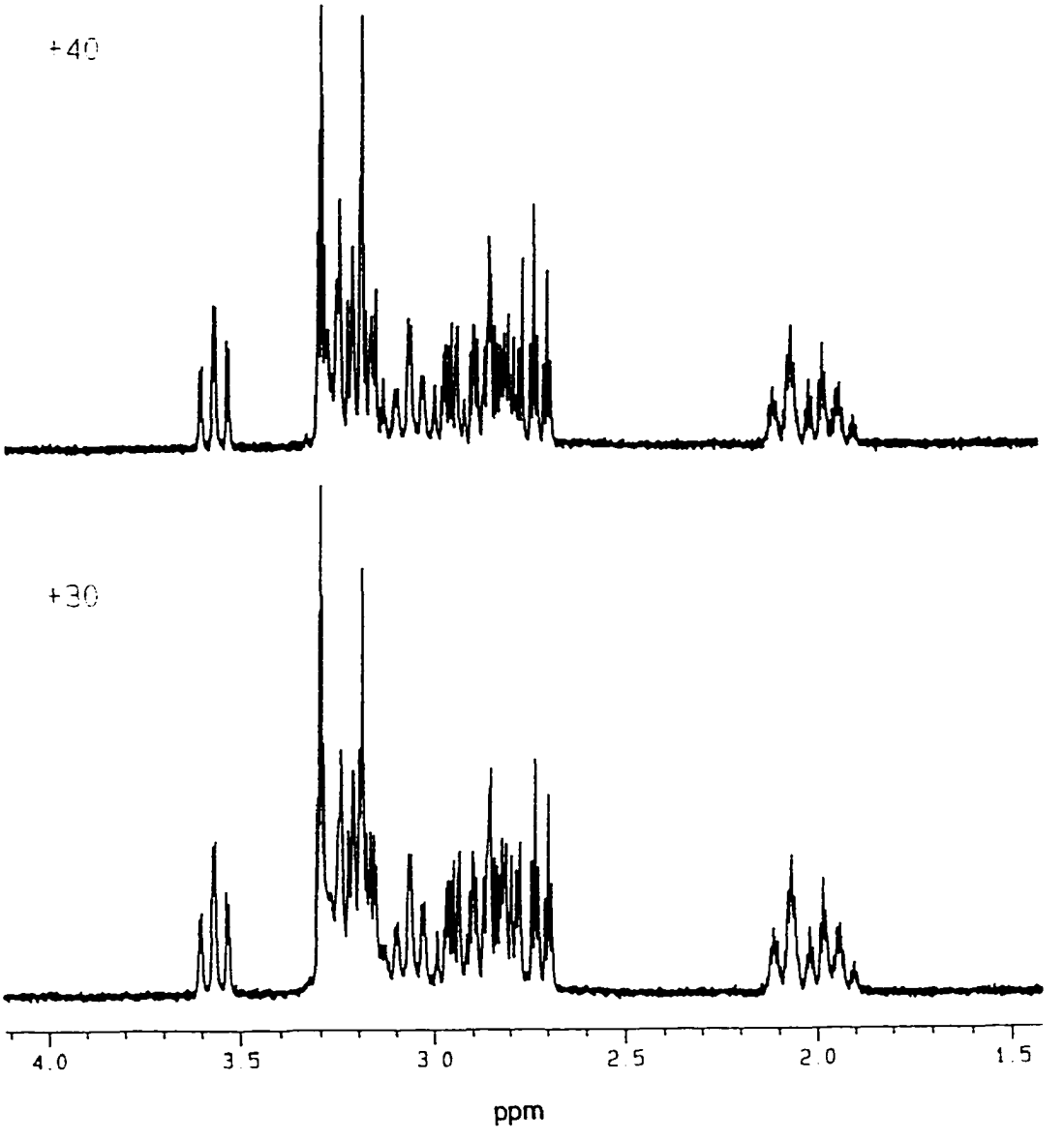

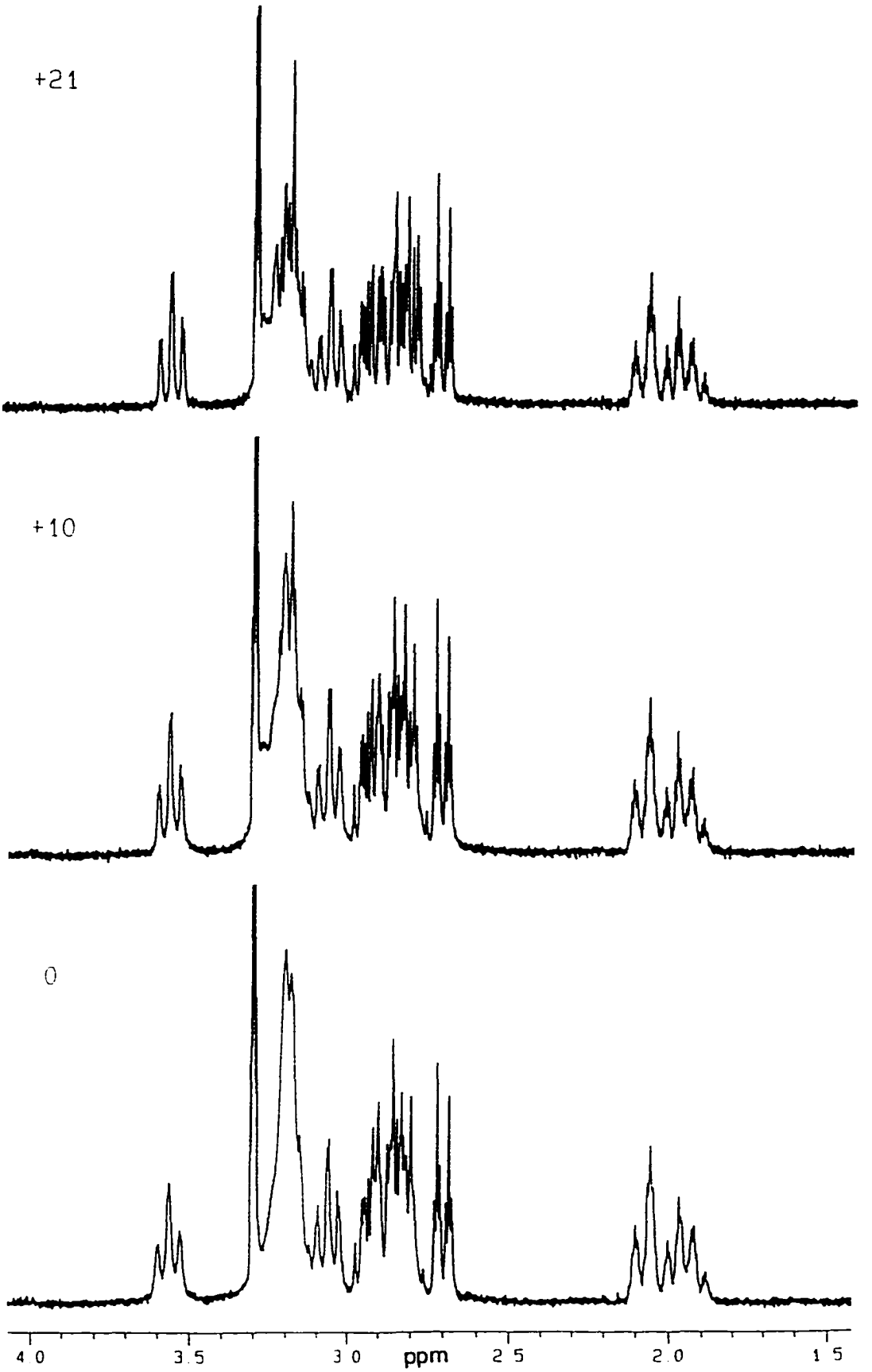
+21
+10
0
4.0
3.5
3.0
ppm
2.5
2.0
1.5

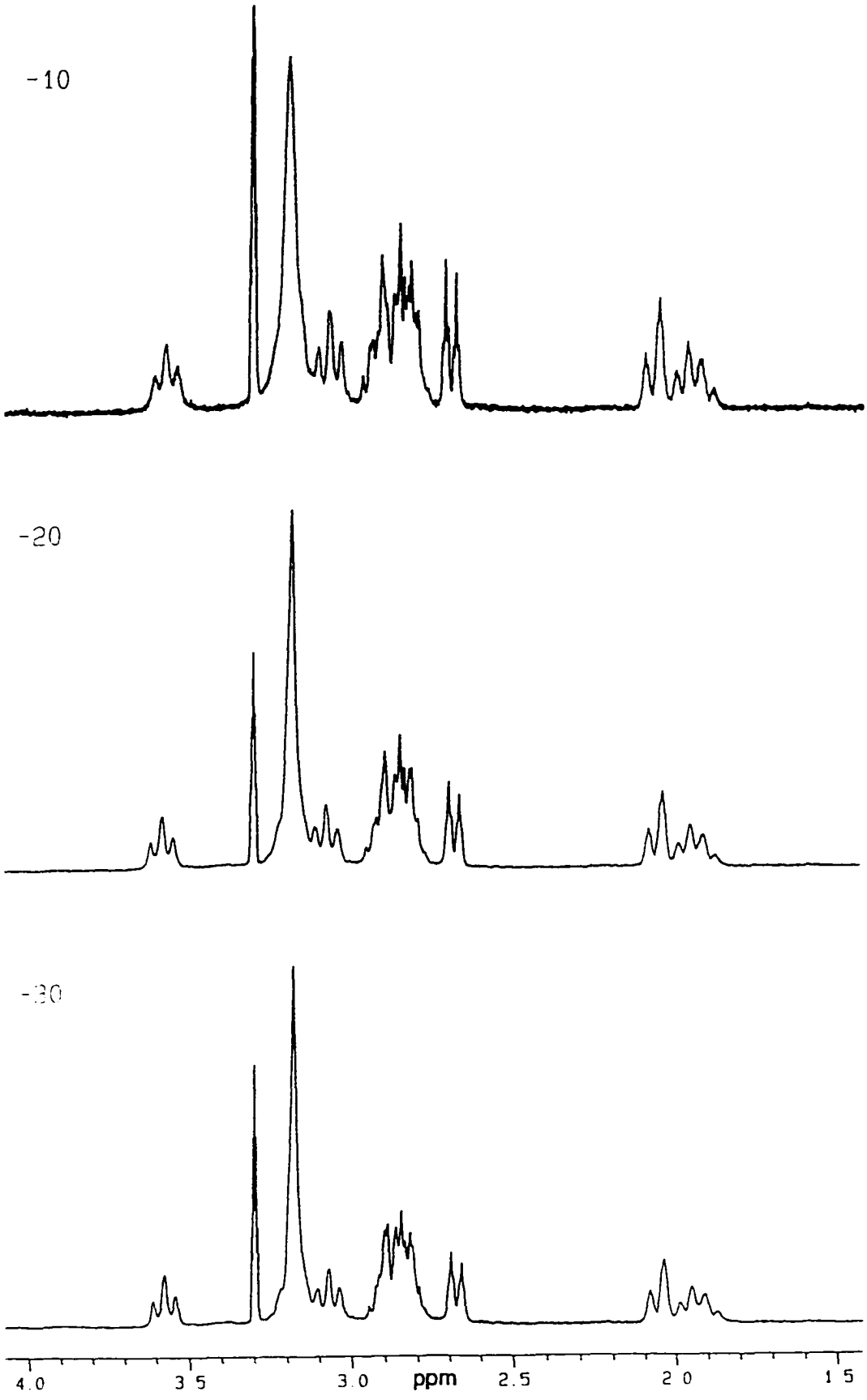
-10
-20
-30
4.0
3.5
3.0
ppm
2.5
2.0
1.5

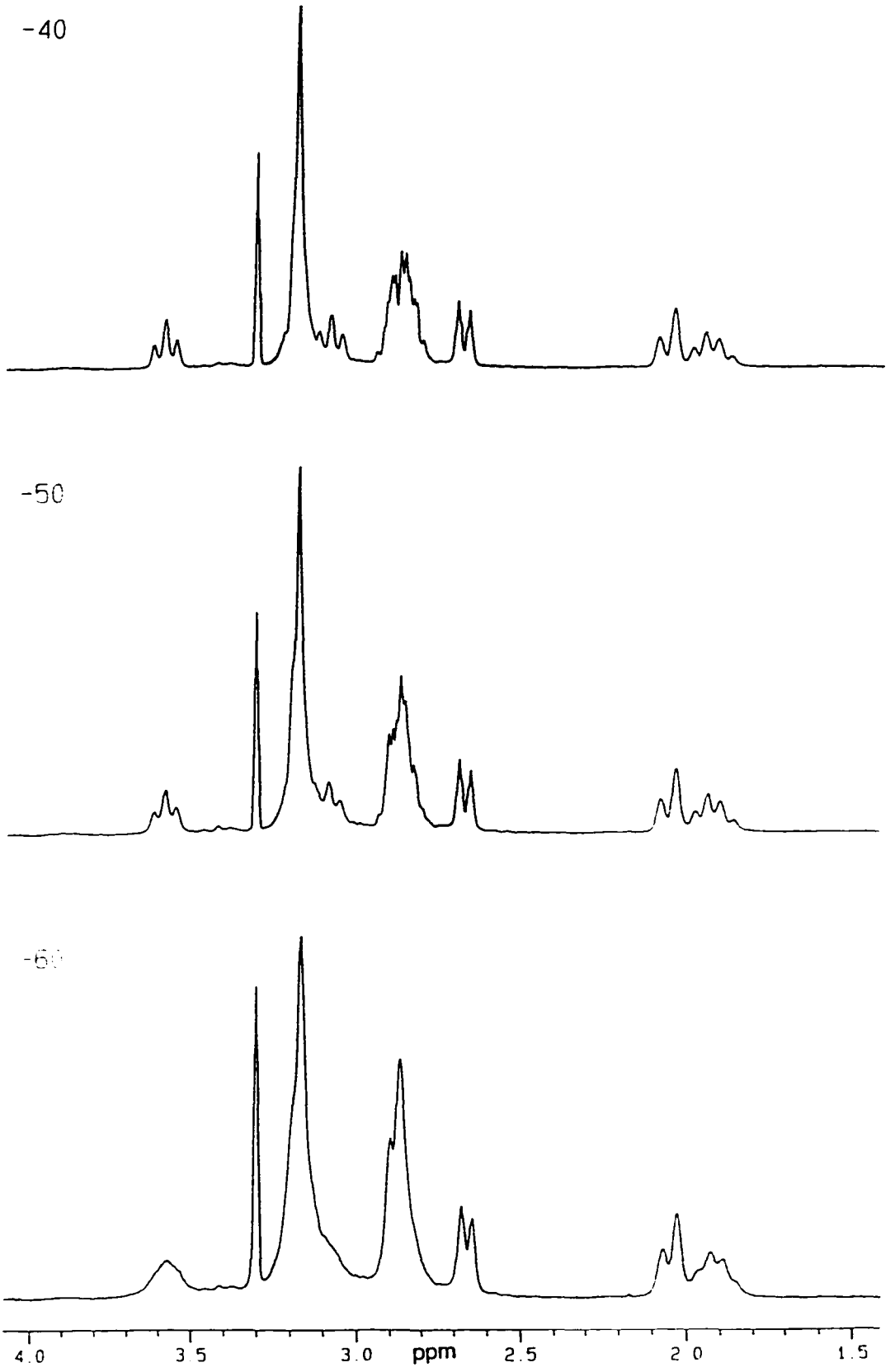
-40
-50
-60
4.0
3.5
3.0
ppm
2.5
2.0
1.5

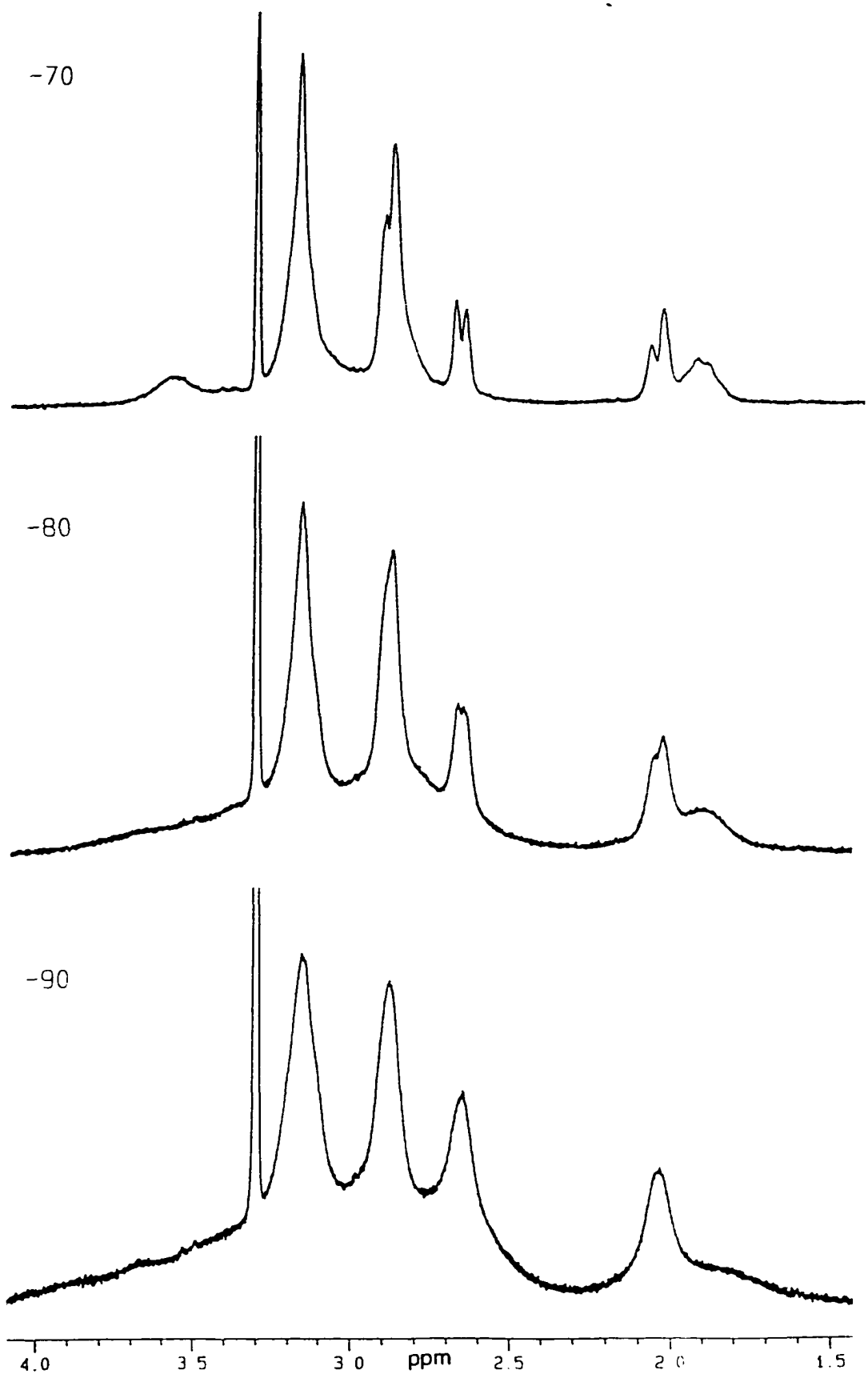
-70
-80
-90
4.0
3.5
3.0
ppm
2.5
2.0
1.5

Chapter 7
Future Studies

The method of synthesizing [10]aneN_2S (**20**) by reacting two equivalents of diaminopropane with thiodiglycolic acid chloride in chloroform, under high dilution conditions, is considered successful, reproducible and more convenient than the Richman and Atkins method. Therefore, application of this method to the syntheses of analogous tridentate ligands is expected to produce similar encouraging results.

The method of synthesizing [10]aneN_4S (**L3**) br reacting [10]aneN_2S (**20**) with the α-chloroamido derivative of propylenediamine was particularly successful, as indicated by the lack of any side products. This method has already been found[128] to be successful in synthesizing the analogous N_4X (X = NH, O) macrobicyclic ligands, and also the corresponding tricyclic ligands, in the present laboratory. Synthesis of other 1,8-N,N'-derivatized cyclam ligands may be achieved satisfactorily by diprotection of dioxocyclam, followed by reduction of the amide groups and reaction of the resulting diprotected cyclam with a suitable di-electrophile.

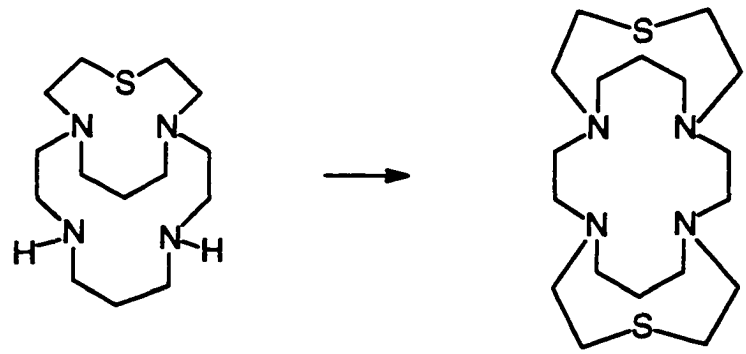

The [9]aneN_4S isomer of the bicycle series could be synthesized by reaction of [9]aneN_2S (**8**) with the β-chloroamido derivative of ethylenediamine, as such reactivity was reported by Bradshaw[129] to be successful but less reactive.

Synthesis of the cryptand isomer of the N_4S_2 tricyclic series could be achieved by reacting the hemi-cryptate isomer of the N_4S macrobicycle (**L2**) with thiodiglycolic acid chloride in chloroform solution under high dilution conditions.

Synthesis of these macrotricyclic ligand isomers by the above methods would allow the study of octahedrally encapsulated metal complexes which are anticipated to behave as interesting outer-sphere electron transfer reagents.

Comparison of the outer-sphere electron transfer behaviour of the three copper(II) N_4S_2-tricyclic ligand isomers should provide considerable insight into the dependence upon ligand rigidity. For example, determination of the self-exchange rates allows calculation of the reorganization energies involved in the electron transfer process.

An X-ray structure investigation of the $[Cu([10]aneN_4S)](ClO_4)_2$ complex is currently in progress. Such a determination is needed in order to gain insight into the coordination properties of this isomer.

Synthesis of a larger batch of $[Ni([10]aneN_4S)(solv)](acetate)_2$ is also an immediate objective, in order to more fully characterize this complex. A comparison of the electrochemical behaviour of the three $[Ni(N_4S)(solv)](ClO_4)_2$ isomers can then be conducted under identical (preferably simultaneous) conditions, such that the observed differences can be confidently attributed to structural (ring strain) effects. The esr spectra of the two newly prepared $[Ni(hemi\text{-}cryptN_4S)(solv)](ClO_4)_2$ and $[Ni([10]aneN_4S)(solv)](ClO_4)_2$ complexes differ markedly from that of the original $[Ni([9]aneN_4S)(solv)](ClO_4)_2$ isomer due to the presence of as yet unexplained splittings of the $g_\perp$ and $g_{//}$ signals. Further characterization of the nickel(III) complexes is therefore needed.

X-ray crystallography[128] of the analogous $[Ni([10]aneN_4O)(solv)](acetate)_2$ complex has determined the N_4 cyclam ring to be in the trans-III configuration, hence, it would be interesting to obtain an X-ray structure of the present sulphur complex.

As mentioned in section 4.3, it is believed that the sulphur bridge of the hemi-cryptate N_4S ligand is more rigid than that of the other two, such that significant strain energy may be induced in the ligand upon coordination of a metal center requiring relatively short axial bond distances. Synthesis, characterization and X-ray crystallography of the cobalt(III) complex is therefore of considerable interest. More detail kinetic studies

of a newly prepared sample of the $[Co([9]aneN_4S)(solv)](ClO_4)_3$ complex are desired. Attempts to obtain coupling constant data from the ambient temperature ^{1}H-NMR spectrum of the $[Pd([9]aneN_4S)](PF_6)_2$ complex by computer iteration of the experimental spectrum are in progress at the time of writing. The coupling constant values will give considerable insight into the relative flexibility of the sulphur bridge and the possibility of the presence of a Pd-S interaction in solution.

Finally, the development of relatively facile synthetic routes to the N_4S macrobicyclic ligands affords the quantities needed to further develop syntheses of tricyclic systems in which one of the bridges provides a hydrophobic pocket (see below) for small molecule activation studies. Also, such ligands would prevent the μ-oxo bridging behaviour of iron(III) complexes (observed in the ferric [9]aneN$_4$S **(L1)** complex), allowing studies of the resulting iron chemisty. The presence of the relatively hard nitrogen donors, offset by the soft donor properties of sulphur, could lead to considerably enhanced $Fe^{2+/3+}$ electron transfer rates due to stabilization of both oxidation states.

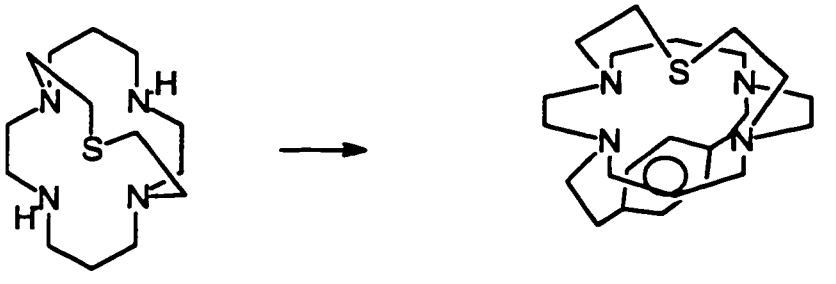

Chapter 8

Experimental Details

8.1. Instrumentation and apparatus:

8.1(a) Spectroscopy:

NMR spectra, both ^{1}H and ^{13}C, were recorded on a Bruker AMX360 or Bruker AC300 high field spectrometer. Either D_2O, using MeOH as external standard, or $CDCl_3$, using TMS as external standard, were used as the solvent. Variable temperature experiments were performed on the Bruker AMX 360 instrument.

Mass spectra of free ligands were recorded on a Finnegan 330 GC-MS instrument by methane chemical ionization and electron impact techniques. Mass spectra of metal complexes were recorded on a Kratos Concept spectrometer either by FAB or electrospray ionization techniques.

Infrared Spectra were recorded on either a Bruker IFS25 (FTIR) spectrometer or a Perkin-Elmer 1330 spectrometer. Solid samples were prepared as KBr discs and oils were coated between NaCl plates.

Ultraviolet-visible (UV-VIS) spectra were recorded on either a Cary 5 UV-VIS-NIR spectrophotometer or a Perkin-Elmer Lambda 4B spectrophotometer. In general, samples were studied as solutions of appropriate concentration in 1 cm quartz cells at ambient temperature.

Centrifugal chromatography was performed on a Harrison Research chromatotron, model 7924T. The plates were coated with TLC grade silica gel (Merck) with gypsum binder and Fluorescent indicator.

Elemental analyses were performed by Canadian Microanalytical Services, Vancouver, B. C.

Crystallography was carried out as described in reference 125. Unit cells and space groups were determined using Weissenberg and precession photography. The crystals were then transferred to either a Picker 4-circle or an Enraf-Nonius CAD4 diffractometer. Solutions of the phase problem were achieved, and the heavy atom position located, using the Direct Methods of the SHELX76 or MULTAN programs.

Electrochemistry was performed using a Princeton Applied Research Model 273 potentiostat-galvanostat, interfaced with an IBM PC microcomputer. The data were recorded and displayed using the "Headstart" program supplied by the Princeton Applied Research Company. The electrochemical cell employed the standard three electrode configuration: platinum working and counter electrodes and $Ag/AgNO_3$ reference electrode. Blank electrolyte solutions were scanned before each run and the ferrocene/ferrocenium couple ($Fc^{0/+1}$) was used as both an external and internal standard to calibrate the reference electrode, $E_{1/2}$ ($Fc^{0/+}$) = 0.15 V *vs.* Ag/Ag^+. All $E_{1/2}$ values were quoted as the potential *vs.* ferrocene, where the $E_{1/2}$ ($Fc^{0/+1}$) was taken as 0.00 V. Acetonitrile (HPLC grade) was dried over CaH_2 and freshly distilled prior to use.

Molecular mechanics calculations were carried out on a Power Macintosh 7100/80 computer using the CAChe Scientific Worksystem™ software package, version 3.7. This software uses the Allinger's widely tested MM2[218] force field modeling program.

8.1(b) Materials:

All starting materials were purchased from Aldrich Chemicals with the exception of HBr/AcOH which was purchased from Fluka Chemicals. Solid chemicals were of reagent grade purity and were used without further purification. Amine liquids such as ethlenediamine, diaminopropane and ethanolamine were purified by vacuum distillation. All solvents were reagent grade or HPLC grade (acetonitrile) and freshly dried and distilled before use. **CAUTION!** Perchlorate salts are explosive and care should be taken when using these compounds.[108]

8.1(c) Methods:

i) Extraction Procedures:

In the course of this work it was often necessary to perform liquid-liquid extractions of amine free ligands. For example, the work-up of borane/THF reduction reactions required extractions to be performed after the 6N HCl reflux. Typically, the ligand sample was dissolved in 2 - 3M NaOH (ca. 10 - 15 ml per gram of amine sample) then extracted six times with an equal or greater volume of organic solvent, usually chloroform. During the course of the extractions, it was noticed that the amount of amine ligand transferred from the aqueous layer was lower than anticipated, particularly for the smaller macrocycles such as [9]aneN_2S and [10]aneN_2S wherein as much as 30% of the ligand was left behind in the aqueous layer. The amine macrocycles synthesized in this work are relatively polar organic amines and therefore have lower partition coefficients.

In order to maximize the amount of amine free ligand extracted into the chloroform layer, continuous extraction procedures are used instead. However, the sulphur containing ligands synthesized in this work were observed to be unstable to heating when dissolved in chloroform. The continuous extraction method requires that the chloroform layer to be boiled constantly for long periods of time such that the ligands were decomposed.

Since the objective of the liquid-liquid extraction was merely to remove the salts (e.g. salts from neutralization and/or borate species) present in the sample, an alternative procedure was used. To the amine free ligand sample was added 25 ml of methanol per gram of ligand. The solution was stirred vigorously for 2 hrs. then centrifuged to remove the undissolved (white) solid salts. The methanol was removed by rotary evaporation then the solid was dried further in vacuo to remove any residual water. To the resulting mixture of ligand and salt was added 25 ml of chloroform per gram of ligand. If the sample was observed to contain a large amount of salts, a small amount (5 ml) of methanol was added first to ensure complete dissolution of the ligand, then addition of the chloroform precipitated out only the salts. The solution was stirred vigorously for 2 hrs. then centrifuged and the solvent was removed from the supernatant by rotary

evaporation (if the sample was still observed to contain white solid salts, it was stirred in chloroform again and stored overnight at 5 °C). The resulting free ligand oil was dissolved in chloroform once again, dried over sodium sulphate, centrifuged and evaporated in vacuo.

Analysis of the solid salts removed showed none of the amine ligand to be present. In the case of borane reduction reactions, it was noticed that further traces of borate salts present in the free ligand oil which, were readily soluble in chloroform, could be removed by dissolving the sample in dry acetonitrile. The presence of borate salts was monitored by ^{11}B-NMR spectroscopy and it was found that this method was usually sufficient to remove all of the borate species.

It was observed that detectable amounts of borate species often transferred into the organic layer when using the conventional liquid-liquid extraction technique. This is presumably because of the presence of a polydispersed suspension of the aqueous layer in the organic layer which facilitates the dissolution of salts. This effect is particularly acute in the case of organic amine hydrochloride salts such as triethylamine hydrochloride.

In cases where the borate species persisted, the free ligand sample was dissolved in pH 13 (NaOH, not buffered) water and passed down a column of DOWEX 1X8-400 anion-exchange resin in the hydroxide form according to the procedure reported by Dietrich, Lehn et al[99]. The neutral amines pass through the packing material while the polyborate species bind effectively and therefore are not eluted.

ii) High Dilution Procedure:

The high dilution principle was frequently used in the course of this work and required a special apparatus similar to those already described in the literature[73] (see figure 8.1). As described in section 2.1 and shown in figure 2.4, the syntheses of macrocyclic ligands by direct methods often require high dilution conditions in order to favour intramolecular condensation of the half-condensed intermediate over intermolecular polymer formation by allowing more time for the half-condensed intermediate to persist before encountering other reactants in the solution. There are several important practical aspects involved which are worthy of mentioning.

The dinucleophile and dielectrophile reagents were both separately dissolved in a small volume (usually 50 ml) of solvent and loaded into identical 100 ml syringes. For reactions using non-chlorinated solvents (acetonitrile, benzene), plastic syringes were used because they are air-tight and the solutions do not fall under their own gravity. The highly reactive diacid chloride electrophiles were not affected by the plastic. It was observed that glass syringes do not have a sufficiently air-tight seal such that the solutions fall even when the pistons are stationary; however, in the case of chlorinated solvents, the 100 ml glass syringes have to be used because the chlorinated solvents swell the rubber seals of the plastic syringes such that the pistons can no longer move. Silicon grease was used to seal the top of the glass syringes and prevent the solutions from falling on their own accord, however, it was difficult to prevent the grease from contaminating the reagent solutions. In the future, teflon syringes should be tried for reactions requiring chlorinated solvents.

The syringes were mounted to a step motor driven holder depicted in figure 8.1. The pistons of the two syringes were simultaneously and slowly advanced by a metal plate which was advanced by an elecronically monitored step motor via spindles. The dilution and feeding rate was controlled by the speed of the spindle.

The 50 ml reagent solutions were added dropwise into a large round bottom flask, usually 5 litre size, containing 2 - 2.5 litres of solvent, over a period of 8 - 10 hours. This slow addition results in reagent concentrations which effectively correspond to one drop of the reagent solution in 2.5 liters. These concentrations are at least four orders of

magnitude lower than if the reagents were added all at once. Assuming the intermolecular collision rates are similar to the diffusion-controlled second order rate constants[43] which are 10^9 - 10^{10} M^{-1} s^{-1}, the average intermolecular collision times are in the 10^{-5} s order of magnitude under these high dilution conditions, as opposed to 10^{-9} s if both reagents are added at once. Regardless of the inaccuracy inherent in these simple theoretical values, it was observed empirically that the high dilution conditions resulted in great improvements of the intramolecular condensation yields, particularly with the [10]aneN_2S diamide (**23**) synthesis reported in section 3.2(d).

Although the slow dropwise addition of the reagents provided the desired high dilution, it was also necessary to ensure homogeneous concentrations via fast mixing of the reaction solution, otherwise the effect of the slow addition is compromised. Conventional overhead stirring conditions were not as effective as desired, especially for the [10]aneN_2S diamide (**23**) synthesis. The salient features of the overhead apparatus used in this work are depicted in figure 8.1.

In order to ensure rapid mixing of the outer annular layers of the solution, the round bottom flask contained three or four glass indents which deflect the outer layers inward towards the stirring paddle. This results in chaotic mixing in which the top of the round bottom is continually washed with splashed solution. This effect also serves to rapidly disperse the drops of reagent solution before they reach the bulk solution.

It was observed that the heights of the stirring paddle and bulk solution in the round bottom flask had significant effects on the cyclization yield. This was because it was necessary to have the flask only half filled such that the top layer of solution was being vigorously mixed, and the paddle low enough to mix the bottom layers. Vigorous mixing and splashing of the top of the solution was probably the most important aspect because it dispersed the drops of reagent solution evenly before they reached the bulk solution.

Finally, it was found that the stirring speed had a significant effect on the cyclization yields, especially in the case of the [10]aneN_2S diamide (**23**) synthesis reported in section 3.2(d) (see table 3.1). Faster stirring speeds were attained using a

specially built overhead stirring apparatus. The apparatus consisted of a 3/4 hp Baldor electic motor, mounted on a solid metal frame, which was attached via a metal connector to a stainless steel stir shaft. The lower portion of the stir shaft (which was removable via a metal connector) was secured via metal bearings to a teflon stir guide which fitted into the B45 neck of the 5 litre round bottom flask. The neck of the flask was attached by two removable circular metal plates to the metal frame. The stirring speed was determined by stroboscopic methods to be up to 1900 rpm which was much improved over the stirring speeds of the previous stirrers (< 600 rpm). It was necessary to install a hard rubber U-joint in the stir shaft to avoid alignment problems and dampen the vibrations which limited the speeds attainable.

Table 8.1. Identification of components shown in figure 8.1

Number in figure 8.1	Component
1	3/4 hp electric motor
2	stainless steel stir shaft
3	hard rubber U-joint
4	removable metal connector
5	metal bearing
6	removable circular metal ring with inner O-ring
7	teflon stir guide
8	wing nuts
9	solid metal frame
10	glass indents
11	syringe holder and step motor

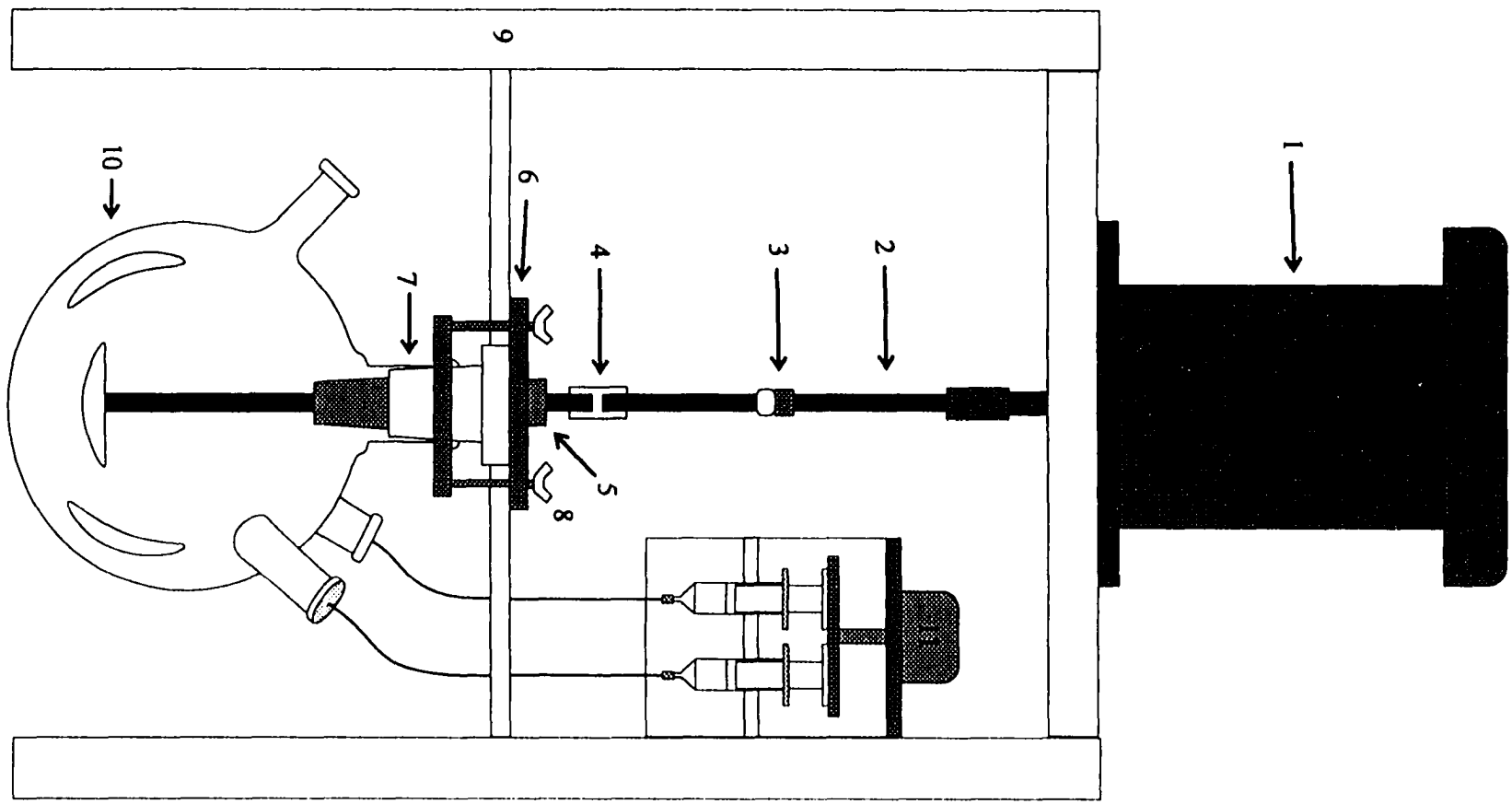

Figure 8.1. Stirring apparatus used in the present study (see table 8.1)

8.2. Synthesis of Ligands (L1-L3) and Compounds 4-30:

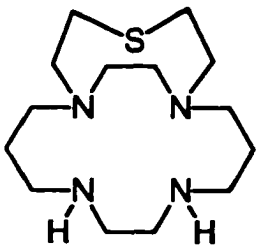

(L1)
[9]aneN$_4$S
bicycle

15-Thia-1,5,8,12-tetraazabicyclo[10.5.2]nonadecane (L1). The procedure reported by Fortier and McAuley[90] was followed in this work without any significant modifications. Yield: 50-60% from **12**. IR: NH stretch, 3276 cm^{-1}; CH stretches, 2800-2900 cm^{-1}. ^{13}C-NMR ($CDCl_3$, ppm relative to TMS standard): 26.7 (C-$\underline{C}H_2$-C); 36.4 ($\underline{C}H_2$-S); 47.3, 48.4, 54.3, 56.7, 58.1, ($\underline{C}H_2$-N). Mass spectrum (CI): m/e 287(M+1), 315(M+29), 327(M+41).

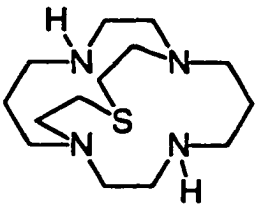

(L2)
Hemi-cryptate
N$_4$S bicycle

17-Thia-1,5,8,12-tetraazabicyclo[6.6.5]nonadecane (L2). To the 7.0g of crude bicyclic diamide mixture (**16**) was added 75 mL (0.075 mol) of 1M BH_3•THF (1 2/3 equiv.'s per tertiary amide[98] x 2 amides per molecule) under N_2 atm. The mixture was stirred at room temperature for 20 min. then refluxed 5 h. The resulting solution was cooled on an ice bath and the excess borane was destroyed by dropwise addition of *ca.* 2-3 mL distilled water (**CAUTION**). The solution was taken to dryness by rotary evaporation. The white solid residue was dissolved in 80 mL 6M HCl and refluxed for 2.4 h. After cooling, the HCl was removed in vacuo. The resulting dry solid was redissolved in aqueous NaOH (2.5g in 30 mL) and extracted (see section 8.1c) into chloroform (6 x 50mL). The organic layers were combined, dried over Na_2SO_4 and taken to dryness. Polyborate materials were removed[99] by dissolving the resulting 4.8g of oily residue in 20mL distilled water (pH 12.5) and chromatographing over a column (3.5cm diam. x 8cm) of DOWEX 1 X 8-400 anion-exchange packing in the hydroxide bound form. The resulting 2.5g of crude free

ligand was purified by complexation to copper(II) perchlorate and chromatography over sephadex CM-C25 cation-exchange packing. To a solution of the copper(II) complex $[Cu(L2)](ClO_4)_2$ (1.75 g, 0.0032 mol) in water (20 mL) was added $Na_2S{\cdot}9H_2O$ (2.9g, 0.012 mol). The solution was refluxed for 2.5 h. then allowed to cool and suction filtered through a glass fritted funnel. The filtrate was made basic by the addition of NaOH (1g) and extracted with $CHCl_3$ (6 x 50mL). The combined extracts were dried over Na_2SO_4 and taken to dryness under reduced pressure, leaving a viscous oil. Yield: 0.550g (1.9 mmol), 7.0% from cyclam. IR: NH stretches, 3200-3300 cm^{-1} (brd). ^{13}C-NMR ($CDCl_3$, ppm relative to TMS standard): 25.8 (C-$\underline{C}H_2$-C); 33.7 ($\underline{C}H_2$-S); 47.5, 51.3, 53.2, 54.3, 58.2 ($\underline{C}H_2$-N). Mass spectrum (CI): m/e 287(M+1), 315(M+29), 327(M+41).

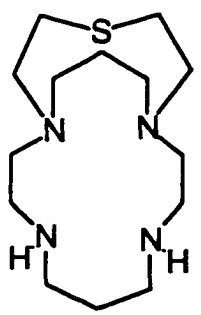

(L3)
[10]aneN$_4$S
bicycle

14-Thia-1,4,8,11-tetraazabicyclo[9.5.3]nonadecane (L3). To 0.500g, 1.6 mmol of [10]aneN$_4$S bicycle diamide (**30**) was added 10 mL of 1M $BH_3{\cdot}THF$ (10 mmol, 6 equiv.) under strict N_2 atmosphere. The slurry was stirred at room temperature for 20 min. then refluxed for 4.5 h. The solution was cooled on an ice bath then the excess borane destroyed (**CAUTION**) by slow dropwise addition of distilled water (ca. 1 mL). The solution was taken to dryness on a rotary evaporator. The resulting white solid residue was dissolved in 20 mL 6N HCl and refluxed for 2.5 h. The solution was cooled to room temperature, taken to dryness on a rotary evaporator and dried further in vacuo. The resulting solid residue was dissolved in 15 mL of 2.5M NaOH and extracted with chloroform (6 x 40 mL). The organic layers were combined, dried over sodium sulphate and taken to dryness in vacuo yielding a colourless oil (crude). Yield: 0.419g (1.5 mmol), 91%. The ligand was then purified by complexation with copper(II) perchlorate and chromatography over sephadex CM-C25 cation-exchange packing.

Purification of (L3). The product ligand was purified by complexation to copper(II) perchlorate and chromatography over sephadex CM-C25 cation-exchange packing. To a solution of 0.649g (1.2 mmol) $[Cu(L3)](ClO_4)_2$ in 20 mL deionized water was added 0.5g (2.1 mmol) $Na_2S \cdot 9H_2O$. The solution was refluxed for 2.5 h. then allowed to cool and suction filtered through a glass fritted funnel. The filtrate was made basic by the addition of NaOH (1.0g) and extracted with chloroform (6 X 50 mL). The combined extracts were dried over sodium sulphate and taken to dryness in vacuo, leaving a viscous colourless oil. Yield: 0.267g (0.93 mmol), 77% (from $[Cu(L3)](ClO_4)_2$). ^{1}H-NMR ($CDCl_3$, ppm relative toTMS): 1.4-1.8 (m, 4H, 2 x C-C$\underline{H_2}$-C); 2.2-3.4 (m, 24H, 2 x C$\underline{H_2}$-S, 10 x C$\underline{H_2}$-N). ^{13}C-NMR ($CDCl_3$, ppm relative to TMS): 29.0 (1C, C-$\underline{C}H_2$-C); 29.3 (1C, C-$\underline{C}H_2$-C); 36.4 (2C, $\underline{C}H_2$-S); 46.7, 51.9, 55.2, 56.0, 57.9 (10C, 5 x $\underline{C}H_2$-N). Mass spectrum (CI): m/e 287 (M+1), 315 (M+29), 327 (M+41).

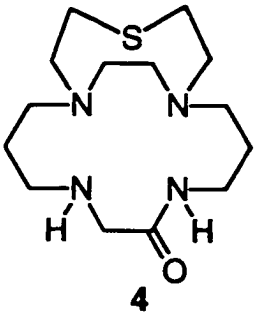

4
monoamido-
[9]aneN$_4$S bicycle

15-Thia-1,5,8,12-tetraazabicyclo[10.5.2]nonadecane-6-one (4). To a solution of the copper complex $[Cu(4)](ClO_4)_2$ (1.22g, 0.0026 mol) in water (20 mL) was added $Na_2S \cdot 9H_2O$ (2.5g, 0.010 mol). The solution was refluxed for 4 h. then allowed to cool and suction filtered through a glass fritted funnel. The filtrate was made basic by the addition of NaOH (1g) and extracted with $CHCl_3$ (6 x 50 mL). The combined extracts were dried over Na_2SO_4 and taken to dryness under reduced pressure, leaving a viscous oil. Yield: 0.60g (2.0 mmol), 77%. IR: NH stretch, 3300 cm^{-1} (s); CH stretches, 2930, 2805 cm^{-1} (s); C=O stretch, 1640 cm^{-1}. ^{13}C-NMR ($CDCl_3$, ppm relative to TMS standard): 25.4, 27.0 (2 x C-$\underline{C}H_2$-C); 32.9, 34.5 (2 x $\underline{C}H_2$-S); 39.7, 48.5, 53.2, 53.3, 53.5, 54.9, 55.3, 57.8, 58.6 (9 x $\underline{C}H_2$-N); 172.3 (C=O). Mass spectrum (CI): m/e 301(M+1), 329(M+29), 341(M+41).

5a. N,N'-*bis*((4-methylphenyl)sulphonyl)*bis*-(2-aminoethyl)sulphide ($TsNH(CH_2)_2S(CH_2)_2NHTs$). To a stirred solution of 80g (0.40 mol) tosylaziridine (**10**) in ethanol/water (800 mL: 200 mL) was added 48.0g (0.20 mol) $Na_2S{\cdot}9H_2O$. The solution was refluxed under N_2 atmosphere for 2 h. The solvent was removed by rotary evaporation and the residue was redissolved in 200 mL distilled water. The aqueous solution was acidified to pH 2-3 with HCl and extracted with 4 x 400 mL dichloromethane. The extracts were combined, dried over sodium sulphate, filtered and taken to dryness in vacuo. The crude solid was usually of sufficient purity such that recrystallization from ethanol was not necessary. Yield: 75g, 88%. ^{1}H-NMR and IR spectra were consistent with that reported[85] in the literature. Mass spectrum (CI): m/e 429(M+1), 457(M+29), 469(M+41).

5b. $TsN(CH_2)_2S(CH_2)_2NTs$ disodium salt. The procedure reported by Fortier and McAuley[90] was used without any significant modification.

6. Ethylene Glycol Ditosylate ($TsO(CH_2)_2OTs$). The procedure reported by Chandrasekhar and McAuley[109] was used with ethylene glycol as the starting material instead of propylene glycol.

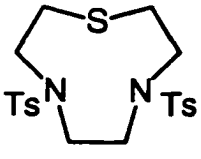

7

4,7-*Bis*((4-methylphenyl)sulphonyl)-1-thia-4,7-diazacyclononane (7). The cyclization of the disodium salt of **5a** with ethylene glycol ditosylate (**6**) was carried out according to the procedure reported[88] in the literature. Yield: 30-40%. ^{1}H-NMR and IR spectra were identical to that reported[88] in the literature. ^{13}C-NMR ($CDCl_3$, ppm relative to TMS): 21.5 ($\underline{C}H_3$); 30.3 ($\underline{C}H_2$-S); 52.1, 53.7 ($\underline{C}H_2$-N); 127.2, 129.8, 134.6, 143.8 (<u>Ts</u>-N). Mass spectrum (CI): m/e 455(M+1), 483(M+29), 495(M+41).

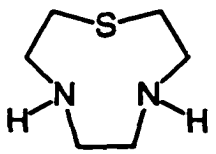

8
[9]aneN$_2$S

1-Thia-4,7-diazacyclononane dihydrobromide (8)•2HBr. The procedure of Koyama and Yoshino[89] was used to hydrolyze the cyclic ditosylate (7). In a typical reaction, 12g of 7 were added to 160 mL of >33% HBr in acetic acid (4.1M, Fluka Chemicals) and refluxed under nitrogen atmosphere for 30 h. The solution was filtered whilst hot through a glass frit filter then concentrated by rotary evaporation. The solid was dissolved in the minimum of distilled water, usually 10 mL, and recrystallized by addition of an equal amount of ethanol/ether 1:3. The white crystalline solid was filtered and washed with ethanol/ether, then ether only, and dried in vacuo. Yield: 3.2g, 40%. ^{1}H-NMR and IR spectra were identical to that reported[85] in the literature. ^{13}C-NMR (D_2O, ppm relative to ethanol standard): 28.1, ($\underline{C}H_2$-S); 42.9, 45.0 (2 x $\underline{C}H_2$-N).

1-Thia-4,7-diazacyclononane (8). The free ligand oil was obtained by dissolving the dihydrobromide salt in 2M NaOH and extracting into chloroform. The combined chloroform extracts were dried over sodium sulphate, filtered and evaporated in vacuo. ^{13}C-NMR (D_2O, ppm relative to ethanol standard): 33.1, ($\underline{C}H_2$-S); 46.5, 47.2 (2 x $\underline{C}H_2$-N). Mass spectrum (CI): m/e 147(M+1), 175(M+29), 187(M+41).

9. Monoethanolamine Ditosylate (TsONHCH$_2$CH$_2$Ts). The synthetic procedure used is an adaptation of the method reported[86] by Wagnon and Jackels. Solid *p*-toluenesulphonyl chloride (800g, 4.2 mol) was added in portions, under N_2 atmosphere, to a mechanically stirred solution of monoethanolamine (122g, 2.0 mol) in dry pyridine (700 mL), producing a viscous yellow slurry. The temperature of the mixture was kept below -10°C but above -30°C using a salt/ice bath (or dry ice/acetone if necessary). The mixture was stirred for 4-5 h. Hydrochloric acid (800 mL of 5M HCl) was then added dropwise so that the temperature was maintained below 10°C. The red oil which formed crystallized to a more solid yellow product on standing. The solid was separated on a large glass frit filter, washed with cold ethanol, and dried under vacuum. Yield: 365g, 46%; m.p. 82-85°C

(lit.[87] m.p. 86-87°C). ^{1}H-NMR and IR spectra were consistent with that reported[87] in the literature.

10

Tosylaziridine (10). To a stirred solution of NaOH (800 mL, 1.4M) at -10°C in a salt/ice bath was added 100g (0.27 mol) monoethanolamine ditosylate (**9**). Stirring was continued for 1.5-2 h. The resulting precipitate was allowed to settle for 3 h. at 10°C. The white solid was collected, washed with cold distilled water, and dried in vacuo. Yield: 51g, 95%; ^{1}H-NMR and IR spectra were consistent with that reported[86] in the literature. Mass spectrum (CI): m/e 198(M+1), 226(M+29), 238(M+41).

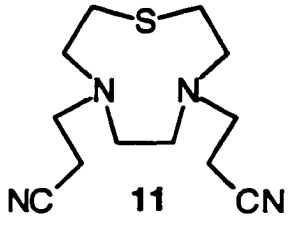

11

4,7-*Bis*(2-cyanoethyl)-1-thia-4,7-diazacyclononane (11). The procedure reported by Fortier and McAuley[90] was used without any significant modifications.

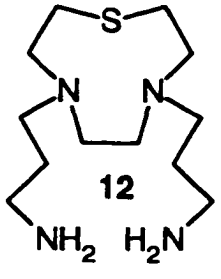

12

4,7-*Bis*(3-aminopropyl)-1-thia-4,7-diazacyclononane (12). The procedure reported by Fortier and McAuley[90] was used without any significant modifications.

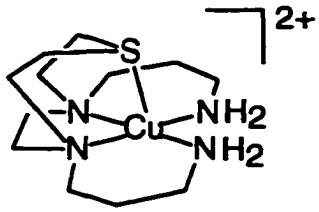

13
$[Cu(12)](ClO_4)_2$

(4,7-*Bis*(3-aminopropyl)-1-thia-4,7-diazacyclononane)copper Diperchlorate {$[Cu(12)](ClO_4)_2$}. The procedure reported by Fortier and McAuley[90] was followed in this work without any significant modifications. Yield: 35-40% from **8**.

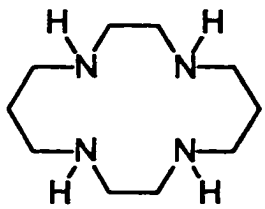

14
$[14]aneN_4$

1,4,8,11-tetraazacyclotetradecane (cyclam). The procedure reported by Barefield et al[82] was used without any significant modifications.

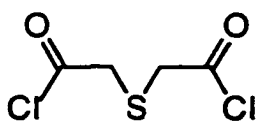

15

Thiodiglycolic acid chloride (15). To a sample of 15g (0.10 mol) of thiodiglycolic acid was 150 mL (2.1 mol) of thionyl chloride (~ 20 equiv.). The solution was stirred at room temperature under strict N_2 atmosphere for 20 h. The unreacted $SOCl_2$ was removed by vacuum distillation (~ 5 x 10^{-2} torr, 5-10°C), leaving a dark oil. Thiodiglycolic acid chloride was obtained in high purity by microdistillation of the oil under vacuum (80 - 100 °C, 10^{-2} torr). Yield: 14.5g (0.078 mol), 78%. ^{1}H-NMR ($CDCl_3$, ppm relative to TMS): 3.86 ($\underline{C}H_2$-S). ^{13}C-NMR ($CDCl_3$, ppm relative to TMS): 44.3 ($\underline{C}H_2$-S); 169.5 ($\underline{C}$=O).

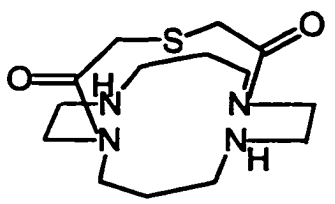

16
hemi-cryptateN_4S
bicycle diamide
(CRUDE)

17-Thia-1,5,8,12-tetraazabicyclo[6.6.5]nonadecane-15,19-dione (crude 16). Dry, twice distilled chloroform was first prepared by refluxing 4.5 litres reagent grade $CHCl_3$ (N_2 atm.) over *ca.* 200-250g phosphorous pentoxide for 8-12 h. The chloroform was fractionally distilled then refluxed (N_2 atm.) for 12 h. over calcium hydride and fractionally distilled again. A 5.50g (0.027 mol) sample of cyclam (**14**) and a 5.13g (0.027 mol) sample of thiodiglycolic acid chloride (**15**), each in 50mL of chloroform, were added simultaneously over a period of 8 h. to 2.5 litres chloroform (N_2 atm., rm. temp.), using the high dilution apparatus described in section 8.1(c). The solution was mechanically stirred at 1170 rpm, as determined by stroboscopic methods. After addition of the reagent solutions was completed, the mixture was stirred for another 5-8 h. The reaction mixture was filtered and the 17g of white solid precipitate was dried in vacuo whereupon the solid was observed to lose 5g of co-crystallized chloroform. The dried solid was dissolved in 50mL 1M NaOH to neutralize the hydrochloride salt. The solution was evaporated to dryness on a rotary evaporator. The solid was stirred vigorously in 50 mL methanol for 2 h., then the insoluble material and NaCl were filtered off. The methanol filtrate was evaporated to dryness on a rotary evaporator then dried in vacuo, yielding 7.0g of a pale yellow solid. This crude mixture was reduced without further purification.

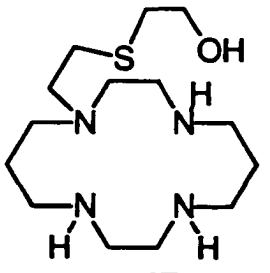

17
Uncyclized N_4S
(proposed structure)

17. The free ligand (**17**) was obtained by removing the copper(II) from $[Cu(17)](ClO_4)_2$ with sodium sulphide then extraction into chloroform according to the procedure described above for **L2**. Yield: 0.11g (0.36 mmol), 1.3% from cyclam. IR: NH stretches, 3200-3350 cm^{-1}; OH stretch, 3100-3300 cm^{-1} (brd). ^{13}C-NMR (D_2O, ethanol internal standard): 25.0, 26.4 (2 x C-$\underline{C}H_2$-C); 28.8, 34.1 (2 x $\underline{C}H_2$-S); 46.1, 46.4, 46.9, 47.3, 48.0,

49.0, 52.1, 52.3, 53.5 (9 x $\underline{C}H_2$-N); 61.0 ($\underline{C}H_2$-OH). Mass spectrum (CI): m/e 305(M+1), 333(M+29), 345(M+41).

18. **Propylene Glycol Ditosylate ($TsO(CH_2)_3OTs$).** The procedure reported by Chandrasekhar and McAuley[109] was used without any significant modifications.

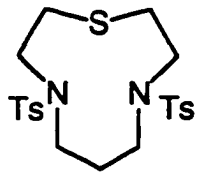

19

4,8-*Bis*((4-methylphenyl)sulphonyl)-1-thia-4,8-diazacyclododecane (19). The procedure reported by Chandrasekhar and McAuley[109] was used. The only significant modification was that the DMF solvent was refluxed and distilled over CaH_2.

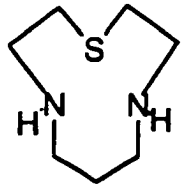

20
[10]aneN_2S

1-Thia-4,8-diazacyclododecane (20). To 2.0 g, 0.011 mol [10]aneN_2S diamide (**23**) was added 45 mL of 1M BH_3•THF (0.044 mol BH_3) under strict nitrogen atmosphere. The slurry was stirred at room temperature for 20 min. then refluxed for exactly 4 hours. The solution was cooled on an ice bath then the excess borane destroyed (**CAUTION**) by slow dropwise addition of distilled water (1 - 2 mL). The solution was taken to dryness on a rotary evaporator. The resulting white solid was dissolved in 40 mL of 6N HCl and refluxed for 2 hours. The solution was cooled to room temperature then taken to dryness on a rotary evaporator and dried further in vacuo. The resulting pale orange solid was dissolved in 25 mL of 2.5M NaOH and extracted (see section 8.1(c) concerning the details of extraction procedures performed in this work) into chloroform (6 X 50 mL). The organic layers were combined, dried over sodium sulphate and taken to dryness yielding a pale yellow or colourless oil. Yield: 1.55g (9.7 mmol), 88%. ^{1}H-NMR ($CDCl_3$, ppm relative to TMS): 1.6 (m, 2H, C-C$\underline{H}_2$-C); 2.6-2.8 (m, 12H). ^{13}C-NMR

($CDCl_3$, ppm relative to TMS): 27.9 (1C, C-$\underline{C}H_2$-C); 35.3 (2C, $\underline{C}H_2$-S); 48.1, 49.7 (4C, 2 X $\underline{C}H_2$-N). Mass spectrum (CI): m/e 161(M+1), 189(M+29), 201(M+41).

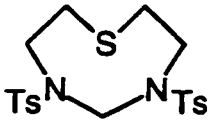

21

4,8-*Bis*((4-methylphenyl)sulphonyl)-1-thia-4,8-diazacyclododecane (21). This side product was consistently produced in the synthesis of **19** reported above.

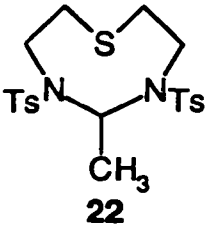

22

4,8-*Bis*((4-methylphenyl)sulphonyl)-1-thia-4,8-diazacyclododecane (22). This side product was consistently produced when the procedure reported by Chandrasekhar and McAuley[109] for the synthesis of **19** was used with the following modification: DMA solvent (refluxed and distilled over CaH_2) was used instead of DMF.

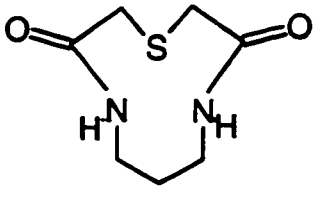

23
[10]aneN_2S
diamide

1-Thia-4,8-diazacyclododecane-3,9-dione (23), [10]aneN_2S diamide. Dry, twice distilled chloroform was first prepared by refluxing 4.5 litres reagent grade chloroform (N_2 atmosphere) over ca. 200-250g phosphorous pentoxide for 12 h. The chloroform was fractionally distilled then refluxed for 12 h. over 50 g calcium hydride and again fractionally distilled. Benzene was dried with sodium metal and freshly distilled before use. An 8.88g, 0.12 mol sample of diaminopropane in 50 mL of benzene and an 11.22g, 0.060 mol sample of thiodiglycolic acid chloride (**15**) in 50 mL of benzene were both added simultaneously from a high precision syringe pump apparatus (see section 8.1c) over a period of 10 h. to 2.5 litres chloroform under N_2 atmosphere at room temperature. The solution was mechanically stirred at 1900 rpm (see section 8.1c). The resulting white precipitate was

removed by filtration and the colorless filtrate was evaporated in vacuo yielding a white solid residue. Yield: 7.1 g (0.038 mol), 63%. M. p. >200 °C. IR: C=O stretch, 1640 cm^{-1} (s, brd). ^{1}H-NMR (D_2O, ppm relative to TMS): 1.65 (m, 2H, C-C<u>H</u>$_2$-C); 3.12 (m, 8H, 2 X C<u>H</u>$_2$-S, 2 X C<u>H</u>$_2$-N). ^{13}C-NMR (D_2O, ppm relative to TMS): 24.9 (C-<u>C</u>H$_2$-C); 36.4, 39.9 (<u>C</u>H$_2$-S, <u>C</u>H$_2$-N); 171.8 (<u>C</u>=O). Mass spectrum (CI): m/e 189 (M+1), 217 (M+29), 229 (M+41). Anal. Calcd for $C_7H_{12}N_2O_2S$: C, 44.66; H, 6.43; N, 14.88. Found: C, 43.77; H, 6.41; N, 14.52.

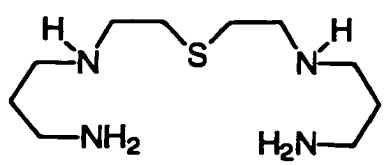

24
[15]aneN$_4$S linear

***Bis*(3,7-diaminoheptane)sulphide (24).** This side product was obtained from the synthesis of [10]aneN$_2$S **(20)** using the moderate stirring conditions reported in section 8.1(c). Yield: 25-30% (from diaminopropane). ^{1}H-NMR ($CDCl_3$, ppm relative to TMS): 1.63 (q, 2H, C-C<u>H</u>$_2$-C); 2.51, 2.62, 2.69, 2.74 (t, 2H, <u>C</u>H$_2$-S and 3 x t, 6H, <u>C</u>H$_2$-N). ^{13}C-NMR ($CDCl_3$, ppm relative to TMS): 32.1, 33.5 (1C, C-<u>C</u>H$_2$-C and 1C, <u>C</u>H$_2$-S); 40.3, 47.3, 48.6 (3C, 3 X <u>C</u>H$_2$-N). Mass spectrum (CI): m/e 235(M+1), 275(M+29).

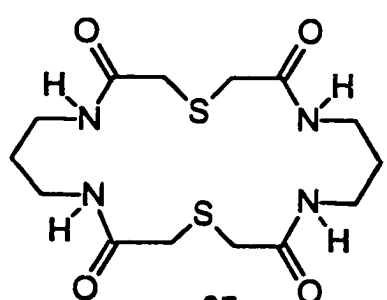

25
[20]aneN$_4$S$_2$ tetraamide
proposed structure only

25 (proposed structure = 1,11-Dithia-8,8,14,18-tetraazacycloeicosane-3,9,13,19-tetra-one). Ligand **(25)** was obtained as a side product from the synthesis of **23** reported above. Yield: 2.1g (5.6 mmol), 18.6%. M. p. >200 °C. IR: C=O stretch, 1640 cm^{-1} (s, br.). ^{13}C-NMR (D_2O, ppm relative to TMS): 28.0 (C-<u>C</u>H$_2$-C); 35.8, 37.4 (<u>C</u>H$_2$S, <u>C</u>H$_2$N); 171.6 (<u>C</u>=O). Mass spectrum (CI): m/e 377(M+1), 405(M+29). Anal. Calcd. for $C_7H_{12}N_2O_2S$: C, 44.66; H, 6.43; N, 14.88. Found: C, 43.88; H, 6.41; N, 13.92.

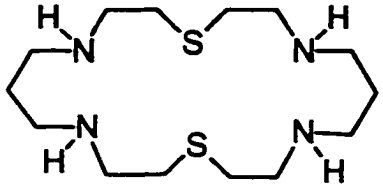

26
[20]aneN$_4$S$_2$
proposed structure only

26 (proposed structure = 1,11-Dithia-4,8,14,18-tetraazacycloeicosane). To 0.750g, 2.0 mmol of **25** in 100 mL dry distilled THF was added 0.90g, 0.024 mol (12 equiv.) of $LiAlH_4$ under N_2 atmosphere. The solution was stirred at room temperature for 20 min. then refluxed for 8 h. After cooling in an ice bath, the excess $LiAlH_4$ was destroyed (**CAUTION**) by slow dropwise addition of 2M NaOH. The solution was taken to dryness on a rotary evaporator and the resulting gelatinous solid residue was stirred vigorously in 50 mL of deionized water. The lithium hydroxide solids were removed by centrifugation and extracted with 50 mL water twice more. The combined 150 mL of supernatant was taken to dryness. The resulting solid residue was stirred vigorously with 150 mL chloroform, filtered to remove undissolved salts and taken to dryness in vacuo yielding 0.53g of viscous pale yellow oil. To the oil dissolved in 50 mL pH 9 water was added 0.60g copper(II) perchlorate dissolved in 20 mL water. The resulting copper(II) complexed mixture was chromatographed over sephadex CM-C25 cation-exchange packing. The major product eluted from the column (0.12M $NaClO_4$ eluent) was a violet coloured complex. The solution was taken to dryness in vacuo. The copper complex was dissolved in 50 mL dry ethanol, filtered to remove the $NaClO_4$ and the filtrate taken to dryness in vacuo. The copper(II) was removed by gently refluxing the complex in 20 mL water (1 h.) with 2 equivalents of Na_2S then filtering to remove the copper sulphide precipitate. The aqueous solution was made basic by the addition of 1g NaOH and extracted with 6 X 50 mL chloroform. The combined chloroform extracts were dried over sodium sulphate, filtered and taken to dryness in vacuo. Yield: 0.240g, 0.75 mmol, 38%. ^{13}C-NMR ($CDCl_3$, ppm relative to TMS): 31.9 (2C, C-$\underline{C}H_2$-C); 38.8 (4C, $\underline{C}H_2$-S); 46.4, 47.8 (8C, 4 X $\underline{C}H_2$-N). Mass spectrum (CI): m/e 321(M+1), 349(M+29).

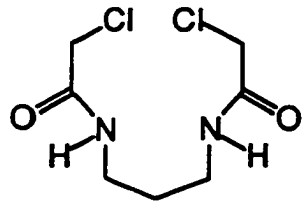

27

N,N'-*bis*(α-chloroamido)diaminopropane (27). A solution of 30 mL (0.37 mol) chloroacetyl chloride in 200 mL dichloromethane was slowly added dropwise to a vigously stirred solution of 14.8g (0.20 mol) diaminopropane and 45g (0.33 mol) potassium carbonate in 250 mL distilled water (rm. temp.). The stirring was continued for 2 h. then the organic layer was separated, dried with sodium sulphate and taken to dryness in vacuo. The white solid residue was recrystallized from methanol. Yield: 21.3g (0.94 mol), 47%. ^{1}H-NMR ($CDCl_3$, ppm relative to TMS): 1.72 (quintet, 2H, C-C$\underline{H_2}$-C); 3.18 (quartet, 4H, C$\underline{H_2}$-N); 4.05 (singlet, 4H, C$\underline{H_2}$Cl). ^{13}C-NMR ($CDCl_3$, ppm relative to TMS): 29.4 (1C, C-$\underline{C}H_2$-C); 36.4 (2C, $\underline{C}H_2$-N); 42.6 (2C, $\underline{C}H_2$Cl); 166.8 (2C, $\underline{C}$=O). Mass spectrum (CI): m/e 227(M+1), 255(M+29).

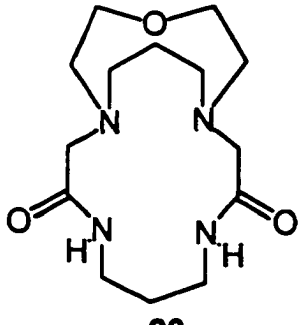

28
[10]aneN$_4$O bicycle diamide

14-Oxa-1,4,8,11-tetraazabicyclo[9.5.3]nonadecane-3,9-dione (28), [10]aneN$_4$O bicycle diamide. A 1.0g (7.0 mmol) sample of 1-Oxa-4,8-diazacyclododecane ([10]aneN$_2$O)[219] was dissolved in 200 mL of dry distilled acetonitrile. A 1.6g (7.0 mmol) sample of N,N'-bis(α-chloro amido)diaminopropane (27) was dissolved in 200 mL acetonitrile. It would have been preferable to dissolve both reagents in only 50 mL but the solubility of 27 was < 450 mg per 50 mL. Both reagent solutions were added simultaneously dropwise in four batches of 50 mL at a time from the syringe pump apparatus (see section 8.1c) over a period of 8-10 h. per 50 mL batch (40 h. total) to 2.5 litres of refluxing (80 °C) dry distilled acetonitrile containing 1.9g, 2.5 equivalents of sodium carbonate under N_2 atm. The solution was mechanically stirred at 1200-1900 rpm using the high dilution apparatus described in

section 8.1(c). The reaction was stopped and allowed to cool to room temperature then filtered. The filtrate was taken to dryness in vacuo, yielding a white powdery solid. Yield: 2.91g (9.26 mmol), 100% (based on [10]aneN_2O). M. p. >200 °C. IR: C=O stretch, 1645 cm^{-1} (s, brd.). ^{1}H-NMR ($CDCl_3$, ppm relative to TMS): 1.4-1.9 (m, 4H, 2 x C-C$\underline{H_2}$-C); 2.4-2.6, 2.8-3.4, 3.6-3.8 (m, 20H, 2 x C$\underline{H_2}$-O, 8 x C$\underline{H_2}$-N). ^{13}C-NMR ($CDCl_3$, ppm relative to TMS): 26.8 (1C, C-$\underline{C}H_2$-C); 27.9 (1C, C-$\underline{C}H_2$-C); 36.3, 39.5, 54.5, 55.2, 60.0 (5C, 4 x $\underline{C}H_2$-N, 1 x $\underline{C}H_2$-O); 170.7 (1C, C=O). Mass spectrum (CI): m/e 315 (M+1), 343 (M+29), 355 (M+41).

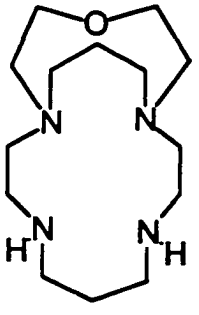

29
[10]aneN_4O
bicycle

14-Oxa-1,4,8,11-tetraazabicyclo[9.5.3]nonadecane (29), [10]aneN_4O bicycle. To 1.00g, 3.4 mmol of [10]aneN_4O bicycle diamide (**28**) was added 100 mL of 1M BH_3•THF (100 mmol) under strict N_2 atmosphere. The slurry was stirred at room temperature for 20 min. then refluxed for 4.5 h. The solution was cooled on an ice bath then the excess borane destroyed (**CAUTION**) by slow dropwise addition of distilled water (ca. 1mL). The solution was taken to dryness on a rotary evaporator. The resulting white solid residue was dissolved in 50 mL 6N HCl and refluxed for 2.5 h. The solution was cooled to room temperature then taken to dryness on a rotary evaporator and dried further in vacuo. The resulting solid residue was dissolved in 30 mL of 2.5M NaOH and extracted with chloroform (6 X 40 mL). The organic layers were combined, dried over sodium sulphate and taken to dryness in vacuo yielding a colorless oil. Yield: 0.742g (2.75 mmol), 82%. ^{1}H-NMR ($CDCl_3$, ppm relative toTMS): 1.4-1.8 (m, 4H, 2 x C-C$\underline{H_2}$-C); 2.2-3.4 (m, 24H, 2 x C$\underline{H_2}$-O, 10 x C$\underline{H_2}$-N). ^{13}C-NMR ($CDCl_3$, ppm relative to TMS): 27.78 (1C, C-$\underline{C}H_2$-C); 27.82 (1C, C-$\underline{C}H_2$-C); 47.1, 47.5, 56.5, 57.7, 58.1 (10C, 5 x $\underline{C}H_2$-N); 73.2 (2C, $\underline{C}H_2$-O). Mass spectrum (CI): m/e 271 (M+1), 299 (M+29), 311 (M+41).

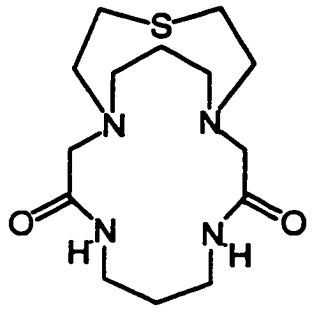

30
[10]aneN$_4$S bicycle diamide

14-Thia-1,4,8,11-tetraazabicyclo[9.5.3]nonadecane-3,9-dione (30), [10]aneN$_4$S bicycle diamide. A sample of 1-Thia-4,8-diazacyclododecane (**20**) ([10]aneN$_2$S) 1.48g, 9.25 mmol was dissolved in 200 mL of dry distilled acetonitrile. A sample of N,N'-bis(α-chloro amido)diaminopropane (**27**) 2.1g, 9.25 mmol was dissolved in 200 mL acetonitrile. It would have been preferable to dissolve both reagents in only 50 mL but the solubility of **27** was < 500 mg per 50 mL. Both reagent solutions were added simultaneously dropwise in four batches of 50 mL at a time from the syringe pump apparatus (see section 8.1c) over a period of 8-10 h. per 50 mL batch (40 h. total) to 2.5 litres of refluxing (80 °C) dry distilled acetonitrile containing 2.5g, 2.5 equivalents of sodium carbonate under N_2 atm. The solution was stirred mechanically at 1900 rpm using the high dilution apparatus described in section 8.1(c). The reaction was stopped and allowed to cool to room temperature then filtered. The filtrate was taken to dryness in vacuo, yielding a white powdery solid. Yield: 2.91g, 9.26 mmol, 100% (based on [10]aneN$_2$S). M. p. >200 °C. IR: C=O stretch, 1645 cm^{-1} (s, brd.). ^{1}H-NMR ($CDCl_3$, ppm relative to TMS): 1.4-1.9 (m, 4H, 2 x C-C$\underline{H}_2$-C); 2.4-2.6, 2.8-3.4, 3.6-3.8 (m, 20H, 2 x C$\underline{H}_2$-S, 8 x C$\underline{H}_2$-N). ^{13}C-NMR ($CDCl_3$, ppm relative to TMS): 26.8 (1C, C-$\underline{C}H_2$-C); 27.9 (1C, C-$\underline{C}H_2$-C); 36.3, 39.5, 54.5, 55.2, 60.0 (5C, 4 x $\underline{C}H_2$-N, 1 x $\underline{C}H_2$-S); 170.7 (1C, C=O). Mass spectrum (CI): m/e 315 (M+1), 343 (M+29), 355 (M+41). Anal. Calcd. for $C_{14}H_{26}N_4O_2S$: C, 53.48; H, 8.33; N, 17.82. Found: C, 50.12; H, 10.32; N, 16.04.

8.3. Synthesis of Metal Complexes (compounds 31-44):

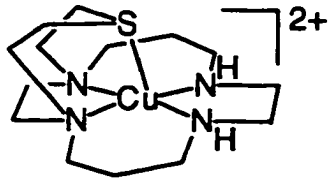

31
$[Cu(L1)](ClO_4)_2$

(15-Thia-1,5,8,12-tetraazabicyclo[10.5.2]nonadecane)copper Diperchlorate {$[Cu(L1)](ClO_4)_2$}. The procedure reported by Fortier and McAuley[90] was followed in this work without any significant modifications. Yield: 50-60% from **12**. IR: NH stretch, 3200-3300 cm^{-1}; ClO_4, 620, 1100 cm^{-1}. Anal. Calcd. for $[Cu(C_{14}H_{30}N_4S)](Cl_2O_8)$: C, 30.63; H, 5.50; N, 10.20. Found: C, 30.11; H, 5.87; N, 9.33.

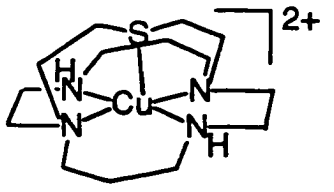

32
$[Cu(L2)](ClO_4)_2$

(17-Thia-1,5,8,12-tetraazabicyclo[6.6.5]nonadecane)copper Diperchlorate {$[Cu(L2)](ClO_4)_2$}. To the 2.5g (*ca.* 8.7 mmol) of crude **L2** free ligand oil was added 3.23g (8.7 mmol) copper(II) perchlorate in 100 mL distilled water. The copper complexed mixture was purified by chromatography over sephadex CM C-25 cation-exchange packing (2.5cm diam. x 20cm). The blue $[Cu(L2)](ClO_4)_2$ complex (third band) was eluted with 0.1M $NaClO_4$. The solution was taken to dryness under reduced pressure, dissolved in ethanol, filtered, and recrystallized from water. Yield: 1.75g (3.2 mmol), 11.8% from cyclam. IR: NH stretches, 3250 cm^{-1}, 3450 cm^{-1} (brd). Anal. Calcd. for $[Cu(C_{14}H_{30}N_4S)](Cl_2O_8)$: C, 30.63; H, 5.50; N, 10.21. Found: C, 30.23; H, 5.36; N, 9.61.

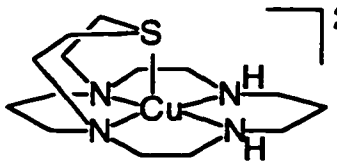

33
$[Cu(L3)](ClO_4)_2$

(14-Thia-1,4,8,11-tetraazabicyclo[9.5.3]nonadecane)copper Diperchlorate {$[Cu(L3)](ClO_4)_2$}. To a solution of the 0.419g (1.5 mmol) **L3** crude oil dissolved in 50 mL deionized water was added a solution of 0.600g, 1.6 mmol copper(II) perchlorate in 30 mL deionized water. The blue copper(II) complexed mixture was chromatographed over sephadex CM-C25 cation-exchange packing and eluted with 0.15M $NaClO_4$. The blue/violet solution was taken to dryness in vacuo, dissolved in 20 mL ethanol, filtered, then evaporated in vacuo. The resulting violet powder was recrystallized from water. Yield: 0.649g (1.2 mmol), (79%). IR: NH stretches, 3460 cm^{-1} (brd), 3515 cm^{-1} (brd). Anal. Calcd. for $[Cu(C_{14}H_{30}N_4S)](Cl_2O_8)$: C, 30.63; H, 5.51; N, 10.21. Found: C, 30.36; H, 5.37; N, 9.98.

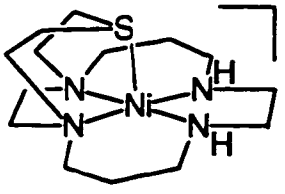

34
$[Ni(L1)](ClO_4)_2$

(15-Thia-1,5,8,12-tetraazabicyclo[10.5.2]nonadecane)nickel Diperchlorate $[Ni(L1)](ClO_4)_2$. The complex $[Ni([9]aneN_4S)](ClO_4)_2$ was synthesized according to the previously published[90] procedure by reaction of the free ligand (**L1**) with nickel(II) perchlorate in ethanolic or aqueous (pH 9-11) solution.

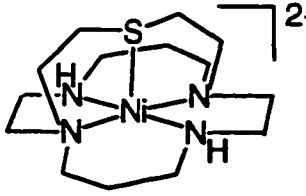

35
$[Ni(L2)](ClO_4)_2$

(17-Thia-1,5,8,12-tetraazabicyclo[6.6.5]nonadecane)nickel Diperchlorate $[Ni(L2)](ClO_4)_2$. To an aqueous solution (10mL, pH 9-10) of **L2** (66mg, 0.23 mmol) was added $[Ni(H_2O)_6](ClO_4)_2$ (84mg, 0.23 mmol) and the mixture refluxed for 2 h. to ensure complete coordination. The solution was evaporated to 1/2 its original volume, and an equal volume of

ethanol added. The solution was filtered to remove excess $[Ni(H_2O)_6](ClO_4)_2$ then recrystallized by slow evaporation to yield deep violet crystals. The crystals were washed with isopropanol then dried under vacuum. Yield: 42 mg (0.08 mmol, 33 %). Anal. Calcd. for $[Ni(C_{14}H_{30}N_4S)](ClO_4)_2$: C, 30.91; H, 5.56; N, 10.30. Found: C, 31.91; H, 6.06; N, 10.39. IR: NH stretches, 3250, 3100 cm^{-1}; ClO_4, 1090 cm^{-1}(brd), 620 cm^{-1}(s).

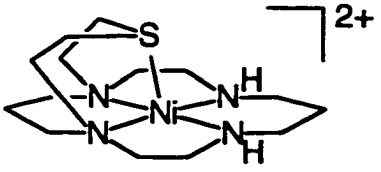

36
[Ni(**L3**)](acetate)$_2$
presumed structure

(14-Thia-1,4,8,11-tetraazabicyclo[9.5.3]nonadecane)nickel Diperchlorate [Ni(L3)](acetate)$_2$. To an acetonitrile solution (5mL) of **L3** (36mg, 0.12 mmol) was added Ni(acetate)$_2$ tetrahydrate (30mg, 0.12 mmol) in 5mL dry ethanol and the mixture refluxed for 0.5 h. to ensure complete coordination. Slow evaporation of the solution yielded pale violet crystals. The crystals were filtered off then dried under vacuum. Yield: 14 mg (0.025 mmol, 21.4 %). IR: NH stretches, 3250, 3130 cm^{-1}; ClO_4, 1100 cm^{-1}(brd), 620 cm^{-1}(s).

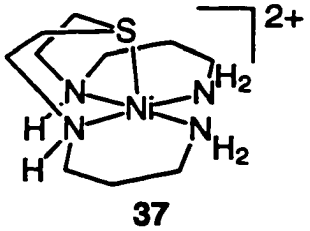

37
[Ni(**24**)](ClO$_4$)$_2$
proposed structure

(*Bis*(3,7-diaminoheptane)sulphide)nickel Diperchlorate {[Ni(24)](ClO$_4$)$_2$}. To a solution of 2.7 g (~16 mmol) of **20/24,** crude mixture (see section 8.5) in 50 mL deionized water was added a solution of 3.5 g (9.6 mmol) nickel(II) perchlorate in 10 mL deionized water. The solution was adjusted to pH 9 with NaOH and refluxed gently for 2 h. The resulting violet solution was filtered then chromatographed over sephadex CM-C25 cation-exchange packing. The blue product complex was eluted with 0.15M $NaClO_4$. The solution was taken to dryness in vacuo then dissolved in ethanol and filtered to remove the insoluble $NaClO_4$. The ethanol filtrate was taken to dryness and the resulting blue solid

was recrystallized from water. Yield: 640 mg (1.3 mmol), 8.1%. λ_{max} /nm (ε /M^{-1} cm^{-1}): 362(6.8), 577(4.8), 967(4.6). Anal. Calcd for $[Ni(C_{10}H_{26}N_4S)](Cl_2O_8)$: C, 24.41; H, 5.33; N, 11.39. Found: C, 24.25; H, 5.24; N, 10.89.

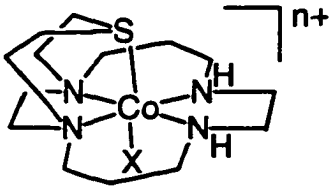

$[Co(L1)(X)](ClO_4)_2$
38: X = OH_2, n=3
39: X = Cl-, n=2
40: X = SCN-, n=2
41: X = $NCCH_3$, n=3

(15-Thia-1,5,8,12-tetraazabicyclo[10.5.2]nonadecane)cobalt(monoaquo) Triperchlorate $[Co([9]aneN_4S)(OH_2)](ClO_4)_3$. To an aqueous solution (25 mL, pH neutral) of [9]aneN$_4$S (**L1**) (140 mg, 0.49 mmol) was added an aqueous solution (25 mL, pH neutral) of $[Co(H_2O)_6](ClO_4)_2$ (200 mg, 0.55 mmol) and activated charcoal (0.2g). Oxygen was bubbled through the stirred mixture (room temperature) for 30 h. After filtration, *ca.* 2 -3 equivalents of $HClO_4$ were added then the dark red solution was recrystallized by slow evaporation. The sample was usually of sufficient purity for further use (based on the NMR spectrum), however, it was occasionally judged to be impure and therefore chromatographed over DOWEX 50X8-400 cation-exchange packing. The resulting red crystalline solid (*ca.* 110 mg) was dissolved in acetonitrile, filtered, then recrystallized by diffusion of diethyl ether to give burgundy crystals (66 mg) of $[Co([9]aneN_4S)(NCCH_3)](ClO_4)_3$ (**41**). Recrystallization from aqueous solution then afforded crystals of $[Co([9]aneN_4S)(OH_2)](ClO_4)_3$ dihydrate. Yield: 42 mg (0.063 mmol, 18%). Anal. Calcd. for $[Co(C_{14}H_{30}N_4S)](ClO_4)_3 \cdot 2H_2O$: C, 24.09; H, 5.20; N, 8.03. Found: C, 24.08; H, 4.86; N, 7.97. IR: NH stretches, 3480, 3360 cm^{-1}; CH bends, 1400 cm^{-1}; ClO_4, 565, 850cm^{-1}(s). ^{13}C-NMR (D_2O, ppm relative to TMS): 23.8 (1C, C-$\underline{C}H_2$-C); 32.9 (1C, $\underline{C}H_2$-S); 45.9, 51.9, 58.5, 59.0, 60.0 (5C, $\underline{C}H_2$-N).

[Co([9]aneN$_4$S)(Cl)](ClO$_4$)$_2$ (39). The chloro complex was prepared by reacting **L1** with one equivalent of cobalt(II) chloride under identical conditions to the procedure reported above for the aquo complex. Yield: 88% (crude); 25-30% (pure).

[Co([9]aneN$_4$S)(SCN)](ClO$_4$)$_2$ (40). To a solution of 3 mg [Co([9]aneN$_4$S)(OH$_2$)](ClO$_4$)$_3$ dihydrate in ~0.5 mL deionized water was added 2 mg NaSCN. The solution was refluxed for 1 h. then recrystallized by slow evaporation. Yield: 1.2 mg, 42%.

[Co([9]aneN$_4$S)(NCCH$_3$)](ClO$_4$)$_3$ (41). The synthesis of the acetonitrile coordinated complex (**41**) is described above in the synthesis of the aquo complex (**38**).

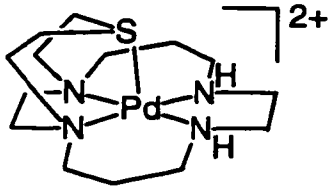

42
[Pd(**L1**)](PF$_6$)$_2$

(15-Thia-1,5,8,12-tetraazabicyclo[10.5.2]nonadecane)palladium diammonium hexafluorophosphate [Pd([9]aneN$_4$S)](PF$_6$)$_2$. To a solution of [9]aneN$_4$S (**L1**) (123.4 mg, 0.70 mmol) in 10 mL of benzonitrile was added a warm, filtered solution of $PdCl_2$ (200 mg, 0.70 mmol) in 10 mL of benzonitrile. The mixture was refluxed at 60 - 80 °C (N_2 atmosphere) for 2 h., then stirred overnight, after which a fine white powdery precipitate formed. The precipitate was separated by centrifugation, dissolved in dry ethanol (*ca.* 10 mL), then an equal volume of saturated NH_4PF_6 (2.3g, 0.014 mol, 10 equiv.) in ethanol was added. The solution was reduced to 10 mL by slow evaporation, filtered to remove excess NH_4PF_6, and the complex was recrystallized by slow diffusion of diethyl ether vapour. The resulting clear yellow crystals of [Pd([9]aneN$_4$S)](PF$_6$)$_2$ were separated by centrifugation then washed with diethyl ether:ethanol (3:2) and dried under vacuum. X-ray quality crystals were obtained by again recrystallizing from ethanol by slow diffusion of diethyl ether vapour. Yield: 58 mg (0.085

mmol, 12 %). Anal. Calcd. for $[Pd(C_{14}H_{30}N_4S)](PF_6)_2$: C, 24.63; H, 4.43; N, 8.21. Found: C, 24.08; H, 4.38; N, 8.18. IR: NH stretches, 3285 cm^{-1}; CH bends, 1390 cm^{-1}; PF_6, 850(brd), 555 cm^{-1}. ^{13}C-NMR (D_2O, ppm relative to TMS): 26.8 (1C, C-$\underline{C}H_2$-C); 32.6 (1C, $\underline{C}H_2$-S); 50.8, 54.0, 59.8, 61.4, 62.9 (5C, $\underline{C}H_2$-N).

$[Pd([9]aneN_4S)](PF_6)_2(ClO_4)$ (43). Solutions of the $[Pd(L1)]^{3+}$ complex were prepared in situ by oxidation with a stoichiometric defficiency of $NO^+ClO_4^-$. The tervalent ion was generated rapidly by the oxidation but was not very stable ($t_{1/2}$ < 5 min) at room temperature.

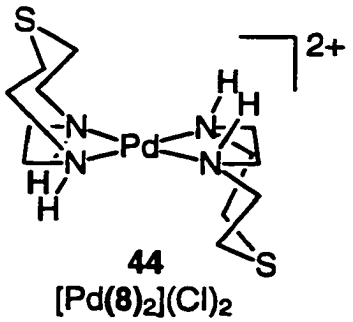

44
$[Pd(8)_2](Cl)_2$

***bis*(1-thia-4,7-diazacyclononane)palladium dichloride monohydrate $[Pd([9]aneN_2S)_2](Cl)_2 \cdot H_2O$.** To a solution of $[9]aneN_2S$ (**8**) (225 mg, 1.5 mmol) in 2.5 mL of ethanol was added a warm, filtered solution of $PdCl_2$ (266 mg, 1.5 mmol) in 5 mL of benzonitrile. The mixture was refluxed (N_2 atmosphere) for 2 h., after which a fine white powdery precipitate formed. The precipitate was separated by centrifugation, dissolved in 3 mL deionized water, and recrystallized by slow evaporation. The resulting X-ray quality, pale yellow crystals of $[Pd([9]aneN_2S)_2](Cl)_2 \cdot H_2O$ were separated by centrifugation, washed with diethyl ether:ethanol (3:2) and dried under vacuum. Yield: 110 mg (0.23 mmol, 16 %). Anal. Calcd. for $[Pd(C_{12}H_{28}N_4S)](Cl)_2 \cdot H_2O$: C, 30.68; H, 6.01; N, 11.93. Found: C, 29.45; H, 6.05; N, 11.44. IR: NH stretches, 3130 cm^{-1}(brd).

8.4. Synthesis of 1-Thia-4,8-diazacyclodecane-3,9-dione (23) using moderate stirring conditions:

1-Thia-4,8-diazacyclododecane-3,9-dione (23), [10]aneN_2S diamide. Dry, twice distilled chloroform was first prepared by refluxing 4.5 litres reagent grade chloroform (N_2 atmosphere) over ca. 200-250g phosphorous pentoxide for 12 h. The chloroform was fractionally distilled then refluxed for 12 h. over 50 g calcium hydride and fractionally distilled again. A 4.44 g, 0.060 mol sample of diaminopropane in 50 mL of chloroform and an 11.22 g, 0.060 mol sample of thiodiglycolic acid chloride (15) in 50 mL of chloroform were both added simultaneously from high precision dropping funnels over a period of 8 h. to 2.5 litres chloroform containing 50 g potassium carbonate (N_2 atmosphere, rm. temp.). The solution was mechanically stirred at 600 rpm. The resulting solution was filtered and the solvent removed in vacuo yielding a white solid. Yield: 1.67 g (0.0088 mol), 14.8%.

8.5. Synthesis of 1-Thia-4,8-diazacyclododecane (20) using excess borane:

1-Thia-4,8-diazacyclododecane (20). To 1.5 g of diamide mixture (23) was added 150 mL of 1M BH_3•THF under N_2 atmosphere. The mixture was stirred at room temperature for 20 min. then refluxed 8 h. The heat was removed from the resulting solution and the excess diborane was destroyed (**CAUTION**) by dropwise addition of ca. 20 - 50 mL absolute ethanol. The solution was taken to dryness on a rotary evaporator. The white solid residue was refluxed in 150 mL of 30% HCl in MeOH for 1.5 h. The solution was taken to dryness on a rotary evaporator then dissolved in ca. 50 mL 3M NaOH and extracted into 4 x 100 mL chloroform. The organic layers were combined, dried over Na_2SO_4 and taken to dryness. Typically, there would be ca. 1.0 g of crude product mixture in the form of a viscous pale brown oil.

REFERENCES

1. Martin, D. F. and Martin, B. B. *Coordination Compounds*; McGraw-Hill: New York, 1964, pp. 25.

2. Cabbiness, D. K.; Margerum, D. W. *J. Am Chem. Soc.* **1969,** *91*, 6540.

3. Ziola, R. F.; Extine, *M. Inorg. Chem.* **1981,** *20*, 2709.

4. Werner, A. *Neuere Anschauungen auf dem Gebieteder anorganischen Chemie* (1906). English translation: Hedley, E. P., Ed. *New Ideas On Inorganic Chemistry;* London Press, 1905.

5. Bethe, H. *Ann. Physik.* **1929**, *3(5)*, 135.

6 Wilkinson, G., Ed. *Comprehensive Coordination Chemistry: The Synthesis, Reactions, Properties and Applications of Coordination Compounds*; Permagon Press: Oxford, 1987, vol. 1-7.

7.(a) Meyers, R. T. *Inorg. Chem.* **1978,** *17*, 952. (b) Bell, C. F., Ed. *Principles and Applications of Metal Chelation;* Oxford University Press, 1979.

8. Lindoy, L., Ed. *The Chemistry of Macrocyclic Ligand Complexes*; University Press, Cambridge, 1989.

9. Melson, Gordon A., Ed. *Coordination Chemistry of Macrocyclic Compounds*; Plenum Press: New York, 1979, chapter 2: "Synthesis of Macrocyclic Complexes", p. 46.

10. Alphen, J. V. *Rec. Trav. Chim. Pays-Bas.* **1936,** *55*, 835.

11. Bosnich, B.; Poon, C. K.; Tobe, M. L. *Inorg. Chem.* **1965,** *4*, 1102. Bosnich, B.; Tobe, M. L; Webb, G. A. *Inorg. Chem.* **1965,** *4*, 1109.

12. Curtis, N. F. *J. Chem Soc.* **1960,** 4409. Curtis, N. F.; House, D. A. *Chem Ind.* **1961,** *42*, 1708.

13. Cabbiness, D. K.; Margerum, D. W. *J. Am. Chem. Soc.* **1969,** *91*, 6540.

14. Cabbiness, D. K.; Margerum, D. W. *J. Am. Chem. Soc.* **1970,** *92*, 2151.

15. Kodama, M.; Kimura, E. *J. Chem. Soc.,* Dalton Trans. **1983**, 2341.

16. Hinz, F. P.; Margerum, D. W. *Inorg. Chem.* **1974**, *13*, 2941.

17. Micheloni, M.; Paoletti, P.; Sabatini, A. *J. Chem. Soc., Dalton Trans.* **1983,** 1189.

18. Billo, E. J. *Inorg. Chem.* **1984,** *23*, 236.

19. Busch, D. H.; Farmery, K.; Goedken, V.; Katovic, A. C.; Melnyk, A. C.; Sperati, C. R.; Tokel, N. *Advan. Chem. Ser.* **1971,** *100*, 44.

20. Hay, R. W.; Bembi, R.; McLaren, F.; Moodie, W. T. *Inorganica Chimica Acta,* **1984,** *85*, 23.

21. Bertini, I.; Gray, H.; Lippard, S. J.; Valentine, J. S., Eds. *Bioinorganic Chemistry;* University Science Books: Mill Valley, California, 1994.

22. Hay, R. Ed. *Bio-Inorganic Chemistry;* Ellis Horwood Limited:Chichester, 1984.

23. Lippard, S. J. *Science* **1993,** *261*, 699.

24. Busch, D.; Alcock, N. W.; *Chem. Rev.* **1994,** *94(3),* 585.

25. Kimura, E; Shiota, T.; Koike, T.; Shiro, M.; Kodama, M. J. *Am. Chem. Soc.* **1990,** *112*, 5805.

26. Kimura, E.; Koike, T. *Comments Inorg. Chem.* **1991,** *11(5,6)*, 285.

27. Henrick, K.; Tasker, P. A.; Lindoy, L. F. *Prog. Inorg. Chem.* **1985,** *33*, 1.

28. Hoard, J. L.; Smith, K. M. Ed. *Porphyrins and Metalloporphyrins*; Elsevier, Amsterdam, 1975, Ch. 8.

29. Collman, J. P.; Schneider, P. W. *Inorg. Chem.* **1966,** *5*,1380.

30. Thöm, V. J.; Foc, C. C.; Boeyens, J. C.; Hancock, R. D. J. *Am. Chem. Soc.* **1984,** *106*, 5947.

31. Connolly, P. J.; Billo, E. J. *Inorg. Chem.* **1987,** *26*, 3224.

32. Hay, R. W.; Norman, P. R. *Inorg. Chim. Acta. Lett.* **1980,** *45*, 139. Hertli, L.; Kaden, T. A. *Helv. Chim. Acta.* **1981,** 64, 33. Richens, D. T.; Adzamli, I. K.; Leupin, P.;

Sykes, A. G. *Inorg. Chem.* **1984,** *23*, 3065. Moore, P.; Sachinidis, J.; Willey, G. R. J. *Chem. Soc., Chem. Commun.* **1983**, 522.

33. Wagner, F.; Barefield, E. K. *Inorg. Chem.* **1976,** *15*, 408.

34. Hay, R. W.; Bembi, R.; Moodie, W. T.; Norman, P. R. J. *Chem. Soc., Dalton Trans.* **1982**, 2131.

35. Mitewa, M.; Bontchev, P. R. *Coord. Chem. Rev.* **1994,** *135/136*, 129.

36. Legget, G. H.; Dunn, B. C.; Vande Linde, A. M. Q.; Ochrymowycz, L. A.; Rorabacher, D. B. *Inorg. Chem.* **1993,** *32*, 5911.

37. Fabbrizzi, L. *Comments Inorg. Chem.* **1985,** *4(1)*, 33.

38. Haines, R. I.; McAuley, A. *Coord. Chem. Rev.* **1981,** *39*, 77.

39. Lovecchio, F. V.; Gore, E. S.; Busch, D. H. J. *Am. Chem. Soc.* **1974,** *96*, 3109.

40. House, D. A. *Comments Inorg. Chem.* **1994,** *16(4)*, 229.

41. Lay, P. A. *Comments Inorg. Chem.* **1991,** *11(5/6)*, 235.

42. Swaddle, T. W. *Comments Inorg. Chem.* **1991,** *12(4)*, 237.

43. Jordan, R. B., Ed. *Reaction Mechanisms of Inorganic and Organometallic Systems;* Oxford University Press: New York, 1991.

44. Poon, C. K. *Coord. Chem. Rev.* **1973,** *10*, 1.

45. Margerum, D. W.; Cayley, Weatherburn, D. C.; Pagenkopt, *Kinetics and Mechanisms of Complex Formation and Ligand Exchange*, in *Coordination Chemistry*; A. E. Martell Ed., ACS monograph, 1978, Vol. 2, p. 1-120.

46. Wilkins, R. G., Ed., *The Study of Kinetics and Mechanism of Reactions of Transition Metal Complexes*; Allyn and Bacon, Inc.: Boston, 1974.

47. Sutin, N. *Acc. Chem. Res.* **1982,** *15*, 275.

48. Marcus, R. A. *Annu. Rev. Phys. Chem.* **1964,** *15*, 155.

49. Sigel, H., Ed., *Metal Ions in Biological Systems;* Marcel Dekker, Inc.: New York, vol. 27.

50. Williams, R. J. P.; da Silva, J. R. R. F.,*Eds. New Trends in Bio-inorganic Chemistry;* Academic Press: London, 1978.

51. Cooper, S. R., Ed. *Crown Compounds: Towards Future Applications*; VCH: New York, N. Y.,1992.

52. Dietrich, B. *Macrocyclic Chemistry: Aspects of Organic and Inorganic Supramolecular Chemistry*; VCH: New York, N. Y., B. Dietrich, P. Viout, J.-M. Lehn, Eds., 1993.

53 Brown, G. M.; Brunschwig, B. S.; Creutz, C.; Endicott, J. F.; Sutin, N. *J. Am. Chem. Soc.* **1979**, *101*, 1298. Fujita, E.; Szalda, D. J.; Creutz, C.; Endicott, J. F.; Sutin, N. *J. Am. Chem. Soc.* **1988**, *110*, 4870.

54. Wolfe, R. S. *Trends Biochem. Sci.* **1985**, 396.

55. Fisher, B.; Eisenberg, R. *J. Am. Chem. Soc.*, **1980**, *102*, 7361

56. Bely, M.; Collin, J. P.; Ruppert, R.; Sauvage, J. P. *J. Chem. Soc., Chem Commun.*, **1984**, 1315. Ibid. J. *Am. Chem. Soc.*, **1986**, *108*, 7461.

57. Fujita, E.; Creutz, C.; Sutin, N.; Brunschwig, S. *Inorg. Chem.* **1993**, *32*, 2657.

58. Shankaran, K.; Sloan, C. P.; Sniekus, V. *Tetrahedron Lett.* 1985, 26, 6001. Beckwith, A. J.; Gara, W. B. J. *Chem. Soc., Perkin II.* **1975**, 795.

59.Ozaki, S.; Matsushita, H.; Ohmori, H. J. J. *Chem. Soc., Chem. Commun.* **1992**, 1120. Ozaki, S.; Horiguchi, I.; Matsushita, H.; Ohmori, H. J. *Tetrahedron Lett.* 1994, *35*, 725. Mubarak, M. S.; Peters, D. G. J. *Electroanal. Chem.* **1992**, *332*, 127.

60. Olivero, S.; Clinet, J. C.; Dunach, E. *Tetrahedron Lett.* **1995**, *36(25)*, 4429.

61. Lehn, J. M.; Sauvage, J. P. *J. Am. Chem. Soc.* **1975**, *97*, 6700.

62. Kauffmann, E.; Lehn, J. M.; Savauge, J. P. *Helvetica Chimica Acta.* **1976**, *59*, 1099.

63. C. Xu, Ph.D. Dissertation, University of Victoria, 1991.

64. Cooper, S. R. *Acc. Chem. Res.* **1988**, *21*, 141.

65. Beinnert, H.; *Coord. Chem. Rev.* **1980**, *33*, 55.

66. Cammack, R. Nickel in metalloproteins; Sykes, A. G., Ed.; Advances in Inorganic Chemistry, Vol. 32, Academic Press, Inc.: New York, 1988.

67. Kuehn, C. G.; Isied S. S. *Prog. Inorg. Chem.* **1980**, *27*, 153.

68. Setzer, W. N.; Ogle, C. A.; Wilson, G. S.; Glass, R. S. *Inorg. Chem.* **1983**, *22*, 266.

69.Rorabacher, D. B.; Martin, M. J.; Koenigbauer, M. J.; Malik, M.; Schroeder, R. R.; Endicott, J. F.; Ochrymowycz, L. A. In Copper Coordination Chemistry: Biochemical and Inorganic Perspectives; Karlin, K. D.; Zubieta, J., Eds.; Adenine Press: Guilderland, NY, 1983, pp. 167.

70. Busch, D. H. *Acc. Chem. Res.* **1978**, *11*, 392.

71. Thöm, V. J.; Fox, C. C.; Boeyens, J. C. A.; Hancock, R. D. J. *Am. Chem. Soc.* **1984**, *106*, 5947. Hancock, R. D.; Wade, P. W.; Ngwenya, M. P.; de Sousa, A. S.; Damu, K. V. **1990**, *29*, 1968.

72. Parker, D., Ed. *Macrocycle Synthesis. A Practical Approach*; Oxford University Press: Oxford, 1996.

73. Karbach, S.; Lohr, W.; Vogtle, F. *Journal of Chemical Research (S).* **1981**, 314.

74. Graf, E.; Lehn, J. M. J. *Am. Chem. Soc.* **1975**, 97, 5022. Graf, E.; Lehn, J. M. *Helv. Chim. Acta.* **1981**, *64*, 1040.

75. Travis, K.; Busch, D. H. *Inorg. Chem.* **1974**, *13*, 2591.

76. Tabushi, I.; Tanaguchi, Y.; Hidefumi, K.*Tetrahedron Letters.* **1977**, *12*, 1049.

77. Richman, J. E.; Atkins, T. J. *J. Am. Chem. Soc.* **1974**, *96*, 2268.

78. Cram, D. J.; Lehn, J. M. *J. Am. Chem. Soc.* **1985**, *107*, 3657.

79. Ogawa, S.; Yamaguchi, T.; Gotoh, N. *J. Chem. Soc., Perkin Trans. I.* **1974**, 976.

80. Carver, F. J.; Hunter, C. A.; Shannon, R. J. *J. Chem. Soc., Chem. Comm.* **1994,** 1277.

81. Krakowiak, K. E.; Bradshaw J. S.; Izatt R. M. *J. Org. Chem.* **1990,** *55*, 3364.

82. Barefield, E. K.; Wagner, F.; Herlinger, A. W.; Dahl, A. R.*Inorg. Synth.* **1976,** *16*, 220.

83.An, H.; Bradshaw, J. S.; Izatt, R. M. *Chem. Rev.* **1992,** *92*, 543. Izatt, R. M.; Pawlak, K.; Bradshaw, J. S. *Chem. Rev.* **1995,** *95*, 2529.

84. Voronkov, M. G.; Knutov, V. I. Russ. *Chem. Rev.* **1991,** *60(12)*, 1293.

85.Hart, S. M.; Boeyens, J. C. A.; Michael, J. P.; Hancock, R. D. J. *Chem. Soc., Dalton Trans.* **1983,** 1601.

86. Wagnon, B. K.; Jackels, S. C. *Inorg. Chem.* **1989,** *28*, 1923.

87. Martin, A. E.; Ford, T. M.; Bulkowski, J. M. *J. Org. Chem.* **1982,** *47*, 412.

88. Boeyens, J. C. A.; Dobson, S. M.; Hancock, R. D. *Inorg. Chem.* **1985,** *24*, 3073.

89. Koyama, H.; Yoshino, T. *Bull. Chem. Soc. Jpn.* **1972,** *45*, 481.

90. Fortier, D. G.; McAuley, A. *Inorg. Chem.* **1989,** *28*, 655.

91. Barefield, E. K.; Wagner, F.; Hodges, K. D. *Inorg. Chem.* **1976,** *15*, 1370.

92. Fortier, D. G.; McAuley, A. *J. Am. Chem. Soc.* **1990,** *112(7)*, 2640.

93. Beveridge, K.; McAuley, A.; Xu, C. *Inorg. Chem.* **1991,** *30(9)*, 2074.

94. Balasubramanian, S. *Inorg. Chem.* **1987,** *26*, 553.

95. Goedken, V. L.; Busch, D. H. *Inorg. Chem.* **1971,** *10*, 2697.

96.(a) Cary, F. A.; Sundberg, R. J., Eds. *Advanced Organic Chemistry, Part B: Reactions and Synthesis. Third edition; Plenum Press: New York and London,* **1990,** p. 145.

(b) Cary, F. A.; Sundberg, R. J., Eds. *Advanced Organic Chemistry, Part A: Structure and Mechanisms. Third edition; Plenum Press: New York and London,* **1990,** p. 467.

97. Bianchi, A.; Garcia-España, E.; Micheloni, M.; Nardi, N.; Vizza, F.*Inorg. Chem.* **1986,** *25,* 4379.

98. Brown, H. C.; Heim, P. *J. Org. Chem.* **1973,** *38(5),* 912.

99. Dietrich, B.; Lehn, J. M.; Sauvage, J. P.; Blanzat, J. *Tetrahedron.* **1973,** *29,* 1629.

100. Rodopolous, T. Unpublished work, 1995.

101. Ramasubbu, A.; Wainwright, K. P.*J. Chem. Soc., Chem. Comm.* **1982,** 277.

102. Buoen, S.; Dale, J. *Acta Chemica Scandinavia B.* **1986,** *40,* 141.

103. Weisman, G. R.; Rogers, M. E.; Wong, E. H.; Jasinski, J. P.; Paight, E. S. *J.* Am. *Chem. Soc.* **1990,** *112(23),* 8604.

104. Helps, I. M.; Parker, D.; Morphy, J. R.; Chapman, J. *Tetrahedron.* **1989,** *45(1),* 219. Chapman, J.; Ferguson, G.; Gallagher, J. F.; Jennings, M. C.; Parker, D.*J. Chem. Soc., Dalton Trans.* **1992,** 345. Helps, I. M.; Parker, D.; Chapman, J.; Ferguson, G. *J. Chem. Soc., Chem. Comm.* **1988,** 1094.

105. Kovacs, Z.; Sherry, D. J. *Chem. Soc., Chem. Commun.* **1995,** 185.

106. Desreux, J. F.; Merciny, E.; Loncin, M. F.*Inorg. Chem.* **1981,** *20,* 987.

107. Springborg, J.; Kofod, P.; Olsen, C. E.; Toftlund, H.; Sotofte, I. *Acta Chemica Scandinavia.* **1995,** *49,* 547.

108. Küppers, H. J.; Wieghardt, K.; Nuber, B.; Weiss, J.; Eckhard, B.; Trautwein, A. X. *Inorg. Chem.* **1987,** *26,* 3762.

109. Wambeke, D. M.; Lippens, W.; Hermann, G. G.; Goeminne, A. M. Bull.*Soc. Chim. Belg.* **1989,** *98(5),* 307. Chandrasekhar, S.; McAuley, A.*J. Chem. Soc., Dalton Trans.* **1992,** 2967.

110. James, T. Chemistry Dept., University of Victoria, 1992. Private communications.

111. Iyer, S. Chemistry Dept., University of Victoria, 1995. Private communications.

112. Bradshaw, J.; An, H.; Krakowiak, K.; Wang, T.; Zhu, C.; Izatt, R. *J. Org. Chem.* **1992**, *57*, 6112.

113. Searle, G. H.; Geue, R. J.; *Aust. J. Chem.* **1984**, *37*, 959. S. Subramanian, Ph.D. Dissertation, University of Victoria, 1989.

114.(a) Cary, F. A.; Sundberg, R. J., Eds. *Advanced Organic Chemistry, Part A: Structure and Mechanisms. Third edition; Plenum Press: New York and London,* **1990**, p. 147, and references therein. (b) ibid p. 63. (c) ibid p. 116-118.

115. *J. Org. Chem.* **1994**, *59*, 2186.

116. Graham, P. G.; Weatherburn, D. C. *Aust. J. Chem.* **1983**, *36*, 2349.

117. Alder, R. W.; Mowlam, R. W.; Vachon, D. J.; Weisman, G. R. *J. Chem. Soc., Chem. Commun.* **1992**, 507.

118. Jurczak, J.; Stankiewicz, T.; Salański, P.; Kaspryk, S.; Lipkowski, P. *Tetrahedron.* **1993**, *49(7)*, 1478.

119.Skoog, Douglas A., Ed. *Principles of Instrumental Analysis. Third edition; Sauders College Publishing: New York,* **1985**, chapter 27.

120. D. G. Fortier, Ph.D. Dissertation, University of Victoria, 1988.

121.(a) Nöth, H.; Wrackmeyer, B. In *Nuclear Magnetic Resonance Spectroscopy of Boron Compounds*; P. Diehl, E. Fluck, R. Kosfield, Eds., ISBN: Springer-Verlag, Berlin, Heidelberg, New York, 1978. (b) Ishihara, K.; Nagasawa, A.; Umemoto, K.; Ito, H.; Saito, K. *Inorg. Chem.* **1994**, *33*, 3811.

122. Helps, I.; Parker, D.; Jankowski, K. J.; Chapman, J.; Nicholson, P. E. *J. Chem. Soc., Perkin Trans I.* **1989**, 2079.

123. Bullens, G. J. *J. Chem. Soc., Dalton Trans.* **1981**, 511. Richman, J. E.; Young, N. C.; Anderson, L. L. *J. Am. Chem. Soc.* **1980**, *102*, 5790.

124. Hancock, R. D. *J. Chem. Ed.* **1992**, *69(8)*, 615.

125. S. Chandrasakar, Ph.D. Dissertation, University of Victoria, 1992.

126. Cotton, F. A.; Wilkinson, G., Eds. In *Advanced Inorganic Chemistry*; John Wiley and Sons: New York, 1986.

127. C. Xu., University of Victoria, unpublished results.

128. Rodopoulos, T. unpublished results, 1996. Beveridge, K. A.; McAuley, A.; Xu, C. *Inorg. Chem.*, **1991**, *30(9)*, 2074.

129. Bradshaw, J. S.; Krakowiak, K. E.; Izatt, R. M. *J. Heterocyclic Chem.* **1989**, *26*, 1431.

130. (a)Cary, F. A.; Sundberg, R. J., Eds. *Advanced Organic Chemistry, Part B: Reactions and Synthesis. Third edition; Plenum Press: New York and London,* **1990,** p. 120. (b) ibid. p. 113.

131. Lawrence, G. A.; Lye, P. G. *Comments Inorg. Chem.* **1994**, *15(5,6)*, 339.

132. Billo, E. J.; Connolly, P. J.; Sardella, D. J.; Jasinski, J. P.; Butcher, R. J.*Inorganic Chimica Acta* **1995**, 19.

133. (a)B. Cameron, Ph.D. Dissertation, University of Victoria, 1993.
(b) L. Cameron, private communications, University of Victoria, 1995. Zabicky, J., Ed. *The Chemistry of Amides*; Interscience Publishers: London, 1970. Wilberg, K. B.; Rablen, P. R.; Rush, D. J.; Keith, T. A. J.*Am. Chem. Soc.* **1995**, *117*, 4261.

134. Bencini, A.; Bianchi, A.; Bazzicalupi, C.; Ciampolini, M.; Fusi, V.; Micheloni, M.; Nardi, N.; Paoli, P.; *Valtancoli, B. Supramolecular Chemistry,* **1994,** *3*, 141.

135. Wareham, R. S.; Kilburn, J. D.; Turner, D. L.; Rees, N. H.; Holmes, D. S. Angew. *Chem. Int. Ed. Engl.* **1995**, *34(23/24)*, 2660.

136. Simmons, H. E.; Park, C. H.; J. *Am. Chem. Soc.* **1968**, *90*, 2429. Simmons, H. E.; Park, C. H.; Uyeda, R. T.; Habibi, M. F. *Trans. N. Y. Acad. Sci., Ser. II* **1979**, 2577.

137. Katritzky, A. R.; Patel, R. C.; Riddell, F. G. Angew.*Chem. Int. Ed. Engl.* **1981**, *20*, 521.

138. Alder, R. W.; Heilbronner, E.; Honegger, E.; McEwen, A. B.; Moss R. E.; Olefirowicz, E.; Petillo, P. A.; Sessions, R. B.; Weisman, G. R.; White, J. M.; Yang, Z. *J.* Am. *Chem. Soc.* **1993**, *115*, 6580.

139. Lipkowitz, K. B. *J. Chem. Ed.* **1995**, *72(12)*, 1070.

140. Kofman, V.; Farver, O.; Pecht, I.; Goldfarb, D. *J. Am. Chem. Soc.* **1996**, *118*, 1201.

141. Gillian, E. N.; Anderson, B. F.; Baker, E. N. *J. Am. Chem. Soc.* **1986**, *108*, 2784.

142. Soloman, E. I.; Baldwin, M. J.; Lowery, M. D. *Chem. Rev.* **1992**, *92*, 521.

143. Cho, K. C.; Che, C. M.; Ng, K. M.; Choy, C. L. *J. Am. Chem. Soc.* **1986**, *108*, 2814.

144. Tsukihara, T.; Aoyama, H.; Yamashita, E.; Tomizaki, T.; Yamaguchi, H.; Shinzawa-Itoh, K.; Nakashima, R.; Yaono, R.; Yoshikawa, S. *Science*, **1995**, *269*, 1069.

145. Ryden, L., In *Copper Proteins and Copper Enzymes*, Lontie, R., Ed.; CRC Press: Boca Raton, FL, 1984; Vol. 3, pp. 157.

146. Fabrizzi, L.; Poggi, A. *J. Chem. Soc., Dalton Trans.* **1984**, 1495.

147. Bernardo, M. M.; Robandt, P. V.; Schroeder, R. R.; Rorabacher, D. B. *J. Am. Chem. Soc.* **1989**, *111*, 1224.

148. Sima, J.; Labuda, J. *Comments Inorg. Chem.* **1993**, *15(2)*, 93.

149. Hosken, G. D.; Hancock, R. D. *J. Chem. Soc., Chem. Commun.* **1994**, 1363. Weisman, G. R.; Wong, E. H.; Hill, D. C.; Rogers, M. E.; Reed, D. P.; Calabrese, J. *J. Chem. Soc., Chem. Commun.* **1996**, 947.

150. Beguin, C.; Chautempts, P.; Marzouki, A. E.; Pierre, J.-L.; Refaif, S. M.; Serratrice, G.; Saint-Aman, E.; Rey, P. *J. Chem. Soc., Dalton Trans.* **1995**, 1939. Sivagnanam, U.; Palaniandavar, M. *J. Chem. Soc., Dalton Trans.* **1994**, 2277.

151. Hung, Y.; Martin, L.; Jackels, S.; Tait, A. M.; Busch, D. H. *J. Am. Chem Soc.* **1977**, *99(12)*, 4029.

152. Comba, P.; Zimmer, M. *J. Chem. Ed.* **1996**, *73(2)*, 108.

153. Burton, V. J.; Deeth, R. J. *J. Chem. Soc., Chem. Commun.* **1995**, 573.

154. Gerloch, M.; Woolley, R. G. *J. Chem. Soc., Dalton Trans.* **1981**, 1714.

155. Forsyth, G. A.; Lockhart, J. C. *J. Chem. Soc., Dalton Trans.* **1994**, 2243. Forsyth, G. A.; Lockhart, J. C. *Supramolecular Chem.* **1994**, *4*, 17.

156. Hedwig, G. R.; Love, J. L.; Powell, H. K. J. *Aust. J. Chem.* **1970**, *23*, 981.

157. Addison, A. W.; Sinn, E. *Inorg. Chem.* **1983**, *22*, 1225.

158. Hay, R. W.; Bembi, R.; Moodie, W. T.; Norman, P. R. *J. Chem. Soc., Dalton Trans.* **1982**, 2131.

159. Siddiqui, S.; Shepherd, R. E. *Inorg. Chem.* **1986**, *25*, 3869.

160. Proctor, I. M.; Hathaway, B. J.; Billing, D. E.; Dudley, R.; Nicholls, P. *J. Chem. Soc. A.* **1969**, 1192. Billing, D. E.; Dudley, R.;Hathaway, B. J.; Tomlinson, A. A. G. *J. Chem. Soc. A.* **1971**, 691.

161. Sivagnanam, U.; Palaniandavar, M. *J. Chem. Soc., Dalton Trans.* **1994**, 2277.

162. Hartman, J. R.; Cooper, S. R. *J. Am. Chem. Soc.* **1986**, *108*, 1202.

163. Fabrizzi, L.; Poggi, A.; Zanello, P. *J. Chem. Soc., Dalton Trans.* **1983**, 2191.

164. Chautemps, P.; Gellon, G.; Morin, B.; Pierre, J. L.; Provent, C.; Refaif, S. M.; Beguin, C. G.; Marzouki, A. E.; Serratrice, G.; Saint-Aman, E. *Bull. Soc. Chim. Fr.* **1994**, *131*, 434.

165. Beguin, C. G.; Chautemps, P.; Marzouki, A. E.; Pierre, J. L.; Provent, C.; Refaif, S. M.; Serratrice, G.; Saint-Aman, E.; Rey, P. *J. Chem. Soc., Dalton Trans.* **1995**, 1939.

166. Jabri, E.; Carr, M. B.; Hausinger, R. P.; Karplus, P. A. *Science* **1995**, *268*, 998.

167. Halcrow, M. A.; Christou, G. *Chem. Rev.* **1994**, *94*, 2421.

168. Drain, C. M.; Sable, D. B.; Corden, B. B. *Inorg. Chem.* **1990**, *29*, 1428.

169. Hon, H.; Olson, K. D.; Summers, M. F.; Wolfe, R. S. *Comments. Inorg. Chem.* **1993**, *15(1)*, 1.

170. Lin, S.; Jaun, B. *Helv. Chim. Acta.* **1992**, *74*, 1725. Ibid. *75*, 1479.

171. Albracht, S. P. J.; Ankel-Fuchs, D.; Bocher, R.; Ellerman, J.; Moll, J.; van der Zwann, J. W.; Thaur, R. K. *Biochim. Biophys. Acta.* **1988**, *955*, 86. Albracht, S. P. J.; Ankel-Fuchs, D.; van der Zwann, J. W.; Fontijn, R. D.; Thaur, R. K.*Biochim. Biophys. Acta.* **1986**, *870*, 50.

172. Eidness, M. K.; Sullivan, R. J.; Schwartz, J. R.; Hartzell, P. L.; Wolfe, R. S.; Flank, A.; Cramer, S. P.; Scott, R. A. *J. Am. Chem. Soc.* **1986**, *108*, 3120.

173. Suh, M. P.; Kim, H. K.; Kim, M. J.; Oh, K. Y.*Inorg. Chem.* **1992**, *31*, 3620. Suh, M. P; Lee, Y. J.; Jeong, J. W. *J. Chem. Soc., Dalton Trans.* **1995**, 1577. Suh, M. P.; Oh, K. Y.; Lee, J. W.; Bae, Y. Y. *J. Am. Chem. Soc.* **1996**, *118*, 777.

174. Kimura, E.; Machida, R.; Kodama, M.*J. Am. Chem. Soc.* **1984**, *106*, 5497.

175. Kimura, E. *Pure Appl. Chem.* **1986**, *58*, 1461.

176. Drago, Russel S., Ed. In *Physical Methods in Chemistry*; W. B. Saunders Company: Philadelphia, London, Toronto, 1977, chapter 10.

177. Rowley, D. A.; Drago, R. S. *Inorg. Chem.***1968**, *7(4)*, 795.

178. Lever, A. B. P. *Coord. Chem. Rev.* **1982**, *43*, 63.

179. Martin, L. Y.; Sperati, C. R.; Busch, D. H. *J. Am. Chem. Soc.* **1977**, *99(9)*, 2968.

180. Sperati, C. R., Ph.D thesis, Ohio State University, 1971.

181. Brubaker, G. R.; Busch, D. H. *Inorg. Chem.* **1966**, *5*, 2114.

182. Wentworth, R. A. D.; Piper, T. S. *Inorg. Chem.* **1965**, *4(5)*, 709.

183. Lever, A. B. P. *Coord. Chem. Rev.* **1968**, *3*, 119.

184. Barefield, E. K.; Wagner, F.*Inorg. Chem.* **1973**, *12(10)*, 2435.

185. Ciampolini, M.; Micheloni, M.; Vizza, F.; Zanobini, F.; Chimichi, S.; Dapporto, P*J. Chem. Soc., Dalton Trans.* **1986**, 505.

186. Olson, D. C.; Vasilevskis, J.*Inorg. Chem.* **1969**, *8*, 1611; *ibid.* **1971**, *10*, 463.

187. Rillema, D. P.; Endicott, J. F.; Papaconstantinou, E.*Inorg. Chem.* **1971**, *10*, 1739.

188. Van der Merwe, M.; Boeyens, J. C. A.; Hancock, R. D. *Inorg. Chem.* **1983**, *22*, 3490.

189. Atkins, P. W., Ed. *Physical Chemistry*; W. H. Freeman and Company: New York, third edition, 1986, chapter 11.

190. Dehayes, L. J.; Busch, D. H. *Inorg. Chem.* **1973**, *12*, 1505, 2010.

191. Hung, Y.; Martin, L. Y.; Jackels, S. C.; Tait, A. M.; Busch, D. H. *J. Am. Chem. Soc.* **1977**, *99(12)*, 4029.

192. Baldwin, M. E.; Chan, S. C.; Tobe, M. L. *J. Chem. Soc.* **1961**, 4637.

193. Jaynes, B. S.; Ren, T.; Liu, S.; Lippard, S. J. *J. Am. Chem. Soc.* **1992**, *114*, 9670.

194. Bushnell, G. W.; Fortier, D.; McAuley, A.*Inorg. Chem.* **1988**, *27*, 2626.

195. Saito, Y., *Spectroscopy and Structure of Metal Chelate Compounds*; K. Nakamoto and P. J. McCarthy, Ed., Wiley: New York, N. Y., 1968.

196. Yamashita, M.; Ito, H.; Toriumi, K.; Ito, T. *Inorg. Chem.* **1983**, *22(10)*, 1566.

197. Hunter, G.; McAuley, A.; Whitcombe, T. W.*Inorg. Chem.* **1988**, *27*, 2634.

198. Blake, A. J.; Crofts, R. D.; de Groot, B.; Schroder, M. *J. Chem. Soc., Dalton Trans.* **1993**, 485.

199. Blake, A. J.; Holder, A. J.; Hyde, T. I.; Schroder, M. *J. Chem. Soc., Chem. Commun.* **1987**, 987.

200. B. Chak, Ph.D. dissertation, University of Victoria, 1993.

201. Hartman, J. R.; Hintsa, E. J.; Cooper, S. R. *J. Chem. Soc., Chem. Commun.* **1984**, 386.

202. Carlin, R. L.; Weissberger, E. *Inorg. Chem.* **1964**, *3*, 611

203. Orpen, A. G.; Connelly, N. G.; *J. Chem. Soc., Chem. Commun.* **1985**, 1310.

204. Krogh-Jespersen, K.; Zhang, X.; Ding, Y.; Westbrook, J. D.; Potenza, J. A.; Schugar, H. J. *J. Am. Chem. Soc.* **1992**, *114*, 4345-4353. Krogh-Jespersen, K.; Zhang, X.; Westbrook, J. D.; Fikar, R.; Nayak, K.; Kwik, W-L.; Potenza, J. A.; Schugar, H. J. *J. Am. Chem. Soc.* **1989**, *111*, 4082-4091.

205. Jackels, S. C.; Farmery, K.; Barefield, E. K.; Rose, N. J.; Busch, D. *Inorg. Chem.* **1972**, *11*, 2893.

206. Beaumont, R. C. *Inorg. Chem.* **1969**, *8*, 1805. Hawkins, C. J.; Sargeson, A. M.; Searle, G. H. *Aust. J. Chem.* **1964**, *17*, 598.

207. Fabrizzi, L. *Comments Inorg. Chem.* **1985**, *4*, 33.

208. Barefield, E. K.; Mocella, M. T.; *J. Am. Chem. Soc.* **1975**, *97*, 4238.

209. Maruthamuthu, P.; Patterson, L. K.; Ferraudi, G. *Inorg. Chem.* **1978**, *17*, 3157.

210. De Santis, G.; Fabrizzi, L.; Poggi, A.; Taglietti, A. *Inorg. Chem.* **1994**, *33*, 134.

211. Pohl, K.; Wieghardt, K.; Kaim, W.; Steenkem, S. *Inorg. Chem.* **1988**, *27*, 440.

212. Comba, P.; Jackson, W. G.; Marty, W.; Zipper, L. *Helvetica Chimica Acta.* **1992**, *75*, 1172. Ahmed, E.; Tobe, M. L. *Inorg. Chem.* **1974**, *13(12)*, 2956.

213. Goodall, D. M.; Hardy, M. J. *J. Chem. Soc., Chem. Comm.* **1975**, 919.

214. B. Cameron and D. A. House, unpublished results.

215. Comba, P.; Jackson, W. G.; Marty, W.; Zipper, L. *Helv. Chim.. Acta.* **1992**, *75*, 1172.

216. Jackson, W. G.; McGregor, B. C.; Jurisson, S. S. *Inorg. Chem.*, **1987**, *26*, 1286-1291.

217. Reid, G.; Blake, A. J.; Hyde, T. I.; Schröder, M. *J. Chem. Soc., Chem. Commun.* **1989**, 1397.

218. Allinger, N. L. *J. Am. Chem. Soc.* **1977**, *99*, 8127.

219. Beveridge, K.; McAuley, A.; Xu, C. *Inorg. Chem.* **1991**, *30*, 2074.

APPENDIX I: Calculation of Dq^{xy} and Dq^{z} ligand field splitting parameters for the three $[Ni(N_4S\text{-bicycle})(solv)]^{2+}$ isomers.

i) $[Ni([9]aneN_4S)(solv)]^{2+}$:

$E(^3B_{2g}) - E(^3B_{1g}) = 10Dq^{xy} = 11{,}834\ cm^{-1}$ (845 nm)

$Dq^{xy} = 1183\ cm^{-1}$, $\sim 1180\ cm^{-1}$

$E(^3E_g^a) - E(^3B_{1g}) = 9{,}615\ cm^{-1}$ (1040 nm) $= 10\ Dq^{xy} - (35/4)D_t$

$D_t = 254\ cm^{-1}$

$D_t = 254\ cm^{-1} = (4/7)[Dq^{xy} - Dq^{z}]$

$Dq^{z} = 736\ cm^{-1}$, $\sim 740\ cm^{-1}$

ii) $[Ni([10]aneN_4S)(solv)]^{2+}$:

$E(^3B_{2g}) - E(^3B_{1g}) = 10Dq^{xy} = 11{,}891\ cm^{-1}$ (841 nm)

$Dq^{xy} = 1190\ cm^{-1}$, $\sim 1190\ cm^{-1}$

$E(^3E_g^a) - E(^3B_{1g}) = 9{,}524\ cm^{-1}$ (1050 nm) $= 10\ Dq^{xy} - (35/4)D_t$

$D_t = 271\ cm^{-1}$

$D_t = 271\ cm^{-1} = (4/7)[Dq^{xy} - Dq^{z}]$

$Dq^{z} = 716\ cm^{-1}$, $\sim 720\ cm^{-1}$

iii) $[Ni(hemi\text{-}cryptN_4S)(solv)]^{2+}$:

$E(^3B_{2g}) - E(^3B_{1g}) = 10Dq^{xy} = 12{,}240\ cm^{-1}$ (817 nm)

$Dq^{xy} = 1224\ cm^{-1},\ \sim 1220\ cm^{-1}$

$E(^3E_g^a) - E(^3B_{1g}) = 9{,}260\ cm^{-1}\ (1080\ nm) = 10\ Dq^{xy} - (35/4)D_t$

$D_t = 341\ cm^{-1}$

$D_t = 341\ cm^{-1} = (4/7)[Dq^{xy} - Dq^z]$

$Dq^z = 627\ cm^{-1},\ \sim 630\ cm^{-1}$

iv) $[Ni([7.12]bicycloN_5)(Br)]^{1+}$ (data obtained from reference 185, [7.12]bicycloN$_5$ = 12,17-Dimethyl-1,5,9,12,17-pentaazabicyclo[7.5.5]nonadecane):

$E(^3B_{2g}) - E(^3B_{1g}) = 10Dq^{xy} = 11{,}001\ cm^{-1}\ (909\ nm)$

$Dq^{xy} = 1100\ cm^{-1},$

$E(^3E_g^a) - E(^3B_{1g}) = 7{,}855\ cm^{-1}\ (1273\ nm) = 10\ Dq^{xy} - (35/4)D_t$

$D_t = 360\ cm^{-1}$

$D_t = 360\ cm^{-1} = (4/7)[Dq^{xy} - Dq^z]$

$Dq^z = 470\ cm^{-1}$